Raquel Comaposada Baró

Role of the p75 neurotrophin receptor ($p75^{NTR}$) in the basal forebrain cholinergic neurons (BFCNs)

Director de tesis:
Dr. Marçal Vilar Cerveró

València, Juliol 2021

Doctorat en Neurociències
de la Universitat de València
Institut de Biomedicina de València (IBV-CSIC)

Marçal Vilar, PhD

Molecular Basis of Neurodegeneration Unit

Biomedicine Institute of Valencia (IBV-CSIC)

e-mail: mvilar@ibv.csic.es

Marçal Vilar Cerveró, Doctor en Ciencias Químicas, Científico Titular y Director de la Unidad de Bases Moleculares de la Neurodegeneración del Instituto de Biomedicina de Valencia del CSIC y Enrique Lanuza Navarro catedrático de la Universidad de València del Departamento de Biología Celular, Biología Funcional y Antropología Física.

CERTIFICAN:

Que Raquel Comaposada Baró, graduada en Bioquímica en la Universidad de Barcelona ha realizado bajo la Tesis doctoral titulada "Role of the neurotrophin receptor p75 ($p75^{NTR}$) in basal forebrain cholinergic neurons (BFCNs)" bajo al supervisión de Marçal Vilar Cerveró (Director) y el tutelaje académico de Enrique Lanuza (Tutor).

En Valencia, Julio de 2021

VILAR CERVERO MARCIAL - DNI 25415779C

Digitally signed by VILAR CERVERO MARCIAL - DNI 25415779C
Date: 2021.07.26 12:35:27 +02'00'

Director de tesis

Marçal Vilar Cerveró

ENRIQUE| LANUZA| NAVARRO

Firmado digitalmente por ENRIQUE|LANUZA| NAVARRO
Fecha: 2021.07.26 12:57:58 +02'00'

Tutor académico

Enrique Lanuza Navarro

Julio de 2021

Quan arriba el moment de mirar enrere i recopilar tots els moments viscuts els últims quatre anys, trobes complicat poder-ho resumir i expressar com voldries. No sé si trobaré les paraules més adequades.

Òbviament, he de començar agraïnt al Dr Marçal Vilar tot el que m'ha ensenyat. Tant a nivell professional com personal. La evolució viscuda ha sigut gegant! També a la Dra Helena Mira, per els seus bons consells i serenitat. Gràcies als dos per ser tant humans.

A tots els companys i companyes de laboratori: Malú, creo que no puedo haber tenido mejor compañera de tesis. Recuerdo un mes que estuvimos juntas cada día, incluidos los fines de semana ¡madre mía, nose cómo no nos matamos! Aunque es tan sencillo trabajar contigo que lo veo imposible. Nunca has puesto una mala cara o dijiste una mala palabra aunque estuviéramos al límite, siempre me ayudaste en todo lo posible (fuera la hora que fuera y el día que fuera) ¡¡¡mil gracias!!!! Nunca te lo podré agradecer suficiente. JuanJu, ¡Qué gran descubrimiento! Aunque tú creas que eres un chico promedio, de 7.5, eres un chico sobresaliente, de 10. Tu seriedad mezclada con tu humor sabes que me da la vida! Gracias por tantas risas, son pura medicina! Jose, tus polillas no se van a olvidar! Gracias por toda la ayuda dada! Lau, no se qué habría echo si no me hubieras acogido en tu casa, gracias, gracias, gracias. Siempre tendrás un sitio en mi corazón. Isa, transmites alegría a todo el que te rodea, gracias por no fallar nunca. Espero que alguna vez podamos volver a Ruidera, es un oasis! Lucía, llàstima que Pruna i Habichuela no s'hagin conegut, encara que no crec que hagués sigut el millor! Stefano, bueno, eres una gran parte del equipo de tarde.

També he d'agraïr a la gent que m'he trobat durant aquests anys, sense ells i elles no hauria sitgut el mateix: Marina, no tinc ni paraules, i crec que tu la vas trobar: ARRELAR. Ets lo millor que m'enduc i no deixaré que es perdi. Victor, esta peninsular te va a echar de menos, eres una gran persona, con un corazón enorme.

Thanks to Prof. Christian Humpel to give me the opportunity to learn with him. Karin, Buket and Dhwani thanks for teaching me and embrace me as you did! I had a great time in Innsbruck thanks to you!

Tampoc puc deixar de banda a la familia, que encara que no han pogut ajudar científicament, sempre han estat al meu costat per animar-me i donar-me suport. Gràcies per ser el refugi i la casa que una necessita. També a les nenes, la meva via d'escapada, sempre us sento al meu costat i m'heu donat la energia que necessitava en els moments més durs.

Rafa, gracias por aguantar mis montañas rusas de humor, cuando ya no podía más, por creer en mí. No puedo tener mejor compañero de viaje.

Y en general quiero agradecer a la familia IBV que hemos creado. Sin vosotros y vosotras esta tesis no habría sido posible!

La realización de este trabajo de tesis doctoral ha sido posible gracias al Proyecto de Investigación: Plan Nacional I+D SAF2017-84096-R del Ministerio de Economía y Competitividad.

The PhD candidate has carried out all the experimental work exposed in the Chapter I of the present thesis, with the exception of the qPCRs that have been conducted with the help of José Vicente Santa-Rita Perez. All the experiments from Chapter II have been carried out by the PhD candidate.

RESUMEN

Las neuronas colinérgicas del prosencéfalo basal están implicadas en procesos cognitivos superiores como la atención y la memoria dado que proyectan en regiones como el hipocampo y la corteza. Estas neuronas expresan altos niveles del receptor de neurotrofinas p75 ($p75^{NTR}$) durante toda su vida. Sin embargo, el papel que juega en la fisiología de estas neuronas no esta del todo claro. En el trabajo experimental de esta tesis hemos estudiado el papel de $p75^{NTR}$ durante el envejecimiento y el papel del corte de $p75^{NTR}$ en neuronas maduras. El primer objetivo se estudio usando una cepa de senescencia acelerada: SAMP8. Este modelo fue cruzado con el *knock-out* de $p75^{NTR}$. Los resultados muestran cómo a edades jóvenes (2 meses) el SAMP8-$p75^{NTR-/-}$ tiene un mayor número de neuronas colinérgicas comparado con SAMP8-$p75^{NTR+/+}$. No obstante, a edades adultas (6 meses) y viejas (10 meses) el número de neuronas disminuye hasta los niveles de SAMP8-$p75^{NTR+/+}$. Además, este mismo resultado fue comprobado en ratones C57BL/6-$p75^{NTR-/-}$. El número de neuronas colinérgicas se comparó a día postnatal 16 y a 2, 10 y 24 meses. Así como en los ratones SAMP8-$p75^{NTR-/-}$, los ratones C57BL/6-$p75^{NTR-/-}$ presentan un aumento en el número de neuronas colinérgicas a día postnatal 16 y una posterior reducción a 2, 10 y 24 meses. La reducción en el número de neuronas colinérgicas va acompañado de una reducción en los niveles de marcadores específicos de neuronas colinérgicas como: ChAT, acetilcolina y Acly en los ratones SAMP8-$p75^{NTR-/-}$ de 6 meses. Los resultados muestran cómo la muerte colinérgica no es debida a una disminución a la respuesta al estrés oxidativo, ya que los ratones SAMP8-$p75^{NTR+/+}$ y los ratones SAMP8-$p75^{NTR-/-}$ tienen la misma respuesta a 6 meses. En cambio, los ratones SAMP8-$p75^{NTR-/-}$ sí que presentan unos niveles distintos en enzimas claves para la síntesis de colesterol. Estos resultados sugieren que los ratones SAMP8-$p75^{NTR-/-}$ podrían tener una desregulación en la homeostasis y síntesis de colesterol y por eso las neuronas colinérgicas degeneran y acaban muriendo. Además se comprobó que la perdida neuronal tiene un efecto en la memoria espacial ya que los ratones SAMP8-$p75^{NTR-/-}$ ejecutan peor el test-Y a los 6 meses de edad.

$p75^{NTR}$ es proteolíticamente procesado por una actividad α-secretasa y posteriormente por la γ-secretasa. Para estudiar el efecto del corte de $p75^{NTR}$ se usaron cultivos primarios de neuronas colinérgicas en los cuales la γ-secretasa se inhibió. Al añadir CE (el inhibidor de la γ-secretasa) se vio un aumento específico en la complejidad y longitud de las neuronas colinérgicas. Además se ha comprobado que este efecto es dependiente de $p75^{NTR}$ ya que en cultivos $p75^{NTR-/-}$ el efecto desaparece. Además hemos comprobado cómo el aumento de complejidad es realizado a través de la proteína RhoA, una proteína reguladora de citoesqueleto. Estos resultados fueron comprobados en rodajas de cultivos organotípicos y la adición del CE causa del mismo modo un aumento en la complejidad de las neuronas colinérgicas. Además, en ratones donde la γ-secretasa esta inhibida genéticamente, hay un

aumento de fibras acetilcolinesterasa en la corteza cerebral y en el hipocampo, sitios de inervación de las neuronas colinérgicas. Esto nos indica un aumento en la complejidad en una situación *in vivo*.

En conclusión esta tesis ha ampliado el conocimiento de $p75^{NTR}$ en las neuronas colinérgicas del prosencéfalo basal. Demostrando una dependencia colinérgica del receptor durante la edad adulta y el envejecimiento, probablemente debido a una desregulación en la homeostasis del colesterol. Además, la acumulación de $p75^{NTR}$-CTF, incrementa la complejidad colinérgica, indicando otro papel de $p75^{NTR}$ en las neuronas colinérgicas modulando su morfología.

ABSTRACT

The basal forebrain cholinergic neurons (BFCNs) are implicated in high cognitive processes such attention and memory as they project to regions like the cortex and the hippocampus. These neurons express high amounts of the p75 neurotrophin receptor ($p75^{NTR}$) during their whole life, nevertheless, the role that the receptor plays in them is not fully understood. During the experimental work of this thesis, the role that $p75^{NTR}$ plays during ageing and the role of the proteolytic processing of $p75^{NTR}$ have been studied. The first objective was achieved using a mouse model of accelerated senescence, SAMP8. This mouse model was crossed with the knock-out of $p75^{NTR}$, obtaining the SAMP8-$p75^{NTR-/-}$ mouse. The results showed how at young ages (2 months) there is an increase in the number of BFCNs in SAMP8-$p75^{NTR-/-}$ compared to SAMP8-$p75^{NTR+/+}$ mice. However, in adult mice (6 months) and aged mice (10 months) the number of cholinergic neurons between SAMP8-$p75^{NTR+/+}$ and SAMP8-$p75^{NTR-/-}$ are the same, indicating a cholinergic neuronal loss. In addition, the same result has been reported in the C57BL/6 background. The number of cholinergic neurons were quantified at postnatal day 16 and 2, 10 and 24 months. The results showed an increase in the number of BFCNs at 16 days old in C57BL/6-$p75^{NTR-/-}$ mice compared to C57BL/6-$p75^{NTR+/+}$ animals. Nevertheless, the levels were reduce at 2, 10 and 24 months in C57BL/6-$p75^{NTR-/-}$ mice. The reduction in the number of cholinergic neurons is accompanied by a reduction in the levels of specific cholinergic markers such as: ChAT, acetylcholine and Acly in SAMP8-$p75^{NTR-/-}$ mice at 6 months. The results showed that neuronal cholinergic death is not due to a reduction in the oxidative stress response, since the SAMP8-$p75^{NTR+/+}$ and the SAMP8-$p75^{NTR-/-}$ have the same oxidative response at 6 months of age. Nonetheless, SAMP8-$p75^{NTR-/-}$ mice present different levels in key enzymes of the cholesterol synthesis and endocytic pathway. Indicating that in the SAMP8-$p75^{NTR-/-}$ mice there might be a deregulation in the homeostasis of cholesterol explaining why cholinergic neurons degenerate. In addition, the cholinergic neuronal loss has a spatial memory effect as the SAMP8-$p75^{NTR-/-}$ mice perform worst the Y-maze test at 6 months compared to 2 months.

The $p75^{NTR}$ is proteolytically cleaved by the α-secretase generating the C-terminal domain, which is further cleaved by the γ-secretase. To study the effect of the $p75^{NTR}$ cleavage, primary cultures of cholinergic neurons were used and the γ-secretase was chemically inhibited. The addition of CE (a γ-secretase inhibitor) to the cholinergic neurons specifically increases their complexity and length. Furthermore, it was seen that this effect is $p75^{NTR}$-dependent as in $p75^{NTR-/-}$ cultures the effect disappears. In addition, we have proved that the increase in complexity is through the inhibition of the RhoA protein, a cytoskeleton regulatory protein. These results were confirmed in organotypic brain slices, as the addition of CE causes the same effect, an increase in the complexity of cholinergic neurons. Furthermore, in mouse models in which the γ-secretase is genetically inhibited, there is an increase in

acetylcholinesterase fibres in the cortex and hippocampus, places of innervation of cholinergic neurons. This is an indication of increased complexity in a *in vivo* situation.

All together the results of this thesis have amplified the knowledge of the $p75^{NTR}$ in the basal forebrain cholinergic neurons. Demonstrating a cholinergic dependence of the receptor during adulthood and ageing, probably to a cholesterol homeostasis deregulation. Moreover, the accumulation of $p75^{NTR}$-CTF, increases cholinergic complexity, indicating another role of $p75^{NTR}$ in the cholinergic neurons regulating their morphology.

CONTENTS

Role Of The P75 Neurotrophin Receptor In Basal Forebrain Cholinergic Neurons

LIST OF ABBREVIATIONS

Aß$_{1-42/1-17}$: Amyloid Beta 1-42/1-17
Acetyl CoA: Acetyl Coenzyme A
ACh: Acetylcholine
AChE: Acetylcholinesterase
Acly: ATP Citrate Synthase
AD: Alzheimer's Disease
ANOVA: Analysis Of Variance
APP: Amyloid Precursor Protein
AraC: Cytosine Arabinoside Hydrochloride
BACE: Beta site APP-Cleaving Enzyme
BB: Band of Broca
BBB: Brain Blood Barrier
BDNF: Brain Derived Neurotropic Factor
BF: Basal Forebrain
BFCN: Basal Forebrain Cholinergic Neuron
BSA: Bovine Serum Albumin
CA1: Cornu Ammonis 1
CamKII: Calcium/Calmodulin-Dependent Protein Kinase II
ChT: Choline co-transporter
ChAT: Choline Acetyltransferase
CNS: Central Nervous System
CiC: Citrate Carrier
CTF: C-Terminal Domain
DAG: Diacylglycerol
DAPI: 2-(4-amidinophenyl)-1H-indole-6-carboxamidine
DBB: Diagonal Band of Broca
DIV: Days in vitro
DMSO: Dimethyl sulfoxide
DNA: Deoxyribonicleic Acid
E: Embryonic day
EEG: Electroencephalogram
EDTA: Ethylenediaminetetraacetic Acid
ER: Endoplasmic Reticulum
Erk: Extracellular signal-regulated kinase
FL: Full Lenght
GABA: Gamma-Aminobutiric Acid
GFAP: Glial Fibrillary Acidic Protein
GDP: Guanosine Diphosphate
GTP: Guanosine Triphosphate
HBSS: Hanks' Balanced Salt Solution
HC: Hippocampus
HDB: Horizontal Diagonal Band of Broca
HEPES: 4-(2-HydroxyEthyl)-1-PiperazineEthaneSulfonic Acid
HMGCR: 3'-Hydroxy-3-MethylGlutaryl-CoA Reductase
HMOX1: Heme Oxygenase 1
HNE: 4-Hydroxynonenal
HRP: Horse Radish Peroxidase
ICD: Intracellular Domain
IP_3: Inositol trisphosphate
JNK: c-Jun N-terminal Kinase
Ldb1: LIM-Domain-Binding Protein 1
LDL: Low Density Lipoprotein
LDLR: Low Density Lipoprotein Receptor
LGE: Lateral Ganglionic Eminence
Lhx8, 6: LIM Homeobox 8, 6
LINGO-1: Leucine rich repeat and Immunoglobin-like domain-containing protein 1
MAPK: Mitogen-Activated Protein Kinase
MCP1/2: Mithocondrial pyruvate carriers 1/2
MGE: Medial Ganglionic Eminences
MRI: Magnetic Resonance Image
mRNA: Messenger RNA
MS: Medial Septum
MW: Multi Well
NBM: Nuclis Basalis of Meynert / Nuclis Basalis Magnocellularis
NF-κB: Nuclear factor κB
Nfr2: Nuclear factor erythroid 2-related factor 2

NGF: Nerve Growth Factor
Nkx2.1: NK-2 homeobox 1
NOR: Novel Object Recognition
NRAGE: Neurotrophin Receptor-Interacting MAGE homolog
NRIF: Neurotrophin Receptor-Interacting Factor
NT-3, -4: Neurotrophin-3, -4
PB: Phosphate Buffer
PBS: Phosphate Buffered Saline
PD: Postnatal Day
PDC: Pyruvate Dehydrogenase Complex
PDL: Poly-D-lysine
PET: Positron Emission Tomography
Pen-Strep: Penicillin/Streptomycin
PFA: Paraformaldehyde
PFC: Prefrontal Cortex
PI3K: Phosphoinositide 3-kinase
PKC: Protein Kinase C
PMSF: Phenylmethylsulfonyl fluoride
PNS: Peripheral Nervous System
POA: Preoptic Area
PLC-γ: Phospholipase C-γ
PSEN1/2: Presinilin-1/2
qPCR: Quantitative real time Polymerase Chain Reaction
RIP: Regulated Intramembrane Proteolysis
RIP2: Receptor Interacting Protein-2
RNA: Ribonucleic acid
ROS: Reactive Oxygen Species
SAMP: Senescence Accelerated Mouse Prone
SAMR: Senescence Accelerated Mouse Resistant
SDS: Sodium Dodecyl Sulfate
SEM: Standard Error of the Mean
SI: Substantia Innominata
SOD1/2: Super Oxid Dismutase 1/2
SREBP: Sterol Regulatory Element-Binding Proteins
TACE: Tumor necrosis factor-alpha converting enzyme
TBS: Tris Buffered Saline
TMD: Transmembrane Domain
TNF: Tumour Necrosis Factor
Trk: Tropomyosin Receptor Kinase
V: Ventricle
VChAT: Veicular ACh Transporter
VDB: Vertical Diagonal Band of Broca
WB: Western Blot

INTRODUCTION

1. The Basal Forebrain

Ageing is an inherent vital phenomenon that, luckily, all of us will suffer. All humans and animals experience bio physiological changes during elderly and is the biggest risk factor to any disease (Wyss-Coray, 2016). The brain is an important organ that suffers from the effects of becoming older. During this process there is an anatomical and functional decline which can be normal or pathological. In a non-pathological ageing different morphological changes might be appreciated; reduction in the brain volume, loss of neurons, increase of glial cells and dendritic alterations such as a decrease in their number and/or complexity. In a pathological ageing, with cognitive impairment, these same changes happen but they are more noticeable and asynchronous and, eventually, it can lead into a severe dementia like Alzheimer's Disease (AD) (Caserta et al., 2009). An important area of the brain that suffers from elderly, among others, is the basal forebrain (BF) and specifically a group of neurons of this area; the basal forebrain cholinergic neurons (BFCNs).

The BF is a heterogeneous area located in the medial-ventral surfaces of the cerebral hemispheres, between Bregma + 1.42 mm up to Bregma - 1.34 mm, comprising an area of 2.76 mm of longitude in the mouse brain **(Figure I1)** (Franklin & Paxinos, 2013). This highly complex region is composed of different types of neurons, like cholinergic and GABAergic interneurons, glutamatergic and calcium binding protein neurons (calbindin, calretinin or parvalbumin positive) (Gritti et al., 1997; Gritti et al., 2003; Henderson et al., 2010). Apart from the aforementioned neurons, in the BF there is a group of cholinergic projection neurons; the BFCNs. These neurons are the major source of acetylcholine (ACh) of the central nervous system (CNS) (Everitt & Robbins, 1997) and they are involved in high cognitive processes, such as attention and memory (Zaborszky et al., 2018). Moreover, BFNCs have been related to cognitive decline and different neurodegenerative diseases such as AD and Parkinsons's Disease (Mega, 2000; Schliebs & Arendt, 2011).

Even though big efforts have been made to study the BFCNs, this is not an easy task. The difficulty relies on the heterogeneity found in this area. As mentioned above, the BF is composed of different types of neurons, being the BFCNs the largest and the most complex ones of the CNS described to date (Wu et al., 2014). BFCNs long axons project into a variety of distal areas and even a single neuron can project to different regions (Mesulam et al., 1983).

Cholinergic neurons receive a widespread group of inputs. At 2016 Hu and colleagues reported the different areas that project to the BFCNs (Hu et al., 2016). Some of these inputs are: cortical, olfactory, entorhinal–hippocampal system, stress-related brain areas and motivation-related areas. All the different inputs highlight the arduous functional role of the BFCNs, demonstrating that this area is processing signals from all over the brain and send it back to

other brain areas, such as the hippocampus (HC) and the prefrontal cortex (PFC) (see below) (Hu et al., 2016).

In rodents, the BFCNs are present in four areas regarding the localisation of their neuronal soma and their projecting area. These areas, in a rostral to caudal order, are; the medial septum (MS), the horizontal and vertical limbs of the diagonal band of Broca (HDB and VDB, respectively), the substantia innominata (SI), and the nucleus basalis magnocellularis (NBM). The MS and the VDB mainly innervate to the HC (Kondo & Zaborszky, 2016), whereas the HDB projects to the olfactory bulb and finally the NBM to the PFC and amygdala (Woolf, 1991) **(Figure I1)**. In primates, the nomenclature is different, all the CNS cholinergic neurons are divided in 10 groups, from Ch1 to Ch10 being the Ch1-Ch4 groups from primates the BFCNs (Blake & Boccia, 2016). Ch1 corresponds to the MS; Ch2 to the VDB; Ch3 to the HDB and Ch4 the NBM complex that includes the SI and the nucleus basalis of Meynert (Mesulam et al., 1983).

At the beginning the different groups of cholinergic neurons were believed to diffused and separate structures (Saper, 1984; Woolf, 1991). However, the BFCNs have a concrete topographical organisation and when looking at them from a three-dimensional perspective, they construct a longitudinal, obliquely (lateromedially) oriented, partially overlapping area **(Figure I1)** (Zaborszky et al., 1999; Wu et al., 2014; Unal et al., 2015; Zaborszky et al., 2015; Ballinger et al., 2016; Jiang et al., 2016).

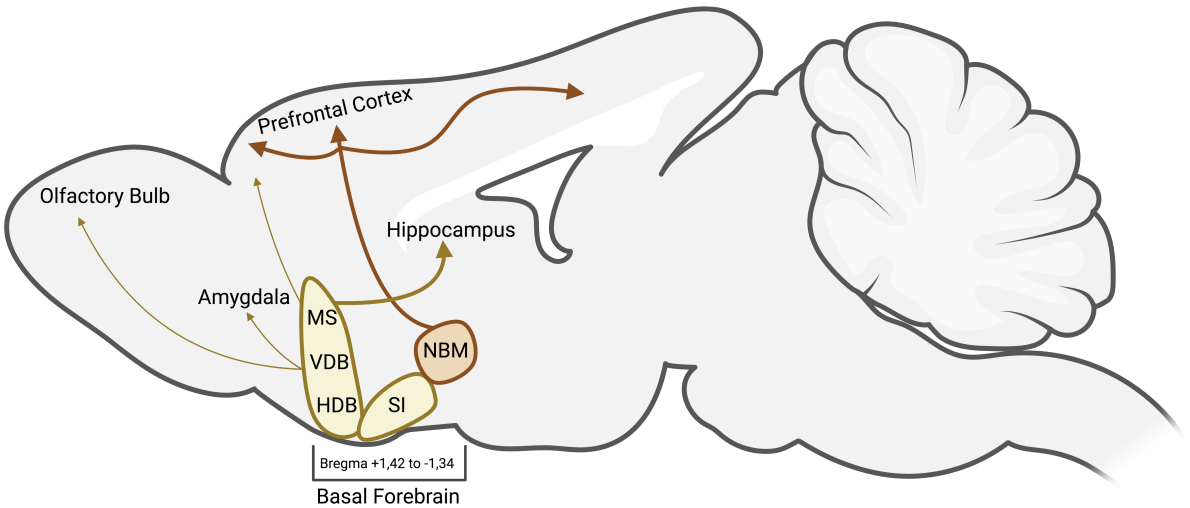

***Figure I1:* Organisation and projection areas of the Basal forebrain cholinergic neurons.** *BFCNs are present in four areas, the MS, the DBB, the SI and the NBM. These areas form a continuum. Each area project to distal brain regions: the MS and the VDB mainly to the hippocampus and the HDB and the NBM mainly to prefrontal cortex. MS: Medial Septum, VDB/HDB: Vertical and Horizontal Diagonal Band of Broca, SI: Substantia Innominata, NBM: Nucleus Basalis Magnocellularis.*

1.1. Development Of The Basal Forebrain Cholinergic Neurons

The development of the brain is a well-organised and complex process in which different steps happen in a very short period of time. All the development is guided thanks to specific signals (exogenous) and specific transcription factors (intrinsic). Every concrete combination of different factors will specify the fate of a neuron and will also guide it during migration, to finally achieve the whole structured brain (Purves et al., 2019).

The BFCNs are originated from neural precursors born in the subpallium or ventral telencephalon, specifically in the medial ganglionic eminence (MGE) at embryonic day 9.5 (E9.5). The cholinergic precursors start to express the homeobox transcription factor Nkx2.1 at E9.5 and the BFCNs keep its expression during their whole life (Allaway & Machold, 2017). In fact, it is known that this transcription factor is needed all over the cholinergic maturation process and life. If Nkx2.1 is removed during embryonic stages, there is a colossal decrease, around the 90 %, in the number of BFCNs compared to wild type animals (Magno et al., 2017). The requirement of Nkx2.1 expression during the whole life of the BFCNs was demonstrated *in vivo* with the deletion of the Nkx2.1 homeobox transcription factor at postnatal stages. The work showed a decrease in the number of BFCNs (Magno et al., 2011). These evidences proved that Nkx2.1 is not only needed during developmental stages, but also to maintain BFCNs integrity during adulthood.

In posterior embryonic stages, as the compartmentalisation increases, other transcription factors start to be expressed. At E10.5 the subpallium is divided into the MGE, the lateral ganglionic eminence (LGE) and the preoptic area (POA). At this stage, Nkx2.1 is expressed in the MGE and the POA and not in the LGE. Two Nkx2.1 downstream transcription factors expressed in the MGE/POA are the LIM-homeodomain 6 and 8 (Lhx6/8). Lhx6 and Lhx8 are thought to compete against each other. Nkx2.1 positive progenitor cells enter into a 'proto-GABAergic' state and express Lhx6. Then, a subset of these cells up-regulate Lhx8 expression, resulting in a down-regulation of Lhx6 and an adoption of the cholinergic fate, while those that retain Lhx6 expression acquire a mature GABAergic fate (Fragkouli et al., 2009).

Other downstream Nkx2.1 transcription factors that are necessary for the final fate of the BFCNs are; a Lhx8 cofactor, the LIM-domain-binding protein 1 (Ldb1) (Zhao et al., 2014), Islet-1 (Isl-1) the expression of which starts at E10.5 in the MGE/POA, and Olig2 (Furusho et al., 2006). Without them, there is a reduction of around the 40 % in the number of cholinergic neurons (Furusho et al., 2006) **(Figure I2)**.

During brain development the time at which the cells undergo the final mitosis, which is called the time of origin, is important. Thanks to choline acetyltransferase (ChAT)

immunohistochemistry co-labeled with H^3 thymidine, the time of origin of the BFCNs was studied. First, Semba and Fibiger (Semba & Fibiger, 1988) determined the time of origin of the neurons in the rat BF, and a year later, in the mouse one (Schambra et al., 1989). In their research, it was proved that the BFCNs are originated in a caudal to rostral gradient, denoting that the peak of post-mitotic ChAT positive neurons happen early in the caudal part of the brain, at E12-E13 in the rat and at E11-E12 in the mouse (Sweeney et al., 1989). Nonetheless, in the most rostral part it ends at E16 in the rat and at E15 in the mouse. Once the neurons have done their last mitosis they radially migrate in a caudal to rostral gradient (Schambra et al., 1989). Once there are in place, they start to send their axons to their respective projection areas (Marin et al., 2000).

BFCNs are highly linked to neurotrophins (NTs), especially to nerve growth factor (NGF), and their receptors, tropomyosin receptor kinase (Trks) and the neurotrophin receptor ($p75^{NTR}$). NTs and their receptors are important during BFCNs development and maturation, but also to maintain them alive during adulthood (Koh & Loy, 1989). The expression of $p75^{NTR}$ in developmental rat brain is first detected at E13 (Koh & Loy, 1989), but only in the most caudal parts, since that these neurons are the first ones to exit the cell cycle and mature. The same occurs in the mouse brain, $p75^{NTR}$ is first detected at E11 in the caudal parts, and at E13 in the rostral areas (Semba, 2004). In fact, the expression of $p75^{NTR}$ begins when the neuron is post-mitotic and it is believed that $p75^{NTR}$ is the first phenotypic trait found in cholinergic neurons, preceding transmitter-specific markers like ChAT (Koh & Loy, 1989).

A high number of studies have been published trying to understand the role that $p75^{NTR}$ plays during BFCNs development. Most of them find an increase in the number of BFCNs in $p75^{NTR-/-}$ mice compared to $p75^{NTR+/+}$ mice (Van der Zee et al., 1996; Yeo et al., 1997; Krol et al., 2000; Naumann et al., 2002; Greferath et al., 2012; Boskovic et al., 2014). However, two studies showed the opposite, a reduction of ChAT positive neurons in mice with $p75^{NTR}$ deletion (Peterson et al., 1997; Peterson et al., 1999). Another research showed no differences (Greferath et al., 2000; Ward et al., 2000). Some authors attributed these differences found when comparing the number of BFCNs to the mice strain used, and suggested that the model developed by Lee et al. has several issues;

1. The knock-out is total, and because of this some regions of the brain that could express $p75^{NTR}$ may affect the physiology of the BFCNs.

2. When the knock-out was generated by Lee et al., the background was mixed: Balb/c and S129/Sv, not pure.

3. Some authors have shown that the mixed background animal model developed by Lee et al. where the exon III of $p75^{NTR}$ is deleted, can generate an intracellular truncated form of $p75^{NTR}$. This isoform can have possible biological effects and the knock-out would not be complete (von Schack et al., 2001). In order to solve these problems, a different $p75^{NTR}$ knock-

out mouse was generated, deleting the exon IV instead of the exon III (Naumann et al., 2002). Interestingly, the same phenotype was found in the BFCNs, an increase in their number when analysed postnatally (Naumann et al., 2002). Recently, a conditional deletion of $p75^{NTR}$ has been described (Boskovic et al., 2014) showing that when breeding with $ChAT^{CRE}$ mouse, an increase in the number of BFCNs is also observed. All these findings point out that during development $p75^{NTR}$ plays a pro-apoptotic role, because when it is not expressed, there is an increase in the number of cholinergic neurons.

TrkA, another NT receptor, is also expressed during the development of the BFCNs. **(Figure I2)** Lhx8 has been shown to promote the expression of TrkA during development, and a positive feedback loop between NGF-TrkA-Lhx8-TrkA was proposed (Tomioka et al., 2014). Two recent publications showed the importance of TrkA in the BFCNs. In Sanchez-Ortiz et al., 2012, they reported the same number of BFCNs when mutant animals were compared to wild type. Nevertheless, they reported a loss in projections and connectivity. In this work the mouse used is a conditional knock-out of $TrkA^{fl/fl}$ crossed with the $dlx5/6i^{CRE}$ mouse (Sanchez-Ortiz et al., 2012). In Muller et al., 2012, they showed a decrease in the number of ChAT (and also $p75^{NTR}$) positive neurons and no loss of connectivity (just the one in accordance with the loss in the number of neurons). In this work the mouse used is a $TrkA^{fl/fl}$ crossed with a $Nestin^{CRE}$ mouse (Muller et al., 2012). A possible explanation for their differences, as Muller et al., 2012 stands out, is the different timing of the CRE expression and in consequence the time of the TrkA deletion. The CRE in the $Nestin^{CRE}$ line is expressed at E11.5 while the expression of the CRE in $dlx5/6i^{CRE}$ mouse starts at E16.5. The time when TrkA is deleted may be important to its function. This idea is supported with another work, (Fagan et al., 1997), where they showed a reduced number of BFCNs in the TrkA total knock-out. Hereby, TrkA expression is necessary in early developmental stages (before E16.5) because if it is not expressed, there is a reduction in the number of BFCNs. Nonetheless, it is important to keep its expression to maintain BFCNs healthy (Sanchez-Ortiz et al., 2012).
Even tough $p75^{NTR}$ and TrkA are expressed in the BFCNs, their ligand, NGF, is expressed and secreted by cholinergic target cells in the HC and in the cortex, more specifically, by pyramidal neurons of the cortex and dentate granule neurons of the HC. Additionally, GABAergic interneurons in the HC and in the BF express NGF (Biane et al., 2014). After cholinergic specification, these complex neurons start to extend their axons and dendrites and make their synaptic contacts prenatally. Nevertheless, they continue growing and making projections until around postnatal day 30 in mice. In that moment they are considered fully mature cholinergic neurons. To finally maintain its characteristics such as; cell survival, axonal and dendritic growth, synaptogenesis and maintenance of the neurotransmitter phenotype, the BFCNs require the expression of the transcription factors mentioned above (Nkx2.1, Lhx8, Isl-1) but also the retrograde transport of NGF via the TrkA-$p75^{NTR}$ receptor system (Kramer et al., 1999; Zweifel et al., 2005).

Thus, the generation and formation of cholinergic neurons, like all other types of neurons, imply many factors that can affect them, like the time of expression of each transcription factor or the presence or absence of NTs.

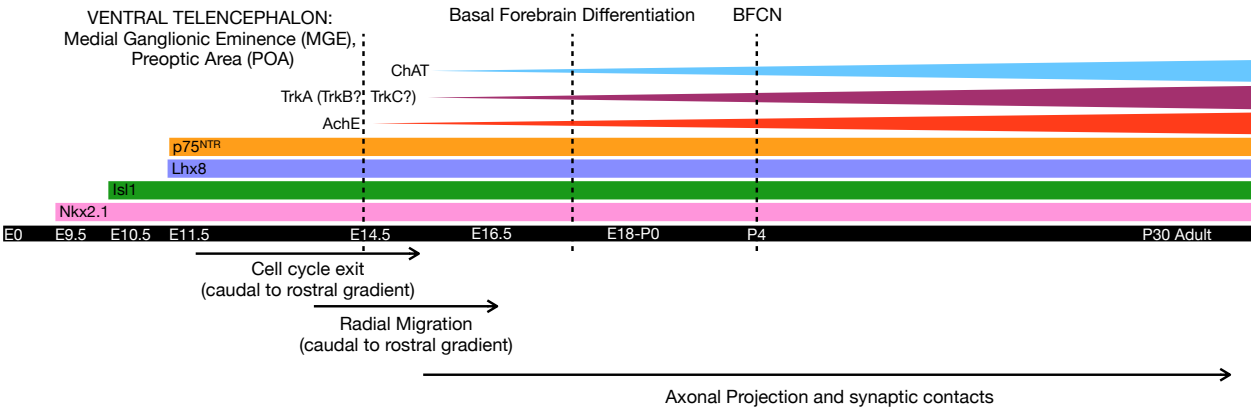

Figure I2: ***Mouse basal forebrain cholinergic neurons gene expression timeline.*** *During embryonic development, the first transcription factor expressed in the BFCNs is Nkx2.1, followed by Isl1, Lhx8 and p75^{NTR}, all at early embryonic stages (E10-E12). After, at mid-late embryonic stages (E15), the expression of AChE starts, finally at late embryonic stages TrkA (TrkB and TrkC is unclear) and ChAT (E16-E18) expression is detected. The expression of all of them is kept throughout the whole life of BFCNs to keep the cholinergic fate.*

1.2. The Neurotransmitter Acetylcholine

The acetylcholine (ACh) was the first substance to be identified as a neurotransmitter (Otto Loewi et al., 1921). ACh is an excitatory neurotransmitter, classified as a small-molecule neurotransmitter, that apart from acting in the neuromuscular junctions and ganglionic synapses at the peripheral nervous system (PNS), it also plays a role in different areas of the CNS. Even though a lot of information is known about the function of the ACh in the PNS, the same does not happen in the CNS. The neurotransmitter ACh follows the normal synthesis-liberation-recycle cycle. ACh is synthesised in the nerve terminals (pre-synaptic neuron) where the two precursors, acetyl Coenzyme A (acetyl-CoA) and choline are chemically bond by ChAT (Jope & Jenden, 1980). Choline is present at high levels in the plasma, around 10 mM, and it is taken up into cholinergic neurons by the high-affinity Na^+-dependent choline co-transporter (ChT). At the same time that one molecule of Na^+ is expelled from the neuron, one choline molecule gets in. On the other hand, the levels of acetyl-CoA in a neuron, both cytosolic and mitochondrial, range from 10 to 7 µmol/L (Ronowska et al., 2018). This acetyl-CoA comes from the lactate imported by neurons, afterwards this lactate is converted into pyruvate. Pyruvate enters into the mitochondria thanks to the two mitochondrial pyruvate carriers, 1 and 2 (MCP1/2). The two MCP form an hetero-oligomeric complex and help pyruvate to cross the inner mitochondrial membrane (McCommis & Finck, 2015). Inside the mitochondria, the pyruvate is oxidative decarboxylated and converted into acetyl-CoA via the pyruvate dehydrogenase complex (PDC). Then, acetyl-CoA is combined with oxaloacetate by the citrate synthase to form citrate and feed the Krebs cycle. This citrate can exit the mitochondria (with the citrate carrier, CiC) and be converted back to acetyl-CoA and oxaloacetate by the ATP citrate lyase (Acly) in the cytosol. The cytosolic acetyl-CoA can have different fates; cholesterol synthesis, fatty acid synthesis and, in addition, in the cholinergic neurons it is used to produce ACh (with the enzyme ChAT) (Prado et al., 2002).

Once the ACh is synthesised, it is loaded into vesicles thanks to the vesicular ACh transporter (VCAhT). This enzyme loads approximately 10000 molecules of ACh into each cholinergic vesicle (Prado et al., 2013). To concentrate the ACh inside the vesicle $2H^+$ are exchanged for 1 ACh, thereby the pH in the lumen of the vesicles is acidic. The vesicles with the ACh will be released into the synaptic cleft when an electric impulse arrives. The ACh will bind their receptors in the post-synaptic membranes: nicotinic and muscarinic acetylcholine receptors (nAChR and mAChR) (Fambrough, 1979). The transmission signal finishes when the ACh is hydrolysed by acetylcholinesterase (AChE) into choline and acetate (that quickly diffuses into the surrounding medium). The AChE enzyme is concentrated in the synaptic cleft (Rotundo, 2003). To close the cycle, the choline is transported into the pre-synaptic neuron and ACh is synthesised again **(Figure I3)**.

A lot of steps are necessary to synthesise and release the acetylcholine, involving a lot of different enzymes that can be regulated. Moreover, these enzymes (ChAT, VCAhT, ChT and AChE) are specific markers for cholinergic neurons.

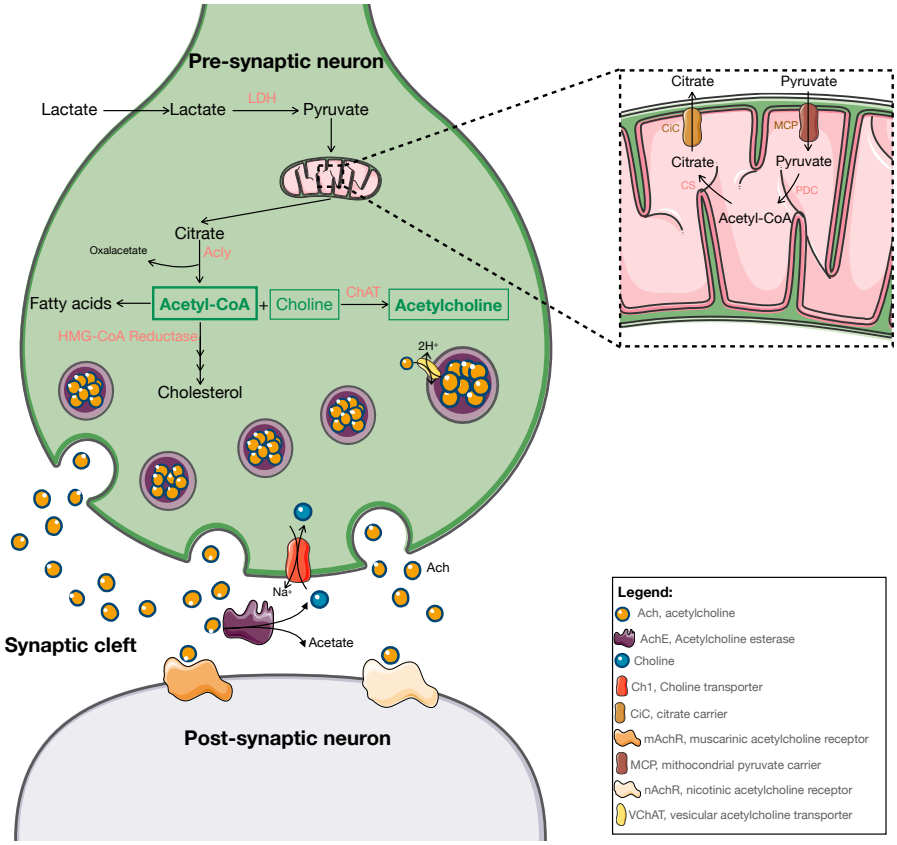

Figure I3: ***Acetylcholine synthesis-liberation-recycle cycle.*** *The lactate enters into the pre-synaptic neuron and is converted into pyruvate that enters into the mitochondria where is oxidative decarboxylated and converted into Acetyl-CoA. Then, acetyl-CoA is combined with oxaloacetate by the citrate synthase to form citrate. This citrate can exit the mitochondria (with the citrate carrier, CiC) and be cleaved back to acetyl-CoA and oxaloacetate by the ATP citrate lyase (Acly) in the cytosol. Acetyl-CoA can follow different routes: cholesterol synthesis, fatty acid synthesis and synthesise the acetylcholine together with a choline and the enzyme ChAT. Once the ACh is synthesised is loaded into vesicles (VCAhT). The ACh is released into the synaptic cleft and binds to its receptors in the post-synaptic membranes: nicotinic and muscarinic acetylcholine receptors (nAChR and mAChR). The transmission signal ends when ACh is hydrolysed by acetylcholinesterase (AChE). The cycle finishes when the choline is transported into the pre-synaptic neuron and ACh is synthesised again.*

1.3. Cognitive Functions Of The Basal Forebrain Cholinergic Neurons

The entire cortex and HC are innervated by topographically organised cholinergic projections (Rye et al., 1984; Lysakowski et al., 1989; Kitt et al., 1994). These two brain regions are involved in superior cognitive processes, such as; memory, attention, learning, arousal and stress. Therefore, the BFCNs are involved in these high cognitive processes.

1.3.1. Cortical functions and pathways

Cortical cognitive functions of the BFCNs have been studied for a long time, mainly because of their correlation with degeneration and the aggravation in AD symptoms (Perry et al., 1978; Bierer et al., 1995). The path of cholinergic fibres ascending from the BF to the cerebral cortex form the extra-thalamic brainstem activating system (Jones, 2004). It is worth to pinpoint that the BFCNs innervate all the six different cortical layers. Historically, due to the lack of proper techniques, the BFCNs were stated to be involved in a wide range of cortical functions (almost all memory tasks); active avoidance, passive avoidance, T-maze alternation learning and retention, radial-maze alternation learning and retention, spatial navigation in the Morris water maze, spatial reversals in an operant chamber or in a T-maze, delayed matching-to sample tasks, brightness discrimination and reversal, and accurate timing of operant responses (Dunnett et al., 1991). However, these studies were made using different NMDA agonists, a non-specific technique, where a lot of other areas and neurons were damaged. Thanks to the selective immunotoxin (192-IgG-saporin) that deletes specifically $p75^{NTR}$-expressing BFCNs, the different cognitive functions related to these neurons were more accurately studied (Wiley et al., 1991). This compound consists in a molecule of saporin, a ribosome-inactivating toxin, combined with a monoclonal antibody (192 IgG) against $p75^{NTR}$. As $p75^{NTR}$ is only expressed in the BFCNs during adulthood it is possible to selectively damage these neurons (Wiley et al., 1991). When new experiments were carried out using the 192 IgG-saporin immunotoxin the substantial damage was limited only to the BF cholinergic neurons, the bast majority of behavioural results could not be reproduced and almost no deficits in learning and memory tasks were seen (Book et al., 1992; Berger-Sweeney et al., 1994; Heckers et al., 1994; Torres et al., 1994; Wenk et al., 1994; Everitt & Robbins, 1997; Chappell et al., 1998).

Nevertheless, these studies showed a link between attention and the BFCNs. Attention is defined as a focused activation of a neuronal network that is relevant to a specific cognitive task (Oken & Salinsky, 1992). Interestingly, attention has been conceptualised as two separate processing streams; goal/cue-driven attention, termed ‘‘top-down” or voluntary, while sensory-driven attention is termed ‘‘bottom-up” or involuntary (Katsuki & Constantinidis, 2014).

The PFC, a target of the cholinergic innervation, is an integral node of circuits underlying attention, exerting a top-down control over sensory cortical areas to enhance task-relevant

cues detection (Ballinger et al., 2016). Thus far, thanks to the immunotoxin, the lesions suggest that the BFCNs may be involved in the control of shifting attention to sensory stimuli that predict a biological relevant event (Wenk, 1997). Another way to study the cognitive functions of the BFCNs is evaluating the electrophysiology of the area. Different studies suggested that BF controls the activation of cortical electroencephalogram (EEG) activity. Cortical activation can be defined as an increased responsiveness of cortical neurons to inputs arriving through sensory pathways and other pathways (Steriade & Deschenes, 1984). Cortical ACh has been shown to participate in the maintenance of cortical activation, which has been proven with the administration of the muscarinic antagonist (receptor of ACh) atropine that induces large slow waves in the cortex similar to those seen during non-rapid eye movement sleep (Longo, 1966), suggesting no cortical activation.

Kanai and Szerb were the first to show the strong tonic correlation between cortical EEG activation and ACh release as a result of reticular formation stimulation. Reticular formation is an afferent BF input (Kanai & Szerb, 1965). Hereby, when the reticular formation is stimulated, the BF is activated and it releases ACh into the cortex. The observation of Kanai and Szerb was supported with other studies in which they directly stimulated the BF and a sevenfold increase in the ACh release was recorded (Casamenti et al., 1986; Rasmusson et al., 1994). Moreover, cortical ACh release is suppressed by anaesthesia (Dudar & Szerb, 1969), is increased during wakefulness and REM sleep (Celesia & Jasper, 1966; Jasper & Tessier, 1971), and is increased by visual (Collier & Mitchell, 1966), auditory (Hemsworth & Mitchell, 1969) or somatosensory stimulation (Kanai & Szerb, 1965; Phillis & York, 1968).

Taking into account that de main source of ACh in the cortex are the BFCNs, their implication can be linked to attentional processes and to the control and maintenance of arousal and sleep states. Furthermore, when EEG were recorded after the injection of the immunotoxin, a general decrease in the EEG power was detected (Kapas et al., 1996). Genetic and optogenetic-assisted cell type identification to extracellularly record cholinergic neurons has also helped determine which cognition aspects cholinergic activity might support (Hangya et al., 2015).

Altogether, evidences showed that at least the cholinergic component is closely related to processes of cortical activation. The effect of ACh blockade by atropine induces large slow waves, whereas ACh release increases during states with high activity in the cortex. Moreover, taking into account both, the histological and anatomical studies of the BF, this area appears to be ideally located to evaluate sensory stimuli and to modulate the responsiveness and attend to it (Everitt & Robbins, 1997; Wenk, 1997; McGaughy et al., 2000; Hampel et al., 2018).

1.3.2. Hippocampal functions and pathways

Until here, the text has focused on the cognitive aspect of attention. Nevertheless, this function is related only to one part of the BFCNs, the NBM, the subset of neurons that innervate the PFC. The MS and the VDB innervate the HC and they are its major source of ACh. More than 90 % of the cholinergic innervation of the HC comes from the MS/VDB (Mesulam et al., 1983), the other 10 % comes from cholinergic interneurons within the very HC (Cassel et al., 1997). The projection pathways that arise from the BF to the HC are called the septo-hippocampal pathways, they are bidirectional and they are composed not only of cholinergic neurons but also of GABAergic and glutamatergic neurons. These pathways are implicated in cognitive processes (Blake & Boccia, 2018), and they have three different routes; the cingular bundle (or supracallosal dorsal route, overlying the corpus callosum), the fornix (also known as infracallosal dorsal route) and the ventral pathway **(Figure I4)** (Gage et al., 1984; Milner & Amaral, 1984). The ventral projection arises from the VDB region and reaches the HC by running over the surface of the amygdaloid complex. Conversely, dorsal fibres are originated in the MS/VDB cells and enter the HC via the fornix and fimbria, as well as the cingular bundle over the genu of corpus callosum (Garcia-Lopez et al., 2015). These septo-hippocampal projections terminate in the cornu ammonis 1 and 3 (CA1, CA3), and dentate regions of the HC. The largest part of cholinergic afferents course through the fimbria–fornix pathways (approximately the 75 %), the supracallosal and ventral pathways contribute to a lesser extent to the cholinergic hippocampal innervations (approximately the 25 %) **(Figure I4)** (Cassel et al., 1997).

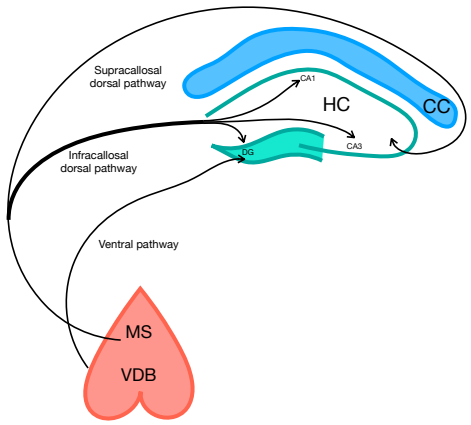

Figure I4: ***Different projection pathways from medial septum to Hippocampus (septo-hippocampal pathways):*** ventral pathway arises from VDB region and reaches the HC by running over the surface of the amygdaloid complex. The infracallosal dorsal fibres (most common) and the supracallosal dorsal fibres originate from MS/VDB and enter the HC.

The best-known cognitive function related to HC is memory. Memory is perhaps the most complex of all the cognitive functions and a variety of different processes are involved in it; first the acquisition of the memory occurs, then there is short- and/or long-term storage of it, and finally the recall and/or extinction (Purves et al., 2019). In addition to all the steps needed to create just one memory, different types of memory can be appreciated. Briefly, the first big

classification is; short-term and long-term memory, and as the name itself indicates, it affects the time memory is retained. Short-term memory is considered as working memory and enables the brain to remember a small amount of information for a short period of time. This is the process we use to hold information in our head while we are engaged in other cognitive processes. Long-term memory can be divided in the implicit and the explicit memory. On the one hand, the implicit, or unconscious memory, encompasses memories that may be procedural, involving learned motor skills; for instance learning how to pipette or how to load a gel. On the other hand, the explicit or conscious memory, as its name indicates, is the intentional collection of factual information, previous experiences, and concepts. Conscious memory can also be subdivided into episodic and semantic. The episodic memory will recall events that happened to you and records information about one's environment and spatial orientation, whereas semantic memory recalls the general knowledge of the world (Purves et al., 2019). In this thesis the focus will be put on spatial and episodic memory since evidence links the BF to them.

Increasing theta activity and neuron synchronisation achieve the promotion of synaptic plasticity, within and across, regions of the HC. It is believed that the neurotransmitter in charge of allowing this efficient encoding of novel information is the ACh (Pavlides et al., 1988; Hyman et al., 2003). In accordance to that, different studies have shown the importance of the liberation of ACh in the formation of spatial memories (Mitsushima et al., 2013). More in concrete, using microdialysis investigators have seen a rise in ACh levels while rats are exploring in the novel object recognition test (NOR). Moreover, both hippocampal ACh release and hippocampal theta activity were increased during exploration or novelty experience, together with stress or arousal (Giovannini et al., 2001; Anzalone et al., 2009). Furthermore, the pharmacological blockade of ACh receptors locally in the hippocampal CA3 or CA1 regions disrupts the encoding of spatial information while sparing retrieval (Rogers & Kesner, 2003).

Regarding evidence at a network level, some studies showed the importance of cholinergic signalling in gamma and theta oscillations. The balance between these oscillations in hippocampal activity has been shown to be important for learning and memory (Duzel et al., 2010; Hasselmo & Stern, 2014). Moreover, cholinergic signalling, coming from the MS can modulate their strength (Lu & Henderson, 2010; Newman et al., 2013; Dannenberg et al., 2015).

To sum up, due to the different innervation areas of the BFCNs, several cognitive functions can be differentiated. The most caudal part, the NBM, liberates ACh into the cortex leading to its activation which has been related to attentional processes. However, the MS and the VDB areas, which innervate the HC, have been suggested to control theta oscillations and induce a state that allows the detection of novelty and formation of new memories (Blake & Boccia, 2016).

1.4. Basal Forebrain Cholinergic Neurons In Ageing, Cognitive Impairment And Alzheimer's Disease

A massive interest in the study of the BFCNs appeared when investigators made the observation that cognitive impairment was linked to a cholinergic hypofunction (Perry et al., 1977; Perry et al., 1978). Different studies reported moderate degenerative changes during ageing in the BFCNs, correlated with a progression in memory deficits. The first evidence showing this interaction was a decrease in ChAT activity with age in human brain samples in the temporal cortex and in the HC (Perry et al., 1977). After that, some research showed a reduction in different cholinergic markers (ChAT, ACh, AChE, mAChR and nAChR binding) (Davies & Maloney, 1976; Perry et al., 1977; Perry et al., 1977;1978; Perry et al., 1992; Sparks et al., 1992) when comparing postmortem brains of AD patients and normal ageing tissue. Moreover, these cholinergic deficiencies were correlated with cognitive impairment. ChAT and AChE activities decrease at the same time as cognitive impairment and senile plaques increase (Perry et al., 1978). Furthermore, magnetic resonance image (MRI) studies showed how cholinergic atrophy (with volume reduction) parallels cognitive decline, specifically in the NBM when patients show mild cognitive impairment and AD (Grothe et al., 2013; Kilimann et al., 2014; Lammers et al., 2018). Closer in time, the positron emission tomography (PET) technology showed a decrease in AChE activity in mild cognitive impairment and early AD (Shinotoh et al., 2000; Rinne et al., 2003).

Leaving human samples aside, cholinergic atrophy has been reported in different rodent models (Koliatsos et al., 1991; Tuszynski, 2000). Even though there is a decrease in all the cholinergic markers, in normal ageing and mild cognitive impairment, no cholinergic neuronal loss has been described at these stages (Schliebs & Arendt, 2011). While at later stages, AD patients with a severe cognitive deficiency, exhibit a profound loss of cholinergic neurons, specifically in the NBM (Whitehouse et al., 1982). Suggesting that the BFCNs suffer from changes in gene expression, impairments in intracellular signalling and cytoskeletal transport that lead to the neuronal atrophy and age-related functional decline. This cholinergic atrophy precedes the neuronal loss reported at late stages in the AD pathology.

Another link of cholinergic atrophy and cognitive impairment was seen when AD patients were treated with AChE inhibitors, promoting an increase in the ACh levels in the synapsis, and ameliorating the worsened cognitive symptoms (Anand & Singh, 2013). Nevertheless, with the administration of the different drugs approved by the FDA to treat AD, AChE inhibitors and cholinomimetic drugs, the disease is not cured, just delayed and palliated.

All these studies led to the cholinergic hypothesis of memory in AD. It stated; a serious loss of cholinergic function in the CNS significantly contributes to the cognitive symptoms associated

with AD and advanced age (Bartus, 2000). One explanation relates cholinergic dysfunction to a decrease in the trophic support, needed for the BFCNs healthiness (see section 3: basal forebrain cholinergic neurons and neurotrophins) (Sofroniew et al., 2001). The importance of the BFCNs in memory and attention and that their dysfunction is undeniably related to a worsening in these functions. However, the treatment of cholinergic hypofunction ameliorates the effects and do not cure the patients, so the BFCNs atrophy might be a consequence of a first deregulation and not the trigger of the dementia. Hereby, other important players might be involved.

2. The Neurotrophins And Their Receptors

2.1. The Neurotrophins

The study of NTs started around 70 years ago when Rita Levi-Montalcini and Stanley Cohen discovered the NGF (Levi-Montalcini & Hamburger, 1951; Cohen et al., 1954; Levi-Montalcini et al., 1954). This event changed the way of understanding vertebrates brain and its development. Since then, a lot of scientific effort has been made to understand the function of the different NTs and their receptors.

The neurotrophic theory defends the regulation of neuronal survival, differentiation and function as the main role of the NTs (Chaldakov et al., 2009). Nevertheless, multiple and variegated new NTs functions have been discovered, such as; axonal and dendritic growth, neurotransmitter release, long-term potentiation, synaptic plasticity and neurodegeneration (Chao, 2003; Franco et al., 2020). Moreover, the NTs can promote the survival of non-neuronal cells and affect different metabolic processes such as; glucose levels, oxidative stress and lipid metabolism (Chaldakov et al., 2009; Chen et al., 2017).

Four different NTs exist in mammals: NGF; brain-derived neurotrophic factor, BDNF (Barde et al., 1982); neurotrophin-3, NT-3 (Maisonpierre et al., 1990) and neurotrophin-4, NT-4 (Hallbook et al., 1991). To carry out their functions, the NTs bind and activate two different types of receptors: the TrKs; TrkA, TrkB and TrkC, and the $p75^{NTR}$. Each NT binds and activates specifically one tyrosine receptor: NGF to TrkA, BDNF and NT-4 to TrkB and NT-3 to TrkC. Additionally, the four NTs and their immature form (pro-neurotrophins) can bind to $p75^{NTR}$ with similar affinity (Rodriguez-Tebar et al., 1991).

The four NTs have similar biochemical characteristics and behave similarly. The NTs are secretory proteins that form non-covalent homodimers. Moreover, all the NTs share 50 % of their amino acid sequence and the final three-dimensional structure of all of them is similar (Lewin & Barde, 1996). Regarding their synthesis, NTs are synthesised as pre-proneurotrophins, once in the endoplasmic reticulum (ER) the pre-sequence is cleaved generating the

proneurotrophins. These proneurotrophins form homodimers and after, the pro domain is cleaved by furin, releasing the mature domain (neurotrophin) that is trafficked to the extracellular space in secretory vesicles in the constitutive pathway (Al-Qudah & Al-Dwairi, 2016).

2.2. The Neurotrophin Receptors

2.2.1. TrkA

TrkA is a member of the tyrosine kinase receptors and its tyrosine kinase activity is promoted when NGF binds to it. The receptor itself consists of the extracellular domain, containing five different domains, one transmembrane domain and the intracellular tyrosine kinase domain. The immunoglobulin-like domain proximal to the membrane (TrkA-d5 domain) is necessary and sufficient for the NGF binding (Wiesmann et al., 1999). In order to activate the receptor, NGF binds the TrkA-d5 domain and induces a conformational change coupled to its transmembrane domain dimerisation (Franco et al., 2020). This state leads to intracellular autophosphorylation of the 3 tyrosines within the kinase domain, enhancing the phosphorylation of the other 2 tyrosines, localised outside the kinase domain. The last ones will serve as docking sites for adaptor proteins that will ultimately trigger intracellular cascades (Mitra, 1991). These cascades will activate diverse neuronal functions such as cell survival and differentiation, axonal and dendritic growth and arborisation, synapse formation and synaptic plasticity (Huang & Reichardt, 2003; Deinhardt & Chao, 2014).

A well-studied pathway is the one triggered by PLC-γ. Once PLC-γ binds the activated TrkA, hydrolyses the phosphatidylinositol-(4,5)-bisphosphate (PI(4,5)P2) into DAG and inositol tri-phosphate (IP3). IP3 leads the release of intracellular Ca^{2+}-dependent enzymes and the phosphatase calcineurin. Additionally, the release of Ca^{2+} and the production of DAG activate the PKC, which stimulates ERK to trigger differentiation and survival **(Figure I5)** (Franco et al., 2020). Shc (Shc homologous and collagen-like) protein is an adaptor protein of TrkA. When TrkA is phosphorylated, Shc binds to TrkA and starts the recruitment of another two proteins (Grb2 and Gab1) that will activate phosphatidylinositol 3-Kinase (PI3K) and consequently the Ras/MAPK signalling cascade. The result of this signalling induces neuronal differentiation via gene expression regulation **(Figure I5)**.
With all these examples it can be stated that the main function of activated TrkA by NGF is to promote intracellular cascades in order to contribute to neuronal survival and differentiation.

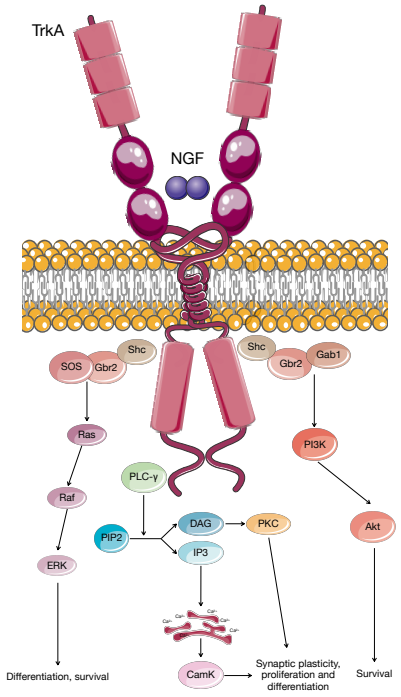

Figure I5: **TrkA signalling pathways.** *When NGF binds the TrkA, the receptor autophosphorilates and recruits adaptor proteins that activate three different survival and differentiation signalling cascades. PLC-γ hydrolyses PIP2 generating DAG and IP3. The DAG activates PKC and IP3 promotes Ca^{2+} liberation from endoplasmic reticulum and activates calcium dependent kinases. The other two routes are dependent of the Shc adaptor protein. Shc can bind Gbr2/SOS and activate MAPKK signalling cascade or bind Gbr2/Gab1 and activate Akt.*

2.2.2. The Neurotrophin Receptor P75

The neurotrophin receptor p75 is a member of the tumor necrosis factor receptor (TNFR) superfamily and is classified as a type I transmembrane protein with a molecular weight of 75 kDa. The protein contains an extracellular domain (ECD) at the N-terminal part of the protein that consists in 4 cysteine-rich motifs (where the NTs bind) followed by a serine/threonine-rich region. The ECD is followed by a single transmembrane domain (TMD) and an intracellular domain (ICD) containing the death domain (Vilar, 2017). $P75^{NTR}$ can be glycosylated with both N- and O-links in the extracellular domain, which is necessary for the receptor to be sorted (Johnson et al., 1986; Yan & Chao, 1991; Baldwin et al., 1992; Yeaman et al., 1997). In addition, the receptor can be palmitoylated. When that occurs, the receptor is translocated into the lipid rafts, and one of the consequences is the prevention of its shedding processing (Underwood et al., 2008).

Once $p75^{NTR}$ is expressed, the intracellular localisation of it is ubiquitous. In neurons can either be found in the somatodendritic compartment and in the most distal part of the axons. Moreover, the receptor can be located in the lipid rafts (Bronfman & Fainzilber, 2004). Different evidences suggested that depending on its localisation, $p75^{NTR}$ can signal differently. For example, if $p75^{NTR}$ is localised in the lipid rafts, it limits the number of co-receptors capable of binding the protein. Scientific data supported that $p75^{NTR}$ move to lipid rafts after ligand stimulation (Higuchi et al., 2003; Zhang et al., 2013). In the lipid rafts, endocytosis, vesicular

transport, and/or endosomal signalling transduction can be facilitated, being a way of the receptor regulation. In the CNS, the expression of p75^{NTR} is high and wide during development (Davies, 1991). Nevertheless, after postnatal stages, its expression is down-regulated and during adulthood is limited to brain injury. Only one neuronal population expresses p75^{NTR} throughout their whole life in the CNS; the basal forebrain cholinergic neurons (Salehi et al., 1996).

P75^{NTR} HOMEOSTASIS: SHEDDING, PROCESSING AND ENDOCYTOSIS

As a transmembrane receptor, different events are kinetically in balance to keep the homeostasis of the receptor and control properly its signalling. Some of those events are; regulated intramembrane proteolysis, recycling endocytosis, signalling endosomes and/or vesicular transport.

A. p75^{NTR} Regulated Intramembrane Proteolysis (RIP)

P75^{NTR} is processed by regulated intramembrane proteolysis (RIP). The half-time life of the receptor is balanced by its synthesis and the RIP. The RIP is thought to have important biological functions since the different fragments generated during shedding can trigger different signals (Kanning et al., 2003). The process consists of a first cleavage of the p75^{NTR} full-length by a membrane metalloproteinase, the TNFα-converting enzyme (TACE, also known as ADAM17). This first cleavage generates the releasing of the ECD and leaves a fragment of 24 kDa anchored into the plasma membrane, called the C-terminal fragment (p75^{NTR}-CTF). The p75^{NTR}-CTF can be further cleaved by the γ-secretase complex generating the intracellular domain (p75^{NTR}-ICD) of 19 kDa **(Figure I6)** (Parkhurst et al., 2010). The proteolysis process is sequential, and the γ-secretase can not further process the receptor until the action of the TACE/ADAM17 has completed. The α-secretase cleavage is facilitated by neurotrophin-induced TrkA activation and phosphorylation of the intracellular region of ADAM17. In a positive feedback loop the p75^{NTR}-ICD enhances Trk signalling pathways (Ceni et al., 2010; Kommaddi et al., 2011).

It has been described that p75^{NTR} can only be shed when it is outside lipid rafts, because of the inability of TACE enzyme to access to them (Gil et al., 2007). P75^{NTR} RIP kinetics induced by ligand is very slow, p75^{NTR}-CTF is not detected until around 12 hours after (Kenchappa et al., 2006), differing, for example, from the 3-5 minutes necessary for Notch processing (Berezovska et al., 2000). The slow shedding kinetics could be correlated with the slow rate of p75^{NTR} endocytosis, as some studies showed how p75^{NTR} RIP happens mostly in the endosomes (Urra et al., 2007). It should also be noted, that p75^{NTR} RIP can change and/or modulate its interaction with other co-receptors, like with TrkA (Jung et al., 2003) and with itself (Sykes et al., 2012).

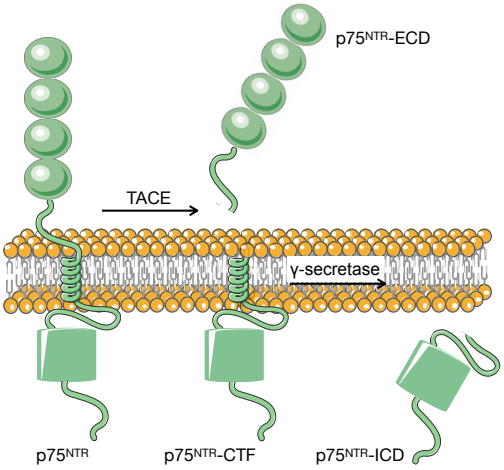

Figure I6: P75NTR Regulated Intramembrane Proteolysis (RIP). The p75NTR full-length (p75NTR-FL) is first cleaved by TACE enzyme, liberating to the extracellular medium the p75NTR extracellular domain (*p75NTR*-ECD) and leaving the p75NTR C-Terminal fragment (*p75NTR*-CTF) anchored into the membrane. After, the γ-secretase cleaves the p75NTR-CTF liberating into the cytosol the intracellular domain (*p75NTR*-ICD).

B. P75NTR endocytic pathways

P75NTR endocytic pathways are not fully understood yet, but lately, some researchers have studied the receptor endocytosis and have helped to understand better the process. In addition, it helped to explain the wide range p75NTR different biological functions from. Interestingly, p75NTR endocytic pathway can be different depending on the neuronal type (McCaffrey et al., 2009; Ascano et al., 2012; Yamashita & Kuruvilla, 2016), on the neuronal localisation, axonal tip or soma, and if it is ligand-activated or not (Bronfman et al., 2003; Saxena et al., 2005; Deinhardt et al., 2007). The existence of different types of endosomes, with different shape and size (and different contents), have been reported in several neuronal types (McCaffrey et al., 2009). These endosomes have big endocytic kinetic differences. For example, p75NTR-NGF internalisation proceeds at a rate $t_{1/2}$ 42–50 min, 3 times slower than TrkA-NGF internalisation (Bronfman et al., 2003). This suggests that each kind of endosome can trigger different signals and have different fates, making it possible for it to be recycled or retrogradely transported through the axon. The evidence of this divergence can be detected when p75NTR binds TrkA, TrkA internalisation is reduced, increasing the time of TrkA signalling into the membrane (Bronfman et al., 2003; Makkerh et al., 2005). In TrkA and p75NTR positive neurons, p75NTR-NGF endocytosis function might be to recycle the NGF into the surface (Saxena et al., 2005; Escudero et al., 2014). Another important aspect to consider is the membrane localisation of the receptors. In fact, the differences in endocytic velocity can be negatively correlated with the cholesterol content of their membranes (Bronfman et al., 2014).

In summary, p75NTR can follow different endocytic pathways; starting as clathrin-dependent (mostly) or -independent. After, the endosomes are directed to early endosomes (Rab5 positive), and from there endosomes are sorted to different routes; the early endosomes can be sent to multi-vesicular bodies/late endosomes (Lamp2 positive) and into the lysosomes (Rab7 positive) for degradation or they can be recycled (Rab4 and Rab11 positive) to the plasma

membrane or if they are “signalling” endosomes being retrograded transported into the somatodentritic compartment. Different responses can be promoted depending on the localisation of the signalling endosome **(Figure I7)** (Ascano et al., 2012; Matusica & Coulson, 2014; Yamashita & Kuruvilla, 2016). Moreover, it has been postulated, that p75^{NTR} RIP occurs in the endosomes, and truly it is possible to find endosomes with p75^{NTR}-FL and endosomes with p75^{NTR}-CTF (Grob et al., 1985; Taniuchi & Johnson, 1985). Nevertheless, all these studies have been made in PNS neurons, so in BFCNs, it might be completely different.

At last, but not least, there is an increasing number of evidences showing the importance of axonal transport in neurodegenerative diseases. Obviously, if NT retrograde transport is impaired and in consequence its survival signalling is altered, neuronal degeneration will occur (Bronfman et al., 2007).

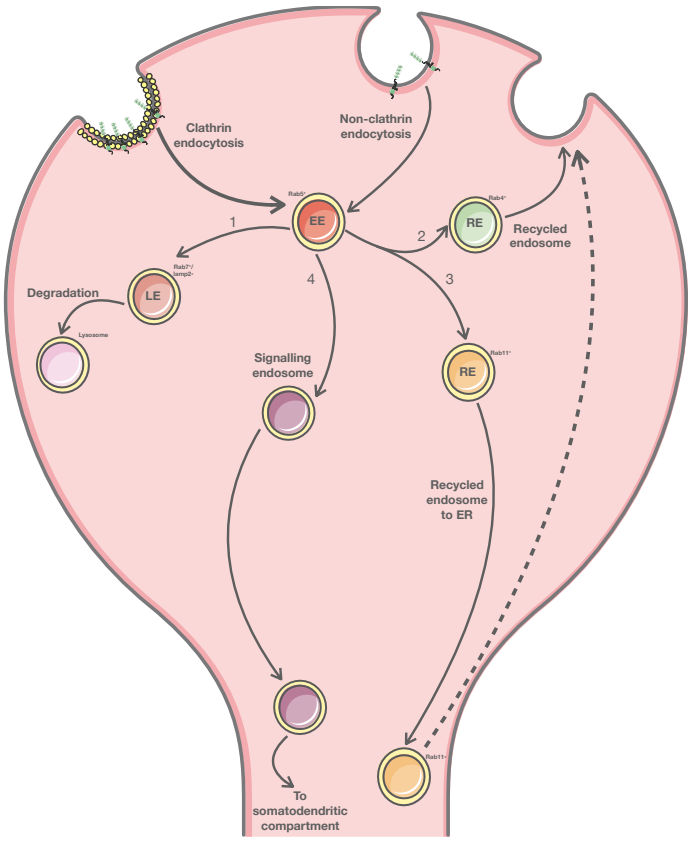

Figure I7: ***General p75^{NTR} endocytic pathway:*** *p75^{NTR} can be endocytated via clatrhin (mostly) or in a non-clathrin-dependent manner. Once in the early endosomes it can be directed into:*

1. *Late endosomes (LE) and to degradation, Rab7 and Lamp2 positive.*
2. *Recycling endosomes and back to the membrane, Rab4 positive.*
3. *Recycling endosomes (RE) and be directed into Endoplasmic Reticulum (ER), Rab11 positive.*
4. *Signalling endosomes and be transported to the somatodendritic compartment.*

P75^{NTR} FUNCTIONS

The neurotrophin receptor p75 is the most promiscuous NT receptor because of its ability to bind to the four NTs plus to pro-neurotrophins (Franco et al., 2020). P75^{NTR} has no intrinsic catalytic activity, it generates the response through the binding of other proteins; co-receptors

or intracellular adapting proteins. Trying to sum all the information from above (localisation, proteolytic process, endocytosis, co-receptors, ligands…) a wide range of different options are possible and in consequence, and not surprisingly, a wide range of functions are associated with $p75^{NTR}$, being $p75^{NTR}$ signalling largely context-dependent.

A. $P75^{NTR}$ and neuronal death

The first known function of $p75^{NTR}$ was neuronal survival, because of its discovery as the NGF receptor (before called, NGF Receptor, NGFR), conversely the most studied function of the receptor has been the pro-apoptotic one. At physiological levels, $p75^{NTR}$ is in charge of the natural development programmed cell death in the PNS. The best well characterised is the pro-apoptotic role of $p75^{NTR}$ together with TrkA, NGF and BDNF in sympathetic neurons (Rabizadeh et al., 1993; Bamji et al., 1998). The system works this way; in the target area of the sympathetic neurons there are limited amounts of NGF and only those reaching the appropriate target on time, will properly activate TrkA and will trigger pro-survival signals. Nevertheless, if the neuron arrives later than supposed or in a non-appropriate place, there will not be enough NGF and, consequently, TrkA will not be activated. Then, $p75^{NTR}$ will be activated by BDNF to trigger apoptosis (Bamji et al., 1998; Majdan et al., 2001). This effect has been seen in other cell populations; hippocampal neurons, oligodendrocytes, trigeminal ganglia, retina neurons, superior cervical ganglion, spinal cord, cerebellar granule neurons (Kraemer et al., 2014) and in the BFCNs (Boskovic et al., 2014).

The many pieces of the puzzle are falling into place when understanding the cellular mechanisms by which $p75^{NTR}$ promotes apoptosis. It is well established that the programmed cell death pathway activated by $p75^{NTR}$ is the JNK cascade, which promotes apoptosis through the mitochondria cascade (Aloyz et al., 1998; Kraemer et al., 2014). Nevertheless, to activate the JNK cascade, different $p75^{NTR}$ adaptor proteins are required. Some known proteins are; TRAFs (TNF receptor-associated factors), specifically, TRAF6 is necessary to trigger neuronal cell death via $p75^{NTR}$. However, TRAF6 does not act alone since it associates with NRIF (neurotrophin receptor-interacting factor) to enhance JNK activation. These two proteins can directly interact or they can bind $p75^{NTR}$ directly **(Figure I8)** (Gentry et al., 2004). RIP2 is another adaptor protein that competes with TRAF6 for the binding to $p75^{NTR}$. In normal conditions there is an equilibrium to achieve the appropriate neuronal number. However, in $RIP2^{-/-}$ mice more TRAF6 is bound to $p75^{NTR}$ and JNK cascade is more active, leading to more apoptosis (Kisiswa et al., 2018).

Another necessary adaptor protein that interacts with $p75^{NTR}$ and helps with the JNK cascade activation is NRAGE (neurotrophin receptor-interacting MAGE homolog) **(Figure I8)**. In fact, NRAGE prevents the association of $p75^{NTR}$ with TrkA, decreasing pro-survival signalling. $TRAF6^{-/-}$, $NRIF^{-/-}$ and $NRAGE^{-/-}$ mice fail to activate JNK cascade and in these transgenic mice

there is an increase in the sympathetic neurons, comparable to the increase seen in $p75^{NTR-/-}$ mice (Yeiser et al., 2004; Linggi et al., 2005; Bertrand et al., 2008).

P38 mitogen-activated protein kinases (MAPK) is activated by a wide range of cellular stresses and when it is phosphorylated and activated, it triggers, among other responses, apoptosis **(Figure I8)** (Zarubin & Han, 2005). Different evidences showed how $p75^{NTR}$ can trigger apoptosis through p38. In human neuroblastoma cell line and dorsal root ganglia it has been reported a p38 activation in a $p75^{NTR}$ manner to induce apoptosis (Costantini et al., 2005; Jiang et al., 2005). In PC12 cells, oligomers of $p75^{NTR}$-CTF induce the activation of caspase-3 cleavage and cell death in a mechanism dependent of TRAF6, JNK and p38 (Franco et al., 2021).

As mentioned above, RIP process of $p75^{NTR}$ and its subsequent products can mediate different intracellular responses and both, $p75^{NTR}$-CTF and $p75^{NTR}$-ICD, have been reported to mediate neuronal death in both TrkA- and TrkB- expressing cells. For example, the release of $p75^{NTR}$-ICD (activated by BDNF) facilitates nuclear translocation of NRIF, in a polyubiquitin TRAF6-dependent mechanism, a necessary event to promote neuronal death activation **(Figure I8)** (Kenchappa et al., 2006). The CTF fragment of $p75^{NTR}$, which has been shown to induce cell death, is a 29 aa region in the cytoplasmic juxtamembrane area known as the 'Chopper domain' the necessary region to induce it (Coulson et al., 2000). The chopper domain activates APAF-1 (apoptotic protease activating factor 1) that activates the apoptosome **(Figure I8)** (Coulson et al., 2004; Coulson et al., 2008).

Another way of $p75^{NTR}$ to promote cell death is through pro-neurotrophins (Lee et al., 2001). To do it, the pro domain of pro-neurotrophins binds Sortilin and the mature domain binds $p75^{NTR}$, facilitating the association of the two receptors and the activation of cell death (Nykjaer et al., 2004; Teng et al., 2005). This pro-apoptotic role of $p75^{NTR}$ is known to take place during neurodevelopment, whereas the expression of $p75^{NTR}$ is afterwards down-regulated in almost all the brain regions. Nevertheless, after cellular damage $p75^{NTR}$ expression is up-regulated and stimulates the death of injured cells.

B. $P75^{NTR}$ and survival

The receptor can promote cell survival on its own but also through the cooperation with Trks, leading to a high affinity receptor complex enhancing Trk signalling.

$p75^{NTR}$ and NF-κB

When the NTs binds $p75^{NTR}$ they activate NF-κB (Pathak & Carter, 2017). It is known that NF-κB promotes neuronal survival. Inactive NF-κB remains in the cytosol as a dimer and bound to its

inhibitor IκB. When IκB is phosphorylated is guided to proteasomal degradation, releasing NF-κB and allowing it to translocate into the nucleus (Baldwin, 2012). The IκB inhibitor is phosphorylated by a cascade that starts with the binding of TRAF6 and RIP2 to $p75^{NTR}$ **(Figure I8)** (Reichardt, 2006). This pro-survival role of $p75^{NTR}$ has been demonstrated in different *in vivo* situations; trigeminal neurons, Schwann cells, cerebellar granule neurons and hippocampal neurons (Middleton et al., 2000; Kraemer et al., 2014; Kisiswa et al., 2018).

$p75^{NTR}$ and TrkA complex

Since 1991 there is evidence indicating that $p75^{NTR}$ and TrkA form a high affinity complex with NGF. With the presence of $p75^{NTR}$, TrkA binds NGF with more affinity (Hempstead et al., 1991). Moreover, when $p75^{NTR}$ is present, TrkA selectively binds NGF and not NT-3 **(Figure I8)** (Benedetti et al., 1993). However, after all these years how the complex is formed is not completely understood. It is known that the transmembrane and intracellular domains of $p75^{NTR}$, but not the neurotrophin-binding portion of the extracellular domain, are required for the high-affinity complex formation (Esposito et al., 2001). Recently, our laboratory has described that $p75^{NTR}$ and TrkA form a complex through their transmembrane domain and the binding of $p75^{NTR}$ to TrkA induces a conformational change on TrkA that may be implicated in improving NGF affinity (Franco et al., 2021). Additionally, the amount of each receptor is important, usually $p75^{NTR}$ is present in higher amounts than TrkA, being TrkA the limiting receptor. Changes in the levels of both receptors can lead to changes in the NGF affinity. For example, during ageing there is a change in the pattern of $p75^{NTR}$ and TrkA expressions, increasing $p75^{NTR}$ and decreasing TrkA. These variations can modify the outcome of the complex (Chao & Hempstead, 1995).

C. $P75^{NTR}$ and axonal growing/retraction (RhoA GTPase)

RhoA is a member of the Rho GTPase family which function in the regulation of axonal growth/retraction. The protein cycles between active/inactive form binding GTP or GDP, respectively. The regulation of RhoA is possible at different levels. RhoGDI binding maintains RhoA in the cytosol away from the plasma membrane where it is activated upon GTP binding. For RhoA activation, RhoGDI needs to detach from RhoA, allowing RhoA to bind to GTP. It has been described that $p75^{NTR}$ activates RhoA in a constitutive manner by the constitutive binding to RhoGDI. In the case of axonal growth inhibition, RhoA is activated upon Nogo receptor, NgR, activation. In this process, three different membrane proteins are mandatory; LINGO-1, NgR and $p75^{NTR}$, being LINGO-1 the bridge protein binding the other two (Mi et al., 2004). When MAG and Nogo are bound to the complex, there is a recruitment of RhoGDI, allowing RhoA to be active. On the other hand, when $p75^{NTR}$ binds to NGF, RhoGDI detaches from $p75^{NTR}$ and inactivates RhoA, permitting axonal growth **(Figure I8)** (Yamashita et al., 1999; Yamaguchi et

al., 2001; Wong et al., 2002; Yamashita et al., 2002). This function of $p75^{NTR}$ is important during development but also in axonal regeneration after injury.

The processing of $p75^{NTR}$ is also implicated in the activation of RhoA. For instance, in cerebellar neurons the inhibition of the γ-secretase with specific inhibitors induces axonal growth and this is due to an inactivation of RhoA (Domeniconi et al., 2005).

D. $P75^{NTR}$ and oxidative stress

An imbalance in the redox state has been recognised as a contributing factor in ageing and in the progression of multiple neurodegenerative diseases including AD (Tonnies & Trushina, 2017). The increase in oxidative stress and therefore of reactive oxygen species (ROS) disrupts the balanced events of a cell by reacting with proteins, nucleic acids and lipids. Consequently, enzymatic activities, signalling pathways and DNA damage repair are disrupted (Chen & Zhong, 2014). When ROS react with lipids, generating lipid peroxidation, a direct product formation is the 4-hydroxynonenal (HNE), a very reactive compound that form adducts with cellular proteins and a key mediator of neuronal apoptosis induced by oxidative stress (Timucin & Basaga, 2017).

When there is an increase in the oxidative stress state, the antioxidant response is activated. The transcription factor NRF2 is activated in high oxidative stress. When NRF2 is activated it translocates into the nucleus and counteracts the increase in ROS levels binding the antioxidant response element (ARE) and initiates the transcription of genes involved in the antioxidant response. Some of these genes are; HMOX1, GSTa, SOD1 and SOD2 (Sivandzade et al., 2019).

The NTs and their receptors have been linked to oxidative stress and might act as regulators of redox balance (Espinet et al., 2015; Cabezas et al., 2019). Specifically, some works showed the pro-apoptotic relation of $p75^{NTR}$ with oxidative stress. It has been described that the expression of $p75^{NTR}$ is up-regulated in oxidative stress conditions (increment of ROS) (Olivieri et al., 2002). Moreover, HNE promotes the $p75^{NTR}$ cleavage, leading to axonal degeneration and apoptosis in mesencephalic neurons (Kraemer et al., 2021). HNE induces sympathetic neuron apoptosis and neurite degeneration, however, neurons from $p75^{NTR-/-}$ mice are resistant to cell death (Kraemer et al., 2014). In addition, primary cell cultures of motor neurons (expressing $p75^{NTR}$) are vulnerable to nitric oxide in a $p75^{NTR}$-dependent manner (Pehar et al., 2004; Pehar et al., 2007). In contrast to the examples before, in PC12 cells, $p75^{NTR}$ (specifically the $p75^{NTR}$-ICD) shows to have a protective role in high ROS conditions (Tyurina et al., 2005).

Thus, even though the role that $p75^{NTR}$ plays in an imbalanced oxidative state is not clear, a great deal of results showed a clear connection between $p75^{NTR}$ and oxidative stress,

nevertheless more research will be necessary to understand the mechanism (Sankorrakul et al., 2021).

E. P75^{NTR} and cholesterol

Cholesterol is a very important membrane sterol. It correctly maintains membrane fluidity, thickness, compressibility, permeability and intrinsic curvature of lipid bilayers. Furthermore, cholesterol participates in lipid-rafts formation (Luo et al., 2020). Therefore, a good cholesterol homeostasis is important for the good functioning of the cell, since when it is altered it leads to different diseases (Benito-Vicente et al., 2018).

To maintain the correct levels of cholesterol, its synthesis, uptake, efflux and accumulation are finally regulated. Cholesterol metabolism in the brain works separately form the rest of the body as it cannot cross the brain blood barrier (BBB). All the cholesterol in the brain is synthesised *de novo (Zhang & Liu, 2015)*. The cholesterol synthesis is a multistep pathway very energetically expensive, it starts from the acetyl-CoA and requires around 30 enzymatic reactions. The rate-limiting enzyme of the cholesterol biosynthesis route is an endoplasmic reticulum protein the 3ß-hydroxy-3ß-methylglutaryl-CoA reducatase (HMGCR) that reduces the 3ß-hydroxy-3ß-methylglytaryl-CoA to mevalonate (Cerqueira et al., 2016). Therefore, this enzyme has a finely regulation at transcriptional, translational and post-translational levels (Sharpe & Brown, 2013). Transcriptional regulation of HMGCR is executed by sterol regulatory element-binding proteins (SREBPs) transcription factors, specifically SREBP-2. When sterol levels are low, SREBP-2 is activated by intramembrane cleavage and the C-terminus enters the nucleus and recognises sterol regulatory elements (SREs) in the DNA and activates the transcription of HMGCR, low density lipoprotein receptor (LDLR) and other cholesterol biosynthesis enzymes (Eberle et al., 2004).

In the brain, the cholesterol is synthesised during embryonic development, reaching its plateau at postnatal week one (Martin et al., 2014). In the adult brain, the most accepted idea is that astrocytes synthesise the cholesterol that then is secreted in ApoE rich lipoproteins and captured by neurons thanks to ApoE binding to the members of the LDL receptor family (Pfrieger, 2003).

Different works have shown that the NTs and their receptors play a role in the cholesterol homeostasis (Colardo et al., 2021). Comparing p75^{NTR} positive and negative PC12 cells, they found an association between the expression of p75^{NTR} and the levels of HMGCR, being the expression of HMGCR higher in p75^{NTR} positive PC12 cells (Yan et al., 2005). This association has also been observed in hippocampal and cholinergic neurons (both expressing p75^{NTR}) where it has been described the correlation between p75^{NTR} and the co-expression of cholesterol synthesis enzymes. Moreover, when p75^{NTR} expression is reduced, the expression

of the cholesterol enzymes are also reduced (Korade et al., 2007). Furthermore, two years later it was reported how p75^{NTR} changes the enzyme levels through NRIF (Korade et al., 2009). In the hepatocyte cells it has also been shown that p75^{NTR} induces SREBP-2 activity, and therefore increases HMGCR expression (Pham et al., 2019). Hereby, the different studies show how p75^{NTR} is likely playing a role in the regulation of cholesterol metabolism.

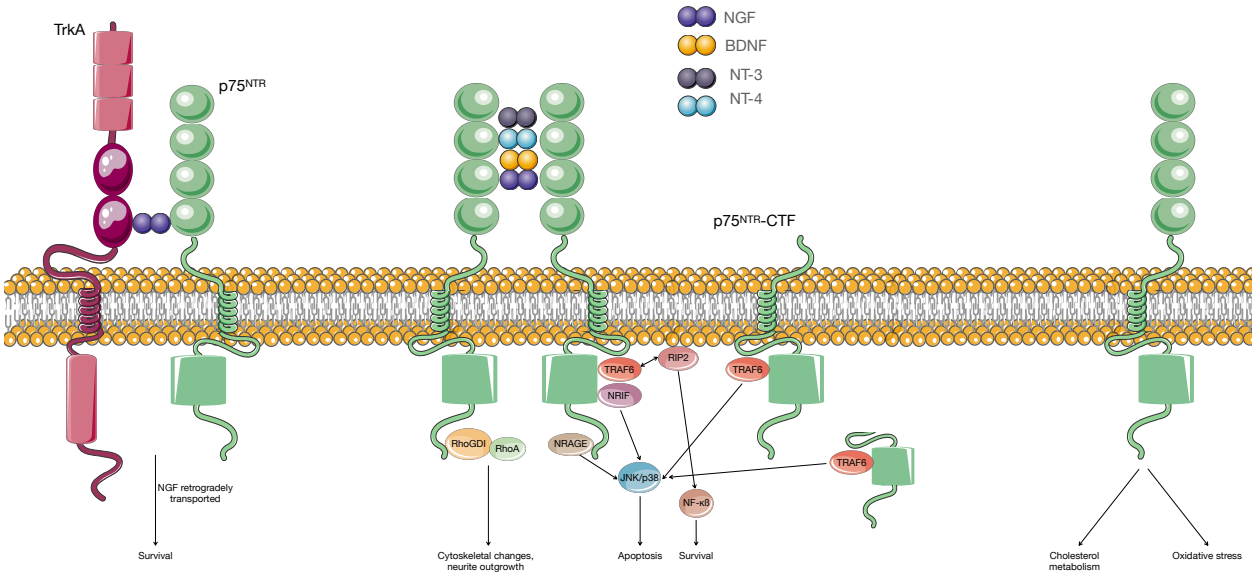

Figure I8: **p75^{NTR} signalling pathways.** *When the NTs bind p75^{NTR} it can trigger a variety of signals. It can potentiate TrkA signalling when interacts with it. It can bind RhoGDI and inhibit RhoA and therefore cause cytoskeletal changes. It can bind TRAF6, NRIF and NRAGE and activate the apoptotic cascade through JNK and/or p38. P75^{NTR}-CTF and p75^{NTR}-ICD can bind TRAF6 and trigger apoptosis. p75^{NTR} can also promote survival through NF-κß. Moreover, it can trigger different metabolic and redox responses.*

4. Basal Forebrain Cholinergic Neurons And Neurotrophins

As aforementioned, the BFCNs are one of the few neuronal populations expressing high levels of $p75^{NTR}$ in the CNS during their whole life. The role of NTs during development has been explained in the BFCNs section. This section will be focused on the role of $p75^{NTR}$ and Trks in the adult, aged and diseased BFCNs. Nevertheless, due to the existing mice models it is complicated to separate the effect of the NTs and their receptors during development and adulthood.

Apart from $p75^{NTR}$ the BFCNs express the different Trks receptors, nevertheless, the expression levels of each of them are different. For example, $p75^{NTR}$ is expressed in 99 % of the mouse BFCNs, TrkA in around 70 % and TrkB in around 80 % (Milne et al., 2015). In another study, with human brains, 54 % of the BFCNs expressed TrkA, 75 % TrkB, and 58 % TrkC and sometimes they co-localised. Furthermore, there are five more times of $p75^{NTR}$ than TrkA receptor in the BFCNs (mouse brain resource: http://mousebrain.org/genesearch.html).

The role that this high amount of $p75^{NTR}$ plays in the BFCNs is not fully understood. It is well stablished that TrkA-$p75^{NTR}$-NGF complex is needed in the first place during development to regulate dendritic and axonal growth and synapse assembly (Ascano et al., 2012). The complex is retrogradely transported from the tips of the dendrites to the somatodendritic compartment and to the nucleus. There, TrkA activates different transcription factors such as; CREB/NFAT/Egr3/SRF that will activate the expression of cytoskeletal components (α-tubulin, β-actin and γ-actin) apart from $p75^{NTR}$ and TrkA itself. The complex can be locally activated in the axons activating short-term axonal growth (Ascano et al., 2012). The NGF–TrkA endosomal complexes in dendrites signal via the MEK/MAPK pathway to modulate the clustering of acetylcholine receptors (nAChRs) and other postsynaptic components (Ascano et al., 2012).

Once the cholinergic neurons are formed, NGF is still indispensable to maintain the levels of ChAT expression and the synthesis of ACh. After NGF withdrawal, neurons undergo atrophic changes like cell shrinkage and reduced transmitter-related gene expression that ends up with cell death (Kramer et al., 1999). However, there is no evidence for a decrease in the levels of NGF, neither NGF mRNA nor protein in the cerebral cortex of aged animals (Alberch et al., 1991; Crutcher & Weingartner, 1991) or patients with Alzheimer's disease, where NGF protein levels may even be increased (Goedert et al., 1986; Crutcher et al., 1993; Scott et al., 1995). However, NGF levels are reduced in the BF of aged mice and AD patients (Alberch et al., 1991; Scott et al., 1995). This evidence suggests an impairment in the retrograde transport, intrinsically linked to neuronal aged changes, generating a reduction in the retrograde transport of NGF and breaking the positive loop, that leads into a downregulation of TrkA expression and cellular atrophy (Cooper et al., 1994; De Lacalle et al., 1996). As a matter of fact, the

percentage of positive Trk neurons is reduced in AD patients (Salehi et al., 1996), TrkA being the most decreased receptor (69 %) (Salehi et al., 1996). Moreover, proNGF is also present in the cortex and can bind $p75^{NTR}$ and TrkA. When both receptors are present, proNGF promotes neurotrophic functions and activates neurite outgrowth and neuronal survival activity (Fahnestock et al., 2004; Masoudi et al., 2009). However, in aged and/or diseased brains where TrkA is reduced and $p75^{NTR}$ is still present, proNGF activates $p75^{NTR}$-dependent apoptotic pathways. In addition, proNGF levels are increased in the cortex of MCI and AD patients (Fahnestock et al., 2001; Peng et al., 2004). In this context, the reduction of the retrograde transport, the loss of TrkA and the accumulation of proNGF creates a reduction in the neurotrophic support and an increase in the proNGF-$p75^{NTR}$ apoptosis signalling that leads to cholinergic neurodegeneration (Fahnestock & Shekari, 2019).

5. Senescence Accelerated Mouse Prone 8

Takeda et al., during the 1980s generated a new murine model of accelerated senescence in order to shorten the time to study ageing problems. They realised while maintaining the AKR/J mice strain, that some of the animals got symptoms of early ageing. Concretely they quoted: *"While continuing the sister-brother mating to maintain this inbred strain -AKR/J line-, we became aware of the presence of certain litters in which most of the mice showed a moderate to severe degree of loss of activity, alopecia and lack of glossiness, skin coarseness, periophthalmic lesions, increased lordokyphosis of the spine and a shortened life span" (Takeda et al., 1981).* Five of these mice with severe "*exhaustion*" were selected to be the progenitors of the senescence-prone line (P) and three other "*normal ageing*" mice, the controls, were selected to be the progenitors of the senescence-resistant line (R). The first breeding was carried out in 1975, and after at least 12 generations, 4 different senescence-prone (P1, P2, P3 and P4) and 3 senescence-resistant (R1, R2 and R3) lines were generated. Nevertheless, after more breedings, two more inbred SAMP strains were bred (P6 and P8) (Takeda et al., 1991). The whole study resulted in the generation of a new model of spontaneous accelerated senescence mice.

SAMP lines recapitulate most of the human ageing problems making them a good murine model to study them. It is important to stand out that these animals have no problems during development, but they age in an accelerated manner after normal development. Therefore, the pattern of ageing in this model has an early onset, irreversible and accelerated senescence rather than a premature ageing or senescence. All different SAMP and SAMR lines share the common accelerated or resistant senescence and also the shortened life span (in the case of SAMP). However, each of them has specific phenotypes and can be classified as a new and different strain because all of them are genetically distinguishable and they clearly have a genetic deviation from the AKR/J strain (Takeda, 1999).

SAMP8 mice have age-related deficits in learning and memory making them good candidates to study cognitive impairments related to age (Miyamoto et al., 1986; Yagi et al., 1988).

5.1. Characteristics Of SAMP8 Mice

Behavioural tests revealed the learning and memory impairments of SAMP8 mice. Later, big efforts have been made to identify the histological hallmarks of these deteriorations. The first distinguished evidence of SAMP8 mice behaviour is the higher spontaneous motor activity compared to SAMR1 mice, though this elevated activity is only seen during the light period. Moreover, the spontaneous motor activity increases with age. Hereby, SAMP8 has hyperactivity during the light period when it is supposed to be resting time for rodents. This hyperactivity was also seen in open-field measurements, entering more times to different squares when compared to SAMR1 (Yagi et al., 1988).

Different works proved a worsening in SAMP8 mice in associative and non-spatial learning tasks compared to age-matched SAMR1 mice. Spatial learning and memory tasks were also proved to be worst in SAMP8 mice. The associative and non-spatial memory was assessed with passive avoidance test and foot shock avoidance task showing a worst long-term memory of SAMP8 mice starting at 2 months (Miyamoto et al., 1986; Yagi et al., 1988; Flood & Morley, 1993). Regarding spatial memory, SAMP8 mice performed worst than SAMR1 mice (at 2 and 8 months) in Morris water task (Miyamoto et al., 1986). In radial arm maze, SAMP8 mice showed spatial memory impairments starting at 4 months (Pallas et al., 2008). Overall, SAMP8 mice showed a deficit in the memory acquisition and in the retention earlier than SAMR1 mice. These characteristics are similar to the ones that aged people present (Akiguchi et al., 2017).

At a molecular level, there is evidence that relates SAMP8 mice with lesions associated with ageing. According to the free radical theory of ageing, the slow generation of high ROS, such as oxygen free radicals, cause oxidative damage to critical cellular components such as lipids, proteins and DNA. These modified cellular components are proposed to be an underlying factor of the ageing process. The generation of ROS is an unavoidable consequence of life in an aerobic environment (Harman, 1994). Moreover, the brain is particularly sensitive to oxidative stress because of its high oxygen utilisation. Different studies showed an increase in the oxidative stress in SAMP8 mice (Sato et al., 1996; Butterfield et al., 1997; Alvarez-Garcia et al., 2006; Stadtman, 2006). Moreover, these results can be linked genetically (Kumar et al., 2000). When hippocampal gene expression of SAMP8 and SAMR1 mice at 4 and 12 months were compared an increase of NADPH;quinone oxidoreductase was found at 12 months in SAMP8 mice. Furthermore, the administration of two antioxidants reversed the memory impairments of SAMP8 mice (Kurokawa et al., 2001; Farr et al., 2003).

Thanks to the sequencing technology, some answers to the accelerated ageing of SAM8 mice could be explained with genetic evidences. Most of the mutations found when the exome of SAMP mice was sequenced are related to DNA repair (base-excision repair, cellular response to DNA damage stimulus, response to DNA damage stimulus) and to stress. Some of the genes that presented mutations are: *Ogg1*, *Tsen2*, *Mbd4*, *Alox5* and *Moxd1 (Tanisawa et al., 2013)*.

Moreover, SAMP8 specifically, has 5 deleterious mutations not found in the other SAMP lines. The most notorious one is found in *the Aifm3* gene (Apoptosis Inducing Factor Mitochondria Associated 3). Even though the specific function of the codifying protein is not clear, the mutation can be contributing to mitochondria bad functioning and the excess of oxidative stress (Xia et al., 1999; Tanisawa et al., 2013). The other genes with specific mutations in SAMP8 mice are: *Ly75, Lnx1, Matn2, Myh11*. *Matn2* and *Lnx1* could explain some of SAMP8 brain problems. Matn2 is an extracellular matrix protein regulated in association with inflammatory axonal injury. The protein has been identified as an important neuronal danger-associated molecule in the CNS that is released in association with tissue damage to elicit a robust pro-inflammatory response by cells of the innate immune system (Jonas et al., 2014). This mutation could explain part of the high neuroinflammation found in SAMP8 mice. *Lnx1* is an E3 ubiquitin-protein ligase that mediates ubiquitination and subsequent proteasomal degradation of different proteins, the most notorious one, NUMB. NUMB binds Notch, modulating its signalling during processes such as cortical neurogenesis. LNX1 protein certainly can act as activator of NOTCH signalling through the ubiquitination of NUMB, controlling better the fate of the neurons. Nevertheless, if *Lnx1* is mutated like in SAMP8 mice, this route is not well regulated and this can be translated into memory and learning problems (Butterfield & Poon, 2005; Young, 2018).

After all this evidence, it is clear that oxidative stress is altered in SAMP8 mice, and that this deregulation plays a role in the ageing status of accelerated ageing in SAMP8. Moreover, antioxidants rescue the changes caused by the impairments (Farr et al., 2003).

The brain is the most susceptible organ to homeostatic changes such as oxygen and ion concentration. Therefore, it is very important to keep it free from toxins and pathogens. To achieve this protection the brain has a unique barrier; the BBB. These tight junctions only allow the crossing of small and lipid soluble components (due to lipid composition of membranes). Other important components that are needed inside the brain have specific transporters, such as glucose (Purves et al., 2019). The loss of BBB properties is a hallmark in neurodegenerative disorders. The breakdown of the BBB can lead to a depletion of the brain homeostasis and consequently a bad functionality of the neurons and the brain itself (Daneman & Prat, 2015). A

BBB dysfunction in aged SAMP8 mice has been reported in different studies (Ueno et al., 1993; Ueno et al., 1997; Pelegri et al., 2007).

Astrocytes are in charge of helping neurons have an excellent surrounding environment allowing them to work perfectly. Astrocytes are usually in a “resting” state, meaning that they perform their usual tasks: give glucose to neurons, uptake neurotransmitters, reduce oxidative stress… Nevertheless, in response to inflammation or injury, astrocytes became reactive, in a process called astrogliosis, when this process occurs, the neuroprotective functions of astrocytes are reduced to increase pro-inflammatory activities. It has been widely reported that during ageing and AD there is an increase of neuroinflammation (Unger, 1998; Lynch et al., 2010; Rodriguez & Verkhratsky, 2011; Verkhratsky et al., 2014). Astrocytes and microglia are the cells in charge of producing pro-inflammatory molecules, such as cytokines. As the alteration of the astrocytes has been reported in ageing, different works studied if SAMP8 have this alteration. The increase of GFAP levels, a protein up-regulated in astrocytic activation, were reported to be higher in SAMP8 animals compared to SAMR1 mice at 4 and 12 months, mostly in HC, entorhinal cortex and brain stem (Wu et al., 2005; Sureda et al., 2006; Grinan-Ferre et al., 2016). *In vitro* experiments also showed a neuroprotective failure of SAMP8 astrocytes (Garcia-Matas et al., 2008). In accordance to astrocytic activation, aged and AD brains also showed microglial activation (Yin et al., 2016; Koellhoffer et al., 2017; Yuan et al., 2020). When microglial cells are activated they produce abundant amounts of toxic substances, including free radicals and glutamate. Additionally, they lose the ability to maintain the debris clearance and immune surveillance. Hence, activation of microglia may be involved in the neuropathology of aged SAMP8 mice and may be associated with their age-related deficits in learning and memory. An increase in CD45 immunoreactivity was reported in aged SAMP8 mice, while this increase does not happen in SAMR1 aged mice (Kawamata et al., 1998; Fernandez et al., 2021).

In SAMP8 mice, lower density and number of spines have been reported in advanced ages but not in SAMR1 mice (Hess et al., 1993; Kawaguchi et al., 1995). Dendritic spines are small protrusions that emerge from the dendrites of the neurons and make synaptic connections. It is believed that the spines are related to plasticity, human disease, ageing and alterations regarding spine morphology or density (Nimchinsky et al., 2002).

As mentioned earlier the BFCNs are related to learning and memory processes and they are decreased/damaged during ageing and AD. Thus, it is not strange to think that SAMP8 mice can have altered cholinergic neurons and therefore some researchers studied if aged SAMP8 mice also recapitulates this deficit. ACh levels have been examined in two different studies, they both see a decrease in ACh levels due to age. Nevertheless, if they compare it with the control strain, SAMR1, there are no differences between them, meaning that ACh decreases

with age, but is not accelerated in the SAMP8 (Ikegami et al., 1992; Kabuto et al., 1995). Regarding ChAT expression a decrease in ChAT immunohistochemical intensity in SAMP8 aged mice (10 months) compared to young was observed, even though they do not report a decrease in number of ChAT positive neurons, just a decrease of ChAT expression (Tooyama et al., 1997; Sasaki et al., 1999). This result can be confirmed with the measure of ChAT activity, being reduced around 50 % in aged SAMP8 mice (from 4 to 8 months). That decrease is not seen in SAMR1 mice of the same age (Strong et al., 2003). In the latest work, a decrease of ChAT positive neurons in the forebrain of aged SAMP8 mice was reported (from 4 to 8 and 12 months old). A decrease in mRNA and protein levels were seen, attributed to the loss of neurons (Wang et al., 2009).

Even though there is a close relationship between the BFCNs and the NTs and their receptors ($p75^{NTR}$ and TrkA) there is no research analysing how NTs expression may or may not change in aged SAMP8 mice. There is only one work that connects the BF, NTs and SAMP8. It analyses NT expression at different ages and they found a decrease in NGF expression in postnatal SAMP8 mice (1 week old), but a higher expression at 1 month and 10 months compared to age-matched SAMR1 mice (Kaisho et al., 1994).

Taken all together, the study of SAMP8 mice and the BFCNs needs further study to clarify if there is a deficit in the neurotrophic support.

To sum up, evidence showed that SAMP8 is a sporadic mouse model that recapitulates a great number of ageing and AD hallmarks. Moreover, if SAMP8 is compared with transgenic mice models of AD that over produce human APP, tau or ApoE, SAMP8 presents some benefits. For example, the transgenic mouse models over-express genes with mutations seen in familiar AD (FAD), and FAD represents only 5 % of AD patients. On the other hand, SAMP8 mice are no knock-in and do not over-produce any human protein, it is just the natural process of ageing, but accelerated. In addition, with transgenic mice it is not possible to study the cause of the disease, just the consequences. In conclusion, we consider SAMP8 mice a good model to study ageing processes.

6. The γ-Secretase Complex

The γ-secretase complex is an aspartyl protease that belongs to the iCLiPs (intramembrane cleaving proteases) family. This multi-complex protein has more than 80 different substrates, all of them type I transmembrane proteins **(Table I1)** (McCarthy et al., 2009; Haapasalo & Kovacs, 2011). The best well-known and studied γ-secretase substrate is the amyloid precursor protein (APP) due to its importance in AD (Wang et al., 2017). Another relevant substrate of the γ-secretase complex is Notch due to its importance in embryonic stages (Siebel & Lendahl, 2017).

The "minimal" core of the γ-secretase complex is formed by four different proteins; presenilin (PS), nicastrin (Nct), anterior pharynx defective 1 (Aph-1) and presenilin-enancer 2 (PEN-2). These proteins are necessary and sufficient for the γ-secretase to carry out its activity and are found in the complex with an stoichiometry of 1:1:1:1 (De Strooper, 2003). The homologous PSs, PS1 and PS2, are the catalytic subunit of the γ-secretase, catalysing the transmembrane cleavage of the substrate (Thinakaran et al., 1997; Wolfe et al., 1999). They exist with a 66 % sequence homology in humans, being the TMDs the most conserved parts (Escamilla-Ayala et al., 2020). Both proteins are ubiquitously expressed, however, a few differences can be found in different developmental stages or between tissues. For example, even though both PS1 and PS2 mRNAs are expressed at similar levels in most of the tissues, there is a major expression of PS1 during development, fact that could explain the differences between the PS1 knock-out mice, being developmental lethal (due to Notch signalling). Nevertheless, PS2 knock-out mice are viable and fertile. Moreover, it has been reported that the expression of PS1 and PS2 is higher in neurons than in microglia (Lee et al., 1996; Kumar & Thakur, 2012). Another difference between both proteins is their cellular localisation. It was not until 2016 that thanks to confocal and CRISPR/Cas9 techniques Sannerud and colleagues decoded the sub-cellular localisation of the different complexes. They found out that the γ-secretase complexes containing PS2 are mostly located in the late endosomes/lysosomes, and in consequence are able to process their substrates there, whereas the γ-secretase complexes containing PS1 are more ubiquitously expressed, including the plasma membrane (Sannerud et al., 2016).

Presenilins were the first identified proteins of the complex. They were first described in a genetic screening of mutations that cause FAD, in that moment more than 250 mutations were identified in *PSEN* genes. Mutations in both *PSEN1* and *PSEN2* have been found and cause FAD. Nevertheless, *PSEN2* mutations tend to have a later age of onset and produce a more slowly progressive disease (Bertram & Tanzi, 2004). FAD-linked *PSEN* mutations lead to a reduction in the γ-secretase activity and cause an increase in the production of amyloidogenic $Aβ_{1-42}$, at the expense of the less non-amyloidogenic $Aβ_{1-40}$ generation, increasing the $Aβ_{1-42}$/$Aβ_{1-40}$ ratio. This toxic function of the γ-secretase has been the foundation of the amyloid

hypothesis for years and the biochemical foundation of the use of γ-secretase inhibitors and/or modulators as a therapeutical approach for AD patients (Alzheimer's Disease Collaborative, 1995; Levy-Lahad et al., 1995; Rogaev et al., 1995; Sherrington et al., 1995). For example, a very promising drug that arrived to clinical phase 3 was Semagacestat (LY-450139, SG), a γ-secretase inhibitor, that showed a dose-dependent decrease in the generation of Aβ in the cerebrospinal fluid of healthy humans. However, when mild-to-moderate AD patients were administrated with SG, detrimental effects were reported in cognition and functionality (Doody et al., 2013).

Due to the importance of the γ-secretase complex in AD, different transgenic mouse models were generated to study the effects of its inhibition. Individual PS2 or conditional PS1 knock-out mice did not show any important features, probably, as the expression of the other PS in the adult brain might be sufficient to ameliorate the effect one PS absence (Herreman et al., 1999; Feng et al., 2001). Therefore, double (PS1 and PS2) null mice were generated. These mice do not form plaques but they exhibit age-related neuronal and synaptic loss among other pathological features (Placanica et al., 2009; Elder et al., 2010). In fact, PSs are necessary for neuronal survival in the adult brain, as mice with no PS showed a reduction in the number of neocortical neurons (Saura et al., 2004), ventricle enlargement caused by a loss of the tissue surrounding the area and an increase in astrogliosis (Feng et al., 2004). The degenerative process starts to be apparent at 6 months of age, and as ageing proceeds, neurodegeneration is more pronounced.

Hereby, even though knock-out mice for PS do not produce plaques, they exhibit a range of pathological as well as physiological changes that mimic many aspects of AD (Elder et al., 2010). Moreover, it has been described that during ageing there is a natural loss of the γ-secretase activity that leads to the accumulation of several protein CTFs that can trigger neurodegeneration (Placanica et al., 2009).

Number	Substrate	Number	Substrate	Number	Substrate
1	Alcadein α	33	IL6R	65	PAM
2	Alcadein γ	34	IR	66	PLXDC2
3	APLP1	35	Ire1α	67	Polyductin (PKHD1)
4	APLP2	36	Ire1 β	68	Protocadherin-α4
5	ApoER2	37	Jagged2	69	Protocadherin-γ-C3
6	AβPP	38	KCNE1	70	Ptprz
7	Betacellulin (BTC)	39	KCNE2	71	RAGE
8	Betaglycan	40	KCNE3	72	RPTPκ
9	CD43	41	KCNE4	73	RPTPμ
10	CD44	42	Klotho	74	ROBO1
11	CSF1R	43	L1	75	SorC3
12	CXCL16	44	LAR	76	SorCS1b
13	CX3CL1	45	LRP1 (LDLR)	77	SorLA (LR11)
14	DCC	46	LRP1 b	78	Sortilin
15	Delta1	47	LRP2 (megalin)	79	Syndecan-1
16	Desmoglein-2	48	LRP6	80	Syndecan-2
17	DNER	49	MUC1	81	Syndecan-3
18	Dystroglycan	50	N-cadherin	82	Tie1
19	E-cadherin	51	Nav-β1	83	Tyrosinase
20	EpCAM	52	Nav-β2	84	TYRP1
21	EphA4	53	Nav-β3	85	TYRP2
22	EphB2	54	Nav-β4	86	Vasorin
23	EphrinB1	55	Nectin-1α	87	VE-cadherin
24	EphrinB2	56	Neuregulin-1	88	VEGF-R1
25	ErbB4	57	Neuregulin-2	89	VLDLR
26	GHR	58	Notch 1		
27	HLA	59	Notch-2		
28	HLA-A2	60	Notch-3		
29	IFNaR2	61	Notch-4		
30	IGF-1R	62	NPR-C		
31	IL-1R1	63	NRADD		
32	IL-1R2	64	p75NTR		

***Table 1:* γ-secretase substrate proteins.** *Addapted from: Haapasalo & Kovacs; 2011.*

RESEARCH AIMS

The main objective in our laboratory is understanding the role of $p75^{NTR}$ in BFCNs during development and ageing (both healthy and pathological). For such objective in this experimental work we will characterise the role of $p75^{NTR}$ in the ageing mouse model SAMP8 and how the proteolytic cleavage of $p75^{NTR}$ impacts the differentiation and survival of BFCNs *in vitro* and *in vivo*.

The specific objectives of this thesis are the following;

1. Quantifying the number of BFCNs in young, adult and ageing SAMP8-$p75^{NTR+/+}$ and SAMP8-$p75^{NTR-/-}$ mice.
2. Studying the effect of $p75^{NTR}$ deletion in SAMP8-$p75^{NTR-/-}$ aged mice.
3. Determining if the deletion of $p75^{NTR}$ in SAMP8 mice has any behavioural consequence.
4. Analysing BFCNs in primary cell cultures and in organotypic slices after the addition of γ-secretase inhibitors.
5. Studying the effect of the γ-secretase inhibition in a transgenic mouse model *in vivo*.

MATERIALS AND METHODS

1. Murine Models, Maintenance And Genotyping

All procedures were approved by the Valencian Community Ethics Committee and conducted in accordance with the Spanish and European Code of Practice for the Care and Use of Animals for Scientific Purposes. Animals were housed in the Biomedicine Institute of Valencia animal facility on a 12 hours light/dark cycle (lights on at 7:00 a.m.), and at a constant temperature of 24 ºC. Food and water were provided *ab libitum.* Breeding colonies were maintained in a Specific pathogen-free (SPF) environment. Both male and female animals were used for all experiments. The different lines used in this work were equally maintained; two females were crossed with one male when they were at least 2 months old. At the moment of the weaning (approximately 21 days old) the mice were separated by gender. To individually identify each animal they were labeled in the ear and the tissue collected was used for genotyping.

The DNA extraction protocol was common for all genotypes: 100 µl of Solution A (25 mM NaOH, 0.2 mM EDTA) were added into the tissue and incubated for 1 hour at 95 ºC. Then, 100 µl of Solution B (40 mM Tris-HCl pH 7.5) were added into the extracted DNA and centrifuged for 10 minutes at 400 g at 4 ºC. The supernatants were collected in new tubes and used as template for the PCR reactions. The DREAM Taq DNA Polymerase (Thermo Scientific, 5 U/µL, EP0704) was used for the PCR reactions.

The PCR mix, primers and cycle conditions of each reaction are specified in the specific mice strain section and listed in **Table M1** and **Table M2 A-B**. The different PCR products were run in an agarose (Crondalab, 8010) gel (% specified in each section) prepared with TAE buffer (1 mM EDTA, 20 mM acetic acid in 40 mM Tris-HCl) and 5 µL/100 mL of Green Safe (Nzytech, MB13201) to stain the DNA. The PCR products were mixed with loading buffer (30 % glycerol, 0.25 % bromophenol blue). Finally, the PCR products were ultraviolet detected and photographed in a transilluminator (16si Plus, Isogen LifeScience) using the Proxima AQ4 software.

1.1. C57BL/6J-p75$^{NTR-/-}$ Mice

The knock-out p75^{NTR} mouse used in this work was obtained from Jackson laboratory (JAX stock #002213) and previously generated by Lee et al. 1992. Briefly, this mouse model was generated with a neomycin cassette that was introduced inside the exon III of p75^{NTR}, disrupting the sequence encoding cysteine repeats 2, 3, and 4, generating a p75^{NTR} unable to bind NGF. Homozygous mice for the mutation are viable and fertile. Nevertheless, the development of sensory and sympathetic neurons is altered in the mutated mice correlated with a loss of sensitivity in their paws, which progress into feet loose (Lee et al., 1992).

To genotype this line the primers p75 WT, p75 MUT and p75 REV **(Table M1)** were used. PCR mix and conditions are enclosed in **Table M2 A-B**. PCR products were run in a 1.5 % agarose gel and a 437 bp band appeared for $p75^{NTR+/+}$ mice, a 270 bp band for $p75^{NTR-/-}$ mice and both for $p75^{NTR+/-}$ mice **(Figure M1 A)**.

Even though $p75^{NTR-/-}$ mice are fertile and viable, the homozygous breedings were challenging. For that reason, breedings were composed of heterozygous ($p75^{NTR+/-}$) male and female mice.

1.2. SAMP8-$p75^{NTR-/-}$ Mice

To evaluate the role of $p75^{NTR}$ during ageing, a new mouse model was generated in Dr. Marçal Vilar's laboratory; the $p75^{NTR}$ mutation was introduced into a SAMP8 background, crossing C57BL/6J-$p75^{NTR-/-}$ animals with SAMP8 mice, generating the new SAMP8-$p75^{NTR-/-}$ mouse model. SAMP8 mice were obtained from Dr. Helena Mira.

To generate the line a SAMP8 male was crossed with a C57BL/6J-$p75^{NTR-/-}$ female. A $p75^{NTR+/-}$ female of the F1 generation was crossed again with a SAMP8 male, reducing the C57BL/6J background and increasing the SAMP8. This procedure was carried during 13 generations in order to obtain a SAMP8-$p75^{NTR+/-}$ mice with a 99.999 % SAMP8 background. The line SAMP8-$p75^{NTR+/-}$ was maintained with heterozygous breedings. The breeding between these heterozygotes mice generated the animals SAMP8-$p75^{NTR+/+}$ and SAMP8-$p75^{NTR-/-}$ used for the thesis.

Genotyping was performed with the same primers and PCR conditions as the C57BL/6J-$p75^{NTR-/-}$ mice.

The common control for SAMP8 is the SAMR1 (Senescence Accelerated Mouse Resistant-1) strain, as these mice do not have an accelerated senescence (Takeda et al., 1981). At the same time that SAMP8 mice were crossed with C57BL/6J-$p75^{NTR-/-}$, SAMR1 was as well crossed with C57BL/6J-$p75^{NTR-/-}$ animals. Nevertheless, after different breedings no SAMR1-$p75^{NTR-/-}$ mice were born and it was impossible to generate both lines in parallel.

1.3. $CamKII^{CRE}$; $PS1^{f/f}$; $PS2^{-/-}$ Mice

This mouse line was obtained from Dr. Carlos Saura from Autonomous University of Barcelona with the written permission of Dr. Jie Shen, from Harvard University for its use.

PS1 complete knock-out mice are not viable and die after birth because of ribcage defects as PS1 is required for the spatiotemporal expression of Notch1 and Dll1, essential proteins for somite segmentation and maintenance of somite borders (Shen et al., 1997). Consequently, the generation of a CRE conditional knock-out mouse for PS1 was necessary. CamKII^{CRE} mice were crossed with PS1 floxed mice (PS1$^{f/f}$) in order to delete PS1 in mature neurons (Yu et al., 2001). The CamKII^{CRE} line was generated with the insertion of a transgene consisting in 8.5 Kb of the α-calcium-calmodulin-dependent kinase II (αCAMKII) promoter followed by the cDNA of the CRE recombinase. With this strategy, the expression of the CRE recombinase is selective in neurons of the postnatal forebrain under the control of the αCamKII. These mice were later crossed with the conditional PS1$^{f/f}$ mice, generated by the same experimenters (Yu et al., 2001). Using homologous recombination in embryonic stem cells, a loxP site and a floxed drug selection cassette were introduced into PS1 introns 1 and 3, respectively **(Figure M2 A)**, flanking PS1 exons 2 and 3 by two loxP sites. The deletion of the exons 2 and 3 generates a smaller and highly unstable PS1 transcript, generating a null allele for PS1 (Yu et al., 2001).

CamKII expression is not restricted to mature neurons, as it has been reported some transient expression in male gonads (Song & Palmiter, 2018). Therefore, if the male carries the CamKII^{CRE+} and the PS1$^{f/f}$, the CRE protein will be expressed in the somites and will recombine, leading to animals with PS1 deletions in the sperm. These animals will generate progeny animals with a widespread PS1 deletion, not specifically in neurons of the postnatal forebrain. These animals are named deleted or PS1$^{\Delta}$. To avoid the problem, the maintenance of the line is restricted to breedings of males CamKII^{CRE-} and females CamKII^{CRE+}. Nevertheless, CamKII can be, in a lower percentage, expressed in female gonads, generating some deleted animals. Accordingly, an extra primer was designed to detect these deleted animals. The primer hybridises a sequence after the second loxP. Therefore, if it has been some CamKII^{CRE} expression in the zygote, and the exons have been deleted in a nonspecific tissue like the ear, a new PCR product will be amplified **(Figure M2 B)**.

For genotyping the line the following primers were used; PS1 WT, PS1 FLOX, PS1 DEL, CamKIICRE FW and CamKIICRE REV, listed in **Table M1**. PCR mix and conditions are enclosed in **Table M2 A-B**. The PCR products were run in a 2.5 % agarose gel. In CRE+ mice a band of 700 bp appeared. In PS1$^{+/+}$ mice (PS1 gene not floxed) a 216 bp band was amplified, in PS1$^{f/f}$ mice a 262 bp band appeared, in PS1$^{+/f}$ both bands were present in the gel. If the CRE was expressed at the embryo a 372 bp band appeared (PS1$^{\Delta}$) **(Figure M2 B)**.

In rodents exist two types of Presenilin, PS1 and PS2. Thus, there is the requirement to delete both presinilins to inhibit completely the γ-secretase catalytic activity. PS2 knock-out mice were obtained from Dr. Carlos Saura from Autonomous University of Barcelona. These mice are viable and fertile (Herreman et al., 1999). For genotyping PS2 line, PS2 WT, PS2 MUT, PS2 REV

primers were used **(Table M1)**. PCR mix and conditions are enclosed in **Table M2 A-B**. The PCR products were run in a 2.5 % agarose gel and in $PS2^{+/+}$ mice a 540 bp band appeared and in $PS2^{-/-}$ a 326 bp band. For heterozygous mice, both bands appeared in the gel **(Figure M1 C)**. PS2 animals were kept with $PS2^{-/-}$ breedings.

$CamKII^{CRE}$;$PS1^{f/f}$ animals were crossed with $PS2^{-/-}$ mice to get the desired triple transgenic mouse: $CamKII^{CRE+}$;$PS1^{f/f}$;$PS2^{-/-}$. As controls, $CamKII^{CRE-}$;$PS1^{f/f}$;$PS2^{-/-}$ animals were used.

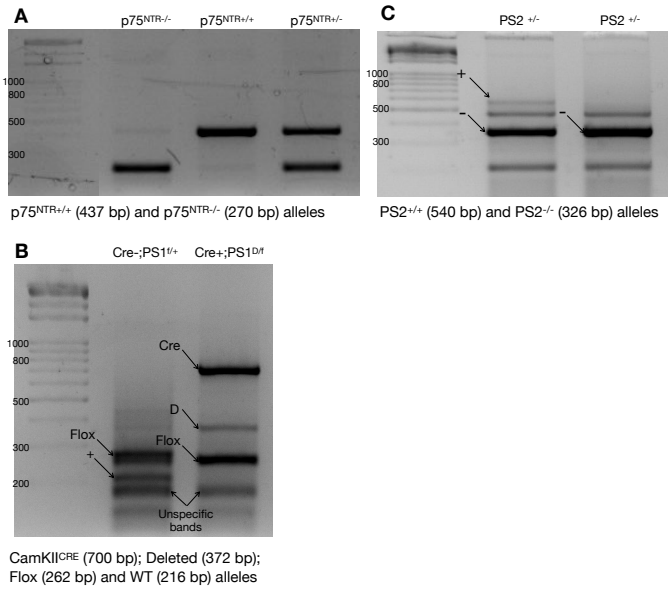

***Figure M1:* Agarose electrophoretic gels of mice genotyping.** **A)** Agarose gel of $p75^{NTR}$ genotype. The band of 437 bp corresponds to the $p75^{NTR+/+}$ and the band of 270 bp to the $p75^{NTR-/-}$. **B)** Agarose gel of $CamKII^{CRE}$;$PS1^{f/f}$ genotype. The band of 700 bp corresponds to CRE+, the band of 372 bp to deleted, the band of 262 bp to Flox and the band of 216 bp to WT. **C)** Agarose gel of PS2 genotype. The band of 540 bp corresponds to $PS2^{+/+}$ and the band of 326 bp to $PS2^{-/-}$.

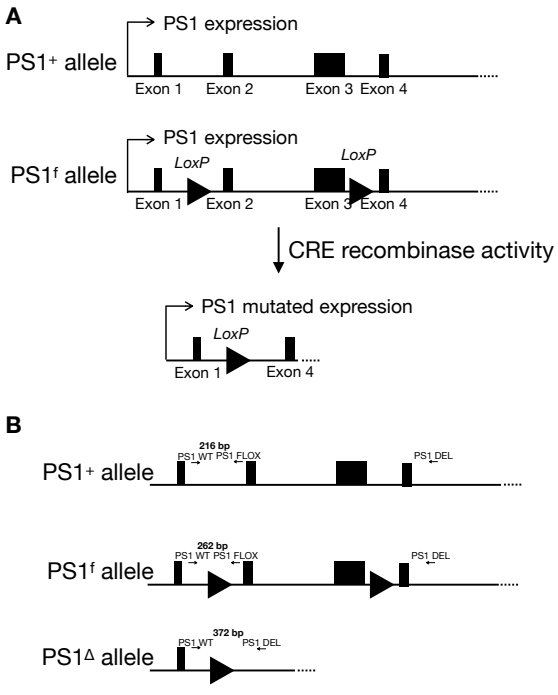

Figure M2:* Schematic representation of transgenic mice lines.** ***A) *PS1 allele representation before (upper scheme) and after (lower scheme) CRE recombinase activity. The black boxes represent the different exons and the triangles the LoxP sequences, located in introns 1 and 3. LoxP sequences will be recognised by CRE and will recombine the gene, deleting exons 2 and 3 and generating a null PS1 protein.* ***B)*** *Genotype strategy to detect null animals.*

Name	Sequence 5' to 3'
CAMKII Cre FW	GCC TGC ATT ACC GGT CGA TGC AAC GA
CAMKII Cre REV	GTG GCA GAT GGC GCG GCA ACA CCA TT
P75 MUT	GAA CTT CCT GAC TAG GGG AGG AGT
P75 REV	GGA CAA ACA GAA CAC AGT GTG TGA
P75 WT	ACC CAT ATA ATC GCT GAG AGA GGA
PS1 DEL	TGC CCC CTC TCC ATT TTC TC
PS1 FLOX	GGT TTC CCT CCA TCT TGG TTG
PS1 WT	TCA ACT CCT CCA GAG TCA GG
PS2 MUT	CAC ACA GAG AGG CTC AAG ATC
PS2 REV	AAG GGC CAG CTC ATT CCT CC
PS2 WT	CAT CTA CAC GCC CTT CAC GG

Table M1: ***Sequence of the primers used for the mice genotyping.***

A

Reactive volume (µL) x sample	$p75^{NTR}$	$\alpha CAMKII^{CRE}$;PS1	PS2
ddH_2O (sterile)	8,9	13	12
Display Buffer 10x	2	2,5	2,5
$MgCl_2$ 50 mM	1	0,5	1
dNTP's 10 mM	1	0,5	0,5
Primers 10 µM	0,6 (each, 3)	1,25 (each, 5)	1,25 (each, 2)
Taq Pol 5 U/µl	0,3	0,25	0,25

B

PCR conditions	$p75^{NTR}$			$\alpha CamKII^{CRE}$;PS1			PS2		
	T (ºC)	Time	Times	T (ºC)	Time	Times	T (ºC)	Time	Times
Initial denaturation	94	3'	1	94	4'	1	94	4'	1
Denaturation	94	30"	35	94	1'	40	94	1'	35
Annealing	62	30"	35	60	1'	40	62	1'	35
Extension	72	40"	35	72	7'	40	72	7'	35
Maintenance	4	∞	∞	4	∞	∞	4	∞	∞

Table M2: ***Conditions of the different mice genotyping.*** ***A)*** *Mix conditions of each PCR.* ***B)*** *Thermocycle conditions of each genotype.*

2. Histological Techniques

2.1. Brain Fixation

Animals were sacrificed with a Pentobarbital overdose and transcardially perfused with 4 % paraformaldehyde (PFA, PanReac, 141451.1211). For it, animals were cut open below the diaphragm and the rib cage was cut rostrally on the lateral edges to expose the heart. A little cut on the right side of the heart was made. After, 20 mL of NaCl 0.9 % were injected through the left ventricle with a 20 mL syringe with a 23 GA needle to remove the blood from the veins. Subsequently, 40 mL of 4 % PFA were injected with a constant flux to perfuse the animal.

2.2. Post-Fixation

The brains were removed and post-fixed overnight with 4 % PFA at room temperature and shaking. The post-fixation time was 2 hours for the brains used to analyse AChE fibres,. The next day (or after the 2 hours) the brains were washed several times with 0.1 M PB, pH 7.4 and kept in 0.1 M PB with 0.005 % sodium azide at 4 ºC until its use.

2.3. Tissue Processing

Depending on the purpose of the brain, they were processed differently:

A. Cryostat processing

The brains of SAMP8-p75^{NTR} and C57BL/6-p75^{NTR} mice were cryoprotected and cut in the cryostat and used for BFCNs counting and GFAP immunostaining. The brains were cryoprotected over night with a solution of 30 % sucrose at 4 ºC to avoid the formation of crystals due to water freezing present in the tissue. After, the brains were fit in O.C.T, Tissue-Tek Embedding Medium for frozen tissue specimens (Sakura, 4583 Finetek Europe) and situated and orientated in a specific mould for freeze (Aname, 70181). After, the tissue was frozen in liquid nitrogen and stored at -80 ºC until its use. Finally, coronal slices (Leica CM1900 cryostat) of 10 µm thickness were collected in gelatinised slides (0.2 % aluminium chromium, 0.5 % gelatine and 1 % sodium azide). Up to 8 parallel series (10 slides/serie) were collected per brain, to achieve a rostral to caudal brain representation from the whole BF. The slices were kept at -20 ºC until its use.

B. Vibratome porcessing

The brains from CamKII^{CRE};PS1$^{f/f}$;PS2$^{-/-}$ strain were cut in the vibratome.
The perfused tissues were coronary cut at 40 µm with the Vibratome (Leica, VT1200) and the sections were collected in 24 multi-well (MW) plate containing 0.1 M PB with 0.005 % sodium azide and stored at 4 ºC until its use.

3. In vitro Techniques

3.1. Organotypic Slice Culture

The technique of organotypic slice culture was learned in Prof. Humpel's laboratory, Innsbruck (Austria), during a 3 months international stay in the third year of the PhD candidate (from September 2020 to December 2020).

To obtain BF fresh slices, mice of postnatal day 8-10 (P8-10) were sacrificed by decapitation. The brain was removed from the skull and the cerebellum cut. The brain was glued (Glue Loctite 401) onto the vibratome (Leica, VT1200) platform with the olfactory bulbs facing up. The platform was positioned inside the inner cuvette of the vibratome previously fulfilled with chilled PL sterile medium (50 % Minimum Essential Medium (MEM, Sigma, 51415C), 2 mM $NaHCO_3$, pH 7.2). Under aseptic conditions, 170 µm coronal brain sections were cut and collected. The organotypic vibrosections were carefully placed onto a 0.4 µm membrane insert (Millipore, PICM03050) within a 6 MW plate. Twelve sections per brain were taken at the level of the NBM (Bregma -0.34 to -1.34). The 12 slices were transferred in 2 plates (6 each) allowing 2 different experimental approaches per animal. The organotypic brain slices were maintained at 37 ºC and 5 % CO_2 for 2 weeks with the following medium: 50 % MEM/HEPES (Sigma, M2645), 10 % heat inactivated horse serum (Gibco), 25 % Hank's solution (Gibco, 24020-091), 2 mM $NaHCO_3$ (Merck, 1.06329.1000), 6.5 mg/ml glucose (Merck, 8342), 2 mM L-glutamine (Gibco, 25030-024), 1 % penicillin/streptomycin (GE Healthcare, SV30010) and pH 7.2. The medium was changed once a week (Humpel, 2018). The different compounds tested were added into the medium since day 0. After 2 weeks the ex *vivo* slices attached to the membranes were fixated for 3 hours with 4 % PFA at 4ºC **(Figure M3)**.

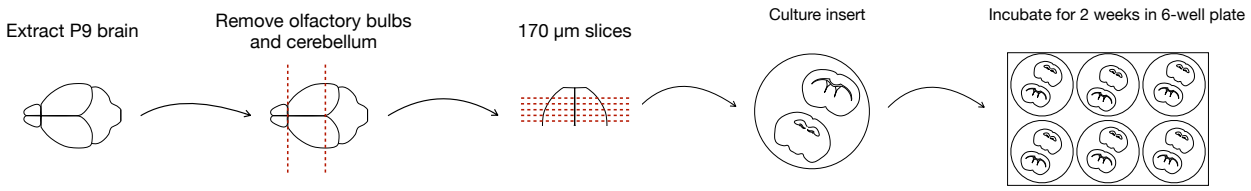

Figure M3: ***Schematic representation of organotypic slices preparation.*** *Brains from postnatal day 8-10 pups were extracted and the olfactory bulbs and cerebellum removed. The brain was placed in a vibratome and cut in 170 µm slices. The slices were freshly placed into an insert and cultured for 2 weeks in a 6 MW plate.*

3.2. Basal Forebrain Cholinergic Neurons Primary Culture

Embryos of 17-18 days (E17-18) were surgically removed and septal areas were dissected from the cerebral tissue in chilled Hanks balanced salt solution (HBSS, 137 mM NaCl, 5.4 mM KCl, 0.17 mM Na_2HPO_4, 0.22 mM KH_2PO_4, 9.9 mM HEPES, 8.3 mM glucose and 11 mM sucrose). All the septums were pooled together and digested with 1 mL of 0.25 % trypsin (Ge Healthcare, SV30037.01) and 0.5 mL of 100 kU DNasa I (GE healthcare, D4263) for 10 minutes at 37 ºC. The fragments were dissociated by aspiration with progressive narrower tips in 0.5 mL of 4 % BSA (Apollo Scientific, BIA3981) and 1 mL of Neurobasal medium (Gibco, Life Technologies, 10888-022) supplemented with 2 % B-27 (Gibco, Life Technologies, 17504-044), 1 % L-glutamine (Gibco, 25030-024) and 0.5 % penicillin/streptomycin (GE Healthcare, SV30010). After tissue dissociation, 2.5 mL of 4 % BSA were added and the tubes were centrifuged for 5 minutes at 300 g at 4 ºC. The supernatant was aspirated and the pellet resuspended in 5 mL of 0.2 % BSA. The cell suspension was filtered in 40 µm nylon filter (Sysmex, 04-0042-2316-5) and living cells counted in the Neubauer chamber. The suspension was centrifuged again and resuspended in NB/B-27 medium and seeded. For immunocytochemical analysis cells were seeded in 24 MW plates with 12 mm diameter pre-coated circular coverslips (VWR, ECN 631-1577). For Western blot analysis or $p75^{NTR}$ immunoprecipitation, cells were seeded in pre-coated p-100 plates. The surfaces were coated with 50 µg/mL poly-D-lysine (Sigma, 27964-99-4) overnight at 4 ºC and 5 µg/mL laminin (Sigma, L2020) for 2 h at 37 °C. The seeding density was 2.10^5 cells/well (Schnitzler et al., 2008). The next day, half of the NB medium was changed, reducing the concentration of B-27 from 2 % to 0.2 % and supplemented with 2 µM of the anti mitotic 1-β-D-Arabinofuranosyl Cytosine, AraC (Sigma, 14794-4) and 100 ng/ml of NGF (Alomone labs, N-245). Neurons were kept at 37 ºC in a humidified incubator in a 5 % CO_2 atmosphere for 11 days (D.I.V 11) for posterior fixation with 2 % PFA for 15 minutes at room temperature.

The protocol to get $p75^{NTR-/-}$ primary neurons was the same as explained above but instead of pooling all the embryos, each septum was dissected and processed individually. The procedure had to be this way because the embryos came from a breeding of heterozygous animals, so each embryo could have a different genotype. At the moment of the brain extraction, the tip of the tail was kept for posterior genotyping (following the same protocol as C57BL6/J-$p75^{NTR-/-}$ genotyping) to identify the cultures of interest. A difference from $p75^{NTR+/+}$ cultures, $p75^{NTR-/-}$ were kept 7 D.I.V.

To evaluate the effect of inhibitors in the primary culture a unique dose of the different chemicals was added to the culture one, two or three days before fixation (D.I.V 8, 9 or 10). The inhibitors evaluated in this work were: the γ-secretase inhibitor Compound E (CE, Millipore, sc-222308) was added at a final concentration of 1 µM; the γ-secretase inhibitor Semagacestat

(SG, Selleckchem LY450139) at 0.1 µM; the α-secretase inhibitor TAPI (Sigma, SML0739) at 10 µM; the RhoCK-inhibitor, Y-27632 (Selleckchem, S1049) at 10 µM; the TrkA activity inhibitor, K252α (Sigma, K1639) at 0.5 µM; human $Aß_{1-42}$ (kindly donated by Dr. Chavez) at 1µM; human $Aß_{1-17}$ (kindly donated by Dr. Chavez) at 1µM or DMSO as vehicle (Sigma, D2650).

3.3. Basal Forebrain Extraction

The BF was extract freshly and freezed at -80 ºC until its use. The mice were sacrificed by dislocation and the brain was extracted and placed in a sterile plate with chilled PBS. The brain was placed under a magnifying glass (Leica S6E), and the olfactory bulbs were removed. A sagittal cut was made along the sagittal seizure to separate the cerebral hemispheres. The hemispheres were carefully separated and elevated until the corpus callosum was identified. Underneath the corpus callosum is located the BF. Three cuts are necessary to liberate the basal forebrain: two parallel cuts to separate the BF from the cortex, and one antiparallel cut to separate the BF from the cerebrum. After soon, the BF was freezed in liquid nitrogen and stored. The BF extracts were used for Western Blotting, immunoprecipitation, RNA extraction and further qPCR, cholesterol measurement, acetylcholine measurements and HNE adducts ELISAs.

4. Protein Detection

4.1. Immunohistochemistry

A. Organotypic slice immunohistochemistry

Chromogenic horseradish peroxidase (HRP) immunohistochemistry was used to detect $p75^{NTR}$ and ChAT in organotypic slices. If not indicated the opposite, all the steps were made at room temperature and shaking.

After fixation the slices were washed 3 times for 5 minutes with 0.1 M PB and permeabilised for 30 minutes in 0.1 % Triton X-100 (Tx, Sigma, 9002-93-1). The slices were then incubated in 20 % methanol, 1 % H_2O_2 for 20 minutes to block the endogenous peroxidases. After, the slices were washed twice for 5 minutes in PB 0.1 M and incubated for 30 minutes in blocking buffer (0.1 % Tx, 0.2 % BSA, 20 % Horse Serum in 0.1 M PB) to avoid unspecificities, and incubated for 2/3 over nights at 4 ºC in primary antibody **(Table M3)** diluted in blocking buffer. The slices were subsequently washed twice for 5 minutes in 0.1 M PB and incubated for 1 hour in the secondary antibody **(Table M4)** diluted in 0.1 M PB. The slices were subsequently washed 3 times with PB 0.1 M before being incubated in ABC Kit (Avidin/Biotin Complex, Vector Labs, PK-6100) for 1 hour. After, the slices were washed 3 times in 50 mM TRIS buffer and stained with DAB (50 mg DAD 3,3'- Diaminobenzidine in 50 mM TRIS, 0.01 % H_2O_2).

Finally, the slices were mounted and coverslipped with a solution of 50 % Mowiol (Polysciences, 17951) and 50 % Dako mounting medium (Sigma, D2522).

B. Tissue immunohistochemistry

For immunofluorescence labelling brain sections were incubated for 1 hour in blocking buffer to avoid unspecificities (0.1 % Tx, 3 % Fetal Bovine Serum (FBS) in 0.1 M PB). The sections were then incubated overnight at 4 ºC in the corresponding primary antibody **(Table M3)** diluted in blocking buffer. The next day the samples were washed 3 times with 0.1 M PB and later incubated for 1 hour at room temperature in the secondary antibody **(Table M4)** diluted in 0.1 M PB. Then, the nucleus were stained with the nuclear marker 4,6-diamidino-2-phenylindoledihydrochloride (DAPI; Sigma, St. Louis, MO, USA) 1:1000, and finally the brain sections were mounted on slides and coverslipped with Dako fluorescence mounting medium.

4.2. AcetylCholinEsterase Staining

To detect AchE fibres, the protocol from Karnovsky and Roots was followed (Karnovsky & Roots, 1964). Brain slices were washed 3 times with 0.1 M sodium acetate buffer pH 6 and incubated 1 hour at 37 ºC in the AchE solution, prepared as described below:
5 mg of acetylcholine iodide were dissolved in 6.5 ml of 0.1 M sodium acetate pH 6. After, the different solutions were consecutively added in agitation: 500 µL of 0.1 M sodium citrate, 1 mL of 30 mM $CuSO_4$, 1 mL of dH_2O and 1 mL of 5 mM $K_3Fe(CN)_6$. After the 1 hour incubation, the free floating brain sections were mounted on the slides and dehydrated by immersing the slices in four steps washes in the following alcohols for 3-5 minutes each.

- EtOH 70 %
- EtOH 95 %
- EtOH 100 % (x2)
- Xilol (x2)

Finally, the slices were coverslipped and mounted with DPX (Millipore, 1.00579.0500).

4.3. Cholesterol and Acetylcholine Measurements

Three BF extracts of each mouse genotype were sent to INCLIVA, *Instituto de Investigación Sanitaria* in Valencia University to analyse the levels of cholesterol and acetylcholine by HPLC (High Performance Liquid Chromatography).

4.4. 4-HNE Adduct Competitive ELISA

The level of oxidative damage in the BF was estimated by the levels of 4-hydroxynonenal (4-HNE), a natural bi-product of lipid peroxidation, an accepted indicator of oxidative cellular

damage (Breitzig et al., 2016). In order to detect 4-HNE adducts, an ELISA kit (cell biolabs, STA-838) was used following the manufacture protocol, briefly: the plate was coated with *"HNE Conjugate"* (10 µg/mL) overnight at 4ºC. The next day the *"HNE Conjugate"* was removed and washed twice with PBS. The plate was blocked in *"Assay Diluent"* for 1 hour at room temperature. After, 50 µl of each BF lysate were added to the plate and incubated for 10 minutes at room temperature on an orbital shaker. 50 µl of anti-HNE antibody were added to the plate and incubated at room temperature for 1 hour and washed 3 times with *"Washing Buffer"*. Subsequently, 100 µL of *"Secondary Anbtibody-HRP Conjugate"* were added to the plate and incubated for 1 hour at room temperature and washed 3 times with *"Washing Buffer"*. The *"Substrate Solution"* was added to the plate and incubated at room temperature for 2-20 minutes. Finally, the reaction was stoped with the *"Stop Solution"*, and the absorbance of each sample read at 450 nm in the Tekan Spark Instrument. A standard curve was generated with 4-HNE-BSA from 0 to 200 µg/mL in parallel with the samples to estimate the sample concentration.

4.5. Flow Cytometry

The flow cytometry assay was performed with disaggregated cells from E-17 septums, prepared following the protocol described in section 3.2. After the last centrifugation of the protocol, the BSA was aspirated and 250000 cells were separated and used as a blank. The rest of the cells were divided in two equal parts and resuspended with 100 µl of 0.5 % BSA. In one tube 0.5 µl of A488-p75^{NTR} antibody were added and in the other one 4 µl of A633-TrkA antibody and incubated for 45 minutes at 4 ºC. Subsequently, the samples were centrifuged 5 minutes at 100 g and resuspended with 500 µL of 0.5 % BSA. The cytometry analysis was made in the *Cytometry Service from Valencia University*.

4.6. Immunocytochemistry

Immunocytochemistry (ICC) was carried out in primary culture neurons. The cells were permeabilised with 0.1 % Tx for 4 minutes at room temperature. If one of the primary antibodies used was ChAT the cells needed an extra incubation in 0.5 % SDS for 5 minutes. After, the cells were blocked in 2 % BSA, 0.1 % Tx in 0.1 M PB for 1 hour followed by an over night incubation at 4 ºC in a humidified chamber with the corresponding primary/ies antibody/ies **(Table M3)**. The next day, unbound antibodies were washed 3 times with 0.1 M PB and bound antibodies were detected incubating in the corresponding secondary/ies antibody/ies **(Table M4)**. Nucleus were stained with DAPI 1:1000 for 10 minutes and samples were mounted on glass slides, and coverslipped with Mowiol and dako.

4.7. Western Blotting

A. Protein Extraction

BF extracts were dissolved in 200 µl of TNE lysis buffer; 137 mM NaCl, 2 mM EDTA, 0.2 % Tx, 1 µM ortovanadate (Millipore, mcproto444), 10 µM NaF and protease inhibitor cocktail (Bimake, B14011) in 50 mM Tris-HCl pH 7.5. To detect HMGCR protein the lysis buffer was supplemented with 1 % SDS. The tissues were dissociated with the help of a manual potter and kept for 30 minutes on ice to extract the total protein. After, the samples were centrifuged for 15 minutes at 20000 g at 4 ºC and the supernatants were collected and transferred into a clean tube.

B. Protein Quantification

Protein concentrations of the lysates were determined using the Bradford assay (Bio-Rad, 5000006) and normalised across all samples with a BSA standard curve.

C. Western Blot sample preparation

Once the samples were quantified the equal amount of 80 µg of protein were prepared. The necessary amount of protein was dissolved in sample buffer: 50 % glycerol in 1 M Tris-HCl pH 6.8, 10 % SDS, 5 % bromophenol blue, 1.25 % β-mercaptoethanol (Sigma, M6250). Then, the samples were denaturalised for 5 minutes at 95 ºC. To detect HMGCR protein the samples were incubated at 37 ºC.

D. Gel preparation. Electrophoresis. Membrane Transference

To resolve the proteins, denaturalising poliacrylamide gels (SDS-PAGE) in reduction conditions were used. The stacking gels were prepared at 5 %: 0.13 % bis-acrylamide (Sigma, A6050), 125 mM Tris-HCl pH 6.8, 0.1 % SDS (PanReac, 205-788-1), 0.1 % ammonium persulfate (PSA), 0.1 % N,N,N',N'-tetramethylethylenediamine (TEMED, Sigma, T7024). The resolving part of the gels were prepared at different percentages depending on the molecular weight of the proteins: X % bis-acrylamide, 375 mM Tris-HCl pH 8.8, SDS, PSA and TEMED at the same concentration as the stacking gel.

The electrophoresis was performed at 100 V and 20 mA in electrophoresis buffer (0.2 M glycine, 1 % SDS in 25 mM Tris-HCl). A pre-stained ladder was used to correctly estimate the molecular weight (Nzytech, MB090). Finally, the gel was transferred to a nitrocellulose blotting membrane (GE Healthcare, 10600001). The electrophoretic transference was performed for 2 hours at 4 ºC at 100 V in transfer buffer (192 mM glycine, 20 % methanol in 25 mM Tris-HCl pH 8.3).

E. Protein Detection

The membranes were blocked in 5 % BSA in T-TBS buffer (200 mM NaCl, 0.1 % Tween 20 (Promega, H515) in 20 mM Tris-borate pH 7.6) for 1 hour and shaking. After, the membranes were incubated overnight at 4 ºC in the corresponding primary antibody **(Table M3)** diluted in T-TBS. The next day, they were washed twice for 30 minutes in T-TBS and incubated for 1 hour in the corresponding fluorescent secondary antibody **(Table M4)**. Finally, the membranes were washed and the fluorescence was detected with Odyssey (Li-Cor). For ChAT detection the chemiluminescent substrate ECL was used to detect HRP conjugates on immunoblots. The intensity of the bands were quantified using Image Studio Lite software.

4.8. Active RhoA Pull Down

In order to detect the amount of RhoA bound to GTP (active form) in primary cultures, Rhotekin pull down assay was carried out. Rhotekin is a protein with a Rho Binding Domain (RBD) that specifically binds to the complex RhoA-GTP but not to RhoA-GDP (inactive form). Primary culture lysates were incubated with Glutathione-Sepharose beads linked to the RBD of Rhotekin and 1 mM $MgCl_2$ in an orbital shaker for 4 hours at 4 ºC. After, the samples were washed 3 times with 0.1 % Tx in TNE and centrifuged for 2 minutes at 100 g. The pellet was dissolved in sample buffer and run in a WB. The amount of active RhoA was determined using a RhoA antibody **(Table M3)**.

4.9. $P75^{NTR}$ Immunoprecipitation

The low amount of endogenous $p75^{NTR}$-CTF in primary cultures is not directly detectable by Western Blot. It is necessary to perform a previous immunoprecipitation. 500 µl of primary culture lysates were incubated overnight with 2 µL of $p75^{NTR}$ antibody (Millipore, 07-476) at 4 ºC in an orbital shaker. The day after, 10 µL of Protein G Agarose beads (ABT, 4RRPG-5) were added to each tube and incubated for 2 hours in an orbital shaker at 4 ºC and centrifuged for 2 minutes at 100 g to precipitate the agarose beads bound to the antibody. The samples were washed in 0.2 % Tx in TNE buffer and used for WB in which $p75^{NTR}$ full-length and $p75^{NTR}$-CTF were detected with $p75^{NTR}$ antibody (Millipore, 07-476) **(Table M3)**.

Primary Antibody	Source	ICC/IHC Dilution	WB Dilution	Comercial reference
Acly	Ms	—	1:1000	Santacruz, sc-517267
ß-Actin	Ms	—	1:1000	Sigma, A5441
Akt	Rb	—	1:1000	Cell Signaling, 4691
ChAT	Gt	1:200	1:1000	Millipore, AB144P
Cleaved Caspase-3	Rb	1:1000	—	Cell Signaling, 2355
HMGCR	Ms	—	1:500	Abcam, Ab242315
P38	Rb	—	1:1000	Cell Signaling, 8690
P44/42	Rb	—	1:1000	Cell Signaling, 4695
$p75^{NTR}$ intercellular	Rb	1:200	1:2000	Millopore, 07-476
$p75^{NTR}$ intercellular	Rb	1:200	—	Abcam, Ab52987
$p75^{NTR}$ intercellular	Rb	1:200	—	Promega, G323A
$p75^{NTR}$-A488 extracellular	Rb	1:400	—	ATS, FL-N01AP
Presenilin 1	Rb	1:200	1:500	Alomone, AIP-011
Presenilin 2	Rb	1:200		Alomone, AIP-012
Phospho Akt	Rb	—	1:1000	Cell Signaling, 4060
Phospho p38	Rb	—	1:1000	Cell Signaling, 4511
Phospho p44/42 (Erk1-2)	Rb	—	1:1000	Cell Signaling, 4370
Phospho- SAPK/JNK	Rb	—	1:1000	Cell Signaling, 4668
RhoA	Rb	—	1:5000	Abcam, ab187027
SAPK/JNK	Rb	—	1:1000	Cell Signaling, 9252
TrkA extracellular	Rb			Alomone, ANT-018
TrkA extracellular-A633	Rb	1:25	—	Alomone, ANT-018-FR
TrkA	Rb			Millipore, 06-574

Table M3: ***Primary antibodies and their characteristics.*** *Rb: antibody made in Rabbit; Ms: antibody made in mouse; Gt: antibody made in goat.*

Specimen	ICC/IHC Dilution	WB Dilution	Comercial Reference
RABBIT			
Biotin hs α-rb			Vector labs, BA-1100
Cy3 dk α-rb	1:500		Jackson, 711-165-152
IRDye 800CW gt α rb	—	1:10000	Li-Cor, 925-32211
MOUSE			
A455 dk α-ms	1:500		Invitrogen, A31570
A488 dk α-ms	1:500		Invitrogen, A21202
IRDye 680LT gt α ms	—	1:10000	Li-Cor, 925-68020
GOAT			
A488 dk α-gt			Jackson, 705-564-147
Biotin rb α-gt	1:700		Jackson, 305-065-003
Cy3 dk α-gt			Jackson, 705-165-147
HRPdk α-gt		1:6000	Santacruz, 2020
STREPTAVIDINS			
Streptavidin Cy2	1:200		Jackson, 016-220-084
Streptavidin Cy3	1:400		Jackson, 016-160-084

Table M4: ***Secondary antibodies and their characteristics.*** *Rb: antibody made in rabbit; Ms: antibody made in mouse; Gt: antibody made in goat; Hs antibody made in horse; Dk: antibody made in donkey.*

5. Image Analysis

5.1. GFAP Intensity

Immunohistochemistry of the astrocytic marker GFAP was carried out in SAMP8 mice slices. Fluorescence images were captured with Confocal SP8 (Leica) and GFAP positive astrocytes of the CA1 area of the HC were analysed with ImageJ software. After setting a threshold, the mean intensity per μm^3 was assessed. A minimum of five different CA1 areas per animal were measured.

5.2. Basal Forebrain Cholinergic Neuron Counting

Coronal brain slices of 10 µm thick were collected in gelatinised slices. The collection started around Bregma 1.34 mm, when the lateral ventricles appear and finished around Bregma -2.50 mm, when the HC occupies half of the brain **(Figure M4)**. That way, all the BF and HC were collected in 7 - 8 series.

To count BFCNs the first slide of each serie was used to perform ChAT IHC. Fluorescence images were captured with Confocal SP8 Microscope (Leica), and ChAT positive neurons were counted.

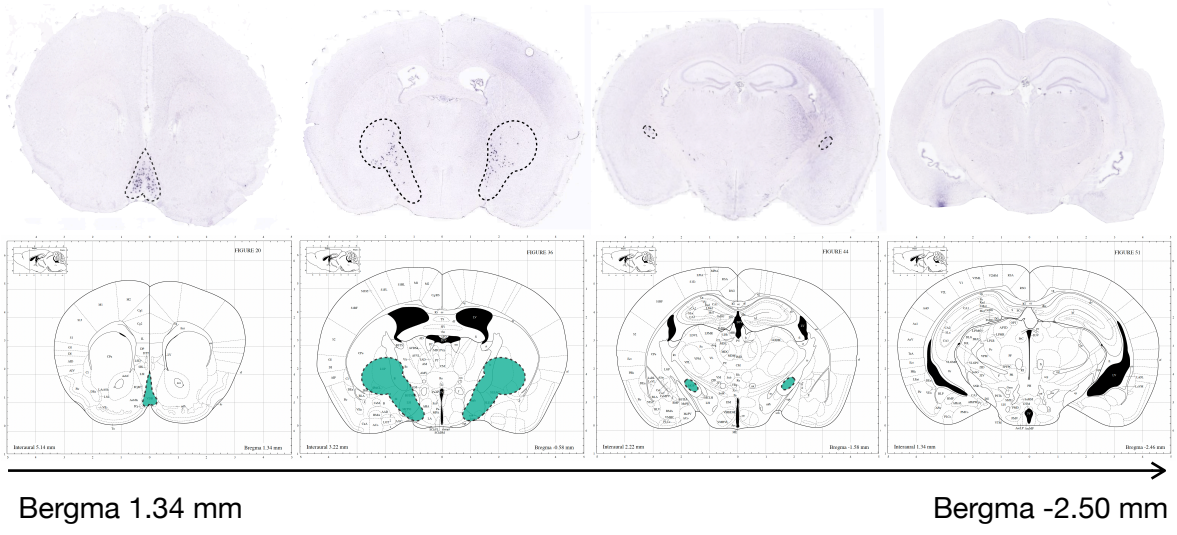

Figure M4: ***Representation through Bregmas of the basal forebrain collection****. The upper panel shows p75^{NTR} In situ hybridisation. The images used are taken from mouse allen brain (https://mouse.brain-map.org). The lower panel shows images of the Paxinos Atlas. The dotted line follows the BF structure.*

5.3. AChE Fibres Quantification

AChE fibres images from HC and cortex of CAMKII^{CRE};PS1$^{f/f}$;PS2$^{-/-}$ animals were captured with DM750 microscope (Leica) and quantified with ImageJ software following the protocol published by Kneynsberg et al., 2016 (Kneynsberg et al., 2016). First, the background of the image was subtracted and a region of interest (ROI) of 140 x 130 pixels was chosen aleatory. Then, an auto threshold with Otsu software was carried out. The analysis particles tool was set up with a range from 0 to ∞ pixel^2. The result was the total area of coloured pixels. Three ROIs of each image were analysed with a minimum of two images per animal.

5.4. Sholl Analysis

To analyse neuronal complexity the Sholl analysis was performed in cholinergic primary culture and organotypic slices. Fluorescence images of neuronal primary culture were taken with a Confocal SP8 microscope (Leica). ChAT and p75^{NTR} positive neurons were analysed. Sholl analysis of organotypic slices was made from chromogenic images were taken with Thunder Microscope (Leica) and p75^{NTR} or ChAT positive neurons were analysed.

Neuronal complexity was assessed with Sholl analysis plugin of ImageJ software. The analysis consist in concentric circles, starting in the soma, and counts the times that a dendrite or axon crosses a particular intersection in a concrete distance. In this work, the number of crossing intersections were counted every 10 µm with a maximum length of 400 µm.

5.5. Cholinergic Death Counting

Cholinergic primary culture cell death induced with H_2O_2, CE, Aß and K-252a chemicals were measured. Of each culture, ChAT positive neurons and double positive neurons for ChAT and cleaved caspase-3, an apoptosis marker, were counted.

6. Gene expression

6.1. RNA Extraction

All the RNA extractions and qPCR were performed with the help of José Vicente Santa-Rita Perez. The BF used were extracted as explained in the section 3.3.

The total RNA from BF was extracted with the kit TRI Reagent® according to the manufacturer instructions. The BF was homogenised in TRI Reagent (250 µl per < 50 mg of tissue) and incubated for 5 minutes to dissociate the nucleoprotein complexes. After, 50 µL of chloroform were added and the samples were mixed vigorously (inverted 15 times) with a following 2 minutes incubation at room temperature. The samples were centrifuged for 15 minutes at 16000 g at 4 °C to separate 3 phases. The upper aqueous phase contains the RNA, the middle phase contains the DNA, and the lower contains the proteins. 70 µl of the aqueous phase were collected in a new tube and 125 µl of isopropanol were aded and mixed vigorously (inverted 15 times). Subsequently, the samples were incubated for 10 minutes and centrifuged at 16000 g for 15 minutes at 4 ºC. The supernatants were removed and the RNA pellets were washed with 150 µl of chilled 70 % ethanol and centrifuged for 5 minutes at 16000 g at 4 °C. The supernatants were removed and the RNA pellets were dried and resuspended in 20 µl of nuclease-free water. RNA concentration and purity (A260/A280 ratio) were determined using a NanoDrop Lite Spectrophotometer (Thermo Scientific). RNA samples were stored at -80 °C until its use.

6.2. RT and q-PCR

The extracted RNA was retrotranscribed to cDNA using the commercial kit PrimeScrpt™ RT reagent kit (Takara, RR037A). 500 ng were retrotranscribed with a single cycle of 15 minutes at 37 ºC and 5 seconds at 85 ºC.
In order to analyse the expression of the different genes quantitative PCR (qPCR) was carried out from cDNA using SyBR Green. The qPCR were run in 96 well PCR plates in the *Applied Biosystems QuantStudio5* system. Primer sequences were designed using the *OligoCalc* tool, *“an online oligonucleotide property calculator (2007)”.* In all cases the primers were designed between exons to avoid a possible amplification of genomic DNA. The resulting products were around 150 bp of length. The same experimental conditions **(Table M5)** were used for all RT-qPCR except the annealing temperature that differed according to each primer **(Table M6)**. In all cases an endogenous expression control (SDHA gene) and a negative control (no cDNA) were used. The expression levels were determined using the 2-ΔΔCt method (Livak & Schmittgen, 2001).

Initial denaturalisation (1 cycle)	95 ºC	10 minutes
Amplification curve (40 cycles)		
Denaturalisation	95 ºC	15 seconds
Annealing	primer TM	1 minute
Dissociation curve (1 cycle)	TM + 5 ºC	15 seconds
	95 ºC	10 seconds
	4 ºC	∞

Table M5: ***Temperatures for all the RT-qPCR.***

Name	Sequence 5' to 3'
ApoE FW	AGGTCCAGGAAGAGCTGCAGA
ApoE REV	CAGCTGTTCCTCCAGCTCCTT
GSTa1 FW	CAGAGTCCGGAAGATTTGGA
GSTa1 REV	CAAGGCAGTCTTGGCTTCTC
HMOX FW	AGGCTAAGACCGCCTTCCT
HMOX REV	TGTGTTCCTCTGTCAGCATCA
LDLR FW	ACCCCTCAAGACAGATGGTX
LDLR REV	CAGCCCAGCTTTGCTCTTAT
NFR2 FW	TTCTTTCAGCAGCATCCTTCTCCAC
NFR2 REV	ACAGCCTTCAATAGTCCCGTCCAG
SDHA FW	AGAGGACAACTGGAGATGGCATT
SDHA REV	AACTTGAGGCTCTGTCCACCAA
SOD1 FW	AGATGACTTGGGCAAAGGTG
SOD1 REV	AATCCCAATCACTCCACAGG
SOD2 FW	CTGGCTTGGCTTCAATAAGG
SOD2 REV	TAAGGCCTGTTGTTCCTTGC

Table M6: ***Sequence of the primers used in the qPCR.***

7. Behavioural Tests

Groups of male and female SAMP8-p75$^{NTR+/+}$ and SAMP8-p75$^{NTR-/-}$ mice of 2 and 6 months of age were used for all the behavioural tests. One week before performing the behavioural tests mice were moved into the behavioural room for habituation and they were housed in cages of 2 animals. In addition, each mouse spend 5 minutes per day during four days with the experimenter. The mice conducted the 3 different test in the following order: Open Field, Y-maze test and Object Recognition Memory test (ORM). Tests were performed with a gap of 3-5 days to let the mouse to rest. The tests were carried out at the same hour and with the same light illumination. Between each mouse the behavioural apparatus was cleaned with 70 % EtOH and the next mouse was not placed on it until the EtOH was evaporated.

7.1. Open Field Test

The open field test consists in a squared black box of 50 x 50 cm and 85 cm elevated from the floor. The box is divided in two areas, the central zone of 42 x 42 cm represents the 40 % of the total surface, and the surrounded periphery zone the 60 % **(Figure M5 A)**. Animals display a natural aversion to brightly open areas (central zone), as these areas leave them exposed to depredators. However, they also have a drive to explore a new environment. The time spend by the mice in each zone and the distance moved is recorded to evaluate anxiety-related parameters, the more anxious the animal is, the more time spends in the periphery (Gould et al., 2009).

Each mouse was individually placed in the same corner of the box facing the wall and was free to explore for 5 minutes. The trajectory, velocity and time spend in each area were recorded with an automatic activity monitoring system (Smart Video Tracking Software, PanLab). The total distance and the mean velocity were used to evaluate general locomotion.

7.2. Spontaneous Alternation Y-Maze

The Y-maze spontaneous alternation test measures episodic memory and takes advantage of the willingness of rodents to explore new areas. Rodents typically prefer to explore a new arm of the maze rather than returning to the one that was previously visited. So, if the animal remembers the arm where it came from and choose a different one, is considered the correct response, whereas returning to the previous arm is considered an error (Kraeuter et al., 2019). The maze consist in 3 opaque arms of 32.5 x 8 cm each, separated each other 120º, generating the shape of a capital Y **(Figure M5 B)**. The mice were placed in the centre of the Y without previous habituation to the maze, and freely explored the maze for 8 minutes. Every time the mice put the four paws in a new arm it was recorded. The correct alternations were

counted for spatial memory parameters. The total number of entries were used to assess general locomotion.

7.3. Novel Object Recognition Memory Test

The novel object recognition (NOR) test evaluates long and short term memory by evaluating the differences in the exploration time in the novel or in the familiar objects (Antunes & Biala, 2012; Lueptow, 2017). The test consist in a 40 x 40 cm squared box and is divided in three temporal phases: habituation, training and test. In the habituation phase, the mice are placed in the empty box for 10 minutes. Twenty-four hours later, the training phase is performed. Each mouse is allowed to explore for 10 minutes the box with 2 identical objects. In this work we used 2 pink rectangles, placed at 8 cm from the walls. The next day, the test phase is conducted placing the mice for 5 minutes in the box with 2 objects: the familiar and the novel. In this work the objects were a pink rectangle (familiar object) and a green triangle (novel object) **(Figure M5 C)**. NOR test is based on the spontaneous tendency of rodents to spend more time exploring a novel object than a familiar one. The choice to explore the novel object reflects the memory of the mice. If the test phase is conducted 2 hours after the training phase, the short-term memory is evaluated. While if the test phase is performed 24 hours after the training phase, it evaluates the long-term memory. In this work only long-term memory has been evaluated. Mice were recorded with a videocamera and the time that each mice spend exploring the novel or the familiar object were counted.

In this test, a normal behaviour is considered when the mouse explores the objects for at least 20 seconds during the five minutes of the test (Lueptow, 2017). Mice that explored less than 20 seconds during the test were eliminated from the results.

8. Statistical Analysis

All the statistical analysis were performed with GraphPad Prism software. The results are represented as mean ± standard error of the mean (SEM). The normal distribution of all data sets were confirmed with the D'Agostino & Peason test. To determine if the differences between 2 groups were significant the unpaired Student's t-test was performed. For multiple comparisons one or two-way analysis of variance (ANOVA) test was used. Initially, it was evaluated if there were significant differences between the groups, then the Tukey's post-hoc test was used to determine the specific differences between groups. In the plots the "n" indicates the number of the independent mice used of each strain and age for each experiment. In all the analysis a p value < 0.05 has been considered statistically significant, and represented as: *$p < 0.05$; **$p < 0.01$; *** $p < 0.001$ and **** $p < 0.0001$.

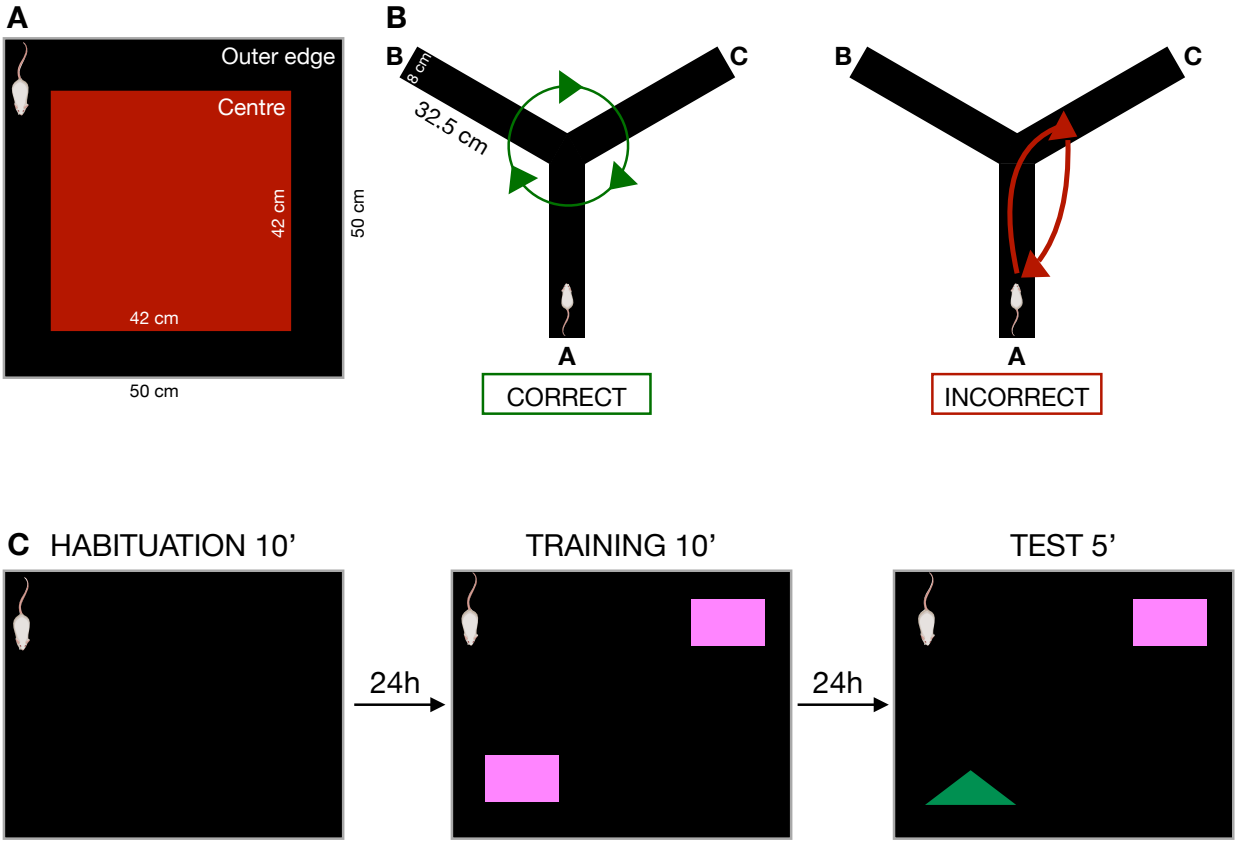

Figure M5: ***Schematic representations of the different behavioural tests carried out.*** ***A)*** *Open field box of 50 x 50 cm. The inner part (centre, red) measures 42 x 42 cm. The mice were always placed at the same corner and the time spent in each area were recorded.* ***B)*** *Y-maze representation, each arm measures 8 x 32.5 cm. The mice were always placed at the A arm and the entries were recorded. If the mouse entered at the 3 different arms consecutively the alternation was considered correct, on the contrary if the mouse resided the same arm or came back to the previous one it was considered incorrect.* ***C)*** *Novel Object Recognition test (NOR) scheme. The mice were placed for habituation 10 minutes in the empty box. The day after, 2 equal objects, 2 pink rectangles, were placed in the box and the mice were free to explore for 10 minutes. The day of the test, 1 of the objects was changed, for a green triangle, the noble object and the mice were free to explore for 5 minutes. The time spend in each object was counted.*

RESULTS

Chapter I

P75^{NTR} IS NECESSARY FOR BASAL FOREBRAIN CHOLINERGIC SURVIVAL DURING AGEING

1.1. Generation Of The Mouse SAMP8-p75$^{NTR-/-}$

To achieve the first objective of this thesis, a new mouse model was generated backcrossing the SAMP8 mice with the p75^{NTR} knock-out mice for 13 generations to finally get the SAMP8-p75$^{NTR-/-}$ model (see Material and Methods section). This mouse model combines the SAMP8 background with the p75^{NTR} null mutation.

The loss of p75^{NTR} protein expression was confirmed either by WB and IHC. Protein lysates from BF dissections were analysed by WB. WB showed that the band corresponding to p75^{NTR} is absent in the SAMP8-p75$^{NTR-/-}$ mice. The levels of actin were used as controls for the total amount of protein. In the **Figure R1 A** the loss of p75^{NTR} signal in SAMP8-p75$^{NTR-/-}$ mice compared to SAMP8-p75$^{NTR+/+}$ is observed. The IHC showed that SAMP8-p75$^{NTR+/+}$ cholinergic neurons (ChAT positive) express p75^{NTR} while in SAMP8-p75$^{NTR-/-}$ no signal of p75^{NTR} is observed, confirming the deletion of the protein **(Figure R1 B)**. In addition, SAMP8-p75$^{NTR-/-}$ conserves some of the most characteristic phenotypical features of the p75$^{NTR-/-}$ mice; the loss of nails at 2 months with subsequent loss of paws at 6 months **(Figure R1 C)**.

After, SAMP8 phenotypic features were evaluated. The half-life of SAMP8-p75$^{NTR+/+}$ and SAMP8-p75$^{NTR-/-}$ mice were 10 and 11.5 months, respectively **(Figure R1 D)**. These results are in agreement with the half-life of 9.7 months previously described for the SAMP8 mice (Akiguchi et al., 2017). In addition to this, SAMP8-p75$^{NTR+/+}$ animals significantly gain weight with age, from 2 to 6 and 10 months, as the control strain SAMR1. However, the null mutant SAMP8-p75$^{NTR-/-}$ mice do not gain weight with age **(Figure R1 E)**. This result agrees with previous publications showing that the deletion of p75^{NTR} increases the energy expenditure as it was shown in the p75$^{NTR-/-}$ feed with a high-fat diet (Baeza-Raja et al., 2016). Another characteristic trait of the SAMP8 strain is the increase in reactive astrocytes with age (Garcia-Matas et al., 2008). We evaluated the amount of reactive astrocytes in the cortex and HC of SAMP8-p75$^{NTR+/+}$ and SAMP8-p75$^{NTR-/-}$ mice by quantifying the intensity of the astrogliosis marker, GFAP, by IHC. The GFAP intensity experiments of SAMP8-p75$^{NTR+/+}$ and SAMP8-p75$^{NTR-/-}$ in CA1 area showed a signal increases of the 50 % between the months 2 and 10, and no differences were observed between the p75^{NTR} genotypes **(Figure R2 A-B)**. We then used protein lysates from BF dissections and quantified the amount of GFAP. The quantification of the GFAP band intensity showed that SAMP8 mice have an increase in GFAP levels compared to SAMR1, suggesting an increase in astrogliosis in that area. Although the difference between SAMP8-p75$^{NTR+/+}$ and SAMR1 mice was statistically significant (*$p < 0.05$) it was not with the SAMP8-p75$^{NTR-/-}$ **(Figure R2 C)**, indicating a tendency to a lower astrogliosis in the p75^{NTR} deleted animals.

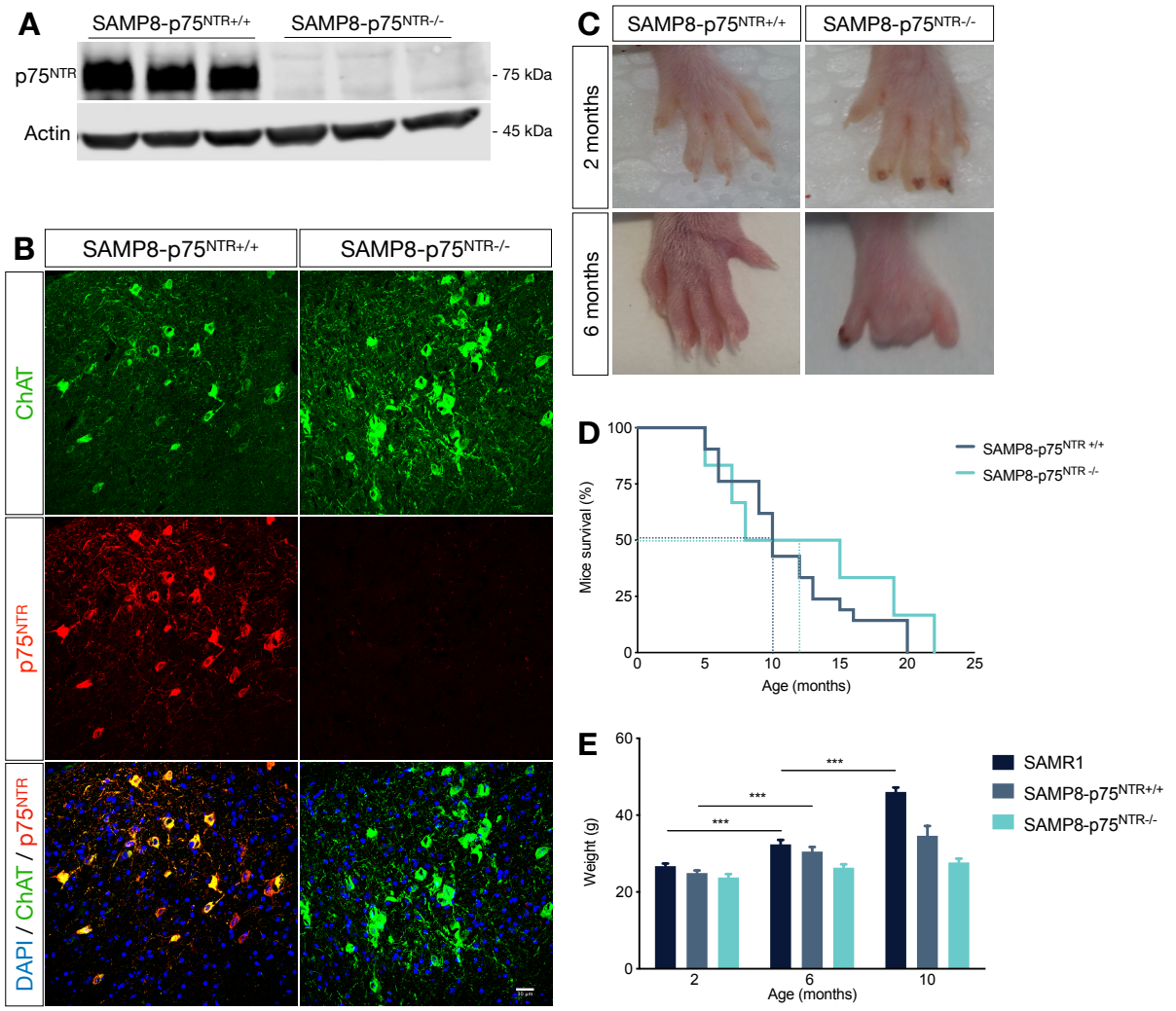

Figure R1: ***Characterisation of SAMP8-p75$^{NTR-/-}$ mouse line.*** ***A)*** *WB of three independent basal forebrain extracts of SAMP8-p75$^{NTR+/+}$ and SAMP8-p75$^{NTR-/-}$. The band corresponding to p75^{NTR} is absent in the SAMP8-p75$^{NTR-/-}$ mice. Actin was used as a control of the total amount of protein loaded.* ***B)*** *Immunohistochemistry of BF cholinergic neurons. ChAT is labeled in green and p75^{NTR} in red. In SAMP8-p75$^{NTR-/-}$ mice the signal of p75^{NTR} is lost.* ***C)*** *Nails and paws of SAMP8-p75$^{NTR+/+}$ and SAMP8-p75$^{NTR-/-}$ mice. SAMP8-p75$^{NTR-/-}$ loses the nails at 2 months and paws at 6 months.* ***D)*** *Survival Kaplan curve of SAMP8-p75$^{NTR+/+}$ and SAMP8-p75$^{NTR-/-}$ mice. The percentage of mice survival is represented in the y-axis and months in the x-axis. The mean half life of SAMP8-p75$^{NTR+/+}$ is 10 months, N = 21 and SAMP8-p75$^{NTR-/-}$ mean half life is 11.5 months, N = 6.* ***E)*** *Differences in weight between SAMR1, SAMP8-p75$^{NTR+/+}$ and SAMP8-p75$^{NTR-/-}$ mice at 2, 6 and 10 months. Mean ± SEM, N < 8. Two way ANOVA followed by Tukey's post-hoc analysis, ***p < 0.001.*

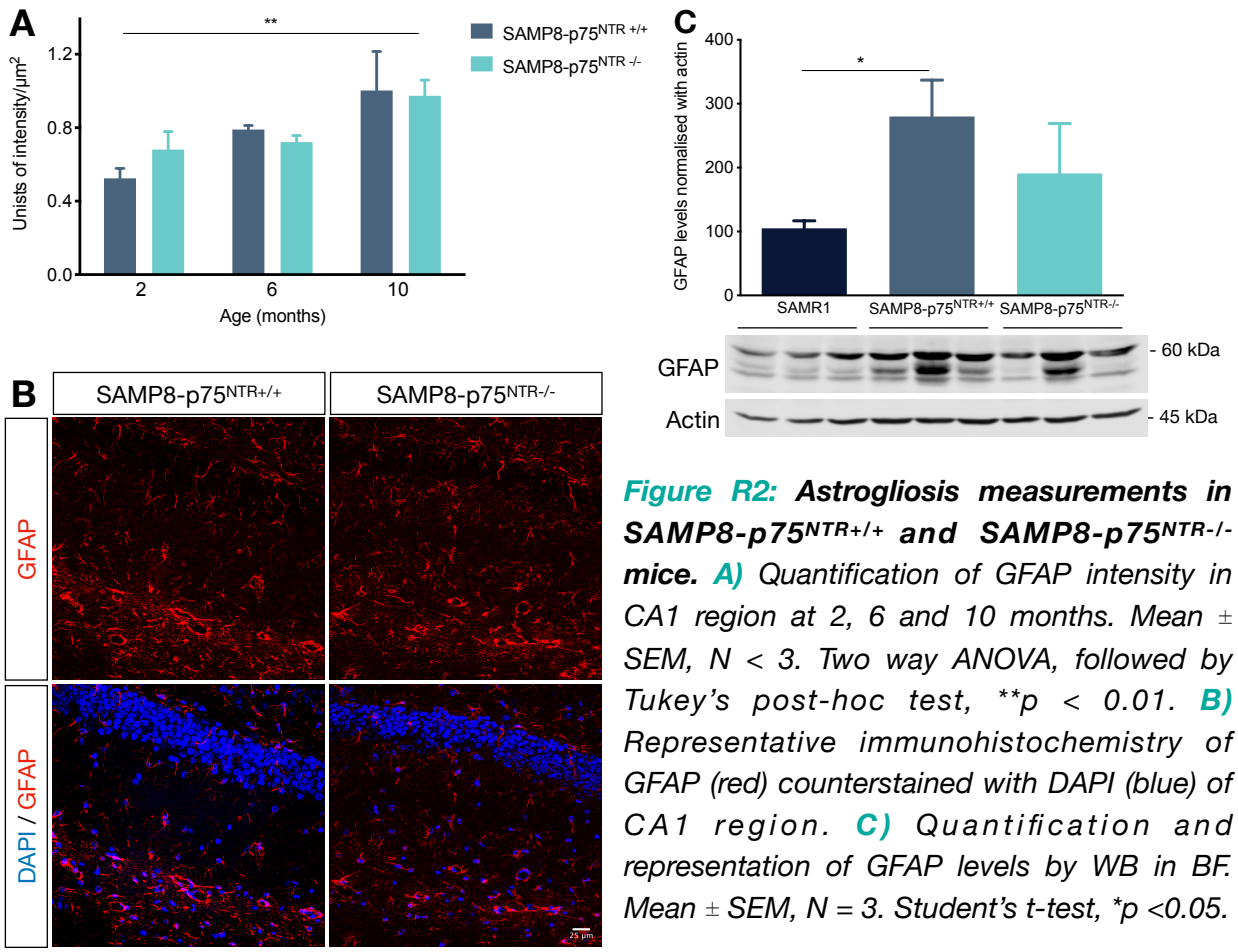

Figure R2:* Astrogliosis measurements in SAMP8-p75$^{NTR+/+}$ and SAMP8-p75$^{NTR-/-}$ mice.** ***A) *Quantification of GFAP intensity in CA1 region at 2, 6 and 10 months. Mean ± SEM, N < 3. Two way ANOVA, followed by Tukey's post-hoc test, **p < 0.01.* ***B)*** *Representative immunohistochemistry of GFAP (red) counterstained with DAPI (blue) of CA1 region.* ***C)*** *Quantification and representation of GFAP levels by WB in BF. Mean ± SEM, N = 3. Student's t-test, *p <0.05.*

1.2. Pro-Survival Role Of P75^{NTR} In Basal Forebrain Cholinergic Neurons During Adulthood And Ageing

To study if the levels of p75^{NTR} change during ageing, BF extracts were used to quantify the levels of the protein of SAMR1 and SAMP8-p75$^{NTR+/+}$ animals of 2 and 6 months of age. At the age of 2 months, SAMP8-p75$^{NTR+/+}$ mice presented a decrease of 45 % in the levels of p75^{NTR} protein in the BF compared to age matched SAMR1 **(Figure R3 A)**. However, at the age of 6 months, SAMP8-p75$^{NTR+/+}$ mice showed a 45 % increase of the protein levels respect to SAMR1 **(Figure R3 B)**.

As p75^{NTR} is only expressed in BF during adulthood, we wondered if the differences seen in the protein levels are because the neurons change the levels of p75^{NTR} during ageing, or if there is a change in the number of BFCNs. To answer this question SAMP8-p75$^{NTR+/+}$ and its control SAMR1 mice were analysed. In addition, the mouse SAMP8-p75$^{NTR-/-}$ was added to the analysis to better understand which is the role of this protein.

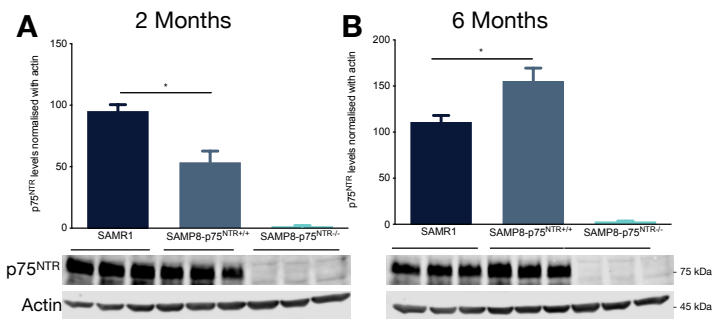

Figure R3: ***p75^{NTR} levels in basal forebrain.*** *Bar diagram of p75^{NTR} levels in the strains SAMR1, SAMP8-p75$^{NTR+/+}$ and SAMP8-p75$^{NTR-/-}$ normalised with actin at the age of **A)** 2 months and **B)** 6 months. Mean ± SEM, N = 6. Student's t-test analysis, * p < 0.05. The WB of p75^{NTR} and actin are showed in the lower panels.*

The number of ChAT positive neurons in the MS/VDB of the BF were quantified. The experiment was performed at 2, 6 and 10 months in SAMR1, SAMP8-p75$^{NTR+/+}$ and SAMP8-p75$^{NTR-/-}$ mice. The results showed that the amount of BFCNs is invariant in SAMR1 and SAMP8-p75$^{NTR+/+}$ mice throughout the whole study 2, 6 and 10 months **(Figure R4 A-C)**, nevertheless, a different effect is observed in SAMP8-p75$^{NTR-/-}$ mice. In this strain the number of ChAT positive neurons exhibit a significant 45 % increase at the age of 2 months **(Figure R4 A-C)**. This increment was already reported in other p75^{NTR} knock-out mice backgrounds (Martinowich et al., 2012; Boskovic et al., 2014). However, the excess of BFCNs disappeared at the age of 6 months with a loss of 37 %, when the 3 mice genotypes had similar numbers of cholinergic neurons in the MS/VDB. From 6 to 10 months only the SAMP8-p75$^{NTR-/-}$ decreased the number of BFCNs **(Figure R4 A-C)**.

The maintenance of cholinergic neurons in SAMR1 and SAMP8-p75$^{NTR+/+}$ mice is appreciated as both lines are straight in the **Figure R4 B**, differing significantly from SAMP8-p75$^{NTR-/-}$ line that has a steeper slope **(Figure R4 B)**.

As the data showed an initial increase in BFCNs at 2 months with a posterior reduction at 6 and 10 months, the levels of ChAT by WB were quantified. The quantification showed no significant differences between SAMR1 and SAMP8-p75$^{NTR+/+}$ mice but a significant reduction in ChAT levels in SAMP8-p75$^{NTR-/-}$ animals at 6 months **(Figure R5 A)**.

The enzyme ATP-citrate lyase, Acly, catalyses the cleavage of citrate into oxaloacetate and acetyl-CoA, the latter serving as common substrate for *de novo* cholesterol and fatty acid synthesis. In addition, in the cholinergic neurons acetyl-CoA is used to generate the neurotransmitter, ACh. This function makes Acly a very important enzyme for cholinergic neurons. Our immunohistochemical results showed that in the adult brain all ChAT positive neurons are also positive for Acly **(Figure R5 B)**. The protein levels of Acly in the BF were quantified at 2 and 6 months in SAMR1, SAMP8-p75$^{NTR+/+}$ and SAMP8-p75$^{NTR-/-}$ mice. The results showed similar protein levels in all 3 mice genotypes at 2 months of age **(Figure R5 C)**.

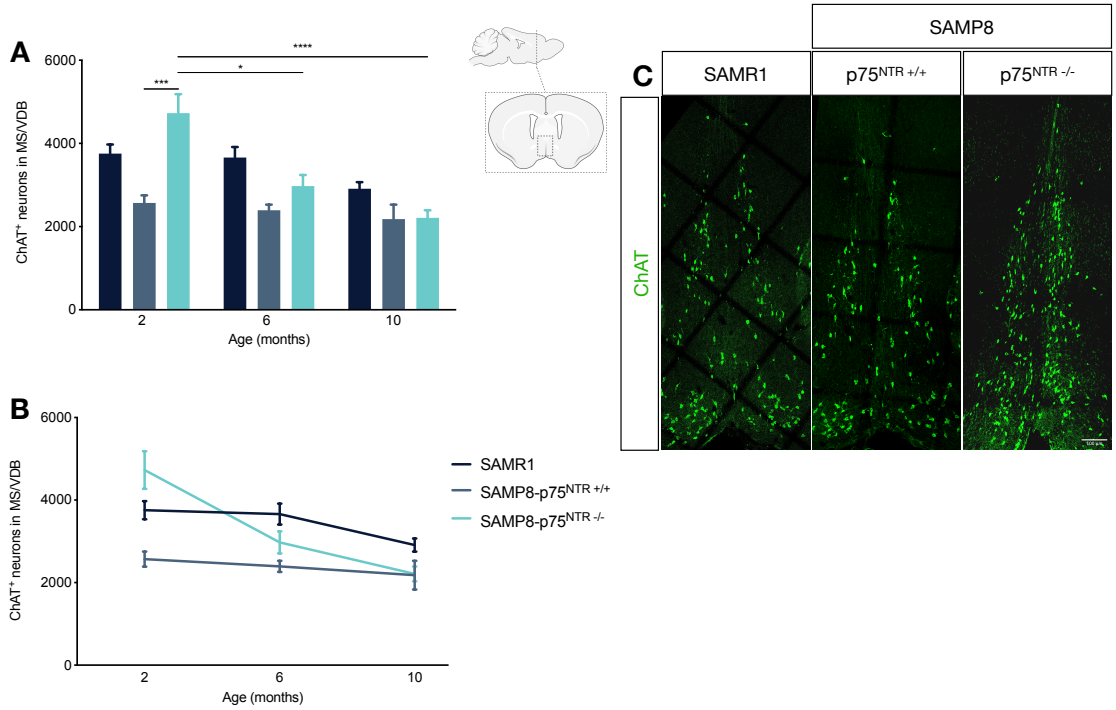

Figure R4: ***Number of Medial Septum cholinergic neurons at different ages in SAMR1, SAMP8-p75$^{NTR+/+}$ and SAMP8-p75$^{NTR-/-}$ mice lines.*** ***A)*** *Quantification of ChAT positive neurons in the MS/VDB. Mean ± SEM, N < 4. Two-way ANOVA followed by Tukey's post-hoc test. *p < 0.05, ***p < 0.001, ****p < 0.0001.* ***B)*** *Number of ChAT positive neurons through age of the different mice lines. Being the slope of SAMP8-p75$^{NTR-/-}$ significantly different from zero, ****p < 0.0001.* ***C)*** *Representative image of medial septum cholinergic neurons labelled with ChAT (green) at 2 months of the different mice lines.*

However, the levels were reduced in SAMP8-p75$^{NTR-/-}$ mice at the age of 6 months, compared to SAMR1 and SAMP8-p75$^{NTR+/+}$ mice **(Figure R5 D)**.

The levels of the cholinergic neurotransmitter ACh were measured at 2 and 6 months from BF tissue **(Figure R5 E)**. The increase in the number of BFCNs in SAMP8-p75$^{NTR-/-}$ mice correlated with an increase in the ACh levels at the age of 2 months compared to SAMP8-p75$^{NTR+/+}$ and SAMR1 control mice **(Figure R5 E)**. However, the tendency changed at 6 months, while SAMR1 and SAMP8-p75$^{NTR+/+}$ had no significant increment in the ACh levels, SAMP8-p75$^{NTR-/-}$ decreased its levels **(Figure R5 E)**, together with the number of cholinergic neurons, ChAT and Acly.

With all these results we can conclude that SAMP8-p75$^{NTR+/+}$ mice do not lose BFCNs during adulthood and ageing. Nevertheless, in SAMP8-p75$^{NTR-/-}$ young mice there is a 50 % increase in the number of BFCNs, translated into an increase of their neurotransmitter acetylcholine. During adulthood and ageing the excess of BFCNs in SAMP8-p75$^{NTR-/-}$ mice is lost, ending with

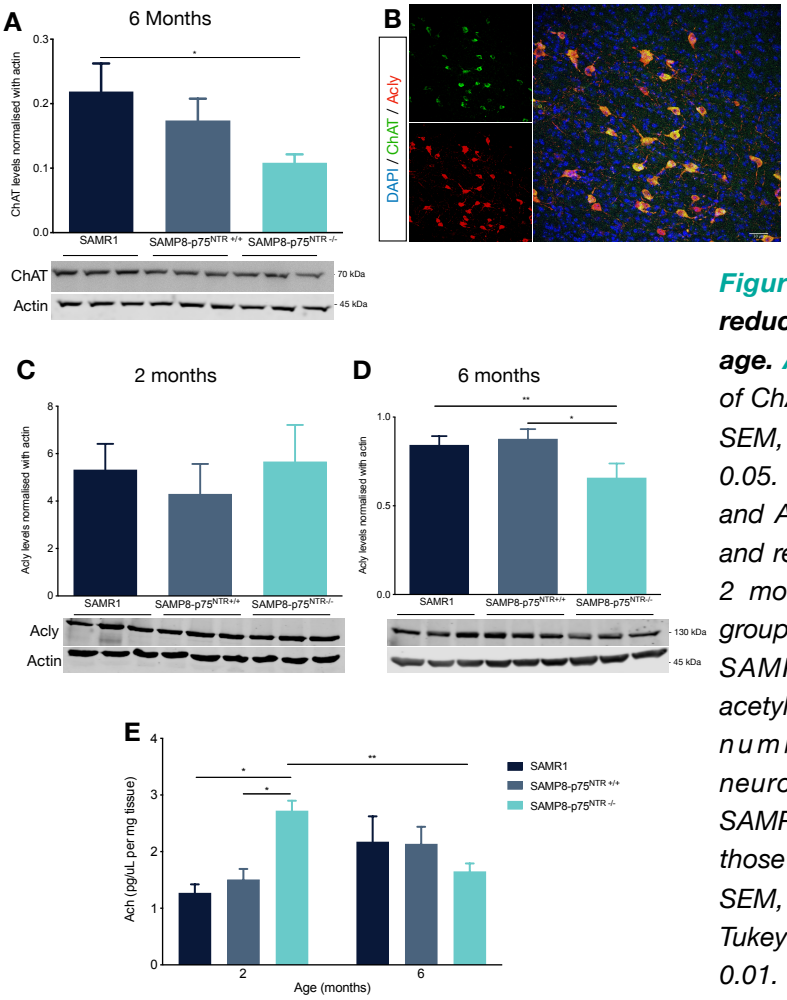

Figure R5: ***Cholinergic markers are reduced in SAMP8-p75$^{NTR-/-}$ mice with age.*** ***A)*** *Quantifications and representation of ChAT Western Blot at 6 months. Mean ± SEM, N = 6. Student's t-test analysis, * p < 0.05.* ***B)*** *Co-localization of ChAT (green) and Acly (red) in the BF.* ***C)*** *Quantification and representation of Acly levels by WB at 2 months* ***D)*** *and 6 months. N = 9 per group. Protein levels of Acly are reduced in SAMP8-p75$^{NTR-/-}$ mice.* ***E)*** *Levels of acetylcholine at 2 and 6 months, as the number of cholinergic neurons, neurotransmitter levels are higher in SAMP8-p75$^{NTR-/-}$ mice at 2 months, and those levels decrease at 6 months. Mean ± SEM, N = 3. Two-way ANOVA followed by Tukey's post-hoc test. *p < 0.05, **p < 0.01.*

the similar numbers of BFCNs as SAMP8-p75$^{NTR+/+}$ and SAMR1 animals. Altogether our data suggest that;

1. The decrease in BFCNs in SAMP8-p75$^{NTR-/-}$ during adulthood is an "adjustment", to remove the excess of these neurons seen at 2 months.
2. p75^{NTR} is needed for BFCNs survival during adulthood and ageing.

However exist the possibility that the effect is only seen in the SAMP8 background. To answer this the number of cholinergic neurons in the C57BL/6 background were analysed.

C57BL/6-p75$^{NTR+/+}$ and C57BL/6-p75$^{NTR-/-}$ animals were analysed at postnatal day 16 and at 2, 10 and 24 months. In C57BL/6-p75$^{NTR+/+}$ animals the number of ChAT positive neurons in the MS/VDB did not change during early postnatal stages, adulthood and ageing (postnatal day 16, 2, 10 and 24 months) **(Figure R6 A-E)**. However, in C57BL/6-p75$^{NTR-/-}$ mice at postnatal day 16 there was a 50 % increase in the number of ChAT positive neurons compared to C57BL/6-p75$^{NTR+/+}$ mice. C57BL/6-p75$^{NTR-/-}$ showed a significant decrease in the number of ChAT positive neurons between postnatal day 16 and 2 months. This decrease continued during adulthood (10 months) and ageing (24 months) **(Figure R6 A-E)**. The same results were

seen in another BF area, the NBM **(Figure R6 B-E)**, and in the whole BF **(Figure R6 C-E)**, suggesting a particular role of $p75^{NTR}$ in the whole BF.

The comparison of the slopes showed a straight line in C57BL/6-$p75^{NTR+/+}$ mice throughout all different ages and C57BL/6-$p75^{NTR-/-}$ showed a negative slope line **(Figure R6 D)**. The lines crossed at the age of 10 months, indicating a decrease in the number of BFCNs in C57BL/6-$p75^{NTR-/-}$ during adulthood and ageing, starting as early as postnatal day 16.

Altogether these results demonstrate that $p75^{NTR}$ plays a dual role in the life of BFCNs in both SAMP8 background (pathological ageing) and C57BL/6 background (healthy ageing). An increase in BFCNs can be seen at young adults, nevertheless, at older ages, there is a reduction in the number of neurons, suggesting that during development the receptor plays a pro-apoptotic role and during adulthood and during ageing a pro-survival role.

1.3. $p75^{NTR}$ Role In The Basal Forebrain Cholinergic Neurons During Ageing

The previous section showed the importance of $p75^{NTR}$ in the BFCNs during adulthood and ageing. Nevertheless, which is the mechanism and the molecular cues that are responsible for the decrease in the number of cholinergic neurons with age without $p75^{NTR}$ is not known. So, our next aim was to understand the role of $p75^{NTR}$ in BFCNs during ageing.

1.3.1. $p75^{NTR}$ Signalling Routes Are Not Affected In SAMP8-$p75^{NTR-/-}$ Mice

The different signalling pathways implicated in $p75^{NTR}$ were analysed. Protein lysates of BF extracts of SAMR1, SAMP8-$p75^{NTR+/+}$ and SAMP8-$p75^{NTR-/-}$ animals at 2 and 6 months of age were analysed by WB.

The first studied protein was p38, a MAPK that when is phosphorylated triggers apoptosis. $P75^{NTR}$ has been shown to modulate p38 activation and induce apoptosis (Pham et al., 2016). The WB showed a slight increase in p-p38 levels in SAMP8-$p75^{NTR-/-}$ mice at the age of 2 months compared to age matched SAMP8-$p75^{NTR+/+}$ **(Figure R7 A)**, indicating a possible increase in apoptosis. Nevertheless, at the age of 6 months, when apoptosis is happening, there were no difference in the levels of p-p38 between the 3 different mice **(Figure R7 B)**. Hereby, p38 is not more active in SAMP8-$p75^{NTR-/-}$ and seems not the responsible for the BFCNs death.

Another pro-apoptotic protein linked to $p75^{NTR}$ is Jnk, an Stress-Activated Protein Kinase (SAPK). In BF lysates analysed by WB no differences were seen in the levels of p-Jnk between

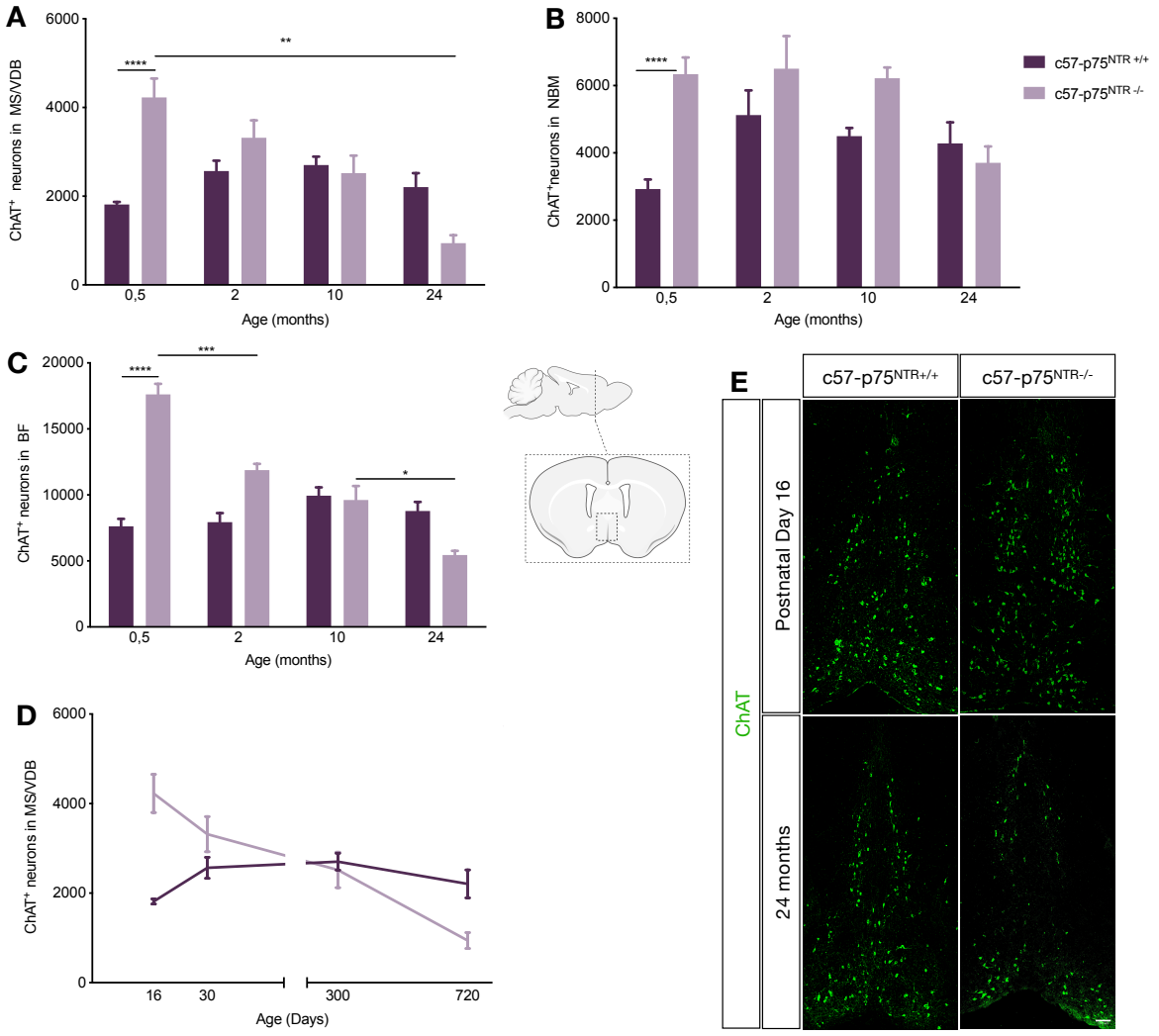

Figure R6: ***Number of ChAT positive neurons in different areas of the basal forebrain at different ages in C57BL/6-p75$^{NTR+/+}$ and C57BL/6-p75$^{NTR-/-}$ mouse lines.*** ***A)*** *Quantification of ChAT positive neurons in the MS/VDB. Mean ± SEM, N < 3. Two-way ANOVA followed by Tukey's post-hoc test. **p < 0.01, ***p < 0.001.* ***B)*** *Quantification of ChAT positive neurons in the NBM. Mean ± SEM, N < 3. Two-way ANOVA followed by Tukey's post-hoc test. ****p < 0.0001.* ***C)*** *Quantification of ChAT positive neurons of the BF. Mean ± SEM, N < 4. Two-way ANOVA followed by Tukey's post-hoc test. *p < 0.05, ***p < 0.001, ****p < 0.0001.* ***D)*** *Representation of the number of ChAT positive neurons through age of the different mouse lines. The slope of C57BL/6-p75$^{NTR-/-}$ is significantly different from zero **** p < 0.0001.* ***E)*** *Representative images of the BF ChAT positive neurons (green) at postnatal day 16 and 24 months of C57BL/6-p75$^{NTR+/+}$ and C57BL/6-p75$^{NTR-/-}$.*

SAMR1, SAMP8-p75$^{NTR+/+}$ and SAMP8-p75$^{NTR-/-}$ mice at 2 months of age **(Figure R7 C)**. No differences were reported either at 6 months **(Figure R7 D)**.

Another possibility would be that p75^{NTR} regulates pro-survival proteins instead of pro-apoptotic ones in the BFCNs. For that reason, 2 different pro-survival proteins were studied, Akt and Erk. WB analysis of p-Erk levels showed no differences between mice at 2 months

(Figure R7 E) and neither at 6 months between SAMR1, SAMP8-p75$^{NTR+/+}$ and SAMP8-p75$^{NTR-/-}$ animals **(Figure R7 F)**. Akt is another protein involved in cellular survival pathways, by inhibiting apoptotic processes. Akt phosphorylation levels were analysed and no differences were reported at 2 months **(Figure R7 G)** and neither at 6 moths **(Figure R7 H)**.

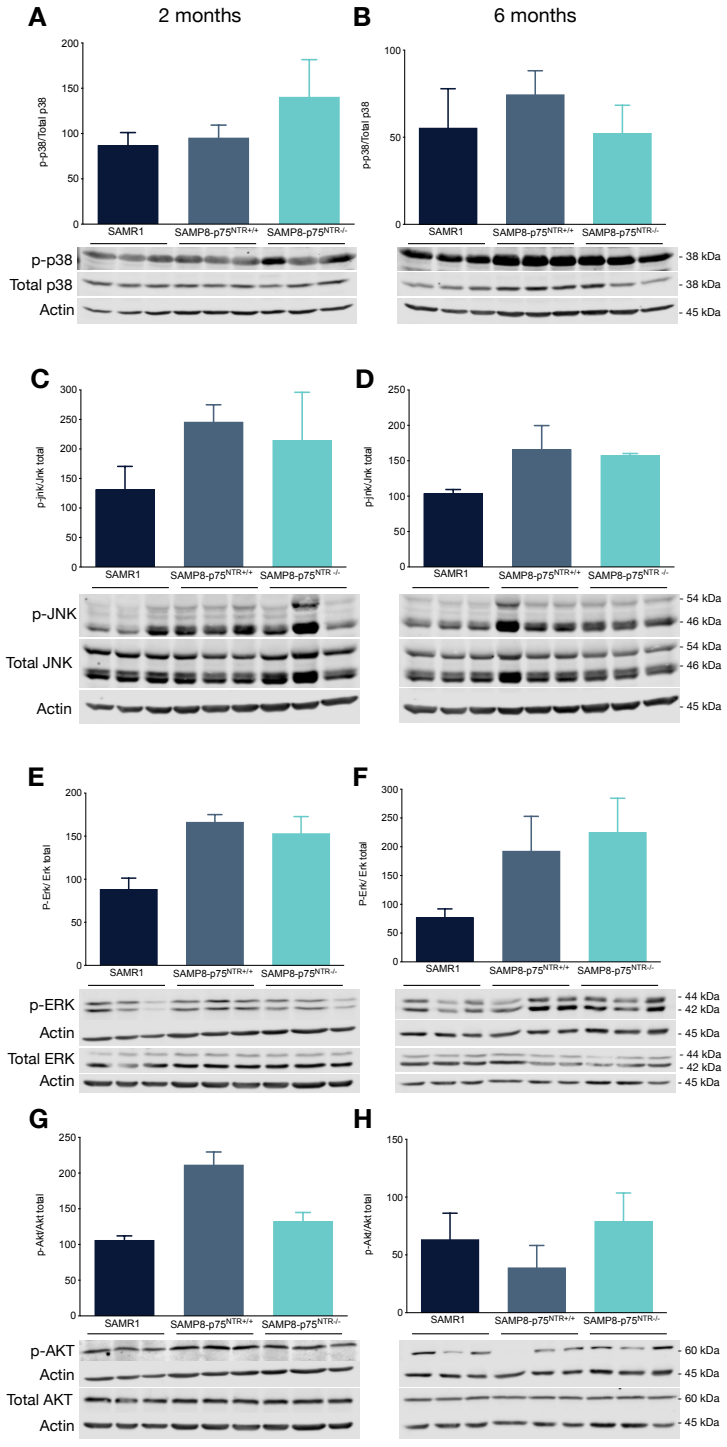

Figure R7:* Analysis of p75^{NTR} signalling routes at different ages in SAMR1, SAMP8-p75$^{NTR+/+}$ and SAMP8-p75$^{NTR-/-}$ mouse lines.** ***A) *Quantification of p-p38 protein levels (normalised with total p38 and actin) at 2 and* ***B)*** *6 months of SAMR1, SAMP8-p75$^{NTR+/+}$ and SAMP8-p75$^{NTR-/-}$ mice.* ***C)*** *Quantification of p-Jnk protein levels (normalised with total Jnk and actin) at 2 and* ***D)*** *6 months of SAMR1, SAMP8-p75$^{NTR+/+}$ and SAMP8-p75$^{NTR-/-}$ mice.* ***E)*** *Quantification of p-Erk levels (normalised with total Erk and actin) at 2 and* ***F)*** *6 months of SAMR1, SAMP8-p75$^{NTR+/+}$ and SAMP8-p75$^{NTR-/-}$.* ***G)*** *Quantification of p-Akt levels (normalised with total Akt and actin) at 2 and* ***H)*** *6 months of SAMR1, SAMP8-p75$^{NTR+/+}$ and SAMP8-p75$^{NTR-/-}$ mice. At the lower panels there is a representative gel of each age. All data is represented as mean ± SEM, N < 3. Student's t-test analysis, n.s.*

1.3.2. p75^{NTR} Does Not Play A Role On The Oxidative Stress Response In The Basal Forebrain

It has been described that SAMP8 background has a higher oxidative stress compared to SAMR1 (Morley et al., 2012). It is also known that p75^{NTR} is linked to oxidative stress routes (Sankorrakul et al., 2021). To determine if SAMP8-p75$^{NTR-/-}$ mice have altered the redox signalling in the BFCNs, an ELISA kit was used to detect HNE adducts, a product consequence of high oxidative stress. BF lysates showed no differences in the amount of HNE adducts between SAMR1, SAMP8-p75$^{NTR+/+}$ and SAMP8-p75$^{NTR-/-}$ mice at the age of 2 months **(Figure R8 A)**. At 6 months of age no significant differences were either found between the 3 different strains **(Figure R8 A)**. In parallel, the response of the BFCNs to oxidative stress was assessed in neuronal primary cultures of C57BL/6-p75$^{NTR+/+}$ and C57BL/6-p75$^{NTR-/-}$ **(Figure R9 A)**. Cholinergic neurons were incubated with different H_2O_2 concentrations (0, 5 and 10 µM) and the percentage of cholinergic apoptosis was quantified with double ChAT and cleaved caspase-3 positive neurons of the total number of ChAT positive neurons. No difference between both genotypes were detected at the different H_2O_2 concentrations used **(Figure R9 B)**, suggesting that p75^{NTR} is not involved in the cell death promoted by the oxidative stress in the BFCNs.

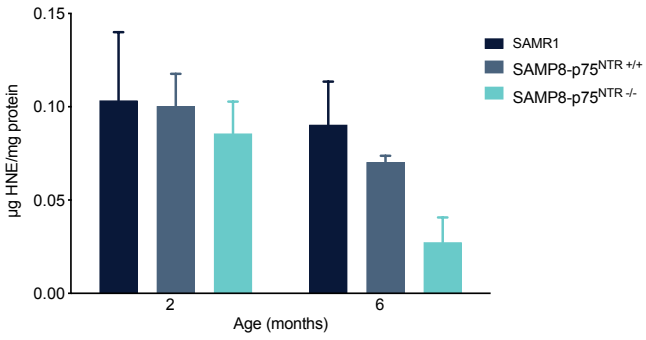

***Figure R8:* HNE adducts ELISA.** *Quantification of HNE adducts in the BF at different ages and genotypes. Data is represented as mean ± SEM, N = 3. Two-way ANOVA followed by Tukey's post-hoc test. n.s.*

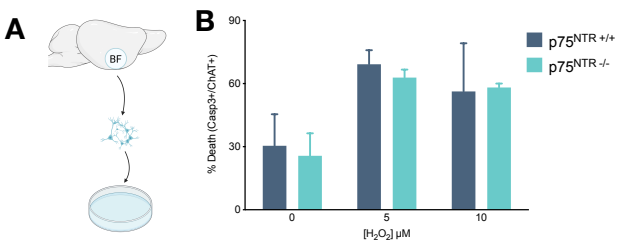

Figure R9:* p75^{NTR} does not change the oxidative response in cholinergic primary culture.** ***A) *Diagram of the generation of the primary culture.* ***B)*** *Percentage of death assessed by cleaved-caspase3 positive neurons divided with ChAT positive neurons at different concentrations of H_2O_2. Data is represented as mean ± SEM, N = 3. One-way ANOVA followed by Tukey's post-hoc test. n.s.*

To further study the role of p75^{NTR} in the oxidative stress response, qPCR of different genes involved in oxidative stress were carried out from BF extracts. The transcription factor NRF2 induces the expression of several anti-oxidant genes such as; HMOX1, GSTa, SOD1 and SOD2 (Buendia et al., 2016) **(Figure R10 A)**. qPCR of BF from SAMR1 and SAMP8 mice showed no differences in the quantity of NRF2 mRNA at 2 moths of age. In contrast, at 6 months SAMP8-p75$^{NTR+/+}$ mice showed a decrease in the expression levels of NRF2 compared to SAMR1 control mice **(Figure R10 B)**. SAMP8-p75$^{NTR-/-}$ animals showed a non-significant reduction (p-value 0.06) in the mRNA levels at 6 months compared to SAMR1 background, indicating that the regulation of NRF2 during ageing is related to SAMP8 strain respect to SAMR1 and it is not associated to p75^{NTR} expression.

NRF2 regulates the expression of HMOX1 (Buendia et al., 2016) and quantification of the mRNA levels of HMOX1 indicated a correlation with the NRF2 mRNA levels. SAMP8-p75$^{NTR+/+}$ and SAMP8-p75$^{NTR-/-}$ mice showed a significant decrease in the expression of HMOX1 at 6 months compared to SAMR1 animals **(Figure R10 C)**. GST1a expression showed a significant decrease in SAMP8-p75$^{NTR+/+}$ mice from 2 to 6 months and no differences between SAMR1 and SAMP8-p75$^{NTR-/-}$ were seen **(Figure R10 D)**. In contrast, there were no differences in the expression of SOD1 or SOD2 genes between mice strains and age **(Figure R10 E-F)**.

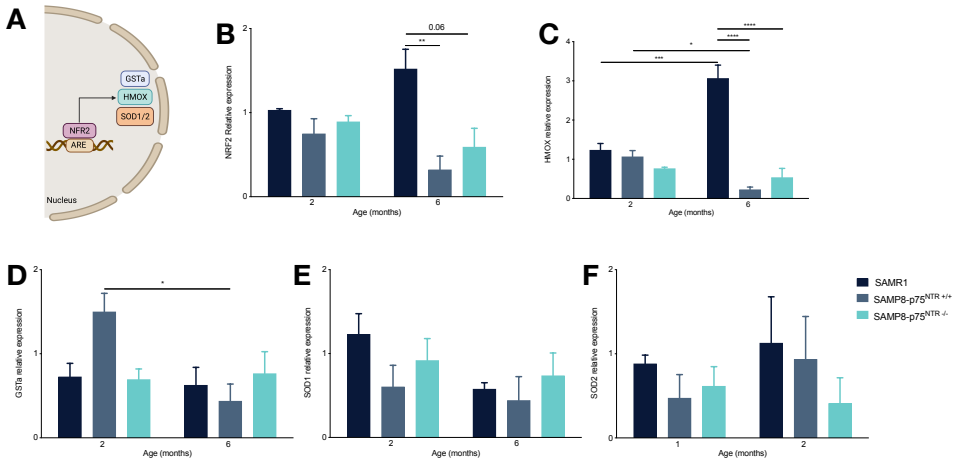

Figure R10: ***SAMP8 background has a reduction in the oxidative response in the basal forebrain compared to SAMR1, but p75^{NTR} does not play a role in it.*** ***A)*** *Scheme of proteins involved in the regulation of oxidative stress response. When NFR2 is activated is translocated into the nucleus and there it binds to ARE sequences and activates the transcription of different genes such as; HMOX, GSTa, SOD1 and SOD2.* ***B)*** *qPCR relative expression of NFR2 transcription factor. SAMP8 mice have a reduction in the expression levels at 6 months.* ***C)*** *qPCR relative expression of HMOX. As NFR2, SAMP8 mice showed an HMOX1 mRNA levels reduction at 6 months.* ***D)*** *qPCR relative expression of GSTa. SAMP8 mice reduce its levels with age.* ***E)*** *qPCR relative expression of SOD1.* ***F)*** *qPCR relative expression of SOD2. All data is represented as mean ± SEM, N = 3. Two-way ANOVA followed by Tukey's post-hoc test. *p < 0.05, **p < 0.01, ***p < 0.001, ****p < 0.0001.*

These results indicate that the main anti-oxidative response in the BF of SAM strains is HMOX1. In addition our results indicated that the higher oxidative stress present in the SAMP8 mice could be the result from a less antioxidant response (i.e less activation of the NRF2/HMOX1 pathway) respect to SAMR1, with no $p75^{NTR}$ implication.

1.3.3. $p75^{NTR}$ Regulates The Expression Of Genes Involved In The Synthesis Of Cholesterol In The Basal Forebrain

Cholinergic neurons are very long and complex projecting neurons (Wu et al., 2014), that require a high amount of lipid and cholesterol synthesis. NTs and $p75^{NTR}$ have been related with cholesterol synthesis in different neuronal types (Korade et al., 2007; Korade et al., 2009). To study if $p75^{NTR}$ have any implications in the cholesterol biosynthesis in BF, different proteins involved in the cholesterol synthesis were analysed by WB and qPCR from SAMR1, SAMP8-$p75^{NTR+/+}$ and SAMP8-$p75^{NTR-/-}$ BF extracts.

The biosynthesis of cholesterol is a highly regulated process. SREBP-2 is cleaved in the ER and translocates to the nucleus to induce the expression of HMGCR, a key and limiting enzyme in the synthesis of cholesterol. HMGCR catalyses the conversion of the HMG-CoA (that comes from acetyl-CoA) to mevalonate in the first step in the synthesis of cholesterol. SREBP-2 also induces the expression of the LDL receptor, LDLR, an important receptor for the neuronal uptake of extracellular cholesterol in the form of LDL particles rich in ApoE. ApoE helps in the interaction between LDL and LDLR to facilitate cholesterol endocytosis **(Figure R11 A)**.

First, the protein levels of HMGCR in the BF were quantified by WB. The quantifications showed a similar HMGCR protein levels at 2 months between the 3 mice genotypes, with a slight increase in the SAMP8-$p75^{NTR-/-}$ **(Figure R11 B)**. This increase in the HMGCR levels in SAMP8-$p75^{NTR-/-}$ was confirmed at the age of 6 months compared to SAMP8-$p75^{NTR+/+}$ (p-value of 0.058) **(Figure R11 C)**. Next, the mRNA levels of LDLR and ApoE by qPCR were analysed. At 2 months of age the expression of LDLR were equal for all strains, but at 6 months SAMR1 and SAMP8-$p75^{NTR-/-}$ showed an increase in LDLR mRNA levels whereas SAMP8-$p75^{NTR+/+}$ mice did not change its levels and presented a decrease when compared with the other 2 mice lines **(Figure R11 D)**. In the same direction, mRNA levels of ApoE showed no differences at 2 months, while at 6 months, there were a decrease in SAMP8 background with age **(Figure R11 E)**, but not in SAMR1 control mice. The cholesterol levels in the BF were measured to confirm if the enzyme and the receptor differences seen were translated into cholesterol changes. At 2 months no differences in cholesterol levels were seen

in SAMR1, SAMP8-p75$^{NTR+/+}$ and SAMP8-p75$^{NTR-/-}$ mice, whereas at 6 months, SAMP8 background showed a reduction of the total cholesterol compared to SAMR1 **(Figure R11 F)**.

In conclusion we found that p75^{NTR} plays a role in the regulation of genes involved in the cholesterol synthesis and homeostasis. There is an induction of genes implicated in the cholesterol that correlates with a decrease in the amount of total cholesterol in the SAMP8-p75$^{NTR-/-}$ mice that may explain why neurons have less survival during ageing. In the next section we ask if the decrease in the number of BFCNs has any implication in different behavioural tasks.

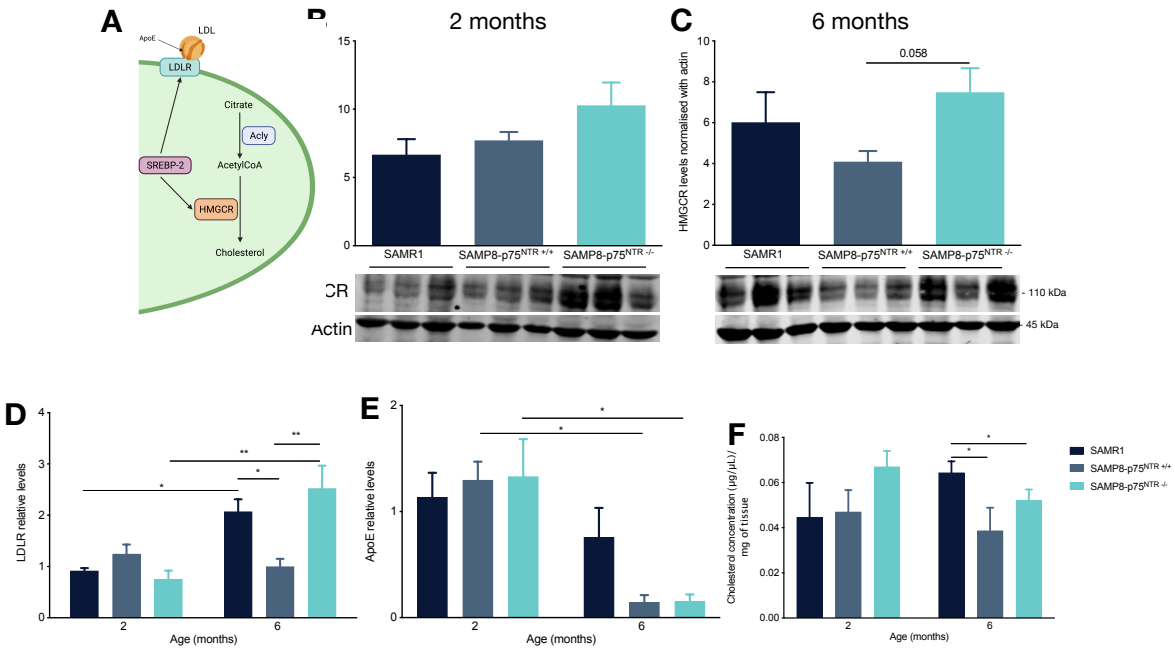

Figure R11: ***p75^{NTR} regulates the expression of the genes involved in the synthesis and homeostasis of cholesterol in the basal forebrain.*** ***A)*** *Scheme of key enzymes in the regulation of cholesterol synthesis. Acetyl-CoA, generated by Acly, can produce cholesterol through HMGCR, key enzyme in cholesterol synthesis regulated by SREBP-2. SREBP-2 also regulates LDLR levels, receptor necessary to uptake the cholesterol.* ***B)*** *Quantification and representation of HMGCR levels by WB at 2* ***C)*** *and 6 months. HMGCR protein levels are higher in SAMP8-p75$^{NTR-/-}$ mice.* ***D)*** *qPCR relative expression of LDLR. LDLR mRNA levels increase with age in SAMR1 and SAMP8-p75$^{NTR-/-}$ mice but not in SAMP8-p75$^{NTR+/+}$.* ***E)*** *qPCR relative expression of ApoE. ApoE mRNA levels decrease with age in SAMP8-p75$^{NTR+/+}$ and SAMP8-p75$^{NTR-/-}$ mice but not in SAMR1.* ***F)*** *Cholesterol levels in BF. SAMP8 background has a cholesterol reduction with age. All data is represented as mean ± SEM, N = 3 (less in Acly protein levels). Student's t-test analysis for Acly and HMGCR protein levels. Two-way ANOVA followed by Tukey's post-hoc test for Acly and LDLR mRNA and cholesterol levels. *p < 0.05, **p < 0.01.*

1.4. The Deletion Of p75^{NTR} In SAMP8 Mice Has An Impact On Behaviour

In order to determine if p75^{NTR} loss has any behavioural implication, different behavioural tests were carried out in a cohort of SAMR1, SAMP8-p75$^{NTR+/+}$ and SAMP8-p75$^{NTR-/-}$ mice at 2 and 6 months of age.

1.4.1. SAMP8 Anxiety Decreases With the Deletion Of p75^{NTR}

The open field test allows the measure of anxiety levels, locomotor activity and exploration activity in rodents (Gould et al., 2009). Anxiety levels are assessed with the percentage of time that the animals spent in the periphery or in the centre of the box. Rodents have an aversion to open spaces (because they are visible to depredators) but they are also willing to explore new areas.

Open field results showed no anxiety levels for SAMR1 mice, as they spent almost half of their time in the centre **(Figure R12 A-C)**. This percentage is lower in SAMP8 mice, they only spent the 15 % of the time in the centre, indicating that SAMP8 is more anxiogenic than SAMR1 mice. Moreover, a significant difference exist between SAMP8-p75$^{NTR+/+}$ and SAMP8-p75$^{NTR-/-}$ mice at 2 and 6 months. SAMP8-p75$^{NTR+/+}$ spends 20 % less time in the centre than SAMP8-p75$^{NTR-/-}$ mice, behaving SAMP8-p75$^{NTR-/-}$ mice more similar to SAMR1 mice **(Figure R12 A-C)**. Hereby, the deletion of p75^{NTR} decreases anxiety levels in SAMP8 background showing a marked tendency to the behaviour of the control strain SAMR1.

Locomotor activity was assessed with open field test and the total distance traveled by the animals were measured. No differences were seen between SAMP8-p75$^{NTR+/+}$ and SAMP8-p75$^{NTR-/-}$ mice at 2 and 6 months **(Figure R12 B-C)**, nevertheless there were a significant decrease in the mobility of SAMP8-p75$^{NTR+/+}$ animals with age not seen in SAMP8-p75$^{NTR-/-}$ mice. Moreover, SAMP8-p75$^{NTR-/-}$ mice move more than SAMR1, indicating a higher hyperactivity **(Figure R12 B-C)**.

1.4.2. The Deletion Of p75^{NTR} In The SAMP8 Has No Effect In Long-Term Memory

Long-term memory was evaluated with novel object recognition test. SAMR1 control mice showed a discrimination ratio higher than 0.5, indicating that they spent more than the half of the time exploring the new object **(Figure R13 A)**, while SAMP8 mice have a discrimination ratio smaller than 0.5, as they spend half of their time in each object, indicating a decrease in the long-term memory **(Figure R13 A)**. No differences were seen between SAMP8-p75$^{NTR+/+}$

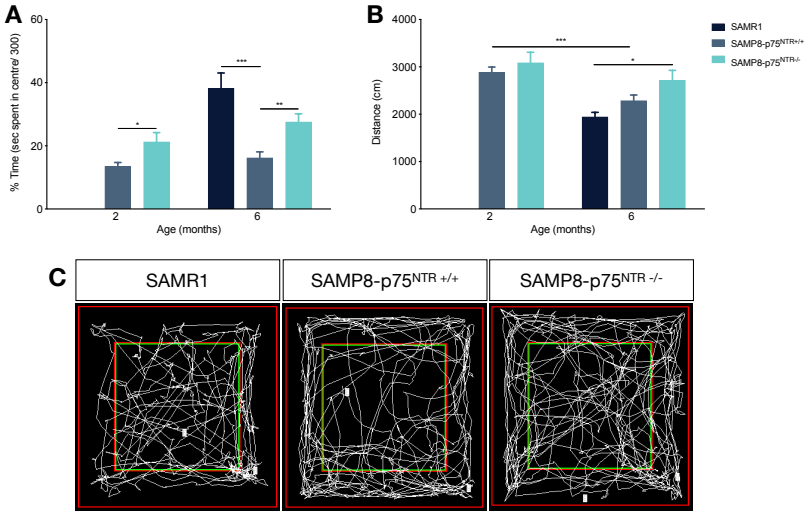

Figure R12: ***SAMP8 anxiety decreases with p75^{NTR} deletion.*** *A) Percentage of the time spent in the centre in the open field test. SAMP8 mice are more anxiogenic than SAMR1 mice. Tough p75^{NTR} deletion partial decreases the anxiety levels. B) Quantification of the distance travelled during the 5 minutes of the open field test at 2 and 6 months. SAMP8 mice showed an hyperactivity that is lost with age. C) Representative images of the different open field measurements. Mean ± SEM, N < 4. Two-way ANOVA followed by Tukey's post-hoc test. *p < 0.05, **p < 0.01, ***p < 0.001.*

and SAMP8-p75$^{NTR-/-}$ mice, thereby the worst performance reported is due to SAMP8 characteristics and is p75^{NTR} independent.
Moreover, in concordance with the open field results, SAMR1 mice spend less time exploring than SAMP8 mice **(Figure R13 B)**.

1.4.3. The Deletion Of p75^{NTR} Causes The Loss Of Spatial Memory With Age

Spatial memory was assessed with the Y-maze test. At young ages, 2 months, there were no differences in the percentage of correct alternations between SAMP8 genotypes **(Figure R14 A)**, nevertheless, SAMP8-p75$^{NTR-/-}$ showed a reduction in the number of correct triplets with age not seen in SAMP8-p75$^{NTR+/+}$ animals, suggesting a lose in spatial memory in the SAMP8-p75$^{NTR-/-}$ mice.

The total number of entries in the arms were quantified **(Figure R14 B)**. Like in the other tests, SAMP8 mice have less mobility with age. Moreover, SAMR1 mice did less entries than SAMP8, suggesting, again, a SAMP8 hyperactivity.

Altogether the decrease in 50 % in the number of BFCNs and in the ACh levels from 2 to 6 months in SAMP8-p75$^{NTR-/-}$ animals may be responsible of the worsening in the cognitive ability. The deletion of p75^{NTR} in the pathological strain SAMP8 induces differences in some of the studied tests, probably depending on the neuronal circuit involved.

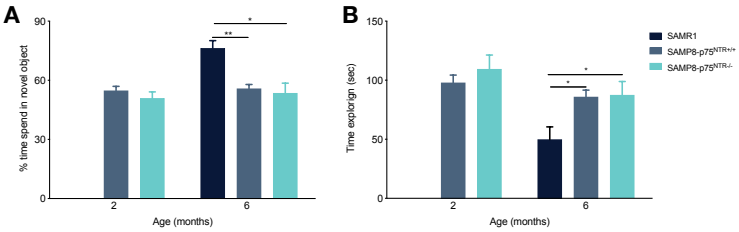

Figure R13: ***The deletion of p75^{NTR} in SAMP8 mice has no effect in long-term memory.*** ***A)*** *Percentage of time spend in the novel object. SAMP8 background showed a loss in long-term memory at 6 months compared to SAMR1 mice.* ***B)*** *Total time of exploration of the two objects. SAMP8 mice showed a bigger time of exploration than SAMR1. Mean ± SEM, N < 4. Two-way ANOVA followed by Tukey's post-hoc test. *p < 0.05, **p < 0.01.*

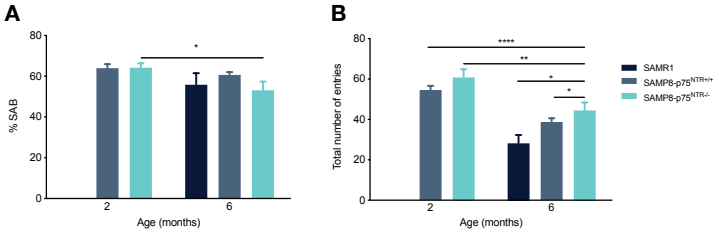

Figure R14: ***p75^{NTR} deletion in SAMP8 mice causes the loss of spatial memory with age.*** ***A)*** *Percentage of SAB (spontaneous alternation behaviour) measured with the number of correct triplets divided per the total triplets. A difference from SAMP8-p75$^{NTR+/+}$ mice, SAMP8-p75$^{NTR-/-}$ loses episodic memory with age.* ***B)*** *Total number of entries in the different arms during 8 minutes. SAMP8 mice loses mobility with age. All test have been made at 2 and 6 months in SAMR1, SAMP8-p75$^{NTR+/+}$ and SAMP8-p75$^{NTR-/-}$ mice. Mean ± SEM, N < 4. Two-way ANOVA followed by Tukey's post-hoc test. *p < 0.05, **p < 0.01, ****p < 0.0001.*

Chapter II

γ-SECRETASE INHIBITION INCREASES BASAL FOREBRAIN CHOLINERGIC NEURONAL COMPLEXITY IN A P75^{NTR} DEPENDENT MANNER

2.1. Basal Forebrain Cholinergic Neuronal Primary Culture Set-up

To study the role of p75^{NTR} shedding in the BFCNs, primary neuronal cultures of basal forebrain were set-up in the laboratory.

The septal area of 17 days embryos was dissected and incubated with A488-p75^{NTR} antibody and/or A633-TrkA antibody and analysed through flow cytometry. The 20 % of the cells were p75^{NTR} positive **(Figure R15 A)** and TrkA positive **(Figure R15 B)**, indicating a proper area localisation and dissection.

The dissociated neurons were cultured and kept alive for 11 days (D.I.V. 11) and fixed for posterior ICC. After 11 D.I.V the 22.12 % of the total nucleus, stained with DAPI, were neurons and the 8.51 % were cholinergic neurons **(Figure R15 C)**. The neuronal population was detected with MAP2, a neuronal specific microtubule protein **(Figure R15 D)**. Cholinergic neurons were detected with p75^{NTR} and ChAT **(Figure R15 E)**. In addition, TrkA, PS1 and PS2 immunocytochemistry were carried out to confirm their expression in cholinergic neurons **(Figure R15 F-H)**.

2.2. The Inhibition Of p75^{NTR} Proteolytic Cleavage Increases Basal Forebrain Cholinergic Neuronal Complexity Through RhoA

2.2.1. The γ-secretase Inhibition Increases Specifically Basal Forebrain Cholinergic Neuronal Complexity

The Compound E (CE), a γ-secretase inhibitor (GSI), was added in BFCNs primary culture and the morphology of cholinergic neurons was studied with Sholl analysis.
An increase in neuronal complexity was detected when an acute dose of CE was added into primary neurons **(Figure R16 A-B)**. A slight effect was already detected after one day, however, the effect increased with time (2 and 3 days) **(Figure R16 A-B)**. In addition to the increase in neuronal complexity, an increase in the length of the neurites was seen **(Figure R16 C)**. The addition of Semagacestat (SG), a GSI drug designed to treat AD that arrived to clinical phase 3, created the same effect; an increase in complexity in BFCNs accentuated at 2 and 3 days **(Figure R16 A-B)**.
The increase in complexity and length was specific for cholinergic neurons as in non-cholinergic neurons (MAP2 positive and ChAT/p75^{NTR} negative), no differences in the complexity were observed when CE was added into the culture for 1, 2 and 3 days **(Figure R17 A-B)**.

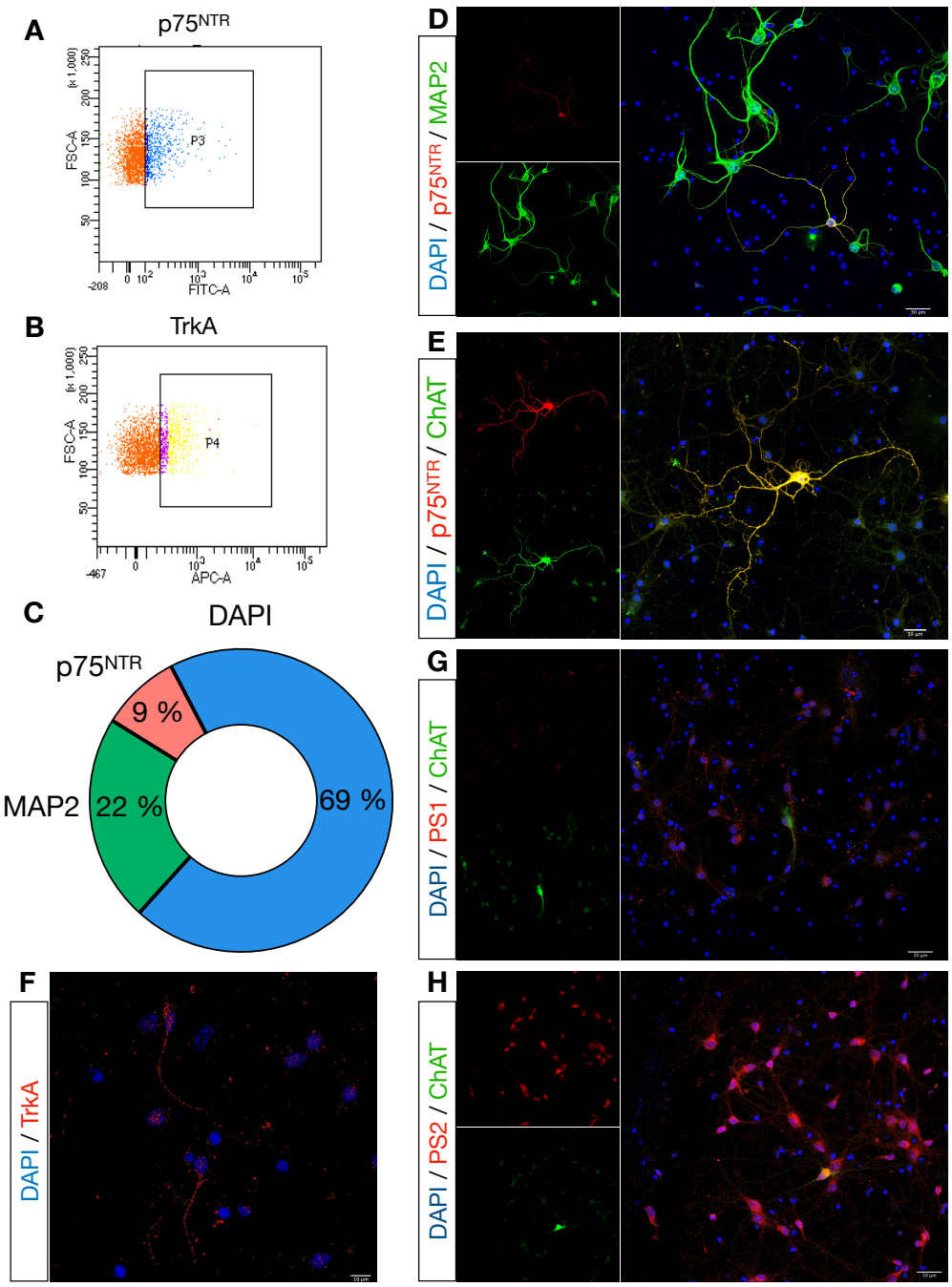

Figure R15: ***Characterisation of basal forebrain cholinergic neurons primary culture.*** ***A)*** *Flow cytometry plot showing the percentage of p75^{NTR} and* ***B)*** *TrkA positive cells after septal disaggregation.* ***C)*** *Percentage of cholinergic neurons after 11 D.I.V. Only 8.5 % of the total neurons were cholinergic.* ***D)*** *Representative image showing MAP2 (green) and p75^{NTR} (red) positive neurons after 11 D.I.V.* ***E)*** *Example of a doubled stained cholinergic neuron with ChAT (green) and p75^{NTR} (red).* ***F)*** *Example of image showing TrkA (red) positive neuron in cholinergic primary culture.* ***G)*** *Example of PS1 (red) and ChAT (green) positive neurons.* ***H)*** *Example of PS2 (red) and ChAT (green) positive neurons.*

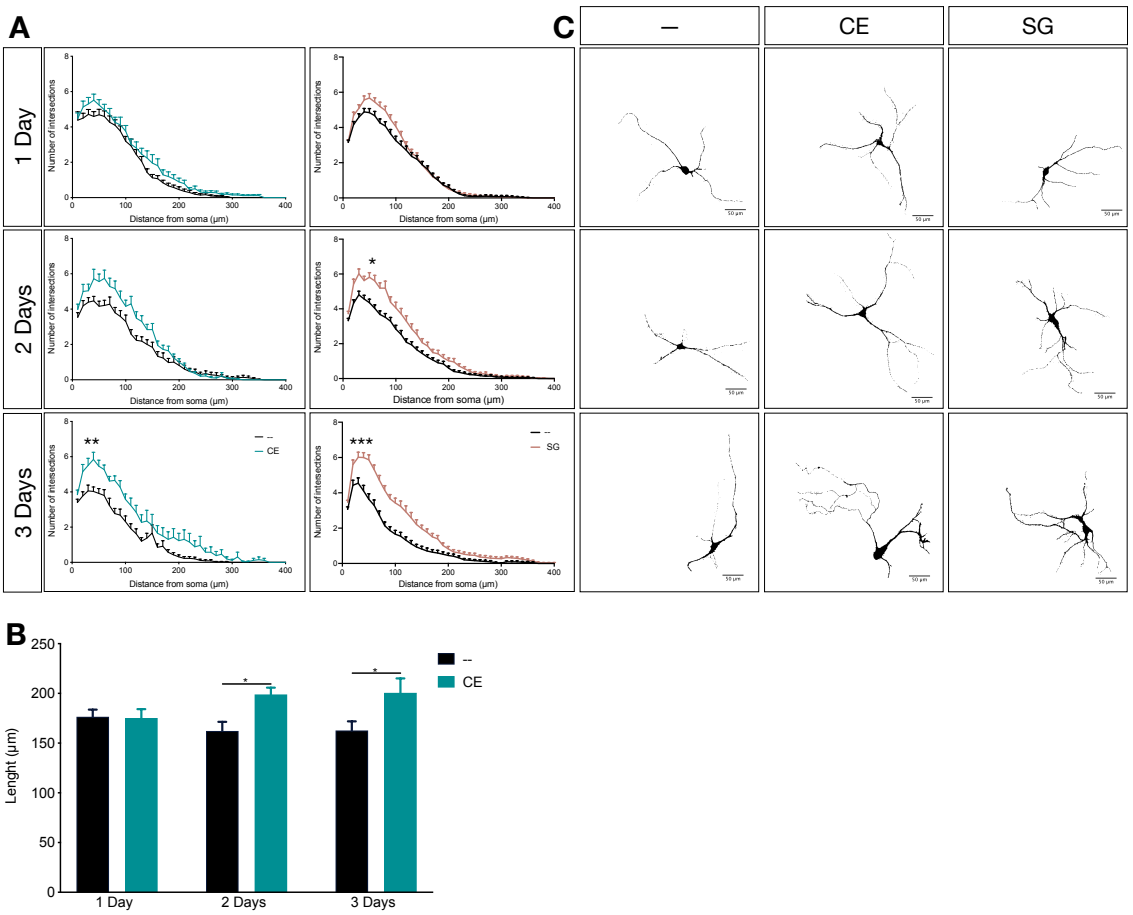

Figure R16: ***γ-secretase inhibition increases basal forebrain cholinergic neuronal complexity and length.*** ***A)*** *Sholl analysis of BFCNs primary culture at D.I.V. 11 and detected with cholinergic markers ChAT and p75^{NTR}. The cultures were incubated for 1, 2 or 3 days with: vehicle (DMSO), γ-secretase inhibitors (CE and Semagacestat). The analysis showed an increase in complexity when the γ-secretase is inhibited starting to be detected at day 1 and significant at day 3. All the data are represented as mean ± SEM, N = 4. Area under the curve and posterior one-way ANOVA test was used to determine the statistical significance, *p < 0.05, **p < 0.01, ***p < 0.001,* ***B)*** *Increase in BFCNs length when CE is added into BFCNs primary culture. Mean ± SEM, N < 4. Two-way ANOVA followed by Tukey's post-hoc test. *p < 0.05.* ***C)*** *Representative BFCNs images showing different complexities upon the indicated conditions at different days.*

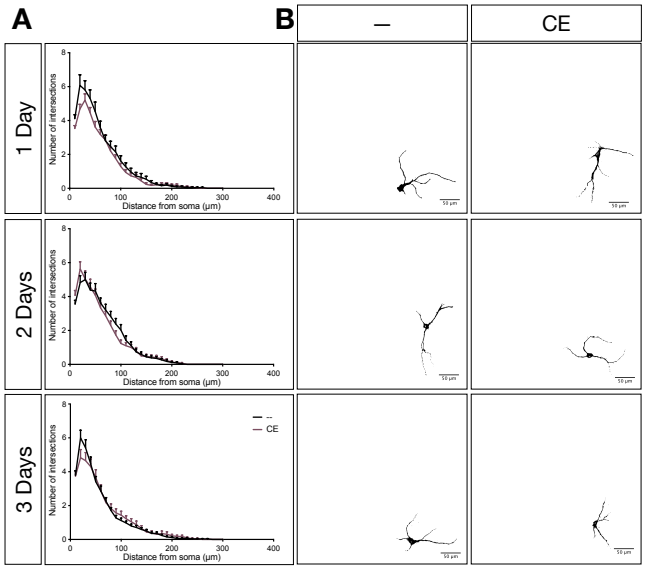

Figure R17: ***γ-secretase inhibition does not increase non cholinergic neuronal complexity.*** ***A)*** *Sholl analysis of non cholinergic neurons at D.I.V 11, detected with neuronal marker MAP2. The cultures were incubated for 1, 2 or 3 days with: vehicle (DMSO) or γ-secretase inhibitor (CE). The analysis showed no differences between treatments. All the data are represented as mean ± SEM, N = 3. Area under the curve and posterior one-way ANOVA test was used to determine the statistical significance.* ***B)*** *Representative neurons showing the same complexity upon the indicated conditions at different days.*

2.2.2. The γ-secretase Inhibition Increases Basal Forebrain Cholinergic Neuronal Complexity In A p75^{NTR} Dependent Manner

As cholinergic neurons express high amounts of p75^{NTR} and p75^{NTR} is a γ-secretase substrate, we hypothesised that the accumulation of p75^{NTR}-CTF, due to an inhibition of the γ-secretase, would be leading the increase of BFCNs complexity.

P75^{NTR} regulated intramembrane proteolysis is a sequential process in which the cleavage of p75^{NTR} by the α-secretase is indispensable for the subsequent γ-secretase cleavage. Therefore, the cultures were treated with CE together with a α-secretase inhibitor, TAPI. The **Figure R18 A-B** shows no increase in complexity when the α-secretase was blocked. Neither when it was added together with CE **(Figure R18 A-B)**. An immunoprecipitation of p75^{NTR} with a p75^{NTR} intracellular antibody was carried out to concentrate p75^{NTR} protein. When the 2 conditions were compared, plus and minus CE, an increase in the levels of p75^{NTR}-CTF were detected **(Figure R18 C)**.

To finally asses that p75^{NTR} is the responsible for the effect, the CE was added into cultures of p75$^{NTR-/-}$ mice and, as a matter of fact, no differences in the complexity of cholinergic neurons were detected after 3 days with CE incubation **(Figure R19 A-B)**.

Altogether, the data suggests that the effect seen on the BFCNs upon GSIs addition is p75^{NTR} dependent and that accumulation of p75^{NTR}-CTF is mediating the increase in BFCNs complexity and length.

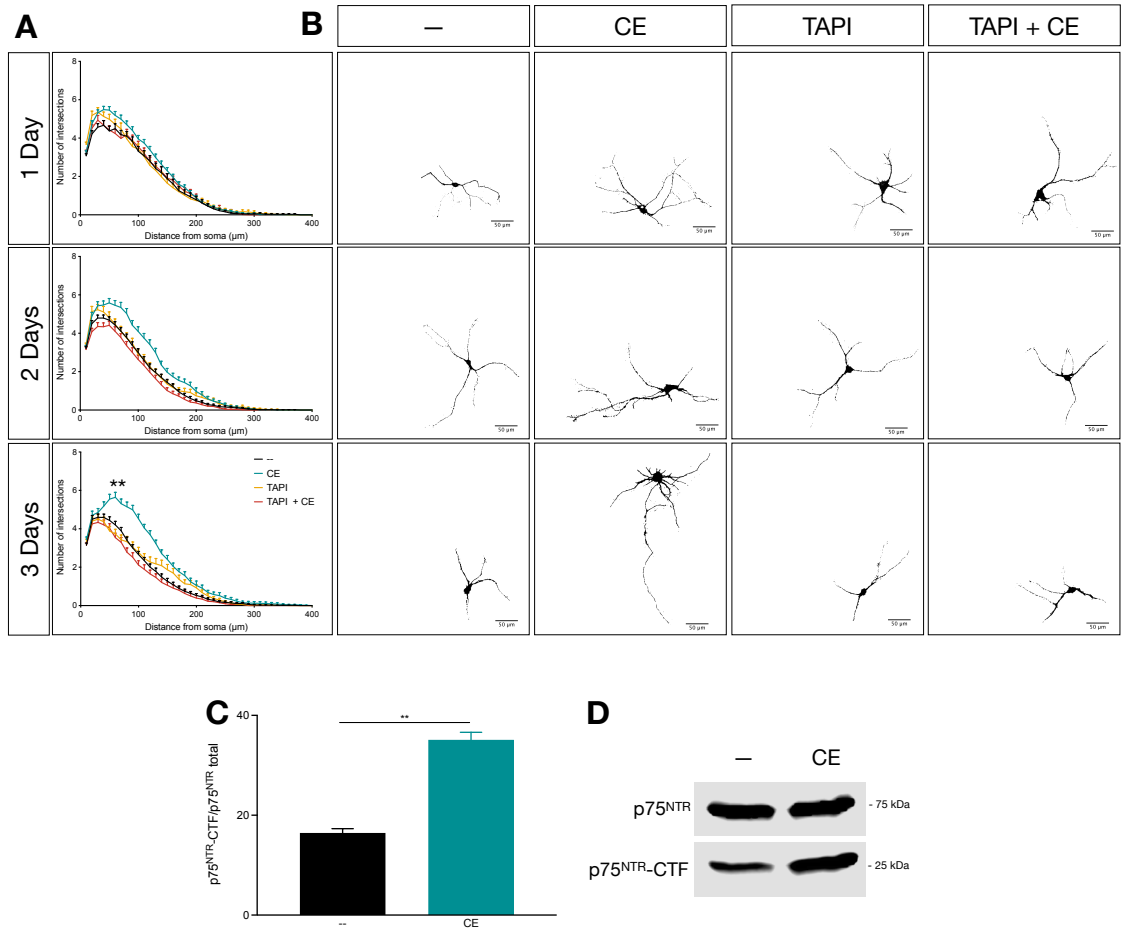

Figure R18: ***γ-secretase inhibition increases basal forebrain cholinergic neuronal complexity and length in a α-secretase dependent manner.*** ***A)*** *Sholl analysis of BFCNs primary culture at D.I.V 11 and detected with cholinergic markers ChAT and p75^{NTR}. The cultures were incubated for 1, 2 or 3 days with: vehicle (DMSO), γ-secretase inhibitor (CE), and α-secretase inhibitor (TAPI). The analysis showed an increase in complexity when the γ-secretase is inhibited starting to be detected at day 1 and significant at day 3. If α-secretase is inhibited the effect is eliminated.* ***B)*** *Representative BFCNs images showing different complexities upon the indicated conditions at different days.* ***C)*** *Quantification of p75^{NTR}-CTF in neuronal cultures. Cultures incubated with CE have more p75^{NTR}-CTF.* ***D)*** *Representative blot of a p75^{NTR} immunoprecipitation incubated with CE. All the data are represented as mean ± SEM, N = 4. Area under the curve and posterior one-way ANOVA test was used to determine the statistical significance, **p < 0.01.*

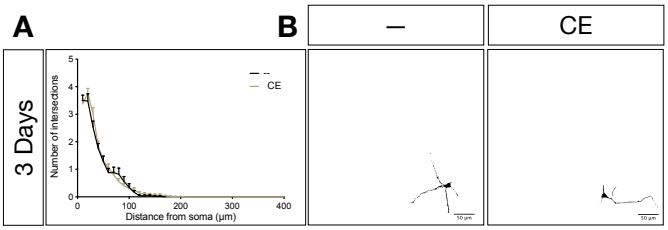

Figure R19: ***γ-secretase inhibition increases basal forebrain cholinergic neuronal complexity and length in a p75^{NTR} dependent manner.*** ***A)*** *Sholl analysis of p75$^{NTR-/-}$ cholinergic neurons of primary culture at D.I.V 7 and detected with neuronal marker ChAT. The cultures were incubated for 3 days with: vehicle (DMSO) or γ-secretase inhibitor (CE). The analysis showed no difference between treatments. All the data are represented as mean ± SEM, N = 6. Area under the curve and posterior student's t-test was used to determine the statistical significance.* ***B)*** *Representative p75$^{NTR-/-}$ cholinergic neurons showing the same complexity upon CE treatment for 3 days.*

2.2.3. p75^{NTR} Acts Through The Small GTPase RhoA To Mediate Basal Forebrain Cholinergic Neuronal Complexity

P75^{NTR} is known regulate RhoA activity, a cytoskeleton regulating protein. P75^{NTR} interacts constitutively with Rho-GDI a protein that inactivates RhoA by sequestering it in the cytosol away from the plasma membrane (Yamaguchi et al., 2001), permitting the RhoA activation and filament contraction (Yamashita & Tohyama, 2003). RhoA triggers mainly its signalling through his downstream effector ROCK.

To check if the increment of BFCNs complexity is due to a RhoA inhibition, the ROCK inhibitor Y-27632, was added into the culture. The ROCK inhibitor generated an increase in the complexity **(Figure R20 A-B)**, similar to the one seen with GSIs. If both inhibitors were added into the culture, a slight increase (not significantly different from both inhibitors alone) in complexity in the area closest to the soma was seen.

To fully confirme the role of RhoA activation downstream of the GSIs, the presence of the active form of RhoA, RhoA-GTP, was detected in cultures using the GST-Rhotekin assay. Rhotekin selectively binds active RhoA-GTP permitting the detection of active RhoA. Primary cultures of BFCNs were incubated with CE and the lysates were analysed by the GST-Rothekin assay showing an increase in the amount of active RhoA in the cells treated with CE **(Figure R20 C-D)**.

In order to confirm our hypothesis about p75^{NTR} implication, the ROCK inhibitor was added into p75$^{NTR-/-}$ culture, and no complexity differences were seen **(Figure R21 A-B)**.

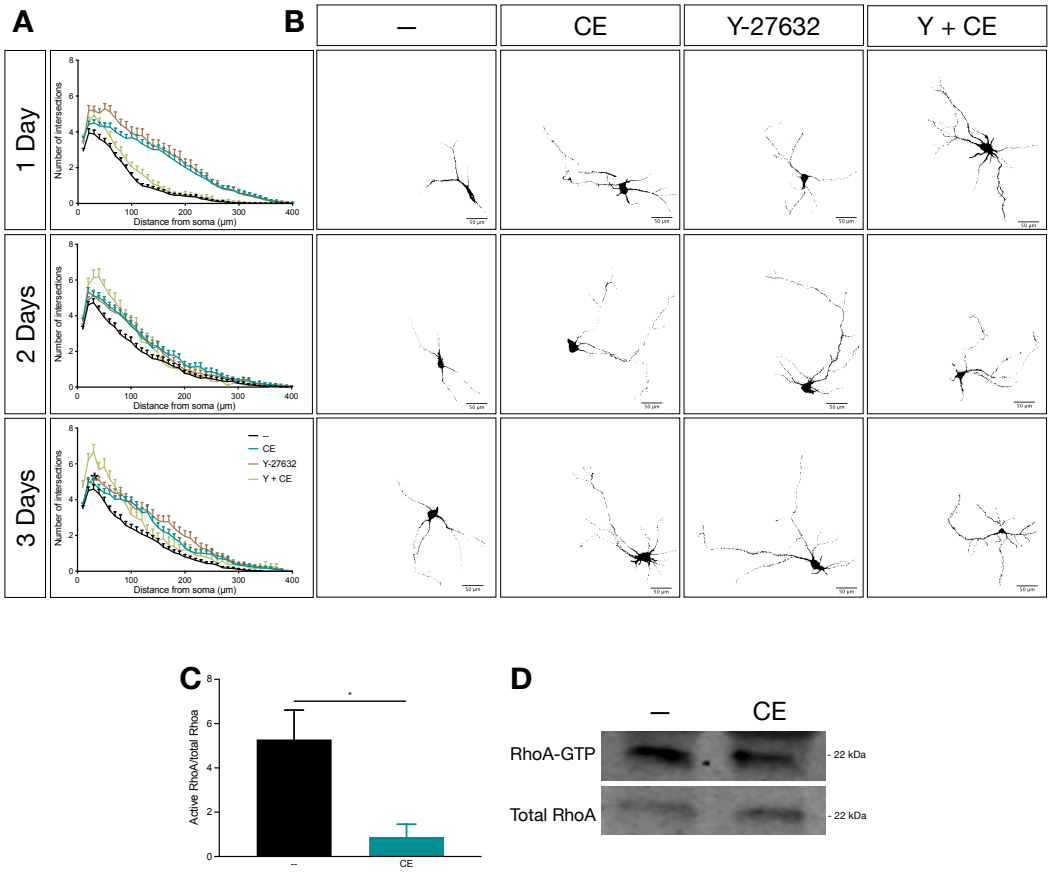

Figure R20: ***p75^{NTR} acts through RhoA to mediate basal forebrain cholinergic neuronal complexity.*** ***A)*** *Sholl analysis of BFCNs primary culture at D.I.V 11 and detected with cholinergic markers ChAT and p75^{NTR}. The cultures were incubated for 1, 2 or 3 days with: vehicle (DMSO), γ-secretase inhibitor (compound E), and ROCK inhibitor (Y-27632). The analysis showed an increase in complexity when the γ-secretase is inhibited starting to be detected at day 1 and significant at day 3. The same effect was seen when RhoA is inhibited. All the data are represented as mean ± SEM, N = 4. Area under the curve and posterior one-way ANOVA test was used to determine the statistical significance, *p < 0.05.* ***B)*** *Representative BFCNs images showing different complexities upon the indicated conditions at different days.* ***C)*** *Quantification of the amount of active RhoA, pulled down with Rothekin.* ***D)*** *Representative gel showing more active RhoA in the condition with vehicle than with CE. Mean ± SEM, N = 3. Student's t-test analysis, * p < 0.05.*

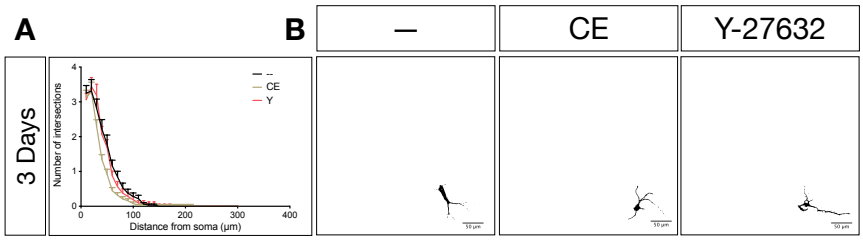

Figure R21: ***γ-secretase inhibition increases basal forebrain cholinergic neuronal complexity and length in a p75^{NTR} dependent manner.*** ***A)*** *Sholl analysis of p75$^{NTR-/-}$ cholinergic neurons at D.I.V 7 and detected with the cholinergic marker ChAT. The cultures were incubated for 3 days with: vehicle (DMSO), γ-secretase inhibitor (CE) or ROCK inhibitor (Y-27632). The analysis showed no differences between treatments. Area under the curve and posterior one-way ANOVA test was used to determine the statistical significance.* ***B)*** *Representative neurons showing the same complexity upon the indicated condition at 3 days.*

2.3. Organotypic Brain Slices Culture Set-up

Primary cultures are a good tool to study physiological effects, but it has some limitations, for example, neurons cannot reach their real target, the cells are dissociated from their environment and they are attached into coated plates. For that reason, an *ex vivo* technique such as organotypic brain slices of BF was used (see Material and Methods for details).

Cholinergic neurons are dependent from neurotrophic factors, specially NGF. BF slices from postnatal mice (P10) were kept for two weeks in culture with or without NGF, and posterior analysed by p75^{NTR} IHC. The quantification showed no significant differences in the number of cholinergic neurons comparing both conditions **(Figure R22 A-B)**. However, neurons incubated with NGF showed a bigger diameter than the neurons without NGF, indicating a healthier neuron **(Figure R22 C-D)**.

2.3.1. Basal Forebrain Cholinergic Neuronal Complexity Increases In Mouse Brain Organotypic Slices When The γ-secretase Is Inhibited

Organotypic slices were used to confirm the effect in the complexity of the γ-secretase inhibition. Therefore, the slices were incubated with CE for two weeks and stained with p75^{NTR} by IHC. Sholl analysis showed an increase in the complexity of cholinergic neurons in the organotypic slices incubated with CE compared to the vehicle **(Figure R23 A)**. In addition, organotypic slices were incubated with the ROCK inhibitor and an increase in the complexity was observed **(Figure R23 B)**, suggesting the same role in both inhibitors. Altogether, this data demonstrated that the higher complexity seen in BFCNs upon GSIs takes place in *ex vivo* experiments as well as in primary neuronal culture in a p75^{NTR} dependent manner through RhoA inactivation.

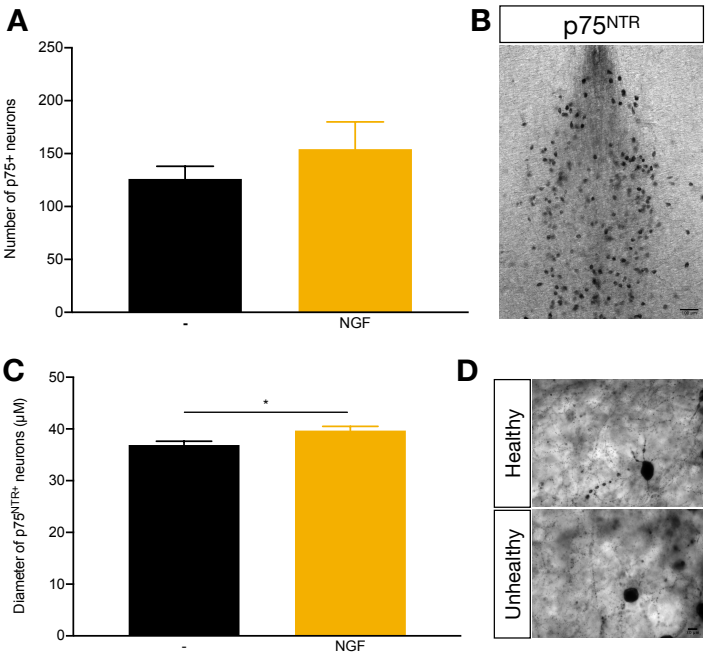

Figure R22: ***Set up of organotypic brain slices culture.*** ***A)*** *Quantification of cholinergic neurons in organotypic slices. The number of p75^{NTR} positive neurons in the basal forebrain of organotypic slices did not change with our without NGF.* ***B)*** *Example of p75^{NTR} IHC of organotypic slices.* ***C)*** *Diameter quantification of p75^{NTR} positive neurons in organotypic slices.* ***D)*** *Representative images of a healthy neuron, with a bigger soma, and unhealthy with a smaller soma.*
*Mean ± SEM, N = 6. Student's t-test, * p < 0.05.*

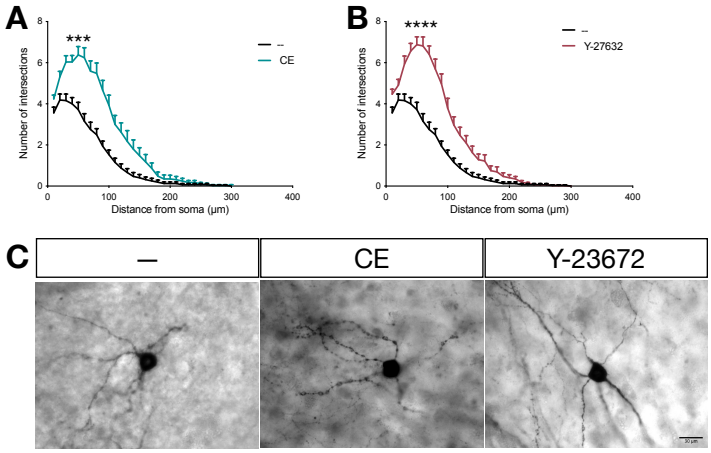

Figure R23: ***γ-secretase inhibition increases basal forebrain cholinergic neuronal complexity in organotypic slices.*** ***A)*** *Sholl analysis of cholinergic neurons of organotypic slices incubated 14 days and detected with cholinergic marker p75^{NTR}. The cultures were incubated since D.I.V. 0 with: vehicle (DMSO) or γ-secretase inhibitor (CE). The analysis showed an increase of complexity in cholinergic neurons treated with CE.* ***B)*** *Sholl analysis of cholinergic neurons of organotypic slices incubated for 14 days and detected with the cholinergic marker p75^{NTR}. The cultures were incubated all days with: vehicle (DMSO) or ROCK inhibitor (Y-27632). The analysis showed an increase in complexity in cholinergic neurons treated with Y-27632.* ***C)*** *Representative neurons showing the complexity upon the indicated condition. Mean ± SEM, N = 3. Area under the curve and posterior Student's t-test was used to determine the statistical significance, ****p < 0.0001.*

2.4. CamKII^{CRE};PS1$^{f/f}$;PS2$^{-/-}$ Mice As A Model To Study γ-secretase Inhibition In The Basal Forebrain Cholinergic Neurons

The previous data was generated from acute chemical inhibition in primary cultures or organotypic slices. To confirm the effect *in vivo*, transgenic mice with null γ-secretase activity, double knock-out mice of PS1 and PS2, were used. PS2$^{-/-}$ mice are viable and fertile, however, PS1$^{-/-}$ mice are lethal and die before birth. Thus the CamKII^{CRE};PS1$^{f/f}$ conditional mouse model was used. As controls, CamKII^{CRE-};PS1$^{f/f}$;PS2$^{-/-}$ (PS2 single knock-out animals) were used. To simplify, from here on named CRE-. For γ-secretase complete activity inhibition CamKII^{CRE+};PS1$^{f/f}$;PS2$^{-/-}$ animals were used. To simplify, from here on named CRE+.

To confirm the proper CRE recombinase activity, PS1 expression was confirmed by IHC in the cortex, where there is the major CamKII expression. The images showed a major loss of PS1 signal at 2 months of age in CRE+ animals compared to CRE- **(Figure R24 A)**. The brains of CRE- and CRE+ animals showed no differences in the brain size at 2 months of age. But at 8 months, CRE+ animals present a reduction of the brain size **(Figure R24 B)**. Correlated with the size, CRE- and CRE+ brains weight the same at two months, but at 8 months brains of CRE+ animals present a significant reduction in the weight **(Figure R24 C)**. This reduction in size and weight can be explained partially due to the enlargement of the ventricles in CRE+ animals at 8 months of age **(Figure R24 D)**. These mouse characteristics were described in Saura et al., 2004.

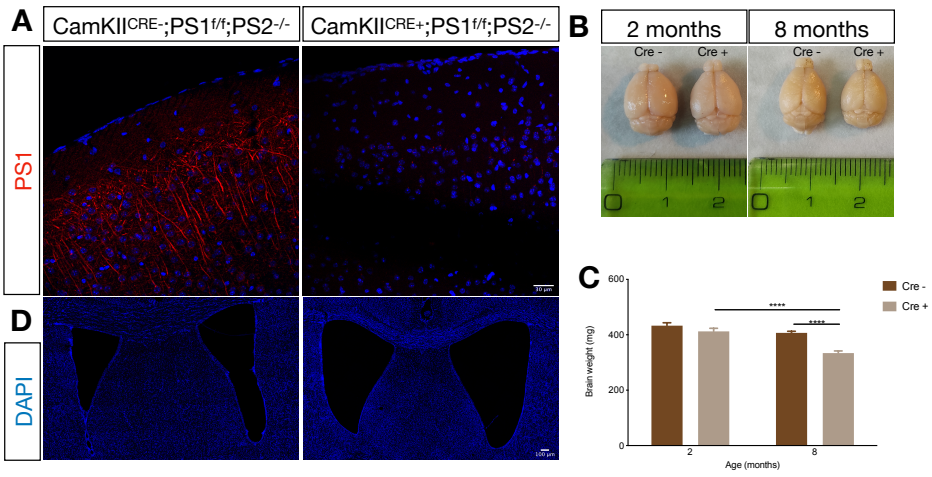

Figure R24: ***CRE+ mice have less brain volume than CRE- mice.*** ***A)*** *PS1 IHC in cortex. CRE+ animals showed a PS1 signal loss (red) compared to CRE- animals.* ***B)*** *Representative brains at 2 and 8 months. CRE+ animals showed a size reduction in brain size at 8 months of age.* ***C)*** *Brain weights of CRE- and CRE+ at 2 and 8 months. CRE+ brains lose weight with age. Mean ± SEM, N < 4. Two-way ANOVA followed by Tukey's post-hoc test. ****p < 0.0001.* ***D)*** *DAPI staining (blue) showing ventricle enlargement in CRE+ animals.*

Nevertheless, our objective was to study the loss of functionality of both PSs in the BFCNs. For that, PS1 loss of expression was confirmed in the BFCNs by IHC and WB. Western blot showed a reduction in the total amount of PS1 in the BF of CRE+ animals at 3 months of age **(Figure R25 A-B)**. By IHC CRE- animals showed PS1 (red) staining localised in the form of dots in BFCNs cholinergic neurons (green) that are not present in CRE+ animals **(Figure R25 C)**.

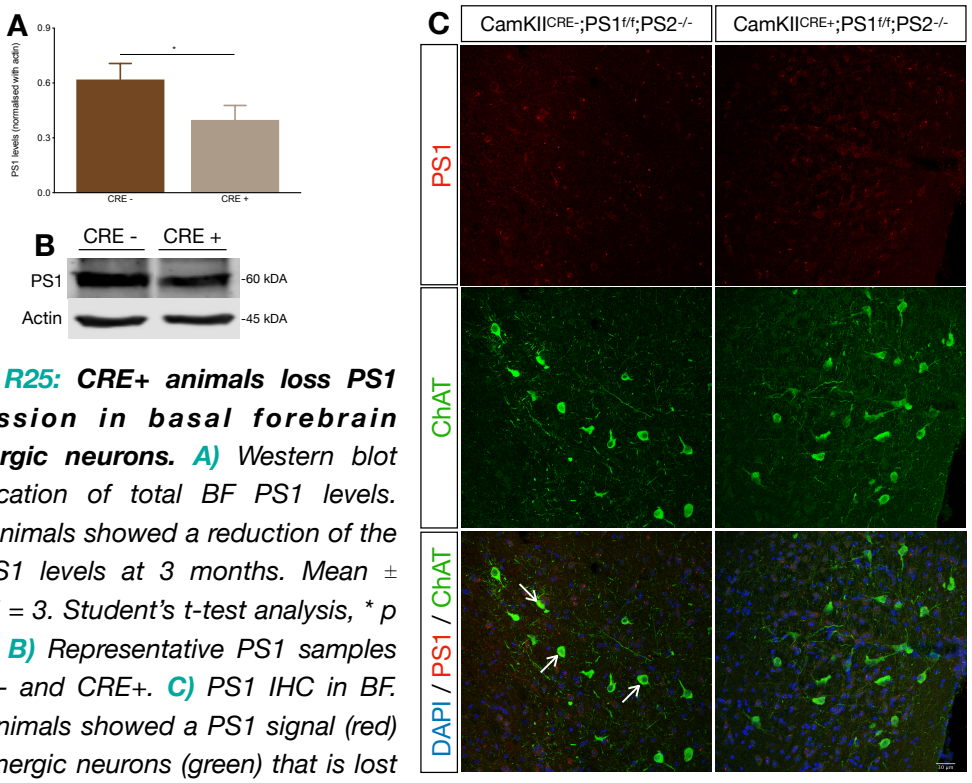

Figure R25: ***CRE+ animals loss PS1 expression in basal forebrain cholinergic neurons.*** ***A)*** *Western blot quantification of total BF PS1 levels. CRE+ animals showed a reduction of the total PS1 levels at 3 months. Mean ± SEM, N = 3. Student's t-test analysis, * p < 0.05.* ***B)*** *Representative PS1 samples of CRE- and CRE+.* ***C)*** *PS1 IHC in BF. CRE- animals showed a PS1 signal (red) in cholinergic neurons (green) that is lost in CRE+ animals.*

2.4.1. The γ-secretase Inhibition Has No effect In Organotypic Brain Slices

In order to study if the complexity seen with the chemical inhibition was also reported in the genetically inhibited animals, organotypic slices of CRE- and CRE+ mice were made and the GSI CE was added into them. The chemical inhibition of the γ-secretase with CE had no complexity effect in CRE+ mice organotypic slices **(Figure R26 A)**. When the ROCK inhibitor was added into the slices, a slight increase in the complexity (no significant) was seen in CRE+ animals **(Figure R26 B)**, indicating a major RhoA inhibition in γ-secretase inhibited mice models.

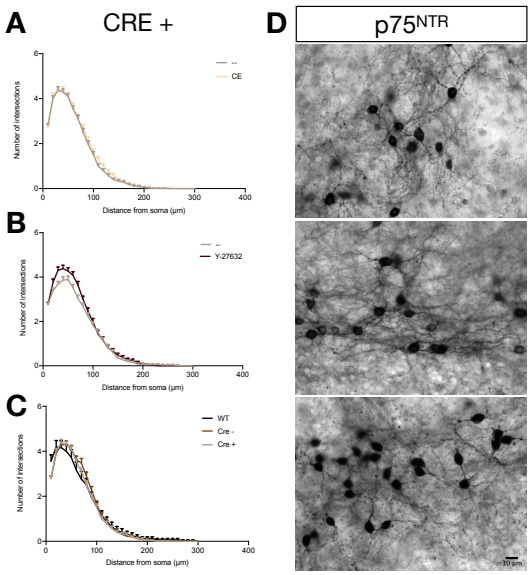

Figure R26: ***The genetic inhibition of the γ-secretase does not increase basal forebrain cholinergic neuronal complexity in organotypic slices.*** ***A)*** *Sholl analysis of cholinergic neurons of organotypic slices incubated for 14 days and detected with p75^{NTR}. The cultures were incubated since D.I.V. 0 with: vehicle (DMSO) or γ-secretase inhibitor (CE). The analysis showed no differences when the CE was added.* ***B)*** *Sholl analysis of cholinergic neurons of organotypic slices incubated for 14 days and detected with p75^{NTR}. The cultures were incubated since D.I.V. 0 with: vehicle (DMSO) or ROCK inhibitor (Y-27632). The analysis showed no differences when the compound was added. Mean ± SEM, N = 3. Area under the curve and posterior Student's t-test was used to determine the statistical significance.* ***C)*** *Basal complexity of BFCNs it is not different in the different genotypes in organotypic slices.* ***D)*** *Representative images of organotypic slices.*

2.4.2. The γ-secretase Inhibition Has An Effect In Basal Forebrain Cholinergic Neuronal Survival And Complexity

The inhibition of the γ-secretase generates hippocampal and cortex neuronal death (Kang & Shen, 2020) so we asked ourselves if BFCNs suffers as well from neurodegeneration when the γ-secretase is inhibited *in vivo*. As showed in **Figure R27 A-B**, at 2 and 4 months of age there were no differences in the number of ChAT positive neurons in the MS/VDB between CRE- and CRE+ mice, nevertheless, at the age of 8 months a decrease in the number of ChAT positive neurons was quantified (p-value of 0.051) **(Figure R27 A-B)**.

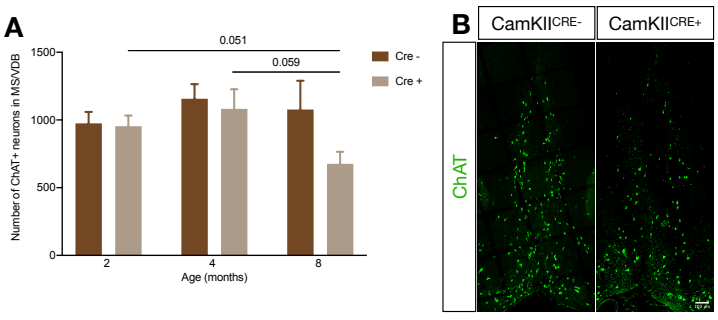

Figure R27: ***The genetic inhibition of the γ-secretase decreases the number of basal forebrain cholinergic neurons with age.*** ***A)*** *ChAT positive neurons in the MS/VDB of CRE- and CRE+ mice. At the age of 2 months there were no differences in the number of cholinergic neurons, but at 8 months CRE+ animals showed a reduction in the number of BFCNs. Mean ± SEM, N < 4. Two-way ANOVA followed by Tukey's post-hoc test.* ***B)*** *Representative images of ChAT (green) positive neurons in the MS/VDB.*

AchE fibres showed an increase of the area of intensity in CRE+ mice compared to CRE- animals in the cortex and in the HC at 2 months of age **(Figure R28 A-B)**, indicating a bigger amount of fibres and therefore an increase in complexity. This result goes in accordance with the chemical inhibition of the γ-secretase.

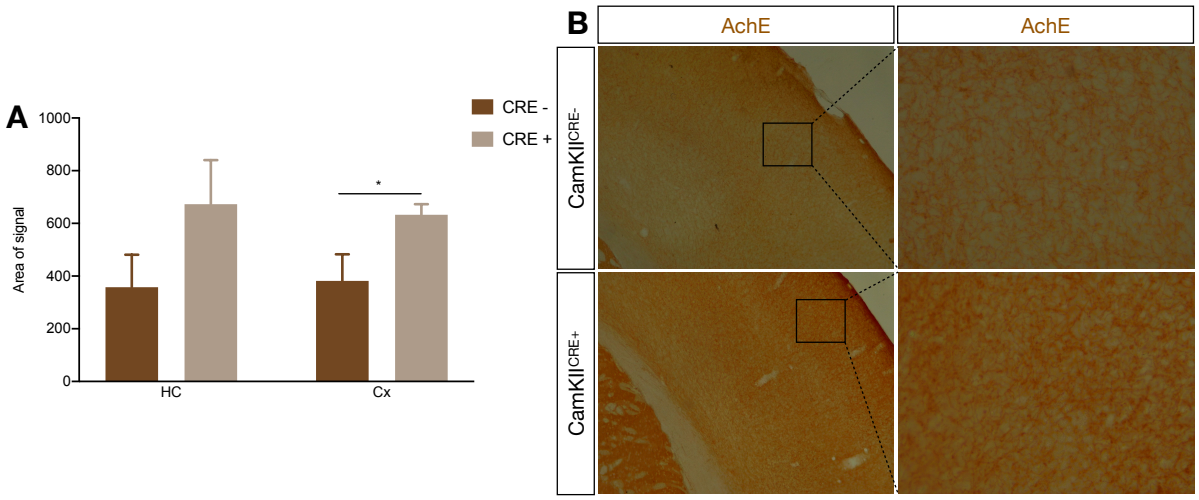

Figure R28: ***The genetic inhibition of the γ-secretase increases AchE fibres in the cortex and in the hippocampus.*** ***A)*** *Quantification of the area with AChE signal in the cortex and in the HC at 2 months. CRE+ animals showed an increase in the area with signal compared to CRE- animals. Mean ± SEM, N < 3. Two-way ANOVA followed by Tukey's post-hoc test.* ***B)*** *Representative images of AChE fibres in CRE+ and CRE- animals in the Cx. Cx: cortex; HC: HC.*

2.5. γ-secretase And TrkA Inhibition Induce Basal Forebrain Cholinergic Neuronal Death In A $p75^{NTR}$-Dependent Manner

Semagacestat is a γ-secretase inhibitor designed to treat AD patients. The drug arrived to clinical phase 3, but at that stage, the clinical trial had to stop due to a worsening in cognitive functions of AD patients (Doody et al., 2013). In addition, a reduction in TrkA signalling in cholinergic neurons of AD patients was reported (Counts & Mufson, 2005; Mufson et al., 2008). With this scenario we wondered if the inhibition of the γ-secretase together with an inhibition of TrkA signalling, like in AD patients, would have any effect.

The survival of cholinergic neurons was assessed through ChAT and Cleaved-caspase-3 double ICC. The inhibition of the γ-secretase or the inhibition of TrkA signalling (with K252a compound) alone were no toxic for the BFNCs after 1, 2 or 3 days of incubation **(Figure R29 A)**. But, the impairment of TrkA signalling together with the inhibition of the γ-secretase produced a significant increase, around 40 %, in cholinergic cell death after 2 and 3 days of incubation **(Figure R29 A)**. This increase in cholinergic neuronal death was completely rescued in $p75^{NTR-/-}$ primary cultures **(Figure R29 A)**, demonstrating a $p75^{NTR}$ dependence mediating cell death upon γ-secretase and TrkA inhibition. **Figure R29 B** shows an example of a ChAT surviving neuron (green) and a ChAT double stained neuron (green and red).

In accordance with it, when human $Aß_{1-42}$ together with K252a is added into the culture, there were an increase in the cholinergic cell death comparable to the one reported with the addition of CE and K252a **(Figure R29 C)**. The effect is specific for the human $Aß_{1-42}$ as the addition of $Aß_{1-17}$ together with K252a did not generate cholinergic death **(Figure R29 C)**.

These data suggest that in adult cholinergic neurons with high expression levels of $p75^{NTR}$, together with TrkA activity impairment, as occurs in BFCNs from elderly people and AD-patients, treatment with GSI drives to cholinergic neuronal apoptosis and cell death.

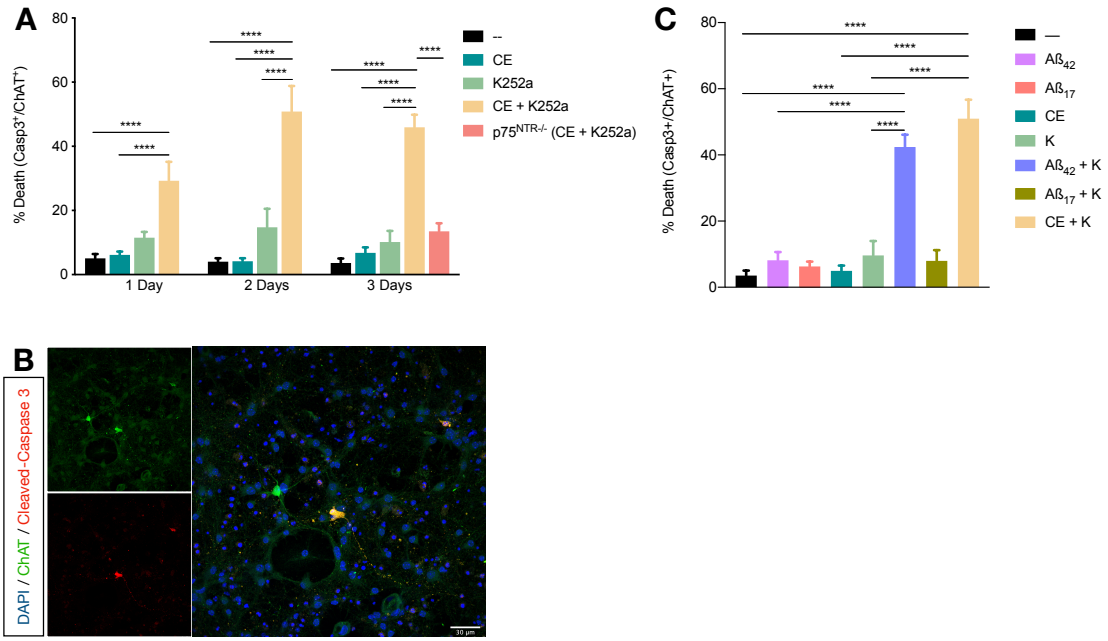

Figure R29: ***TrkA signalling inhibition and γ-secretase inhibition together cause basal forebrain cholinergic neuronal death in a p75^{NTR} dependent manner.*** ***A)*** *Apoptotic cell death analysis of mature BFCNs (ChAT^{+}) from p75$^{NTR+/+}$ and p75$^{NTR-/-}$ mice at D.I.V 11. BFCNs were incubated with vehicle (DMSO), γ-secretase inhibitor (CE), and TrkA inhibitor (k252a), over 3 days and stained for cleaved caspase-3. Quantification of cleaved caspase-3^{+}/ChAT^{+} cells in the respective immunofluorescences showed a significant cell death increase upon inhibition of TrkA signalling and γ-secretase. The effect is rescued in p75$^{NTR-/-}$ neurons. Mean ± SEM, N = 3. Two-way ANOVA followed by Tukey's post-hoc test. ****p < 0.0001.* ***B)*** *Representative BFCNs confocal images stained for ChAT (green) and cleaved caspase-3 (red).* ***C)*** *Apoptotic cell death analysis of BFCNs. Neurons were incubated with vehicle (DMSO), γ-secretase inhibitor (CE) TrkA inhibitor (k252a), Aß$_{1-42}$, Aß$_{1-17}$ or in combination over 3 days and stained for cleaved caspase-3. Quantification of cleaved caspase-3^{+}/ChAT^{+} cells in the respective immunofluorescences showed a significant cell death increase upon inhibition of TrkA signalling and γ-secretase. Mean ± SEM, N = 3. Student's t-test analysis, ****p < 0.0001.*

DISCUSSION

The present thesis focuses on the study of p75^{NTR} in the basal forebrain cholinergic neurons. Fundamentally, the work has been divided in two objectives: studying the role of the receptor during ageing, and assessing the role of p75^{NTR}-regulated intramembrane proteolysis in mature cholinergic neurons. Our interest in BFCNs stems from their critical role in superior cognitive processes such attention, memory and learning, but more importantly for their susceptibility to degeneration during ageing and AD (Ballinger et al., 2016). Cholinergic neurons maintain high levels of the neurotrophin receptor p75 throughout their whole life, although the role of the receptor is ambiguous. Thereby, our work has contributed to shed light to part of this unknown function.

Chapter I comprises the results obtained with a new transgenic mouse developed in our laboratory. This new mouse model has a deletion on the p75^{NTR} gene in the SAMP8 background, which allows the study of cholinergic neurodegeneration during ageing. Chapter II explains the results obtained regarding the role of p75^{NTR}-regulated intramembrane proteolysis in mature cholinergic neurons.

1. p75^{NTR} Plays A Survival Role In Basal Forebrain Cholinergic Neurons During Adulthood And Ageing

A null p75^{NTR} mouse model was generated many years ago by Lee et al., 1992. Since then a plethora of studies have used this murine model to study the role of p75^{NTR} in BFCNs. If p75$^{NTR-/-}$ mice show any differences in the number of cholinergic neurons during their youth is still debatable. Some researchers showed a decrease in the number of cholinergic neurons in p75^{NTR} knock-out mice (Peterson et al., 1997; Peterson et al., 1999), others showed no differences (Greferath et al., 2000; Ward et al., 2000), and the vast majority showed an increase in the number of BFCNs, which correlates with the results from the present thesis (Yeo et al., 1997; Krol et al., 2000; Naumann et al., 2002; Greferath et al., 2012; Boskovic et al., 2014). It is important to highlight that even though the mutation of p75^{NTR} is the same in nearly all the previously published research, the background from the mice used in those studies was different. The studies which reported a decrease in the number of BFCNs used mice with a mixed background (Balb/c-129/Sv). However, the two studies reporting no differences used mice with a 129/Sv background. All the other research has been made with Balb/c or C57BL/6 pure lines. In addition, Naumann et al., 2002 generated a new null p75^{NTR} mice, with the exon IV deleted, and reported an increase in the number of cholinergic neurons. In the work of Boskovic et al., 2014, a p75$^{NTRfl/fl}$ conditional mouse was generated, and an increase in the number of cholinergic neurons was also reported when mice were bred with ChAT^{CRE}. Although it is not proved, the differences in mice background are a good explanation to understand the changes reported in the number of BFCNs throughout the literature.

Our results confirmed the increase previously observed in the number of BFCNs at 2 months of age in C57BL/6-p75$^{NTR-/-}$ mice. Additionally, our new transgenic mice SAMP8-p75$^{NTR-/-}$ also show an increase in the number of BFCNs at young ages. These two mouse lines have a complete different background, hereby, we can conclude that during development one of the roles of p75^{NTR} in BFCNs is pro-apoptotic, since its deletion induces an increase in the number of BFCNs in different mice lines. However, other hypothesis could not be discarded, since they might play a role in neuronal precursor proliferation or in cell cycle withdrawal.

Apart from the characterisation at young ages (2 months), the number of BFCNs were quantified in a longitudinal study, from 2 to 10 months, in the case of SAMP8 (accelerated ageing), and from postnatal day 16 to 24 months in the case of C57BL/6 (healthy ageing). To our knowledge, this long-term study has not been described before. Our results show a significant reduction in the number of cholinergic neurons in SAMP8-p75$^{NTR-/-}$ mice, which is accompanied with a reduction in the cholinergic protein markers ChAT and Acly. ChAT is the enzyme that synthesises the neurotransmitter ACh, therefore if there is a reduction in the number of cholinergic neurons, a decrease in ChAT protein levels will follow. Acly plays a very important role in cholinergic neurons, since it is the enzyme that catalyses the cleavage of citrate into oxaloacetate and acetyl-CoA. Acetyl-CoA is the primary substrate for ACh synthesis, cholesterol and fatty acids, so our results show a correlation between a reduction in the number of BFCNs and a reduction in Acly levels. The levels of ACh are also reduced in SAMP8-p75$^{NTR-/-}$ mice at 6 months in parallel with the number of cholinergic neurons.

Importantly, if cholinergic neurons have died or if they have lost their cholinergic features remain unknown. A good way to solve it would be using a conditional cholinergic CRE mice with a GFP reporter. The combination of SAMP8-p75$^{NTR-/-}$ mice with a ChAT^{CRE} mice and a GFP reporter would label cholinergic neurons with green fluorescence for their whole life. Therefore, if the number of BFCNs and the number of green neurons were the same at 6 months, very probably there would be neuronal death. Nonetheless, if there was a bigger number of green neurons than ChAT positive neurons, it would indicate a loss in cholinergic characteristics.

2. SAMP8-p75$^{NTR-/-}$; A Mouse Model To Study Cholinergic Degeneration

Cholinergic synapses are ubiquitous in the CNS. The BFCNs project to HC and neocortex. These areas are critically important for memory, learning and attention (Ballinger et al., 2016). Interestingly, cholinergic neurons gained importance when different studies reported their degeneration in human AD brains (Davies & Maloney, 1976; Perry et al., 1978; Heckers et al., 1994; Mesulam, 1999). These observations were the origin of AD cholinergic hypothesis, which proposes a progressive loss of limbic and neocortical cholinergic innervation in AD brains (Harrison, 1986).

The unique long and complex morphology of cholinergic neurons make them specially vulnerable to structural degeneration in the ageing brain. The long axons demand a perfectly regulated and unaltered transport, a healthy membrane, and proper protein turn-over and maintenance. All these requirements lead to high metabolic demands (Wu et al., 2014; Li et al., 2018). Therefore, any disturbance can drive to degeneration making cholinergic neurons very sensitive. Recent studies have raised the importance of the BF. They proved that the degeneration of the BFCNs precedes and foresees the cortical spread of the AD pathology, challenging the widely held believe that AD has a cortical origin (Schmitz et al., 2016; Fernandez-Cabello et al., 2020).

Cholinergic neurodegeneration has been studied in different mouse models, all of them transgenic models of AD that over-express human APP, or human APP with *PSEN1* FAD-related mutations. Single APP models over-express a mutant form of human APP that results in elevated levels of Aβ and ultimately to amyloid plaques. The Tg2576 model over-expresses the APP isoform 695 with the Swedish mutation (KM670/671NL). This mouse model presents an impairment in cholinergic transmission (Apelt et al., 2002), loss of ACh release (Laursen et al., 2014) and alterations in cholinergic neurotransmitter receptors density (Klingner et al., 2003). All the cholinergic deficiencies reported started at 17 months of age and no cholinergic loss was reported in any of the aforementioned studies (Apelt et al., 2002; Klingner et al., 2003; Laursen et al., 2014). The APP23 mouse model contains the same APP mutation that Tg2576 mouse but inserted in another promoter. This mouse model presents a modest decrease in cortical cholinergic enzyme activity and a decrease in cholinergic fibre length at 15 months of age (Boncristiano et al., 2002). However, no loss of cholinergic neurons was reported. The mouse model TgCRND8 contains the human APP isoform 695 with two mutations, the Swedish (KM670/671NL) and the Indiana (V717F). This mouse presents a significant cholinergic dysfunction and a 39 % decrease in the number of cholinergic neurons at 7 months (Bellucci et al., 2006). The 5xFAD mouse expresses human APP and *PSEN1* transgenes with a total of five AD-linked mutations. In 5xFAD animals, the lesion of cholinergic fibres in cortex occurred earlier than the cholinergic neuron loss reported at 9 months (Yan et al., 2018).

The SAMP8 model has been considered by some authors as a good model of sporadic AD. SAMP8 develops an early and accelerated senescence, thereby it is used to study ageing, since it recapitulates a wide range of the changes that occur during it (Takeda et al., 1991). Different to transgenic mouse models, SAMP8 has not been genetically manipulated, it was generated through breedings between mice showing an aged phenotype (Takeda et al., 1981). Concretely, SAMP8 mice have a shortened life span and accelerated senescence in addition to problems in learning and memory (Miyamoto et al., 1986; Ikegami et al., 1992). Moreover, the SAMP8 model recapitulates many features observed in early AD pathogenesis such as; oxidative stress, glial activation and BBB dysfunction (Akiguchi et al., 2017). All these

symptoms become apparent at 6 months of age (Moreno, 2015) and makes SAMP8 mice a very good model to study early events of the disease, minimising waiting times for aged mice (Pallas et al., 2008).

Our results showed a 50 % reduction in the number of cholinergic neurons in SAMP8-p75$^{NTR-/-}$ mice at 6 months of age. Therefore, our new mouse SAMP8-p75$^{NTR-/-}$ is currently the model in which animals lose cholinergic neurons early in life. Hereby, SAMP8-p75$^{NTR-/-}$ mice allow the study of cholinergic neurodegeneration at early ages when compared to the other existing mouse models.

3. Basal Forebrain Cholinergic Neurons Do Not Degenerate For A Redox State Imbalance

Our next aim was understanding the mechanisms by which cholinergic neurons degenerate due to p75^{NTR} deletion. When comparing different signalling pathways and biochemical outputs, we observed big differences between the control senescence mouse SAMR1 and the SAMP8, regardless of the p75^{NTR} expression. This suggests that background differences could mask the effect of p75^{NTR}. One of this biochemical evidence is oxidative stress. The oxidative stress response in the different mice genotypes was measured by quantifying the expression levels of NRF2 and several of its targets. SAMP8 mice show a decreased response to oxidative stress compared to SAMR1 mice, with a significant reduction of NRF2 levels and its target gene HMOX1. However, no differences between SAMP8-p75$^{NTR+/+}$ and SAMP8-p75$^{NTR-/-}$ mice are observed. These results indicate a deficit in the oxidative response in SAMP8 background compared to SAMR1 mice, with no role of p75^{NTR} in this response. These results are in line with previous studies in which a higher oxidative stress was seen in SAMP8 background (Nomura et al., 1989; Liu & Mori, 1993; Sato et al., 1996). Therefore, the imbalanced oxidative stress response reported is caused by the senescence background of SAMP8 mice, and the deletion of p75^{NTR} does not make cholinergic neurons less vulnerable to oxidative stress. We also confirm these results *in vitro* with BFCNs primary cell cultures from p75$^{NTR+/+}$ and p75$^{NTR-/-}$ mice in the presence of H_2O_2, and no differences in the percentage of death are observed. These results contrast with a recent report which suggests that p75^{NTR} plays a pro-apoptotic role upon oxidative stress in cultured sympathetic neurons (Kraemer et al., 2014). If this difference is due to the neuronal cell type or the oxidative stress used (H_2O_2 in our work and HNE in theirs) should be further investigated.

4. SAMP8-p75$^{NTR-/-}$ Mouse Presents Differences In The Cholesterol Synthesis

Cholesterol is a major component of cell membranes and the precursor of steroid hormones. Therefore, it impacts nearly all aspects of cellular structure and function. In BFCNs cholesterol is especially important due to their big complexity, their long neurites and their synapsis. The biosynthesis of cholesterol is an energetically expensive and complex process that involves more than 30 chemical reactions (Cerqueira et al., 2016). In the brain, cholesterol has to be synthesised *de novo* because the BBB prevents the entry of lipoproteins from the plasma (Pfrieger, 2003). In the adult brain, it is widely accepted that cholesterol is synthesised by astrocytes and then delivered to neurons in the form of LDL or VLDL particles enriched with ApoE. These particles bind receptors of the LDL receptor family (LDLR, LRP1, SORLA…) through ApoE and are endocyted by neurons, which is followed by cholesterol release to the cytosol. All the steps related to cholesterol synthesis and transport are finely controlled and regulated. Disturbances in cholesterol levels, either high or low, can effect essential cellular processes and cause neurodegeneration. In aged and AD brains differences in cholesterol levels have been reported. There are studies that showed an increase in the total amount of cholesterol (Cutler et al., 2004; Grimm et al., 2012) whereas others reported reduced levels (Mulder et al., 1998; Molander-Melin et al., 2005; Wang et al., 2014).

In this thesis we observe a big difference between proteins related to cholesterol in SAMR1 and SAMP8 background and also between SAMP8-p75$^{NTR+/+}$ and SAMP8-p75$^{NTR-/-}$ mice. At 2 months, there are no differences between any protein and/or strain. All the differences are reported after 4 months, that is when age deficits start in SAMP8. At 6 months, there is an increase in the levels of HMGCR and LDLR mRNA levels in SAMP8-p75$^{NTR-/-}$ when compared to SAMP8-p75$^{NTR+/+}$. In addition, SAMP8 background shows a reduction in ApoE levels and a reduction in the total amount of cholesterol.

With these results we proposed a model for the decrease in the number of cholinergic neurons in p75^{NTR} deleted mice. As previously mentioned, it is widely accepted that in the adult brain neurons stop producing cholesterol and astrocytes are the ones in charge to synthesise it. Nevertheless, a study showed that cholinergic neurons maintain *HMGCR* expression during adulthood (and *dHCR7* expression, another key enzyme in the cholesterol synthesis) (Korade et al., 2007). They also showed that HMGCR levels decreased when p75^{NTR} expression was silenced (Korade et al., 2007). Hereby, our model proposes that in normal conditions, as cholinergic neurons are complex and their necessity of cholesterol is higher, they keep their own synthesis of cholesterol during adulthood. The levels of the enzymes involved in cholesterol synthesis in cholinergic neurons are up-regulated by p75^{NTR}, therefore in a p75$^{NTR-/-}$

mice, cholinergic neurons lose their capacity to synthesise cholesterol themselves and, thereupon, astrocytes have to produce it. Since the ApoE levels are decreased in SAMP8 background, LDLR-mediated internalisation of cholesterol is impaired. An increment of the LDLR mRNA levels is seen, which may account for the increase in the internalisation of cholesterol. The system would detect low levels of neuronal cholesterol inducing the expression of HMGCR and LDLR, which we have detected by WB and qPCR, respectively. In this model, the total amount of cholesterol is not significantly altered but a reduction of cholesterol synthesis and internalisation is presumed in cholinergic neurons **(Figure D1)**. This model is supported by other results from our laboratory, of a parallel thesis, which shows the same increment of HMGCR and LDLR levels in a different mouse strain, C57BL6/J.

However, this hypothesis still needs to be demonstrated. Our Achilles heel is that all the data has been generated from whole BF lysates and in the area, together with cholinergic neurons, there are astrocytes, microglia and other neuronal types. This is a limitation since our results cannot be specifically assigned to cholinergic neurons. To confirm or deny the proposed model, future experiments are mandatory. For example, if we could confirm that cholinergic neurons in p75$^{NTR-/-}$ mice do not express HMGCR we would overcome this downside. However we are limited by the quality of the antibodies, a problem that could not be solved in this work. Another interesting experiment would be the quantification of cholesterol levels, specifically in cholinergic neurons, which would confirm if p75$^{NTR-/-}$ mice have a reduced amount of cholesterol in those neurons. Finally, another proposal would entail a culture of pure cholinergic neurons, which would be co-cultured with astrocytes.

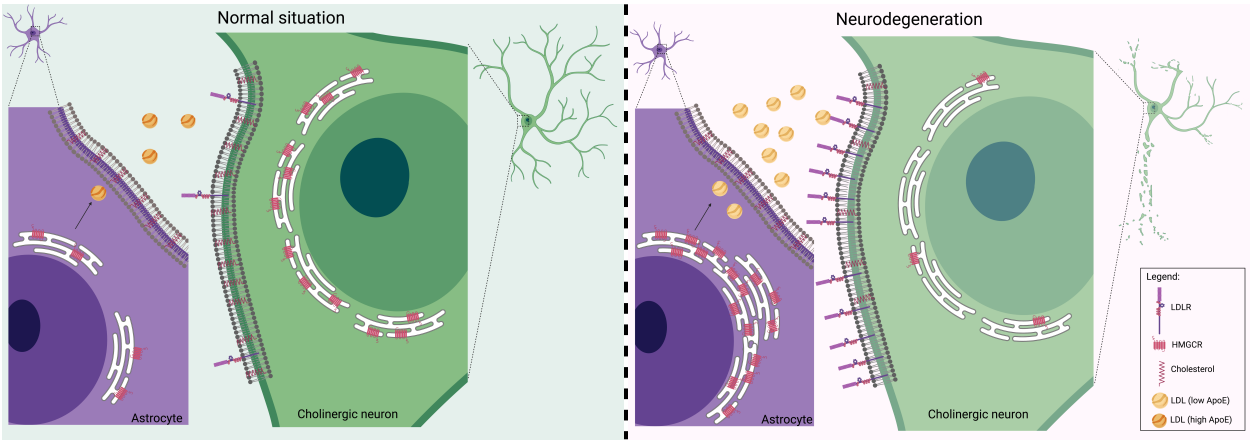

Figure D1: Model of cholinergic neurodegeneration. *In a normal situation, astrocytes synthesis cholesterol for the neurons and is transported in LDL rich in ApoE. This particles bind to LDLR and are endocytated for the neurons. As cholinergic neurons need big amounts of cholesterol they synthesise their own cholesterol. In a neurodegenerative scenario, p75^{NTR} knock-out mice, cholinergic neurons do not have the enzymes to synthesise the cholesterol, therefore astrocytes have to do it for them. Once astrocytes have synthesised the cholesterol this is transported in LDL particles low in ApoE. Hereby, particles bind worst to the LDLR and cholinergic neurons suffers from a cholesterol deficit.*

5. The Cholinergic Decrease Has An Impact On Behaviour

Three behavioural tests were performed to study the effects of cholinergic loss; anxiety, long-term memory and spatial memory in SAMP8-p75$^{NTR\ -/-}$ mice.

The open field test was used to measure anxiety. Our results show an increase in anxiety in SAMP8 mice when compared to SAMR1, in agreement with other reports (Yanai & Endo, 2016). Furthermore, p75^{NTR} removal has an impact on SAMP8 anxiety since this reduces it, suggesting that the deletion of p75^{NTR} in SAMP8 background is anxiolytic. Nevertheless, Martinowich et al., 2012, found an anxiogenic phenotype in C57BL/6-p75$^{NTR-/-}$ mouse, contrary to our results (Martinowich et al., 2012). This might be due to the different anxiolytic baseline of SAMP8 and C57BL/6 mice.

The novel object recognition test was used to asses long-term memory. Interestingly, we found no differences between SAMP8-p75$^{NTR+/+}$ and SAMP8-p75$^{NTR-/-}$ mice, having both of them a significantly worse long-term memory than the control mice SAMR1. This result indicates a loss of long-term memory in SAMP8 mice in a p75^{NTR}-independent manner.

SAMP8-p75$^{NTR-/-}$ mice had a worse performance regarding the spontaneous alternation Y-maze test at 6 months when compared to 2 months, whereas SAMP8-p75$^{NTR+/+}$ had the same performance at both ages. This result suggests that the decrease in the number of cholinergic neurons from 2 to 6 months in SAMP8-p75$^{NTR-/-}$ has a negative impact on spatial memory. The cholinergic projections from the septal area to HC have been proposed to be important in cognition by modulating properties of the HC network (Teles-Grilo Ruivo & Mellor, 2013). Other studies have shown a decrease in spatial memory in p75$^{NTR-/-}$ mice in the water Morris test (Peterson et al., 1999; Wright et al., 2004; Dokter et al., 2015). This can be explained by a 45 % increase in the number of cholinergic neurons in SAMP8-p75$^{NTR-/-}$ mice together with an increase in the innervation to HC. Nonetheless, at 6 months of age the number of cholinergic neurons are not significantly different between SAMP8-p75$^{NTR-/-}$ and SAMP8-p75$^{NTR+/+}$ and therefore, a cholinergic denervation within HC may impact the hippocampal-dependent spatial memory activities.

6. The γ-secretase As A Therapeutical Target For Alzheimer's Disease

AD is the most common type of dementia, since around 75 % of patients diagnosed with dementia suffer AD (Alzheimer's Fact and Figures, (2021). AD is mainly caused by two types of alterations in the brain: the hyper-phosphorylation of the tau protein which forms neurofibrillary tangles (Brion et al., 2001), and the deposition of extracellular amyloid beta plaques. The amyloid hypothesis postulates that Aß plaques, which come from the γ-secretase shedding of

the APP, are the main cause of AD (Castro et al., 2019). The amyloid theory raised from the genetic analysis of patients with FAD in which mutations in *APP*, *PSEN1* and *PSEN2* genes were identified. *PSEN1* and *PSEN2* encode for PS1 and PS2 proteins, respectively, and they are the catalytic components of the γ-secretase complex. When *PSEN1* mutations were discovered, they were linked to a phenotype of a toxic gain of function, increasing the formation of the insoluble and amyloidogenic $Aß_{1-42}$, instead of the non-amyloidogenic and common $Aß_{1-40}$ (Jarrett et al., 1993; Duff et al., 1996; Scheuner et al., 1996). This knowledge led pharmaceutical companies to design γ-secretase inhibitors as promising therapeutical drugs to treat AD by reducing the amount of toxic $Aß_{1-42}$. The reduction of the circulating levels of Aß in AD mouse models increase the expectations of the treatment. One of the leading compounds, Semagacestat (LY450139, Lilly), arrived to clinical trial phase III, but soon-after the trial had to be stopped due to a worsening in the cognitive performance of the patients. In addition, skin cancer problems appeared in patients treated with Semagacestat (Doody et al., 2013). The unexpected secondary effects are now partially understood. The γ-secretase complex mediates the proteolytic cleavage of over 100 substrates, so its inhibition caused an imbalance between many physiological proteins. Notch is a γ-secretase substrate and the inhibition of its cleavage leads to skin cancer in mice (Li et al., 2007), therefore the secondary effects observed in the skin with Semagacestat could be due to an inhibition of Notch cleavage. An explanation for the cognitive secondary effects could be that the 90 % of the reported *PSEN1* and *PSEN2* mutations have been found to lead to a loss of γ-secretase function, which opposes the previous gain of function theory (Chavez-Gutierrez et al., 2012). A better understanding of γ-secretase biology and substrates will help to improve drugs for the treatment of AD.

$P75^{NTR}$ is one of the γ-secretase substrates (Kraemer et al., 2014). The RIP of $p75^{NTR}$ has been suggested to play different biological functions (Kraemer et al., 2014). When the γ-secretase is inhibited there is a $p75^{NTR}$-CTF accumulation that has been mainly related to the pro-apoptotic activity seen in hippocampal and cerebellar granule neurons (Vicario et al., 2015), and also in dorsal root ganglia (Underwood et al., 2008).

$P75^{NTR}$ is highly expressed in BFCNs and its loss is an early and key hallmark of AD (Schliebs & Arendt, 2011). Hereby, understanding the effect that GSIs might cause to BFCNs is important and can help understand the γ-secretase functioning in order to design better treatments.

7. The γ-secretase Inhibition Increases Basal Forebrain Cholinergic Neuronal Complexity

In the present thesis, the effect of γ-secretase inhibition in BFCNs has been studied at physiological conditions in primary cell cultures, organotypic slices and *in vivo*.

The cohort of chemical γ-secretase inhibition experiments in primary culture and organotypic slices showed important morphology changes in BFCNs in a $p75^{NTR}$-dependent manner. Morphology alterations are linked to cytoskeleton changes. A protein that regulates the actin cytoskeleton is RhoA (Kuhn et al., 2000). Previous studies have shown the implication of $p75^{NTR}$ in the regulation of axonal elongation through RhoA (Yamashita et al., 1999; Yamaguchi et al., 2001; Yamashita et al., 2002; Yamashita & Tohyama, 2003). The current model states that $p75^{NTR}$ displaces the RhoA inhibitor (RhoA-GDI) from RhoA, which in turn activates RhoA (Yamaguchi et al., 2001). When a NT binds $p75^{NTR}$, it liberates RhoA-GDI which binds RhoA inactivating it (Gehler et al., 2004). With this system an equilibrium is generated to maintain the cytoskeleton stability. Herein, we show that the accumulation of $p75^{NTR}$-CTF due to the inhibition of the γ-secretase decreases the amount of active RhoA-GTP. The effect is similar when RhoA signalling is inhibited using a specific inhibitor of one of its downstream proteins, ROCK. These results suggest that accumulation of $p75^{NTR}$-CTF inhibits RhoA allowing the increase in complexity of BFCNs.

From a molecular point of view we propose the model shown in the **Figure D2**. In our model of work, cholinergic neurons would have a controlled levels of inactive and active RhoA to maintain its morphology. In conditions of high activation of RhoA, for instance in the presence of myelin membrane proteins like Nogo or MAG, neurons would have an axonal rejection and growth inhibition (Park et al., 2010). This would be similar to the cortical neurons in the presence of myelin (Domeniconi et al., 2005). Here we described the other side of the equilibrium, when in the presence of γ-secretase inhibitors, the accumulation of $p75^{NTR}$-CTF induces the inactivation of RhoA below its basal levels enhancing neuronal complexity. This would be the case of a gain of function of $p75^{NTR}$, which would mimic a $p75^{NTR}$ constitutively activated by NTs **(Figure D2)**.

We wanted to go further and confirm if in a transgenic mouse model with the deletion of both PSs subunits the increase in the complexity was occurring. Two different experiments were carried out in transgenic mice with PS2 (single) or PS1 and PS2 (double) deletions. The complexity of the BFCNs in organotypic slices of wild type and single and double PS knock-out was analysed in the presence of CE by Sholl analysis. PSs complete null slices incubated with CE do not show an increase in neuronal complexity compared to the slices incubated with

the vehicle, suggesting that inhibition of the γ-secretase is required to inhibit the activity of RhoA and neurite growth. Theoretically, if the γ-secretase was genetically inhibited, a basal increase of the complexity between double PS knock-out mice respect to wild-type slices should be appreciated. Nevertheless we do not see any differences in complexity between double knock-out and wild-type mice. However, when double PS knock-out adult mice (2 months) were analysed by AChE staining, which labels the extensive network of the cholinergic neurites innervations, an increase in the total pixel area is observed when compared to single PS knock-out. This result suggests that in the absence of an active γ-secretase there is a basal increase in neurite complexity. The discrepancy between both experiments might be due to differences in the age of the mice. Organotypic slices were made at postnatal day 8-10 and the slices were kept alive for 2 weeks. Therefore, when the slices were analysed they were 23-25 days old. At this age, PS1 levels have not decreased yet, whereas at 2 months PS1 levels are no longer present in adult neurons (Yu et al., 2001).

The changes in cholinergic morphology can have different effects at a synaptic level and in the connectivity, which might be translated into cognitive changes. In fact, a study showed that the double knock-out mice have problems in spatial memory before neurodegeneration (Saura et al., 2004). The BFCNs are related to spatial memory and a deregulation in the number of synapsis, can lead into problems in spatial memory. Even though an increase of fibres is reported, we have not confirmed if these fibres make more synaptic contacts. If that was the case, it would not be difficult to envision that the increase in cholinergic projecting fibres to HC and cortex can have some cognitive effects.

8. The γ-secretase Inhibition Together With A TrkA Impaired Activity Increases Basal Forebrain Cholinergic Neuronal Death

Our results differ from previous reports, showing that the increase in $p75^{NTR}$-CTF generates neuronal death. However, the neuronal populations where they reported this death, hippocampal and cerebellar neurons, the levels of $p75^{NTR}$ expression are low and there are undetectable levels of TrkA in the adult brain. This is an important difference when compared to BFCNs which express these NT receptors during their whole life, since the consequences of the inhibition of the γ-secretase complex in the BFCNs can be completely different, as the context is completely different.

In the case of the BFCNs, the increase in $p75^{NTR}$-CTF on its own did not cause neuronal death but an increase in complexity. Despite this, the cholinergic neurons analysed in our work were young neurons. At these ages, the levels of $p75^{NTR}$ and TrkA are equilibrated, and there is a proper pro-survival TrkA-NGF signalling. Nevertheless, during healthy and pathological ageing the levels of TrkA decrease while the levels of $p75^{NTR}$ are maintained (Ginsberg et al., 2006), the

TrkA decrease results in a reduced pro-survival signalling in cholinergic neurons. In this context, an ageing situation was simulated with BFCNs primary culture adding a TrkA activity inhibitor. When BFCNs were treated together with the GSI and the TrkA activity inhibitor there was a significant increase in cholinergic death. This result suggests that the formation of $p75^{NTR}$-CTF *per se* is not indicative of a pro-death signal if TrkA is active, and that in the absence of TrkA signalling, $p75^{NTR}$-CTF is able to trigger cell death.

In double PS knock-out mice cholinergic neuronal loss is seen at 8 months of age. These mice present a cortical and hippocampal degeneration starting at 6 months of age (Saura et al., 2004). As cortical neurons are the ones that generate the NGF for cholinergic neurons, a decrease in the NGF-TrkA signalling can be occurring. The decrease in the neurotrophic transport together with the $p75^{NTR}$-CTF accumulation can mediate cholinergic death. Other CTFs can be enhancing cholinergic death, but $p75^{NTR}$-CTF is a good candidate to be its cause, since $p75^{NTR}$ high levels found in cholinergic neurons alongside with a decrease in NGF-TrkA signalling.

In summary, the data presented in this thesis show the importance of $p75^{NTR}$ for BFCNs. We postulate a dual role of the receptor as, at young ages, there is an increase in the number of cholinergic neurons, indicating a pro-apoptotic role. Nevertheless, during adulthood and ageing this role switches into a pro-survival one as $p75^{NTR-/-}$ cholinergic neurons end up dying earlier than $p75^{NTR+/+}$ cholinergic neurons, partially due to the modulation of neuronal cholesterol homeostasis.

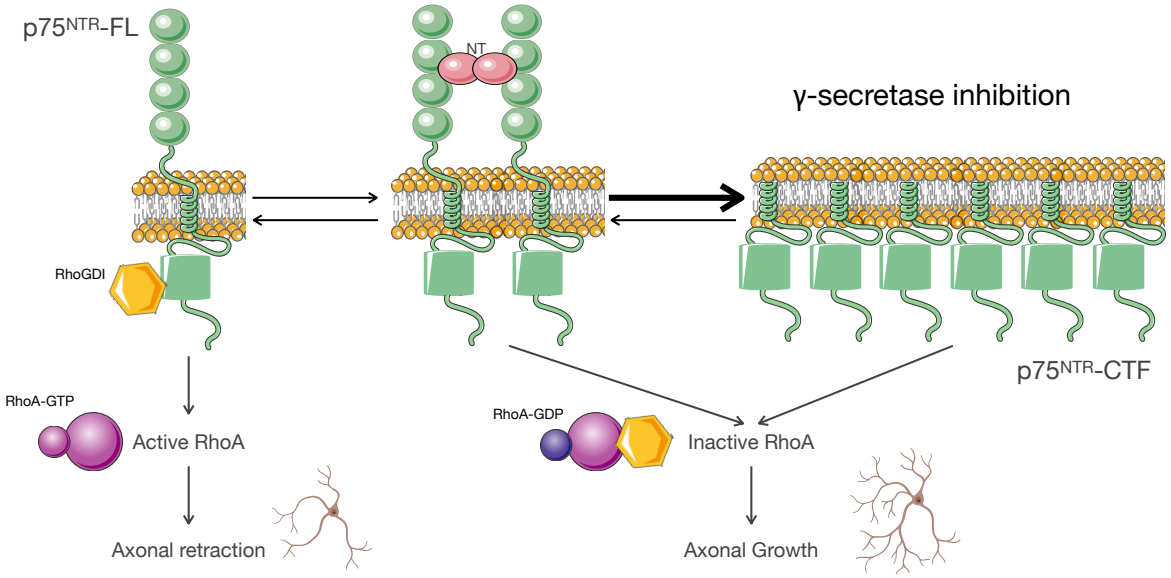

Figure D2: ***Cytoskeleton modulation through p75^{NTR}.*** *The cell keeps an equilibrium between active and inactive RhoA. Nonetheless when there is an accumulation of p75^{NTR}-CTF, due to a γ-secretase inhibition, the equilibrium is moved to a RhoA inactivation.*

CONCLUSIONS

1. A new mouse model has been generated: SAMP8-p75$^{NTR-/-}$.
2. The deletion of p75^{NTR} increases the number of BFCNs at young ages in SAMP8-p75$^{NTR-/-}$ mice.
3. The deletion of p75^{NTR} reduces the number of BFCNs in adults and old SAMP8-p75$^{NTR-/-}$ mice.
4. The deletion of p75^{NTR} in SAMP8 background changes the expression of enzymes related to cholesterol synthesis and uptake in the brain.
5. The deletion of p75^{NTR} in SAMP8 background causes a decrease in spatial memory.
6. The chemical inhibition of the γ-secretase increases BFCNs complexity and length in primary cell cultures and in organotypic slices.
7. p75^{NTR}-CTF increases BFCNs complexity through RhoA inactivation.
8. The genetic inhibition of the γ-secretase increases AChE fibres *in vivo*.
9. The genetic inhibition of the γ-secretase causes BFCNs loss starting at 8 months.

RESUMEN

Introducción

El envejecimiento es un proceso biológico que sufre cualquier ser vivo con el paso del tiempo y se caracteriza por un conjunto de cambios fisiológicos a nivel estructural y funcional. El descenso gradual de las funciones biológicas en órganos, aparatos y sistemas termina con el fallecimiento. Además, el envejecimiento es el mayor factor de riesgo para cualquier enfermedad (Wyss-Coray, 2016). Uno de los órganos más afectados por el envejecimiento es el cerebro. Una area del cerebro que sufre especialmente es el prosencéfalo basal, el cual está situado en la parte medial-ventral del cerebro. El prosencéfalo basal está dividido en cuatro regiones: el septum medial, la banda de *Broca* horizontal, la banda de *Broca* vertical, y el *nucleus basallis magnocellularis* **(Figura 1)**. El prosencéfalo basal contiene las neuronas colinérgicas, entre otros tipos de neuronas como las GABAergicas o las interneuronas (Blake & Boccia, 2016). Las neuronas colinérgicas del prosencéfalo basal son neuronas de proyección complejas y largas que inervan a sitios distales del cerebro como la corteza y el hipocampo. Estas neuronas son las principales productoras del neurotransmitor acetilcolina en el sistema nervioso central (CNS) (Ballinger et al., 2016). Debido a las regiones donde proyectan, como el hipocampo y la corteza, las neuronas colinérgicas del prosencéfalo basal están involucradas en procesos cognitivos superiores como la atención y la memoria (Baxter & Chiba, 1999).

Las neuronas colinérgicas del prosencéfalo basal adquirieron una gran importancia desde 1977, cuando se descubrió que durante el transcurso de la Enfermedad de Alzheimer (EA) sufren una degeneración y posterior muerte (Perry et al., 1977). Estos resultados explicaban la perdida de marcadores colinérgicos como ChAT, acetilcolina y acetilcolinesterasa observada en los cerebros de pacientes que habían sufrido la EA (Davies & Maloney, 1976), y posteriormente esta degeneración colinérgica se correlacionó con una perdida cognitiva del enfermo, generando así la hipótesis colinérgica de la EA (Harrison, 1986). En los últimos años nuevos resultados han mostrado como la EA empieza en el prosencéfalo basal en vez de la corteza como se había creido hasta ahora, volviendo a hacer hincapié en la importancia de las neuronas colinérgicas del prosencéfalo basal (Schmitz et al., 2016; Fernandez-Cabello et al., 2020).

Las neuronas colinérgicas son dependientes de neurotrofinas. Las neurotrofinas, como su nombre indica, son factores tróficos que ayudan a las neuronas a sobrevivir, crecer y diferenciarse. En mamíferos hay cuatro neurotrofinas, el NGF (del inglés, *Nerve Growth Factor*); el BDNF (del inglés, *Brain Derived Neurotrophic Factor*); la neurotrofina-3 y la neurotrofina-4. Para ejercer sus funciones las neurotrofinas se unen a dos tipos de receptores: los tirosina quinasa, que engloban TrkA, TrkB y TrkC, y al receptor de neurotrofinas p75 ($p75^{NTR}$). Las cuatro neurotrofinas pueden unirse y activar a $p75^{NTR}$, a diferencia de los receptores Trk, donde cada tipo de Trk es activado por una neurotrofina específica: el NGF se une y activa a TrkA; el

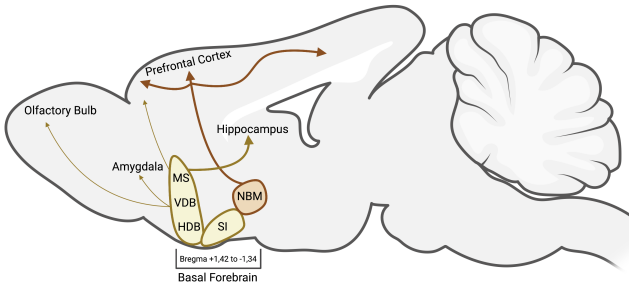

Figura 1: ***Organización y areas de proyección de las neuronas colinérgicas del prosencéfalo basal.*** *Las neuronas colinérgicas del prosencéfalo basal se dividen en cuatro areas, el medial septum, MS; la banda horizontal y vertical de Broca, HBB-VDB; y el nucleus basalis magncelularis, NBM, formado un continuo. Cada area proyecta a una zona distal distinta de el cerebro el MS y VDB mayoritariamente proyectan al hipocampo, la HDB y el NBM mayoritariamente al cortex prefrontal.*

BDNF y la NT-4 a TrkB, y la NT-3 a TrkC (Franco et al., 2020). Los Trks tienen actividad quinasa propia y al autofoforilarse activan sus rutas de señalización. Sin embargo, al contrario de lo qué sucede con los Trks, el receptor $p75^{NTR}$ no tiene actividad propia. Tras su activación desencadena todas las respuestas mediante la interacción con proteínas adaptadoras. La activación de $p75^{NTR}$ por distintas neurotrofinas así como por la diversidad de proteínas adaptadoras, permite que este receptor participe en múltiples y diversas funciones que son dependientes de contexto (Vilar, 2017). El receptor $p75^{NTR}$ no solo homodimeriza, sino que además tiene capacidad de formar heterodímeros con otros receptores como Trks, Sortilin, el receptor de Nogo… multiplicando de esta manera sus funciones. Así mismo, $p75^{NTR}$ sufre un procesamiento proteolítico secuencial, RIP (del inglés, *Regulated Intramembrane Proteolysis*) que conducirá a la degradación de la proteína. El procesamiento de la proteína $p75^{NTR}$ empieza con la actuación de la α-secretasa, que dará lugar al fragmento C-terminal ($p75^{NTR}$-CTF), el cual queda unido a la membrana, y se liberará el dominio extracellular ($p75^{NTR}$-ECD). Posteriormente, el domino $p75^{NTR}$-CTF es procesado por el complejo de la γ-secretasa, liberando al citosol el dominio intracelular ($p75^{NTR}$-ICD). El proceso de RIP de $p75^{NTR}$ sirve para su homeostasis y los distintos productos del RIP poseen un papel señalizador, ampliando las funciones de este receptor.

$p75^{NTR}$ tiene una expresión generalizada durante el desarrollo embrionario del CNS. Sin embargo, su expresión se reduce tras el nacimiento y su expresión queda recluida a las neuronas colinérgicas del prosencéfalo basal que mantienen la expresión de este receptor a lo largo de toda su vida. En condiciones de daño cerebral también se produce un pico de expresión de este receptor.

A pesar de los numerosos trabajos que demuestran la expresión del receptor en las neuronas colinérgicas todavía son desconocidas las funciones que el receptor realiza en estas neuronas. Es por ello por lo que la presente tesis se ha centrado en estudiar el papel del receptor de neurotrofinas p75 en las neuronas colinérgicas del prosencéfalo basal.

Específicamente, el papel que juega durante el envejecimiento y el papel que tiene el procesamiento proteolítico de $p75^{NTR}$ en neuronas colinérgicas maduras.

Para cumplir el primer objetivo, se utilizaron ratones con un fondo genético de senescencia acelerada, los ratones SAMP8 (del inglés, *Senescence Accelerated Mouse Prone 8*). Estos ratones fueron generados a partir de cruces de ratones de la línea AKR/J con un fenotipo de envejecimiento (Takeda et al., 1981). Algunos de estos fenotipos consistían en pérdida de actividad, de pelo, de brillo, así como lesiones perioftálmicas, lordocifosis y una reducida esperanza de vida. De este modo Takeda et al., separaron y mantuvieron a los animales que presentaban las características de envejecimiento prematuro hasta obtener 8 cepas de animales SAMP. Así pues, los ratones SAMP8 tienen un desarrollo normal pero presentan una senescencia acelerada, teniendo una vida media de alrededor de 10 meses, un 63 % más corta que la vida media de sus ratones control SAMR1 (del inglés: *Senescence Accelerated Mouse Resistant 1*) (Takeda et al., 1991). Específicamente los ratones SAMP8 presentan problemas de memoria y aprendizaje, y se ha aceptado como modelo de envejecimiento y también como modelo de la EA ya que presentan muchas patologías asociadas a la enfermedad (Nomura et al., 1989; Morley et al., 2012). Algunas de estas son: incremento del estrés oxidativo, incremento de la glia reactiva, incremento en astrocitos reactivos y disfunción en la barrera hematoencefálica (Akiguchi et al., 2017).

Objetivos

El objetivo general de la tesis fue estudiar el papel del receptor de neurotrofinas $p75^{NTR}$ en las neuronas colinérgicas del prosencéfalo basal. Este objetivo general fue dividido en dos específicos y estos en sub-objetivos:

1. Estudiar el papel del receptor de neurotrofinas p75 durante el envejecimiento en las neuronas colinérgicas del proséncefalo basal.

    1.1. Generar y comprobar un nuevo modelo de ratón: SAMP8-$p75^{NTR-/-}$.
    1.2. Determinar el número de colinérgicas en edades jóvenes (2 meses), adultas (6 meses) y viejas (10 meses) en los ratones SAMP8-$p75^{NTR+/+}$ y SAMP8-$p75^{NTR-/-}$.
    1.3. Estudiar el efecto de la deleción de $p75^{NTR}$ en el ratón SAMP8-$p75^{NTR-/-}$.
    1.4. Evaluar el efecto en el comportamiento de la deleción de $p75^{NTR}$ en el ratón SAMP8-$p75^{NTR-/-}$.

2. Estudiar el papel del corte de $p75^{NTR}$ en neuronas colinérgicas maduras del prosencéfalo basal.
    2.1. Establecer cultivos primarios de neuronas colinérgicas.
    2.2. Estudiar el efecto de la inhibición química de la γ-secretasa en cultivo primario y cultivo organotípico de neuronas colinérgicas.
    2.3. Estudiar el efecto de la inhibición genética de la γ-secretasa *in vivo*.

Resultados

En este trabajo hemos querido ahondar el papel del receptor p75 durante el envejecimiento del prosencéfalo basal, ya que como se ha mencionado anteriormente las neuronas colinérgicas de esta region expresan el receptor durante toda su vida. Para ello se ha cruzado el ratón SAMP8 con el ratón c57-p75$^{NTR-/-}$, hasta obtener el ratón SAMP8-p75$^{NTR-/-}$. Una vez obtenido el ratón, se han cuantificado las neuronas colinérgicas del prosencéfalo basal a edad joven, 2 meses, a edad adulta, 6 meses y a edad vieja, 10 meses. Los resultados muestran un incremento en el número de neuronas colinérgicas a los 2 meses en los ratones SAMP8-p75$^{NTR-/-}$ comparado con los ratones SAMP8-p75$^{NTR+/+}$. Sin embargo, este incremento se ve reducido a edades adultas y viejas, terminando las dos cepas con el mismo número de neuronas cólinergicas, indicando una muerte de neuronas colinérgicas en los ratones nulos de p75^{NTR}.

Una vez descubierto que las neuronas colinérgicas del prosencéfalo basal se mueren sin el receptor, se analizaron distintas rutas que podrían estar afectadas en la zona durante el envejecimiento. Una de las rutas estudiadas fue la del estrés oxidativo. Mediante niveles de expresión, se cuantificaron distintos genes involucrados en la respuesta al estrés: Nfr2, HMOX1, SOD1 y SOD2. Pero no se encontraron diferencias entre ellos. Entonces estudiamos la ruta del colesterol. El colesterol es un esterol necesario para el buen funcionamiento de las membranas lipídicas controlando su fluidez, permeabilidad, forma celular… Se ha demostrado en varios trabajos que hay una desregulación en sus niveles durante el envejecimiento y la EA (Martin et al., 2014). En el cerebro, a diferencia de el resto de órganos, el colesterol tiene que ser sintetizado *de novo*, ya que la barrera hematoencefálica previene su entrada. Es por ello que una buena regulación de su síntesis y degradación es importante para mantener sus niveles adecuados. Las proteínas SREBP (del inglés: *Sterol Regulatory Element-Binding Proteins*) y específicamente la SREBP-2 regula la transcripción de genes relacionados con la síntesis y absorción del colesterol como son la HMGCR (del inglés, *HMG-CoA Reductase*) y el receptor de LDL (del inglés, *Low-Density Lipoprotein)*. Los niveles HMGCR y LDLR fueron analizados en los ratones SAMP8-p75$^{NTR+/+}$ y SAMP8-p75$^{NTR-/-}$ a 2 y 6 meses. Mientras no se encontraron diferencias entre los niveles de las proteínas a 2 meses, el ratón SAMP8-p75$^{NTR-/-}$ presenta un aumento de la enzima HMGCR así como del receptor LDL. Estos resultados nos muestran una posible desregulación en las rutas de síntesis del colesterol, pudiendo explicar la muerte de las neuronas colinérgicas. Además, se quiso comprobar si la perdida en el numero de neuronas colinérgicas tenía algún efecto en el comportamiento. Para ello se realizaron tres tests distintos: el test de campo abierto para medir ansiedad, el test del reconocimiento de objeto nuevo para medir memoria a largo plazo y el test de la Y para medir memoria espacial. Los resultados mostraron como el ratón SAMP8-p75$^{NTR-/-}$ reduce los niveles de ansiedad de

los ratones SAMP8. Sin embargo, no se vieron diferencias en la memoria a largo plazo, siendo ya baja en los ratones SAMP8. Así mismo, si se cuantificó una pérdida en la memoria espacial en los ratones SAMP8-p75$^{NTR-/-}$ de 2 a 6 meses, que podría estar correlacionada con la pérdida de neuronas colinérgicas.

El segundo objetivo de la tesis consistió en estudiar el papel de la inhibición de la γ-secretasa en las neuronas colinérgicas del prosencéfalo basal. La importancia recae en la teoría amiloidogénica de la EA que describe cómo hay un aumento en los niveles de Aß$_{1-42}$ que provienen del corte amiloidogénico por la γ-secretasa de la proteína APP (del inglés, Amyloid Precursor Protein). El Aß$_{1-42}$ es tóxico ya que sus propiedades insolubles llevan a una agregación de la proteína que termina formando placas de Aß que son tóxicas para las neuronas. Estas placas Aß son la causa de la degeneración neuronal en la EA. Esta teoría se postuló cuando se descubrieron las mutaciones ligadas a la enfermedad de Alzheimer familiar (EAF) de los genes *PSEN1* y *PSEN2*. De estos genes se transcriben a las proteínas presinilina 1 (PS1) y presinilina 2 (PS2), respectivamente, que son las unidades catalíticas del complejo de la γ-secretasa (Castro et al., 2019). En ese momento las mutaciones de *PSEN1* y *PSEN2* se relacionaron con una ganancia de función tóxica de la γ-secretasa, incrementado la formación de la forma insoluble Aß$_{1-42}$ y disminuyendo la forma no amiloidogénica Aß$_{1-40}$ (Jarrett et al., 1993; Duff et al., 1996; Scheuner et al., 1996). Este echo llevo a las compañías farmacéuticas a desarrollar inhibidores de la γ-secretasa para así disminuir los niveles de Aß tóxico y tratar la EA. Hubo un fármaco muy prometedor que llego hasta fase clínica III, el Semagacestat (LY450139, Lilly). Sin embargo, cuando los pacientes fueron administrados con el fármaco, no mejoraron sus habilidades cognitivas, sino todo lo contrario, empeoraron. Además, tuvieron problemas de cáncer de piel (Doody et al., 2013). No se sabe específicamente el porqué de los efectos secundarios pero hay varias teorías bien fundamentadas. Para empezar, la γ-secretasa tiene alrededor de 100 sustratos, no solo la proteína APP, así pues otros fragmentos C-terminales podrían estar acumulándose y generar daño. De echo, esa es la razón de el cáncer de piel, ya que en la piel se encuentra Notch, una proteína procesada por la γ-secretasa y se ha visto en ratones que si su corte es inhibido, aumentan las posibilidades de cáncer de piel (Li et al., 2007). Además, más tarde se comprobó que las mutaciones descritas generaban una pérdida de función a la proteína y no una ganancia como se pensaba (Chavez-Gutierrez et al., 2012). Así pues, son necesarios mas estudios para entender mejor la biología del complejo de la γ-secretasa para así poder diseñar mejores fármacos y tratar la EA. Por ello consideramos importante saber cómo afecta la inhibición de la γ-secretasa en unas neuronas tan afectadas en la EA como son las neuronas colinérgicas del prosencéfalo basal.

Para ello se usaron cultivos primarios de neuronas colinérgicas en los cuales se inhibió químicamente la γ-secretasa con el Compuesto E (CE). Al realizar un análisis morfológico, se comprobó un aumento en la complejidad de las neuronas colinérgicas. Además, este efecto es

dependiente de $p75^{NTR}$, ya que el mismo experimento realizado en cultivos de $p75^{NTR-/-}$ no genera un incremento en la complejidad. El mismo efecto se comprobó *ex vivo*, usando cultivos organotípicos del prosencéfalo basal, ya que al añadir CE a los cultivos, se observaba un aumento en la complejidad específicamente de las neuronas colinérgicas.

Quisimos hacer un paso más y estudiar si el mismo efecto es visto en ratones con la γ-secretasa inhibida genéticamente debido a la deleción de la PS1 y la PS2. Y efectivamente, un aumento en fibras acetilcolinestarasa es cuantificado.

Conclusiones

1. Un nuevo modelo de ratón de senescencia acelerada con $p75^{NTR}$ delecionado ha sido generado: SAMP8-$p75^{NTR-/-}$. Este ratón ha sido caracterizado y mantiene las características de SAMP8.
2. La deleción de $p75^{NTR}$ en los ratones SAMP8-$p75^{NTR-/-}$ genera un incremento en el número de neuronas colinérgicas a edades jóvenes (2 meses). Sin embargo, este incremento neuronal es perdido a edades adultas (6 meses) y viejas (10 meses). Sugiriendo un papel de pro-supervivencia de $p75^{NTR}$ en las neuronas colinérgicas del prosencéfalo basal durante la madurez y vejez.
3. La deleción de $p75^{NTR}$ no tiene efecto en la respuesta al estrés oxidativo, pero sí en los niveles de enzimas que regulan la síntesis y la absorción de colesterol en los ratones SAMP8-$p75^{NTR-/-}$.
4. La deleción de $p75^{NTR}$ en los ratones SAMP8-$p75^{NTR-/-}$ tiene un efecto en los niveles de ansiedad del ratón. Además, los ratones SAMP8-$p75^{NTR-/-}$ presentan una pérdida en la memoria espacial de los 2 a los 6 meses de edad.
5. La inhibición de la γ-secretasa genera un incremento en la complejidad de las neuronas colinérgicas del prosencéfalo basal. Este incremento en la complejidad es dependiente de $p75^{NTR}$.

Metodología

Parte I
Generación de un modelo de ratón con senescencia acelerada y p75^{NTR} delecionado

Para llevar a cabo el primer objetivo, el ratón SAMP8, un modelo de envejecimiento acelerado, fue cruzado con un ratón que contiene la proteína p75^{NTR} delecionada, c57-p75$^{NTR-/-}$ generado por Lee et al., 1992 (Lee et al., 1992). Después de 12 generaciones cruzando un SAMP8 con un p75$^{NTR-/-}$ se obtuvo un nuevo modelo de ratón: SAMP8-p75$^{NTR-/-}$. El nuevo modelo fue caracterizado y se comprobaron que las características mas importantes del ratón SAMP8 así como la correcta deleción de p75^{NTR}.

Cuantificación de las neuronas colinérgicas del prosencéfalo basal

Para la cuantificación de las neuronas colinérgicas del prosencéfalo basal se usaron ratones SAMP8-p75$^{NTR+/+}$ y ratones SAMP8-p75$^{NTR-/-}$ de 2, 6 y 10 meses de edad. Para ello a la edad correspondiente los ratones fueron perfundidos y el cerebro fue extraído para posterior post-fijación y procesado. En este trabajo, los cerebros fueron crioprotegidos y cortados en el criostato para la realización posterior de immunohistoquímica de fluorescencia. Para contar las neuronas colinérgicas del prosencéfalo basal se realizo una immunohistoquímica usando el anticuerpo ChAT, un marcador específico de neuronas colinérgicas.

Estudio del efecto de la deleción de p75^{NTR} en los ratones SAMP8

Para estudiar cambios en los niveles de distintos mRNA y proteínas en el prosencéfalo basal de ratones SAMP8-p75$^{NTR-/-}$ se realizaron extractos frescos de la zona que fueron rápidamente congelados con nitrógeno líquido para preservar todos sus elementos. Estos extractos podían ser procesados de manera distinta.

Si el fin era estudiar la cantidad de mRNA que había en los extractos del prosencéfalo basal, primero de todo se extrajo el RNA de la muestra, para luego retrotranscribirlo a cDNA y ese usarlo cómo molde para los distintos genes. Esta estrategia fue usada para estudiar la respuesta al estrés oxidativo comparando ratones SAMP8-p75$^{NTR+/+}$ con ratones SAMP8-p75$^{NTR-/-}$.

Por otro lado, si el objetivo era medir los niveles de proteínas el extracto fue lisado con una solución de extracción de proteína para luego ser corrida en un gel de acrilamida y transferida a una membrana realizando un western blot. En la membrana se detectaron las proteínas de interés con anticuerpos primaros específicos. Esta estrategia fue usada para

estudiar los cambios en los niveles de distintas enzimas relacionadas con la síntesis de colesterol.

Estudios de comportamiento

Para evaluar si la eliminación del receptor en los ratones SAMP8 tenía alguna consecuencia a nivel de comportamiento, se realizaron 3 tests distintos a ratones SAMP8-p75$^{NTR+/+}$ y a ratones SAMP8-p75$^{NTR-/-}$ a 2 y 6 meses de edad. Los distintos tests usados evaluaron los niveles de ansiedad, la memoria a largo plazo y la memoria espacial.

Para estudiar los niveles de ansiedad se realizó el test de campo abierto, donde los ratones pueden explorar libremente durante 5 minutos una caja donde no han estado antes. El test se basa en la aversión que tienen los roedores para estar en sitios abiertos, ya que es donde los depredadores los pueden atacar, sin embargo, un roedor quiere explorar los sitios nuevos, por tanto, un ratón que pase más tiempo en la periferia de la caja, alejado del campo abierto, será un ratón con niveles mas altos de ansiedad que un ratón que pase más tiempo explorando el centro.

Para determinar la memoria a largo plazo en los ratones SAMP8-p75$^{NTR-/-}$ y SAMP8-p75$^{NTR+/+}$ se usó el test de reconocimiento de un objeto nuevo. Este test se divide en tres fases: habituación, ensayo y test. En la primera fase, el ratón explora una caja vacía durante 10 minutos. Al día siguiente, el ratón es puesto en la misma caja que contiene dos objetos idénticos. En esta tesis se usaron dos rectángulos rosas. Durante 5 minutos el ratón es libre para explorar los dos objetos. El día de el test, que se realiza 24 horas después del ensayo, uno de los dos objetos es cambiado por uno nuevo, en este trabajo un triangulo verde, y el ratón puede explorar durante 5 minutos los dos objetos. Si el ratón recuerda el objeto familiar, va a pasar más tiempo explorando el nuevo, en cambio si no recuerda el objeto, va a explorar los dos objetos durante el mismo tiempo.

Para estudiar la memoria espacial se uso el test-Y de alternación espontánea. Este test consiste en 3 brazos unidos que forman una Y mayúscula. Durante el test, el ratón es libre para entrar en los tres brazos y explorar, así pues, cada vez que entra en un brazo distinto al anterior es contado como una alternancia correcta, en cambio si el ratón vuelve al brazo anterior, indicando una pérdida de memoria, se considera una alternancia errónea.

Parte II

Establecimiento de cultivos primarios de neuronas colinérgicas

Para poner a punto la técnica de los cultivos primarios, se siguió el protocolo de (Schnitzler et al., 2008). Brevemente, a embriones de 17 días se les diseccionó el cerebro y separó el septum. Luego, las neuronas de la zona fueron disgregadas químicamente, con tripsina, y luego mecánicamente a través de pipeteo. Una vez disgregadas, las células fueron lavadas y filtradas para eliminar las meninges y posibles restos de suciedad. Por último, las células fueron contadas y sembradas en placas de 24 pocillos previamente cubiertos con poly-D-lisina y laminina. Las neuronas se mantuvieron 11 días en cultivo para que adquirieran un estadio maduro. Durante ese período de incubación se les añadieron los distintos químicos usados para evaluar el efecto de la inhibición de la γ-secretasa. Una vez pasados los 11 días las neuronas fueron fijadas y las neuronas colinérgicas fueron detectadas específicamente a través de la immunocitoquímica de fluorescencia contra ChAT y/o $p75^{NTR}$. Además, también se realizaron cultivos de ratones $p75^{NTR-/-}$ para comprobar si el efecto visto era dependiente del receptor.

Establecimiento de cultivos organotípicos

La técnica de los cultivos organotípicos fue aprendida durante una estancia internacional realizada en el tercer año de tesis en el laboratorio del Prof. Humpel, en Innsbruck, Austria.

La técnica consiste en cortar el cerebro a rodajas y mantenerlas en vida. En este trabajo, se usaron ratones que tenían una edad postnatal de 8 a 10 días. Para ello los ratones fueron sacrificados por decapitación y el cerebro fue extraído. Luego, este fue pegado a la platina de el vibratomo y se realizaron cortes de un grosor de 170 µm. Las rodajas obtenidas fueron transferidas a un inserto, dentro de una placa de 6 pocillos con medio donde se mantuvieron vivas durante dos semanas. Después de las dos semanas los cultivos fueron fijados y las neuronas colinérgicas fueron específicamente detectadas con el marcador ChAT a través de immunohístoquímica de campo claro, usando la reacción química de la peroxidase de rábano.

Estudio de la morfología de las neuronas colinérgicas del prosencéfalo basal

Una vez se realizó la detección de las neuronas colinérgicas, tanto de cultivo primario como de los cultivos organotípicos se tomaron imágenes con el microscopio confocal para hacer un análisis posterior. El análisis realizado fue el análisis de Sholl, este consiste en anillos concéntricos que empiezan en el soma, en cada anillo se cuantifica cuantas intersecciones hay, es decir, cuántas neuritas o axones hay a cierta distancia del soma. Este análisis morfológico permite saber la complejidad y la longitud de cada neurona, y poder así comprar distintas condiciones.

Estudio de la inhibición de la γ-secretasa in vivo

Para profundizar con el estudio del rol del corte $p75^{NTR}$ en las neuronas cólinérgicas, se usaron ratones modificados genéticamente en los cuales tenían delecionadas la PS1 y la PS2. En el caso de la PS2, el raton consistía en un *knock-out* total, en cambio para la deleción de la PS1 los ratones eran condicionales ya que la expresión de la PS1 en estadios embrionarios es necesaria y los ratones *knock-out* totales mueren. Para ello, la Cre recombinasa estaba expresada bajo el promotor de la CamkII, proteína que se expresa en neuronas maduras. Este ratón fue cruzado con un raton con el gen de la presinilna 1 floxeado, $PS1^{f/f}$. Así pues, cuando la CRE y el $PS1^{f/f}$ estuvieran en el mismo ratón, se delecionaría PS1 en neuronas maduras, evitando el problema de muerte embrionaria. A su vez, el *knock-out* de la PS2 fue cruzado con el ratón condicional de la PS1 para obtener el ratón deseado con doble *knock-out.* Este ratón fue descrito en (Yu et al., 2001).

Los ratones transgénicos de interés fueron sacrificados a 2, 4 y 8 meses. Para ello se les inyectó una sobredosis de pentobarbital para realizar una posterior perfusión. Al terminar con la perfusión, el cerebro fue extraído, post-fijado y cortado al vibratomo.
Con el tejido se realizaron dos procedimientos distintos. Por un lado, se cuantificaron las neuronas colinérgicas del prosencéfalo basal realizando una immunohistoquímica de fluorescencia contra ChAT.

Además, se realizó una tinción de acetilcolinesterasa, que marca las fibras colinérgicas para estudiar la complejidad de ellas. La tinción de acetilcolinesterasa se realizó siguiendo el protocolo de (Karnovsky & Roots, 1964). Brevemente, se preparó una solución que contiene 5 mg de acetilcolina iodada, 0.1 M de acetato sódico, 0.1 M de citrato sódico, 30 mM de $CuSO_4$ y 5 mM de $K_3Fe(CN)_6$.

BIBLIOGRAPHY

(2021). 2021 Alzheimer's disease facts and figures. *Alzheimers Dement* 17(3): 327-406.

Akiguchi, I, Pallas, M, Budka, H, Akiyama, H, Ueno, M, Han, J, . . . Hosokawa, M (2017). SAMP8 mice as a neuropathological model of accelerated brain aging and dementia: Toshio Takeda's legacy and future directions. *Neuropathology* 37(4): 293-305.

Al-Qudah, MA & Al-Dwairi, A (2016). Mechanisms and regulation of neurotrophin synthesis and secretion. *Neurosciences (Riyadh)* 21(4): 306-313.

Alberch, J, Perez-Navarro, E, Arenas, E & Marsal, J (1991). Involvement of nerve growth factor and its receptor in the regulation of the cholinergic function in aged rats. *J Neurochem* 57(5): 1483-1487.

Allaway, KC & Machold, R (2017). Developmental specification of forebrain cholinergic neurons. *Dev Biol* 421(1): 1-7.

Aloyz, RS, Bamji, SX, Pozniak, CD, Toma, JG, Atwal, J, Kaplan, DR & Miller, FD (1998). p53 is essential for developmental neuron death as regulated by the TrkA and p75 neurotrophin receptors. *J Cell Biol* 143(6): 1691-1703.

Alvarez-Garcia, O, Vega-Naredo, I, Sierra, V, Caballero, B, Tomas-Zapico, C, Camins, A, . . . Coto-Montes, A (2006). Elevated oxidative stress in the brain of senescence-accelerated mice at 5 months of age. *Biogerontology* 7(1): 43-52.

Alzheimer's Disease Collaborative, G (1995). The structure of the presenilin 1 (S182) gene and identification of six novel mutations in early onset AD families. *Nat Genet* 11(2): 219-222.

Anand, P & Singh, B (2013). A review on cholinesterase inhibitors for Alzheimer's disease. *Arch Pharm Res* 36(4): 375-399.

Antunes, M & Biala, G (2012). The novel object recognition memory: neurobiology, test procedure, and its modifications. *Cogn Process* 13(2): 93-110.

Anzalone, S, Roland, J, Vogt, B & Savage, L (2009). Acetylcholine efflux from retrosplenial areas and hippocampal sectors during maze exploration. *Behav Brain Res* 201(2): 272-278.

Apelt, J, Kumar, A & Schliebs, R (2002). Impairment of cholinergic neurotransmission in adult and aged transgenic Tg2576 mouse brain expressing the Swedish mutation of human beta-amyloid precursor protein. *Brain Res* 953(1-2): 17-30.

Ascano, M, Bodmer, D & Kuruvilla, R (2012). Endocytic trafficking of neurotrophins in neural development. *Trends Cell Biol* 22(5): 266-273.

Baeza-Raja, B, Sachs, BD, Li, P, Christian, F, Vagena, E, Davalos, D, . . . Akassoglou, K (2016). p75 Neurotrophin Receptor Regulates Energy Balance in Obesity. *Cell Rep* 14(2): 255-268.

Baldwin, AN, Bitler, CM, Welcher, AA & Shooter, EM (1992). Studies on the structure and binding properties of the cysteine-rich domain of rat low affinity nerve growth factor receptor (p75NGFR). *J Biol Chem* 267(12): 8352-8359.

Baldwin, AS (2012). Regulation of cell death and autophagy by IKK and NF-kappaB: critical mechanisms in immune function and cancer. *Immunol Rev* 246(1): 327-345.

Ballinger, EC, Ananth, M, Talmage, DA & Role, LW (2016). Basal Forebrain Cholinergic Circuits and Signaling in Cognition and Cognitive Decline. *Neuron* 91(6): 1199-1218.

Bamji, SX, Majdan, M, Pozniak, CD, Belliveau, DJ, Aloyz, R, Kohn, J, . . . Miller, FD (1998). The p75 neurotrophin receptor mediates neuronal apoptosis and is essential for naturally occurring sympathetic neuron death. *J Cell Biol* 140(4): 911-923.

Barde, YA, Edgar, D & Thoenen, H (1982). Purification of a new neurotrophic factor from mammalian brain. *EMBO J* 1(5): 549-553.

Bartus, RT (2000). On neurodegenerative diseases, models, and treatment strategies: lessons learned and lessons forgotten a generation following the cholinergic hypothesis. *Exp Neurol* 163(2): 495-529.

Bellucci, A, Luccarini, I, Scali, C, Prosperi, C, Giovannini, MG, Pepeu, G & Casamenti, F (2006). Cholinergic dysfunction, neuronal damage and axonal loss in TgCRND8 mice. *Neurobiol Dis* 23(2): 260-272.

Benedetti, M, Levi, A & Chao, MV (1993). Differential expression of nerve growth factor receptors leads to altered binding affinity and neurotrophin responsiveness. *Proc Natl Acad Sci U S A* 90(16): 7859-7863.

Benito-Vicente, A, Uribe, KB, Jebari, S, Galicia-Garcia, U, Ostolaza, H & Martin, C (2018). Familial Hypercholesterolemia: The Most Frequent Cholesterol Metabolism Disorder Caused Disease. *Int J Mol Sci* 19(11).

Berezovska, O, Jack, C, McLean, P, Aster, JC, Hicks, C, Xia, W, . . . Hyman, BT (2000). Rapid Notch1 nuclear translocation after ligand binding depends on presenilin-associated gamma-secretase activity. *Ann N Y Acad Sci* 920: 223-226.

Berger-Sweeney, J, Heckers, S, Mesulam, MM, Wiley, RG, Lappi, DA & Sharma, M (1994). Differential effects on spatial navigation of immunotoxin-induced cholinergic lesions of the medial septal area and nucleus basalis magnocellularis. *J Neurosci* 14(7): 4507-4519.

Bertram, L & Tanzi, RE (2004). The current status of Alzheimer's disease genetics: what do we tell the patients? *Pharmacol Res* 50(4): 385-396.

Bertrand, MJ, Kenchappa, RS, Andrieu, D, Leclercq-Smekens, M, Nguyen, HN, Carter, BD, . . . De Backer, O (2008). NRAGE, a p75NTR adaptor protein, is required for developmental apoptosis in vivo. *Cell Death Differ* 15(12): 1921-1929.

Biane, J, Conner, JM & Tuszynski, MH (2014). Nerve growth factor is primarily produced by GABAergic neurons of the adult rat cortex. *Front Cell Neurosci* 8: 220.

Bierer, LM, Haroutunian, V, Gabriel, S, Knott, PJ, Carlin, LS, Purohit, DP, . . . Davis, KL (1995). Neurochemical correlates of dementia severity in Alzheimer's disease: relative importance of the cholinergic deficits. *J Neurochem* 64(2): 749-760.

Blake, MG & Boccia, MM (2016). Basal Forebrain Cholinergic System and Memory. 253-273.

Blake, MG & Boccia, MM (2018). Basal Forebrain Cholinergic System and Memory. *Curr Top Behav Neurosci* 37: 253-273.

Boncristiano, S, Calhoun, ME, Kelly, PH, Pfeifer, M, Bondolfi, L, Stalder, M, . . . Jucker, M (2002). Cholinergic changes in the APP23 transgenic mouse model of cerebral amyloidosis. *J Neurosci* 22(8): 3234-3243.

Book, AA, Wiley, RG & Schweitzer, JB (1992). Specificity of 192 IgG-saporin for NGF receptor-positive cholinergic basal forebrain neurons in the rat. *Brain Res* 590(1-2): 350-355.

Boskovic, Z, Alfonsi, F, Rumballe, BA, Fonseka, S, Windels, F & Coulson, EJ (2014). The role of p75NTR in cholinergic basal forebrain structure and function. *J Neurosci* 34(39): 13033-13038.

Breitzig, M, Bhimineni, C, Lockey, R & Kolliputi, N (2016). 4-Hydroxy-2-nonenal: a critical target in oxidative stress? *Am J Physiol Cell Physiol* 311(4): C537-C543.

Bronfman, FC, Escudero, CA, Weis, J & Kruttgen, A (2007). Endosomal transport of neurotrophins: roles in signaling and neurodegenerative diseases. *Dev Neurobiol* 67(9): 1183-1203.

Bronfman, FC & Fainzilber, M (2004). Multi-tasking by the p75 neurotrophin receptor: sortilin things out? *EMBO Rep* 5(9): 867-871.

Bronfman, FC, Lazo, OM, Flores, C & Escudero, CA (2014). Spatiotemporal intracellular dynamics of neurotrophin and its receptors. Implications for neurotrophin signaling and neuronal function. *Handb Exp Pharmacol* 220: 33-65.

Bronfman, FC, Tcherpakov, M, Jovin, TM & Fainzilber, M (2003). Ligand-induced internalization of the p75 neurotrophin receptor: a slow route to the signaling endosome. *J Neurosci* 23(8): 3209-3220.

Buendia, I, Michalska, P, Navarro, E, Gameiro, I, Egea, J & Leon, R (2016). Nrf2-ARE pathway: An emerging target against oxidative stress and neuroinflammation in neurodegenerative diseases. *Pharmacol Ther* 157: 84-104.

Butterfield, DA, Howard, BJ, Yatin, S, Allen, KL & Carney, JM (1997). Free radical oxidation of brain proteins in accelerated senescence and its modulation by N-tert-butyl-alpha-phenylnitrone. *Proc Natl Acad Sci U S A* 94(2): 674-678.

Butterfield, DA & Poon, HF (2005). The senescence-accelerated prone mouse (SAMP8): a model of age-related cognitive decline with relevance to alterations of the gene expression and protein abnormalities in Alzheimer's disease. *Exp Gerontol* 40(10): 774-783.

Cabezas, R, Baez-Jurado, E, Hidalgo-Lanussa, O, Echeverria, V, Ashraf, GM, Sahebkar, A & Barreto, GE (2019). Correction to: Growth Factors and Neuroglobin in Astrocyte Protection Against Neurodegeneration and Oxidative Stress. *Mol Neurobiol* 56(4): 2352.

Casamenti, F, Deffenu, G, Abbamondi, AL & Pepeu, G (1986). Changes in cortical acetylcholine output induced by modulation of the nucleus basalis. *Brain Res Bull* 16(5): 689-695.

Caserta, MT, Bannon, Y, Fernandez, F, Giunta, B, Schoenberg, MR & Tan, J (2009). Normal brain aging clinical, immunological, neuropsychological, and neuroimaging features. *Int Rev Neurobiol* 84: 1-19.

Cassel, JC, Duconseille, E, Jeltsch, H & Will, B (1997). The fimbria-fornix/cingular bundle pathways: a review of neurochemical and behavioural approaches using lesions and transplantation techniques. *Prog Neurobiol* 51(6): 663-716.

Castro, MA, Hadziselimovic, A & Sanders, CR (2019). The vexing complexity of the amyloidogenic pathway. *Protein Sci* 28(7): 1177-1193.

Celesia, GG & Jasper, HH (1966). Acetylcholine released from cerebral cortex in relation to state of activation. *Neurology* 16(11): 1053-1063.

Ceni, C, Kommaddi, RP, Thomas, R, Vereker, E, Liu, X, McPherson, PS, . . . Barker, PA (2010). The p75NTR intracellular domain generated by neurotrophin-induced receptor cleavage potentiates Trk signaling. *J Cell Sci* 123(Pt 13): 2299-2307.

Cerqueira, NM, Oliveira, EF, Gesto, DS, Santos-Martins, D, Moreira, C, Moorthy, HN, . . . Fernandes, PA (2016). Cholesterol Biosynthesis: A Mechanistic Overview. *Biochemistry* 55(39): 5483-5506.

Chaldakov, GN, Tonchev, AB & Aloe, L (2009). NGF and BDNF: from nerves to adipose tissue, from neurokines to metabokines. *Riv Psichiatr* 44(2): 79-87.

Chao, MV (2003). Neurotrophins and their receptors: a convergence point for many signalling pathways. *Nat Rev Neurosci* 4(4): 299-309.

Chao, MV & Hempstead, BL (1995). p75 and Trk: a two-receptor system. *Trends Neurosci* 18(7): 321-326.

Chappell, J, McMahan, R, Chiba, A & Gallagher, M (1998). A re-examination of the role of basal forebrain cholinergic neurons in spatial working memory. *Neuropharmacology* 37(4-5): 481-487.

Chavez-Gutierrez, L, Bammens, L, Benilova, I, Vandersteen, A, Benurwar, M, Borgers, M, . . . De Strooper, B (2012). The mechanism of gamma-Secretase dysfunction in familial Alzheimer disease. *EMBO J* 31(10): 2261-2274.

Chen, SD, Wu, CL, Hwang, WC & Yang, DI (2017). More Insight into BDNF against Neurodegeneration: Anti-Apoptosis, Anti-Oxidation, and Suppression of Autophagy. *Int J Mol Sci* 18(3).

Chen, Z & Zhong, C (2014). Oxidative stress in Alzheimer's disease. *Neurosci Bull* 30(2): 271-281.

Cohen, S, Levi-Montalcini, R & Hamburger, V (1954). A Nerve Growth-Stimulating Factor Isolated from Sarcom as 37 and 180. *Proc Natl Acad Sci U S A* 40(10): 1014-1018.

Colardo, M, Martella, N, Pensabene, D, Siteni, S, Di Bartolomeo, S, Pallottini, V & Segatto, M (2021). Neurotrophins as Key Regulators of Cell Metabolism: Implications for Cholesterol Homeostasis. *Int J Mol Sci* 22(11).

Collier, B & Mitchell, JF (1966). Release of acetylcholine from the cerebral cortex during stimulation of the optic pathway. *Nature* 210(5034): 424-425.

Cooper, JD, Lindholm, D & Sofroniew, MV (1994). Reduced transport of [125I]nerve growth factor by cholinergic neurons and down-regulated TrkA expression in the medial septum of aged rats. *Neuroscience* 62(3): 625-629.

Costantini, C, Rossi, F, Formaggio, E, Bernardoni, R, Cecconi, D & Della-Bianca, V (2005). Characterization of the signaling pathway downstream p75 neurotrophin receptor involved in beta-amyloid peptide-dependent cell death. *J Mol Neurosci* 25(2): 141-156.

Coulson, EJ, May, LM, Osborne, SL, Reid, K, Underwood, CK, Meunier, FA, . . . Sah, P (2008). p75 neurotrophin receptor mediates neuronal cell death by activating GIRK channels through phosphatidylinositol 4,5-bisphosphate. *J Neurosci* 28(1): 315-324.

Coulson, EJ, Reid, K, Baca, M, Shipham, KA, Hulett, SM, Kilpatrick, TJ & Bartlett, PF (2000). Chopper, a new death domain of the p75 neurotrophin receptor that mediates rapid neuronal cell death. *J Biol Chem* 275(39): 30537-30545.

Coulson, EJ, Reid, K, Shipham, KM, Morley, S, Kilpatrick, TJ & Bartlett, PF (2004). The role of neurotransmission and the Chopper domain in p75 neurotrophin receptor death signaling. *Prog Brain Res* 146: 41-62.

Counts, SE & Mufson, EJ (2005). The role of nerve growth factor receptors in cholinergic basal forebrain degeneration in prodromal Alzheimer disease. *J Neuropathol Exp Neurol* 64(4): 263-272.

Crutcher, KA, Scott, SA, Liang, S, Everson, WV & Weingartner, J (1993). Detection of NGF-like activity in human brain tissue: increased levels in Alzheimer's disease. *J Neurosci* 13(6): 2540-2550.

Crutcher, KA & Weingartner, J (1991). Hippocampal NGF levels are not reduced in the aged Fischer 344 rat. *Neurobiol Aging* 12(5): 449-454.

Cutler, RG, Kelly, J, Storie, K, Pedersen, WA, Tammara, A, Hatanpaa, K, . . . Mattson, MP (2004). Involvement of oxidative stress-induced abnormalities in ceramide and cholesterol metabolism in brain aging and Alzheimer's disease. *Proc Natl Acad Sci U S A* 101(7): 2070-2075.

Daneman, R & Prat, A (2015). The blood-brain barrier. *Cold Spring Harb Perspect Biol* 7(1): a020412.

Dannenberg, H, Pabst, M, Braganza, O, Schoch, S, Niediek, J, Bayraktar, M, . . . Beck, H (2015). Synergy of direct and indirect cholinergic septo-hippocampal pathways coordinates firing in hippocampal networks. *J Neurosci* 35(22): 8394-8410.

Davies, AM (1991). Nerve growth factor synthesis and nerve growth factor receptor expression in neural development. *Int Rev Cytol* 128: 109-138.

Davies, P & Maloney, AJ (1976). Selective loss of central cholinergic neurons in Alzheimer's disease. *Lancet* 2(8000): 1403.

De Lacalle, S, Cooper, JD, Svendsen, CN, Dunnett, SB & Sofroniew, MV (1996). Reduced retrograde labelling with fluorescent tracer accompanies neuronal atrophy of basal forebrain cholinergic neurons in aged rats. *Neuroscience* 75(1): 19-27.

De Strooper, B (2003). Aph-1, Pen-2, and Nicastrin with Presenilin generate an active gamma-Secretase complex. *Neuron* 38(1): 9-12.

Deinhardt, K & Chao, MV (2014). Trk receptors. *Handb Exp Pharmacol* 220: 103-119.

Deinhardt, K, Reversi, A, Berninghausen, O, Hopkins, CR & Schiavo, G (2007). Neurotrophins Redirect p75NTR from a clathrin-independent to a clathrin-dependent endocytic pathway coupled to axonal transport. *Traffic* 8(12): 1736-1749.

Dokter, M, Busch, R, Poser, R, Vogt, MA, von Bohlen Und Halbach, V, Gass, P, . . . von Bohlen Und Halbach, O (2015). Implications of p75NTR for dentate gyrus morphology and hippocampus-related behavior revisited. *Brain Struct Funct* 220(3): 1449-1462.

Domeniconi, M, Zampieri, N, Spencer, T, Hilaire, M, Mellado, W, Chao, MV & Filbin, MT (2005). MAG induces regulated intramembrane proteolysis of the p75 neurotrophin receptor to inhibit neurite outgrowth. *Neuron* 46(6): 849-855.

Doody, RS, Raman, R, Farlow, M, Iwatsubo, T, Vellas, B, Joffe, S, . . . Semagacestat Study, G (2013). A phase 3 trial of semagacestat for treatment of Alzheimer's disease. *N Engl J Med* 369(4): 341-350.

Dudar, JD & Szerb, JC (1969). The effect of topically applied atropine on resting and evoked cortical acetylcholine release. *J Physiol* 203(3): 741-762.

Duff, K, Eckman, C, Zehr, C, Yu, X, Prada, CM, Perez-tur, J, . . . Younkin, S (1996). Increased amyloid-beta42(43) in brains of mice expressing mutant presenilin 1. *Nature* 383(6602): 710-713.

Dunnett, SB, Everitt, BJ & Robbins, TW (1991). The basal forebrain-cortical cholinergic system: interpreting the functional consequences of excitotoxic lesions. *Trends Neurosci* 14(11): 494-501.

Duzel, S, Munte, TF, Lindenberger, U, Bunzeck, N, Schutze, H, Heinze, HJ & Duzel, E (2010). Basal forebrain integrity and cognitive memory profile in healthy aging. *Brain Res* 1308: 124-136.

Eberle, D, Hegarty, B, Bossard, P, Ferre, P & Foufelle, F (2004). SREBP transcription factors: master regulators of lipid homeostasis. *Biochimie* 86(11): 839-848.

Elder, GA, Gama Sosa, MA, De Gasperi, R, Dickstein, DL & Hof, PR (2010). Presenilin transgenic mice as models of Alzheimer's disease. *Brain Struct Funct* 214(2-3): 127-143.

Escamilla-Ayala, A, Wouters, R, Sannerud, R & Annaert, W (2020). Contribution of the Presenilins in the cell biology, structure and function of gamma-secretase. *Semin Cell Dev Biol* 105: 12-26.

Escudero, CA, Lazo, OM, Galleguillos, C, Parraguez, JI, Lopez-Verrilli, MA, Cabeza, C, . . . Bronfman, FC (2014). The p75 neurotrophin receptor evades the endolysosomal route in neuronal cells, favouring multivesicular bodies specialised for exosomal release. *J Cell Sci* 127(Pt 9): 1966-1979.

Espinet, C, Gonzalo, H, Fleitas, C, Menal, MJ & Egea, J (2015). Oxidative stress and neurodegenerative diseases: a neurotrophic approach. *Curr Drug Targets* 16(1): 20-30.

Esposito, D, Patel, P, Stephens, RM, Perez, P, Chao, MV, Kaplan, DR & Hempstead, BL (2001). The cytoplasmic and transmembrane domains of the p75 and Trk A receptors regulate high affinity binding to nerve growth factor. *J Biol Chem* 276(35): 32687-32695.

Everitt, BJ & Robbins, TW (1997). Central cholinergic systems and cognition. *Annu Rev Psychol* 48: 649-684.

Fagan, AM, Garber, M, Barbacid, M, Silos-Santiago, I & Holtzman, DM (1997). A role for TrkA during maturation of striatal and basal forebrain cholinergic neurons in vivo. *J Neurosci* 17(20): 7644-7654.

Fahnestock, M, Michalski, B, Xu, B & Coughlin, MD (2001). The precursor pro-nerve growth factor is the predominant form of nerve growth factor in brain and is increased in Alzheimer's disease. *Mol Cell Neurosci* 18(2): 210-220.

Fahnestock, M & Shekari, A (2019). ProNGF and Neurodegeneration in Alzheimer's Disease. *Front Neurosci* 13: 129.

Fahnestock, M, Yu, G, Michalski, B, Mathew, S, Colquhoun, A, Ross, GM & Coughlin, MD (2004). The nerve growth factor precursor proNGF exhibits neurotrophic activity but is less active than mature nerve growth factor. *J Neurochem* 89(3): 581-592.

Fambrough, DM (1979). Control of acetylcholine receptors in skeletal muscle. *Physiol Rev* 59(1): 165-227.

Farr, SA, Poon, HF, Dogrukol-Ak, D, Drake, J, Banks, WA, Eyerman, E, . . . Morley, JE (2003). The antioxidants alpha-lipoic acid and N-acetylcysteine reverse memory impairment and brain oxidative stress in aged SAMP8 mice. *J Neurochem* 84(5): 1173-1183.

Feng, R, Rampon, C, Tang, YP, Shrom, D, Jin, J, Kyin, M, . . . Tsien, JZ (2001). Deficient neurogenesis in forebrain-specific presenilin-1 knockout mice is associated with reduced clearance of hippocampal memory traces. *Neuron* 32(5): 911-926.

Feng, R, Wang, H, Wang, J, Shrom, D, Zeng, X & Tsien, JZ (2004). Forebrain degeneration and ventricle enlargement caused by double knockout of Alzheimer's presenilin-1 and presenilin-2. *Proc Natl Acad Sci U S A* 101(21): 8162-8167.

Fernandez, A, Quintana, E, Velasco, P, Moreno-Jimenez, B, de Andres, B, Gaspar, ML, . . . Cano, E (2021). Senescent accelerated prone 8 (SAMP8) mice as a model of age dependent neuroinflammation. *J Neuroinflammation* 18(1): 75.

Fernandez-Cabello, S, Kronbichler, M, Van Dijk, KRA, Goodman, JA, Spreng, RN, Schmitz, TW & Alzheimer's Disease Neuroimaging, I (2020). Basal forebrain volume reliably predicts the cortical spread of Alzheimer's degeneration. *Brain* 143(3): 993-1009.

Flood, JF & Morley, JE (1993). Age-related changes in footshock avoidance acquisition and retention in senescence accelerated mouse (SAM). *Neurobiol Aging* 14(2): 153-157.

Fragkouli, A, van Wijk, NV, Lopes, R, Kessaris, N & Pachnis, V (2009). LIM homeodomain transcription factor-dependent specification of bipotential MGE progenitors into cholinergic and GABAergic striatal interneurons. *Development* 136(22): 3841-3851.

Franco, ML, Comaposada-Baró, R & Vilar, M (2020). Chapter 5 - Neurotrophins and Neurotrophin Receptors. Hormonal Signaling in Biology and Medicine. Litwack, G, Academic Press**:** 83-106.

Franco, ML, Garcia-Carpio, I, Comaposada-Baro, R, Escribano-Saiz, JJ, Chavez-Gutierrez, L & Vilar, M (2021). TrkA-mediated endocytosis of p75-CTF prevents cholinergic neuron death upon gamma-secretase inhibition. *Life Sci Alliance* 4(4).

Franco, ML, Nadezhdin, KD, Goncharuk, SA, Mineev, KS, Arseniev, AS & Vilar, M (2020). Structural basis of the transmembrane domain dimerization and rotation in the activation mechanism of the TRKA receptor by nerve growth factor. *J Biol Chem* 295(1): 275-286.

Franco, ML, Nadezhdin, KD, Light, TP, Goncharuk, SA, Soler-Lopez, A, Ahmed, F, . . . Vilar, M (2021). Interaction between the transmembrane domains of neurotrophin receptors p75 and TrkA mediates their reciprocal activation. *J Biol Chem*: 100926.

Franklin, KBJ & Paxinos, G (2013). Paxinos and Franklin's The mouse brain in stereotaxic coordinates.

Furusho, M, Ono, K, Takebayashi, H, Masahira, N, Kagawa, T, Ikeda, K & Ikenaka, K (2006). Involvement of the Olig2 transcription factor in cholinergic neuron development of the basal forebrain. *Dev Biol* 293(2): 348-357.

Gage, FH, Bjorklund, A & Stenevi, U (1984). Cells of origin of the ventral cholinergic septohippocampal pathway undergoing compensatory collateral sprouting following fimbria-fornix transection. *Neurosci Lett* 44(2): 211-216.

Garcia-Lopez, R, Pombero, A, Dominguez, E, Geijo-Barrientos, E & Martinez, S (2015). Developmental alterations of the septohippocampal cholinergic projection in a lissencephalic mouse model. *Exp Neurol* 271: 215-227.

Garcia-Matas, S, Gutierrez-Cuesta, J, Coto-Montes, A, Rubio-Acero, R, Diez-Vives, C, Camins, A, . . . Cristofol, R (2008). Dysfunction of astrocytes in senescence-accelerated mice SAMP8 reduces their neuroprotective capacity. *Aging Cell* 7(5): 630-640.

Gehler, S, Gallo, G, Veien, E & Letourneau, PC (2004). p75 neurotrophin receptor signaling regulates growth cone filopodial dynamics through modulating RhoA activity. *J Neurosci* 24(18): 4363-4372.

Gentry, JJ, Rutkoski, NJ, Burke, TL & Carter, BD (2004). A functional interaction between the p75 neurotrophin receptor interacting factors, TRAF6 and NRIF. *J Biol Chem* 279(16): 16646-16656.

Gil, C, Cubi, R & Aguilera, J (2007). Shedding of the p75NTR neurotrophin receptor is modulated by lipid rafts. *FEBS Lett* 581(9): 1851-1858.

Ginsberg, SD, Che, S, Wuu, J, Counts, SE & Mufson, EJ (2006). Down regulation of trk but not p75NTR gene expression in single cholinergic basal forebrain neurons mark the progression of Alzheimer's disease. *J Neurochem* 97(2): 475-487.

Giovannini, MG, Rakovska, A, Benton, RS, Pazzagli, M, Bianchi, L & Pepeu, G (2001). Effects of novelty and habituation on acetylcholine, GABA, and glutamate release from the frontal cortex and hippocampus of freely moving rats. *Neuroscience* 106(1): 43-53.

Goedert, M, Fine, A, Hunt, SP & Ullrich, A (1986). Nerve growth factor mRNA in peripheral and central rat tissues and in the human central nervous system: lesion effects in the rat brain and levels in Alzheimer's disease. *Brain Res* 387(1): 85-92.

Gould, TD, Dao, DT & Kovacsics, CE (2009). The Open Field Test. Mood and Anxiety Related Phenotypes in Mice: Characterization Using Behavioral Tests. Gould, TD. Totowa, NJ, Humana Press**:** 1-20.

Greferath, U, Bennie, A, Kourakis, A, Bartlett, PF, Murphy, M & Barrett, GL (2000). Enlarged cholinergic forebrain neurons and improved spatial learning in p75 knockout mice. *Eur J Neurosci* 12(3): 885-893.

Greferath, U, Trieu, J & Barrett, GL (2012). The p75 neurotrophin receptor has nonapoptotic antineurotrophic actions in the basal forebrain. *J Neurosci Res* 90(1): 278-287.

Grimm, MO, Rothhaar, TL & Hartmann, T (2012). The role of APP proteolytic processing in lipid metabolism. *Exp Brain Res* 217(3-4): 365-375.

Grinan-Ferre, C, Palomera-Avalos, V, Puigoriol-Illamola, D, Camins, A, Porquet, D, Pla, V, . . . Pallas, M (2016). Behaviour and cognitive changes correlated with hippocampal neuroinflammaging and neuronal markers in female SAMP8, a model of accelerated senescence. *Exp Gerontol* 80: 57-69.

Gritti, I, Mainville, L, Mancia, M & Jones, BE (1997). GABAergic and other noncholinergic basal forebrain neurons, together with cholinergic neurons, project to the mesocortex and isocortex in the rat. *J Comp Neurol* 383(2): 163-177.

Gritti, I, Manns, ID, Mainville, L & Jones, BE (2003). Parvalbumin, calbindin, or calretinin in cortically projecting and GABAergic, cholinergic, or glutamatergic basal forebrain neurons of the rat. *J Comp Neurol* 458(1): 11-31.

Grob, PM, Ross, AH, Koprowski, H & Bothwell, M (1985). Characterization of the human melanoma nerve growth factor receptor. *J Biol Chem* 260(13): 8044-8049.

Grothe, M, Heinsen, H & Teipel, S (2013). Longitudinal measures of cholinergic forebrain atrophy in the transition from healthy aging to Alzheimer's disease. *Neurobiol Aging* 34(4): 1210-1220.

Haapasalo, A & Kovacs, DM (2011). The many substrates of presenilin/gamma-secretase. *J Alzheimers Dis* 25(1): 3-28.

Hallbook, F, Ibanez, CF & Persson, H (1991). Evolutionary studies of the nerve growth factor family reveal a novel member abundantly expressed in Xenopus ovary. *Neuron* 6(5): 845-858.

Hampel, H, O'Bryant, SE, Molinuevo, JL, Zetterberg, H, Masters, CL, Lista, S, . . . Blennow, K (2018). Blood-based biomarkers for Alzheimer disease: mapping the road to the clinic. *Nat Rev Neurol* 14(11): 639-652.

Hangya, B, Ranade, SP, Lorenc, M & Kepecs, A (2015). Central Cholinergic Neurons Are Rapidly Recruited by Reinforcement Feedback. *Cell* 162(5): 1155-1168.

Harman, D (1994). Free-radical theory of aging. Increasing the functional life span. *Ann N Y Acad Sci* 717: 1-15.

Harrison, PJ (1986). Pathogenesis of Alzheimer's disease--beyond the cholinergic hypothesis: discussion paper. *J R Soc Med* 79(6): 347-352.

Hasselmo, ME & Stern, CE (2014). Theta rhythm and the encoding and retrieval of space and time. *Neuroimage* 85 Pt 2: 656-666.

Heckers, S, Ohtake, T, Wiley, RG, Lappi, DA, Geula, C & Mesulam, MM (1994). Complete and selective cholinergic denervation of rat neocortex and hippocampus but not amygdala by an immunotoxin against the p75 NGF receptor. *J Neurosci* 14(3 Pt 1): 1271-1289.

Hempstead, BL, Martin-Zanca, D, Kaplan, DR, Parada, LF & Chao, MV (1991). High-affinity NGF binding requires coexpression of the trk proto-oncogene and the low-affinity NGF receptor. *Nature* 350(6320): 678-683.

Hemsworth, BA & Mitchell, JF (1969). The characteristics of acetylcholine release mechanisms in the auditory cortex. *Br J Pharmacol* 36(1): 161-170.

Henderson, Z, Lu, CB, Janzso, G, Matto, N, McKinley, CE, Yanagawa, Y & Halasy, K (2010). Distribution and role of Kv3.1b in neurons in the medial septum diagonal band complex. *Neuroscience* 166(3): 952-969.

Herreman, A, Hartmann, D, Annaert, W, Saftig, P, Craessaerts, K, Serneels, L, . . . De Strooper, B (1999). Presenilin 2 deficiency causes a mild pulmonary phenotype and no changes in amyloid precursor protein processing but enhances the embryonic lethal phenotype of presenilin 1 deficiency. *Proc Natl Acad Sci U S A* 96(21): 11872-11877.

Hess, DT, Patterson, SI, Smith, DS & Skene, JH (1993). Neuronal growth cone collapse and inhibition of protein fatty acylation by nitric oxide. *Nature* 366(6455): 562-565.

Higuchi, H, Yamashita, T, Yoshikawa, H & Tohyama, M (2003). PKA phosphorylates the p75 receptor and regulates its localization to lipid rafts. *EMBO J* 22(8): 1790-1800.

Hu, R, Jin, S, He, X, Xu, F & Hu, J (2016). Whole-Brain Monosynaptic Afferent Inputs to Basal Forebrain Cholinergic System. *Front Neuroanat* 10: 98.

Huang, EJ & Reichardt, LF (2003). Trk receptors: roles in neuronal signal transduction. *Annu Rev Biochem* 72: 609-642.

Humpel, C (2018). Organotypic Brain Slice Cultures. *Curr Protoc Immunol* 123(1): e59.

Hyman, JM, Wyble, BP, Goyal, V, Rossi, CA & Hasselmo, ME (2003). Stimulation in hippocampal region CA1 in behaving rats yields long-term potentiation when delivered to the peak of theta and long-term depression when delivered to the trough. *J Neurosci* 23(37): 11725-11731.

Ikegami, S, Shumiya, S & Kawamura, H (1992). Age-related changes in radial-arm maze learning and basal forebrain cholinergic systems in senescence accelerated mice (SAM). *Behav Brain Res* 51(1): 15-22.

Jarrett, JT, Berger, EP & Lansbury, PT, Jr. (1993). The carboxy terminus of the beta amyloid protein is critical for the seeding of amyloid formation: implications for the pathogenesis of Alzheimer's disease. *Biochemistry* 32(18): 4693-4697.

Jasper, HH & Tessier, J (1971). Acetylcholine liberation from cerebral cortex during paradoxical (REM) sleep. *Science* 172(3983): 601-602.

Jiang, L, Kundu, S, Lederman, JD, Lopez-Hernandez, GY, Ballinger, EC, Wang, S, . . . Role, LW (2016). Cholinergic Signaling Controls Conditioned Fear Behaviors and Enhances Plasticity of Cortical-Amygdala Circuits. *Neuron* 90(5): 1057-1070.

Jiang, Y, Zhang, JS & Jakobsen, J (2005). Differential effect of p75 neurotrophin receptor on expression of pro-apoptotic proteins c-jun, p38 and caspase-3 in dorsal root ganglion cells after axotomy in experimental diabetes. *Neuroscience* 132(4): 1083-1092.

Johnson, D, Lanahan, A, Buck, CR, Sehgal, A, Morgan, C, Mercer, E, . . . Chao, M (1986). Expression and structure of the human NGF receptor. *Cell* 47(4): 545-554.

Jonas, A, Thiem, S, Kuhlmann, T, Wagener, R, Aszodi, A, Nowell, C, . . . Gresle, M (2014). Axonally derived matrilin-2 induces proinflammatory responses that exacerbate autoimmune neuroinflammation. *J Clin Invest* 124(11): 5042-5056.

Jones, BE (2004). Activity, modulation and role of basal forebrain cholinergic neurons innervating the cerebral cortex. *Prog Brain Res* 145: 157-169.

Jope, RS & Jenden, DJ (1980). The utilization of choline and acetyl coenzyme A for the synthesis of acetylcholine. *J Neurochem* 35(2): 318-325.

Jung, KM, Tan, S, Landman, N, Petrova, K, Murray, S, Lewis, R, . . . Kim, TW (2003). Regulated intramembrane proteolysis of the p75 neurotrophin receptor modulates its association with the TrkA receptor. *J Biol Chem* 278(43): 42161-42169.

Kabuto, H, Yokoi, I, Mori, A, Murakami, M & Sawada, S (1995). Neurochemical changes related to ageing in the senescence-accelerated mouse brain and the effect of chronic administration of nimodipine. *Mech Ageing Dev* 80(1): 1-9.

Kaisho, Y, Miyamoto, M, Shiho, O, Onoue, H, Kitamura, Y & Nomura, S (1994). Expression of neurotrophin genes in the brain of senescence-accelerated mouse (SAM) during postnatal development. *Brain Res* 647(1): 139-144.

Kanai, T & Szerb, JC (1965). Mesencephalic Reticular Activating System and Cortical Acetylcholine Output. *Nature* 205: 80-82.

Kang, J & Shen, J (2020). Cell-autonomous role of Presenilin in age-dependent survival of cortical interneurons. *Mol Neurodegener* 15(1): 72.

Kanning, KC, Hudson, M, Amieux, PS, Wiley, JC, Bothwell, M & Schecterson, LC (2003). Proteolytic processing of the p75 neurotrophin receptor and two homologs generates C-terminal fragments with signaling capability. *J Neurosci* 23(13): 5425-5436.

Kapas, L, Obal, F, Jr., Book, AA, Schweitzer, JB, Wiley, RG & Krueger, JM (1996). The effects of immunolesions of nerve growth factor-receptive neurons by 192 IgG-saporin on sleep. *Brain Res* 712(1): 53-59.

Karnovsky, MJ & Roots, L (1964). A "Direct-Coloring" Thiocholine Method for Cholinesterases. *J Histochem Cytochem* 12: 219-221.

Katsuki, F & Constantinidis, C (2014). Bottom-up and top-down attention: different processes and overlapping neural systems. *Neuroscientist* 20(5): 509-521.

Kawaguchi, S, Kishikawa, M, Sakae, M & Nakane, Y (1995). Age-related changes in basal dendrite and dendritic spine of hippocampal pyramidal neurons (CA1) among SAMP1TA/Ngs--quantitative analysis by the rapid Golgi method. *Mech Ageing Dev* 83(1): 11-20.

Kawamata, T, Akiguchi, I, Maeda, K, Tanaka, C, Higuchi, K, Hosokawa, M & Takeda, T (1998). Age-related changes in the brains of senescence-accelerated mice (SAM): association with glial and endothelial reactions. *Microsc Res Tech* 43(1): 59-67.

Kenchappa, RS, Zampieri, N, Chao, MV, Barker, PA, Teng, HK, Hempstead, BL & Carter, BD (2006). Ligand-dependent cleavage of the P75 neurotrophin receptor is necessary for NRIF nuclear translocation and apoptosis in sympathetic neurons. *Neuron* 50(2): 219-232.

Kilimann, I, Grothe, M, Heinsen, H, Alho, EJ, Grinberg, L, Amaro, E, Jr., . . . Teipel, SJ (2014). Subregional basal forebrain atrophy in Alzheimer's disease: a multicenter study. *J Alzheimers Dis* 40(3): 687-700.

Kisiswa, L, Fernandez-Suarez, D, Sergaki, MC & Ibanez, CF (2018). RIP2 Gates TRAF6 Interaction with Death Receptor p75(NTR) to Regulate Cerebellar Granule Neuron Survival. *Cell Rep* 24(4): 1013-1024.

Kitt, CA, Hohmann, C, Coyle, JT & Price, DL (1994). Cholinergic innervation of mouse forebrain structures. *J Comp Neurol* 341(1): 117-129.

Klingner, M, Apelt, J, Kumar, A, Sorger, D, Sabri, O, Steinbach, J, . . . Schliebs, R (2003). Alterations in cholinergic and non-cholinergic neurotransmitter receptor densities in transgenic Tg2576 mouse brain with beta-amyloid plaque pathology. *Int J Dev Neurosci* 21(7): 357-369.

Kneynsberg, A, Collier, TJ, Manfredsson, FP & Kanaan, NM (2016). Quantitative and semi-quantitative measurements of axonal degeneration in tissue and primary neuron cultures. *J Neurosci Methods* 266: 32-41.

Koellhoffer, EC, McCullough, LD & Ritzel, RM (2017). Old Maids: Aging and Its Impact on Microglia Function. *Int J Mol Sci* 18(4).

Koh, S & Loy, R (1989). Localization and development of nerve growth factor-sensitive rat basal forebrain neurons and their afferent projections to hippocampus and neocortex. *J Neurosci* 9(9): 2999-0318.

Koliatsos, VE, Clatterbuck, RE, Nauta, HJ, Knusel, B, Burton, LE, Hefti, FF, . . . Price, DL (1991). Human nerve growth factor prevents degeneration of basal forebrain cholinergic neurons in primates. *Ann Neurol* 30(6): 831-840.

Kommaddi, RP, Thomas, R, Ceni, C, Daigneault, K & Barker, PA (2011). Trk-dependent ADAM17 activation facilitates neurotrophin survival signaling. *FASEB J* 25(6): 2061-2070.

Kondo, H & Zaborszky, L (2016). Topographic organization of the basal forebrain projections to the perirhinal, postrhinal, and entorhinal cortex in rats. *J Comp Neurol* 524(12): 2503-2515.

Korade, Z, Kenchappa, RS, Mirnics, K & Carter, BD (2009). NRIF is a regulator of neuronal cholesterol biosynthesis genes. *J Mol Neurosci* 38(2): 152-158.

Korade, Z, Mi, Z, Portugal, C & Schor, NF (2007). Expression and p75 neurotrophin receptor dependence of cholesterol synthetic enzymes in adult mouse brain. *Neurobiol Aging* 28(10): 1522-1531.

Kraemer, BR, Clements, RT, Escobedo, CM, Nelson, KS, Waugh, CD, Elliott, AS, . . . Schemanski, MT (2021). c-Jun N-terminal Kinase Mediates Ligand-independent p75(NTR) Signaling in Mesencephalic Cells Subjected to Oxidative Stress. *Neuroscience* 453: 222-236.

Kraemer, BR, Snow, JP, Vollbrecht, P, Pathak, A, Valentine, WM, Deutch, AY & Carter, BD (2014). A role for the p75 neurotrophin receptor in axonal degeneration and apoptosis induced by oxidative stress. *J Biol Chem* 289(31): 21205-21216.

Kraemer, BR, Yoon, SO & Carter, BD (2014). The biological functions and signaling mechanisms of the p75 neurotrophin receptor. *Handb Exp Pharmacol* 220: 121-164.

Kraeuter, AK, Guest, PC & Sarnyai, Z (2019). The Y-Maze for Assessment of Spatial Working and Reference Memory in Mice. *Methods Mol Biol* 1916: 105-111.

Kramer, BM, Van der Zee, CE & Hagg, T (1999). P75 nerve growth factor receptor is important for retrograde transport of neurotrophins in adult cholinergic basal forebrain neurons. *Neuroscience* 94(4): 1163-1172.

Krol, KM, Crutcher, KA, Kalisch, BE, Rylett, RJ & Kawaja, MD (2000). Absence of p75(NTR) expression reduces nerve growth factor immunolocalization in cholinergic septal neurons. *J Comp Neurol* 427(1): 54-66.

Kuhn, TB, Meberg, PJ, Brown, MD, Bernstein, BW, Minamide, LS, Jensen, JR, . . . Bamburg, JR (2000). Regulating actin dynamics in neuronal growth cones by ADF/cofilin and rho family GTPases. *J Neurobiol* 44(2): 126-144.

Kumar, A & Thakur, MK (2012). Presenilin 1 and 2 are expressed differentially in the cerebral cortex of mice during development. *Neurochem Int* 61(5): 778-782.

Kumar, VB, Franko, MW, Farr, SA, Armbrecht, HJ & Morley, JE (2000). Identification of age-dependent changes in expression of senescence-accelerated mouse (SAMP8) hippocampal proteins by expression array analysis. *Biochem Biophys Res Commun* 272(3): 657-661.

Kurokawa, T, Asada, S, Nishitani, S & Hazeki, O (2001). Age-related changes in manganese superoxide dismutase activity in the cerebral cortex of senescence-accelerated prone and resistant mouse. *Neurosci Lett* 298(2): 135-138.

Lammers, F, Borchers, F, Feinkohl, I, Hendrikse, J, Kant, IMJ, Kozma, P, . . . BioCog, c (2018). Basal forebrain cholinergic system volume is associated with general cognitive ability in the elderly. *Neuropsychologia* 119: 145-156.

Laursen, B, Mork, A, Plath, N, Kristiansen, U & Bastlund, JF (2014). Impaired hippocampal acetylcholine release parallels spatial memory deficits in Tg2576 mice subjected to basal forebrain cholinergic degeneration. *Brain Res* 1543: 253-262.

Lee, KF, Li, E, Huber, LJ, Landis, SC, Sharpe, AH, Chao, MV & Jaenisch, R (1992). Targeted mutation of the gene encoding the low affinity NGF receptor p75 leads to deficits in the peripheral sensory nervous system. *Cell* 69(5): 737-749.

Lee, MK, Slunt, HH, Martin, LJ, Thinakaran, G, Kim, G, Gandy, SE, . . . Sisodia, SS (1996). Expression of presenilin 1 and 2 (PS1 and PS2) in human and murine tissues. *J Neurosci* 16(23): 7513-7525.

Lee, R, Kermani, P, Teng, KK & Hempstead, BL (2001). Regulation of cell survival by secreted proneurotrophins. *Science* 294(5548): 1945-1948.

Levi-Montalcini, R & Hamburger, V (1951). Selective growth stimulating effects of mouse sarcoma on the sensory and sympathetic nervous system of the chick embryo. *J Exp Zool* 116(2): 321-361.

Levi-Montalcini, R, Meyer, H & Hamburger, V (1954). In vitro experiments on the effects of mouse sarcomas 180 and 37 on the spinal and sympathetic ganglia of the chick embryo. *Cancer Res* 14(1): 49-57.

Levy-Lahad, E, Wijsman, EM, Nemens, E, Anderson, L, Goddard, KA, Weber, JL, . . . Schellenberg, GD (1995). A familial Alzheimer's disease locus on chromosome 1. *Science* 269(5226): 970-973.

Lewin, GR & Barde, YA (1996). Physiology of the neurotrophins. *Annu Rev Neurosci* 19: 289-317.

Li, T, Wen, H, Brayton, C, Das, P, Smithson, LA, Fauq, A, . . . Wong, PC (2007). Epidermal growth factor receptor and notch pathways participate in the tumor suppressor function of gamma-secretase. *J Biol Chem* 282(44): 32264-32273.

Li, X, Yu, B, Sun, Q, Zhang, Y, Ren, M, Zhang, X, . . . Qiu, Z (2018). Generation of a whole-brain atlas for the cholinergic system and mesoscopic projectome analysis of basal forebrain cholinergic neurons. *Proc Natl Acad Sci U S A* 115(2): 415-420.

Linggi, MS, Burke, TL, Williams, BB, Harrington, A, Kraemer, R, Hempstead, BL, . . . Carter, BD (2005). Neurotrophin receptor interacting factor (NRIF) is an essential mediator of apoptotic signaling by the p75 neurotrophin receptor. *J Biol Chem* 280(14): 13801-13808.

Liu, J & Mori, A (1993). Age-associated changes in superoxide dismutase activity, thiobarbituric acid reactivity and reduced glutathione level in the brain and liver in senescence accelerated mice (SAM): a comparison with ddY mice. *Mech Ageing Dev* 71(1-2): 23-30.

Livak, KJ & Schmittgen, TD (2001). Analysis of relative gene expression data using real-time quantitative PCR and the 2(-Delta Delta C(T)) Method. *Methods* 25(4): 402-408.

Longo, VG (1966). Behavioral and electroencephalographic effects of atropine and related compounds. *Pharmacol Rev* 18(2): 965-996.

Lu, CB & Henderson, Z (2010). Nicotine induction of theta frequency oscillations in rodent hippocampus in vitro. *Neuroscience* 166(1): 84-93.

Lueptow, LM (2017). Novel Object Recognition Test for the Investigation of Learning and Memory in Mice. *J Vis Exp*(126).

Luo, J, Yang, H & Song, BL (2020). Mechanisms and regulation of cholesterol homeostasis. *Nat Rev Mol Cell Biol* 21(4): 225-245.

Lynch, AM, Murphy, KJ, Deighan, BF, O'Reilly, JA, Gun'ko, YK, Cowley, TR, . . . Lynch, MA (2010). The impact of glial activation in the aging brain. *Aging Dis* 1(3): 262-278.

Lysakowski, A, Wainer, BH, Bruce, G & Hersh, LB (1989). An atlas of the regional and laminar distribution of choline acetyltransferase immunoreactivity in rat cerebral cortex. *Neuroscience* 28(2): 291-336.

Magno, L, Barry, C, Schmidt-Hieber, C, Theodotou, P, Hausser, M & Kessaris, N (2017). NKX2-1 Is Required in the Embryonic Septum for Cholinergic System Development, Learning, and Memory. *Cell Rep* 20(7): 1572-1584.

Magno, L, Kretz, O, Bert, B, Ersozlu, S, Vogt, J, Fink, H, . . . Naumann, T (2011). The integrity of cholinergic basal forebrain neurons depends on expression of Nkx2-1. *Eur J Neurosci* 34(11): 1767-1782.

Maisonpierre, PC, Belluscio, L, Squinto, S, Ip, NY, Furth, ME, Lindsay, RM & Yancopoulos, GD (1990). Neurotrophin-3: a neurotrophic factor related to NGF and BDNF. *Science* 247(4949 Pt 1): 1446-1451.

Majdan, M, Walsh, GS, Aloyz, R & Miller, FD (2001). TrkA mediates developmental sympathetic neuron survival in vivo by silencing an ongoing p75NTR-mediated death signal. *J Cell Biol* 155(7): 1275-1285.

Makkerh, JP, Ceni, C, Auld, DS, Vaillancourt, F, Dorval, G & Barker, PA (2005). p75 neurotrophin receptor reduces ligand-induced Trk receptor ubiquitination and delays Trk receptor internalization and degradation. *EMBO Rep* 6(10): 936-941.

Marin, O, Anderson, SA & Rubenstein, JL (2000). Origin and molecular specification of striatal interneurons. *J Neurosci* 20(16): 6063-6076.

Martin, MG, Pfrieger, F & Dotti, CG (2014). Cholesterol in brain disease: sometimes determinant and frequently implicated. *EMBO Rep* 15(10): 1036-1052.

Martinowich, K, Schloesser, RJ, Lu, Y, Jimenez, DV, Paredes, D, Greene, JS, . . . Lu, B (2012). Roles of p75(NTR), long-term depression, and cholinergic transmission in anxiety and acute stress coping. *Biol Psychiatry* 71(1): 75-83.

Masoudi, R, Ioannou, MS, Coughlin, MD, Pagadala, P, Neet, KE, Clewes, O, . . . Fahnestock, M (2009). Biological activity of nerve growth factor precursor is dependent upon relative levels of its receptors. *J Biol Chem* 284(27): 18424-18433.

Matusica, D & Coulson, EJ (2014). Local versus long-range neurotrophin receptor signalling: endosomes are not just carriers for axonal transport. *Semin Cell Dev Biol* 31: 57-63.

McCaffrey, G, Welker, J, Scott, J, der Salm, L & Grimes, ML (2009). High-resolution fractionation of signaling endosomes containing different receptors. *Traffic* 10(7): 938-950.

McCarthy, JV, Twomey, C & Wujek, P (2009). Presenilin-dependent regulated intramembrane proteolysis and gamma-secretase activity. *Cell Mol Life Sci* 66(9): 1534-1555.

McCommis, KS & Finck, BN (2015). Mitochondrial pyruvate transport: a historical perspective and future research directions. *Biochem J* 466(3): 443-454.

McGaughy, J, Everitt, BJ, Robbins, TW & Sarter, M (2000). The role of cortical cholinergic afferent projections in cognition: impact of new selective immunotoxins. *Behav Brain Res* 115(2): 251-263.

Mega, MS (2000). The cholinergic deficit in Alzheimer's disease: impact on cognition, behaviour and function. *Int J Neuropsychopharmacol* 3(7): 3-12.

Mesulam, MM (1999). Neuroplasticity failure in Alzheimer's disease: bridging the gap between plaques and tangles. *Neuron* 24(3): 521-529.

Mesulam, MM, Mufson, EJ, Wainer, BH & Levey, AI (1983). Central cholinergic pathways in the rat: an overview based on an alternative nomenclature (Ch1-Ch6). *Neuroscience* 10(4): 1185-1201.

Mi, S, Lee, X, Shao, Z, Thill, G, Ji, B, Relton, J, . . . Pepinsky, RB (2004). LINGO-1 is a component of the Nogo-66 receptor/p75 signaling complex. *Nat Neurosci* 7(3): 221-228.

Middleton, G, Hamanoue, M, Enokido, Y, Wyatt, S, Pennica, D, Jaffray, E, . . . Davies, AM (2000). Cytokine-induced nuclear factor kappa B activation promotes the survival of developing neurons. *J Cell Biol* 148(2): 325-332.

Milne, MR, Haug, CA, Abraham, IM & Kwakowsky, A (2015). Estradiol modulation of neurotrophin receptor expression in female mouse basal forebrain cholinergic neurons in vivo. *Endocrinology* 156(2): 613-626.

Milner, TA & Amaral, DG (1984). Evidence for a ventral septal projection to the hippocampal formation of the rat. *Exp Brain Res* 55(3): 579-585.

Mitra, G (1991). Mutational analysis of conserved residues in the tyrosine kinase domain of the human trk oncogene. *Oncogene* 6(12): 2237-2241.

Mitsushima, D, Sano, A & Takahashi, T (2013). A cholinergic trigger drives learning-induced plasticity at hippocampal synapses. *Nat Commun* 4: 2760.

Miyamoto, M, Kiyota, Y, Yamazaki, N, Nagaoka, A, Matsuo, T, Nagawa, Y & Takeda, T (1986). Age-related changes in learning and memory in the senescence-accelerated mouse (SAM). *Physiol Behav* 38(3): 399-406.

Molander-Melin, M, Blennow, K, Bogdanovic, N, Dellheden, B, Mansson, JE & Fredman, P (2005). Structural membrane alterations in Alzheimer brains found to be associated with regional disease development; increased density of gangliosides GM1 and GM2 and loss of cholesterol in detergent-resistant membrane domains. *J Neurochem* 92(1): 171-182.

Moreno, MD (2015). Estudio de la actividad de las células madre neurales adultas en el modelo de ratón SAMP8, Autonomous University of Madrid.

Morley, JE, Armbrecht, HJ, Farr, SA & Kumar, VB (2012). The senescence accelerated mouse (SAMP8) as a model for oxidative stress and Alzheimer's disease. *Biochim Biophys Acta* 1822(5): 650-656.

Mufson, EJ, Counts, SE, Perez, SE & Ginsberg, SD (2008). Cholinergic system during the progression of Alzheimer's disease: therapeutic implications. *Expert Rev Neurother* 8(11): 1703-1718.

Mulder, M, Ravid, R, Swaab, DF, de Kloet, ER, Haasdijk, ED, Julk, J, . . . Havekes, LM (1998). Reduced levels of cholesterol, phospholipids, and fatty acids in cerebrospinal fluid of Alzheimer disease patients are not related to apolipoprotein E4. *Alzheimer Dis Assoc Disord* 12(3): 198-203.

Muller, M, Triaca, V, Besusso, D, Costanzi, M, Horn, JM, Koudelka, J, . . . Minichiello, L (2012). Loss of NGF-TrkA signaling from the CNS is not sufficient to induce cognitive impairments in young adult or intermediate-aged mice. *J Neurosci* 32(43): 14885-14898.

Naumann, T, Casademunt, E, Hollerbach, E, Hofmann, J, Dechant, G, Frotscher, M & Barde, YA (2002). Complete deletion of the neurotrophin receptor p75NTR leads to long-lasting increases in the number of basal forebrain cholinergic neurons. *J Neurosci* 22(7): 2409-2418.

Newman, EL, Gillet, SN, Climer, JR & Hasselmo, ME (2013). Cholinergic blockade reduces theta-gamma phase amplitude coupling and speed modulation of theta frequency consistent with behavioral effects on encoding. *J Neurosci* 33(50): 19635-19646.

Nimchinsky, EA, Sabatini, BL & Svoboda, K (2002). Structure and function of dendritic spines. *Annu Rev Physiol* 64: 313-353.

Nomura, Y, Wang, BX, Qi, SB, Namba, T & Kaneko, S (1989). Biochemical changes related to aging in the senescence-accelerated mouse. *Exp Gerontol* 24(1): 49-55.

Nykjaer, A, Lee, R, Teng, KK, Jansen, P, Madsen, P, Nielsen, MS, . . . Petersen, CM (2004). Sortilin is essential for proNGF-induced neuronal cell death. *Nature* 427(6977): 843-848.

Oken, BS & Salinsky, M (1992). Alertness and attention: basic science and electrophysiologic correlates. *J Clin Neurophysiol* 9(4): 480-494.

Olivieri, G, Otten, U, Meier, F, Baysang, G, Dimitriades-Schmutz, B, Muller-Spahn, F & Savaskan, E (2002). Oxidative stress modulates tyrosine kinase receptor A and p75 receptor (low-affinity nerve growth factor receptor) expression in SHSY5Y neuroblastoma cells. *Neurol Clin Neurophysiol* 2002(2): 2-10.

Pallas, M, Camins, A, Smith, MA, Perry, G, Lee, HG & Casadesus, G (2008). From aging to Alzheimer's disease: unveiling "the switch" with the senescence-accelerated mouse model (SAMP8). *J Alzheimers Dis* 15(4): 615-624.

Park, KJ, Grosso, CA, Aubert, I, Kaplan, DR & Miller, FD (2010). p75NTR-dependent, myelin-mediated axonal degeneration regulates neural connectivity in the adult brain. *Nat Neurosci* 13(5): 559-566.

Parkhurst, CN, Zampieri, N & Chao, MV (2010). Nuclear localization of the p75 neurotrophin receptor intracellular domain. *J Biol Chem* 285(8): 5361-5368.

Pathak, A & Carter, BD (2017). Retrograde apoptotic signaling by the p75 neurotrophin receptor. *Neuronal Signal* 1(1): NS20160007.

Pavlides, C, Greenstein, YJ, Grudman, M & Winson, J (1988). Long-term potentiation in the dentate gyrus is induced preferentially on the positive phase of theta-rhythm. *Brain Res* 439(1-2): 383-387.

Pehar, M, Cassina, P, Vargas, MR, Castellanos, R, Viera, L, Beckman, JS, . . . Barbeito, L (2004). Astrocytic production of nerve growth factor in motor neuron apoptosis: implications for amyotrophic lateral sclerosis. *J Neurochem* 89(2): 464-473.

Pehar, M, Vargas, MR, Robinson, KM, Cassina, P, Diaz-Amarilla, PJ, Hagen, TM, . . . Beckman, JS (2007). Mitochondrial superoxide production and nuclear factor erythroid 2-related factor 2 activation in p75 neurotrophin receptor-induced motor neuron apoptosis. *J Neurosci* 27(29): 7777-7785.

Pelegri, C, Canudas, AM, del Valle, J, Casadesus, G, Smith, MA, Camins, A, . . . Vilaplana, J (2007). Increased permeability of blood-brain barrier on the hippocampus of a murine model of senescence. *Mech Ageing Dev* 128(9): 522-528.

Peng, S, Wuu, J, Mufson, EJ & Fahnestock, M (2004). Increased proNGF levels in subjects with mild cognitive impairment and mild Alzheimer disease. *J Neuropathol Exp Neurol* 63(6): 641-649.

Perry, EK, Gibson, PH, Blessed, G, Perry, RH & Tomlinson, BE (1977). Neurotransmitter enzyme abnormalities in senile dementia. Choline acetyltransferase and glutamic acid decarboxylase activities in necropsy brain tissue. *J Neurol Sci* 34(2): 247-265.

Perry, EK, Johnson, M, Kerwin, JM, Piggott, MA, Court, JA, Shaw, PJ, . . . Perry, RH (1992). Convergent cholinergic activities in aging and Alzheimer's disease. *Neurobiol Aging* 13(3): 393-400.

Perry, EK, Perry, RH, Blessed, G & Tomlinson, BE (1977). Necropsy evidence of central cholinergic deficits in senile dementia. *Lancet* 1(8004): 189.

Perry, EK, Perry, RH, Blessed, G & Tomlinson, BE (1978). Changes in brain cholinesterases in senile dementia of Alzheimer type. *Neuropathol Appl Neurobiol* 4(4): 273-277.

Perry, EK, Perry, RH, Gibson, PH, Blessed, G & Tomlinson, BE (1977). A cholinergic connection between normal aging and senile dementia in the human hippocampus. *Neurosci Lett* 6(1): 85-89.

Perry, EK, Tomlinson, BE, Blessed, G, Bergmann, K, Gibson, PH & Perry, RH (1978). Correlation of cholinergic abnormalities with senile plaques and mental test scores in senile dementia. *Br Med J* 2(6150): 1457-1459.

Peterson, DA, Dickinson-Anson, HA, Leppert, JT, Lee, KF & Gage, FH (1999). Central neuronal loss and behavioral impairment in mice lacking neurotrophin receptor p75. *J Comp Neurol* 404(1): 1-20.

Peterson, DA, Leppert, JT, Lee, KF & Gage, FH (1997). Basal forebrain neuronal loss in mice lacking neurotrophin receptor p75. *Science* 277(5327): 837-839.

Pfrieger, FW (2003). Cholesterol homeostasis and function in neurons of the central nervous system. *Cell Mol Life Sci* 60(6): 1158-1171.

Pham, DD, Bruelle, C, Thi Do, H, Pajanoja, C, Jin, C, Srinivasan, V, . . . Lindholm, D (2019). Caspase-2 and p75 neurotrophin receptor (p75NTR) are involved in the regulation of SREBP and lipid genes in hepatocyte cells. *Cell Death Dis* 10(7): 537.

Pham, DD, Do, HT, Bruelle, C, Kukkonen, JP, Eriksson, O, Mogollon, I, . . . Lindholm, D (2016). p75 Neurotrophin Receptor Signaling Activates Sterol Regulatory Element-binding Protein-2 in Hepatocyte Cells via p38 Mitogen-activated Protein Kinase and Caspase-3. *J Biol Chem* 291(20): 10747-10758.

Phillis, JW & York, DH (1968). Pharmacological studies on a cholinergic inhibition in the cerebral cortex. *Brain Res* 10(3): 297-306.

Placanica, L, Zhu, L & Li, YM (2009). Gender- and age-dependent gamma-secretase activity in mouse brain and its implication in sporadic Alzheimer disease. *PLoS One* 4(4): e5088.

Prado, MA, Reis, RA, Prado, VF, de Mello, MC, Gomez, MV & de Mello, FG (2002). Regulation of acetylcholine synthesis and storage. *Neurochem Int* 41(5): 291-299.

Prado, VF, Roy, A, Kolisnyk, B, Gros, R & Prado, MA (2013). Regulation of cholinergic activity by the vesicular acetylcholine transporter. *Biochem J* 450(2): 265-274.

Purves, D, Augustine, GJ, Fitzpatrick, D, Hall, WC, LaMantia, A-S, Mooney, RD, . . . White, LE (2019). Neuroscience.

Rabizadeh, S, Oh, J, Zhong, LT, Yang, J, Bitler, CM, Butcher, LL & Bredesen, DE (1993). Induction of apoptosis by the low-affinity NGF receptor. *Science* 261(5119): 345-348.

Rasmusson, DD, Clow, K & Szerb, JC (1994). Modification of neocortical acetylcholine release and electroencephalogram desynchronization due to brainstem stimulation by drugs applied to the basal forebrain. *Neuroscience* 60(3): 665-677.

Reichardt, LF (2006). Neurotrophin-regulated signalling pathways. *Philos Trans R Soc Lond B Biol Sci* 361(1473): 1545-1564.

Rinne, JO, Kaasinen, V, Jarvenpaa, T, Nagren, K, Roivainen, A, Yu, M, . . . Kurki, T (2003). Brain acetylcholinesterase activity in mild cognitive impairment and early Alzheimer's disease. *J Neurol Neurosurg Psychiatry* 74(1): 113-115.

Rodriguez, JJ & Verkhratsky, A (2011). Neuroglial roots of neurodegenerative diseases? *Mol Neurobiol* 43(2): 87-96.

Rodriguez-Tebar, A, Dechant, G & Barde, YA (1991). Neurotrophins: structural relatedness and receptor interactions. *Philos Trans R Soc Lond B Biol Sci* 331(1261): 255-258.

Rogaev, EI, Sherrington, R, Rogaeva, EA, Levesque, G, Ikeda, M, Liang, Y, . . . et al. (1995). Familial Alzheimer's disease in kindreds with missense mutations in a gene on chromosome 1 related to the Alzheimer's disease type 3 gene. *Nature* 376(6543): 775-778.

Rogers, JL & Kesner, RP (2003). Cholinergic modulation of the hippocampus during encoding and retrieval. *Neurobiol Learn Mem* 80(3): 332-342.

Ronowska, A, Szutowicz, A, Bielarczyk, H, Gul-Hinc, S, Klimaszewska-Lata, J, Dys, A, . . . Jankowska-Kulawy, A (2018). The Regulatory Effects of Acetyl-CoA Distribution in the Healthy and Diseased Brain. *Front Cell Neurosci* 12: 169.

Rotundo, RL (2003). Expression and localization of acetylcholinesterase at the neuromuscular junction. *J Neurocytol* 32(5-8): 743-766.

Rye, DB, Wainer, BH, Mesulam, MM, Mufson, EJ & Saper, CB (1984). Cortical projections arising from the basal forebrain: a study of cholinergic and noncholinergic components employing combined retrograde tracing and immunohistochemical localization of choline acetyltransferase. *Neuroscience* 13(3): 627-643.

Salehi, A, Verhaagen, J, Dijkhuizen, PA & Swaab, DF (1996). Co-localization of high-affinity neurotrophin receptors in nucleus basalis of Meynert neurons and their differential reduction in Alzheimer's disease. *Neuroscience* 75(2): 373-387.

Sanchez-Ortiz, E, Yui, D, Song, D, Li, Y, Rubenstein, JL, Reichardt, LF & Parada, LF (2012). TrkA gene ablation in basal forebrain results in dysfunction of the cholinergic circuitry. *J Neurosci* 32(12): 4065-4079.

Sankorrakul, K, Qian, L, Thangnipon, W & Coulson, EJ (2021). Is there a role for the p75 neurotrophin receptor in mediating degeneration during oxidative stress and after hypoxia? *J Neurochem*.

Sannerud, R, Esselens, C, Ejsmont, P, Mattera, R, Rochin, L, Tharkeshwar, AK, . . . Annaert, W (2016). Restricted Location of PSEN2/gamma-Secretase Determines Substrate Specificity and Generates an Intracellular Abeta Pool. *Cell* 166(1): 193-208.

Saper, CB (1984). Organization of cerebral cortical afferent systems in the rat. II. Magnocellular basal nucleus. *J Comp Neurol* 222(3): 313-342.

Sasaki, K, Tooyama, I, Li, AJ, Oomura, Y & Kimura, H (1999). Effects of an acidic fibroblast growth factor fragment analog on learning and memory and on medial septum cholinergic neurons in senescence-accelerated mice. *Neuroscience* 92(4): 1287-1294.

Sato, E, Oda, N, Ozaki, N, Hashimoto, S, Kurokawa, T & Ishibashi, S (1996). Early and transient increase in oxidative stress in the cerebral cortex of senescence-accelerated mouse. *Mech Ageing Dev* 86(2): 105-114.

Saura, CA, Choi, SY, Beglopoulos, V, Malkani, S, Zhang, D, Shankaranarayana Rao, BS, . . . Shen, J (2004). Loss of presenilin function causes impairments of memory and synaptic plasticity followed by age-dependent neurodegeneration. *Neuron* 42(1): 23-36.

Saxena, S, Howe, CL, Cosgaya, JM, Steiner, P, Hirling, H, Chan, JR, . . . Kruttgen, A (2005). Differential endocytic sorting of p75NTR and TrkA in response to NGF: a role for late endosomes in TrkA trafficking. *Mol Cell Neurosci* 28(3): 571-587.

Schambra, UB, Sulik, KK, Petrusz, P & Lauder, JM (1989). Ontogeny of cholinergic neurons in the mouse forebrain. *J Comp Neurol* 288(1): 101-122.

Scheuner, D, Eckman, C, Jensen, M, Song, X, Citron, M, Suzuki, N, . . . Younkin, S (1996). Secreted amyloid beta-protein similar to that in the senile plaques of Alzheimer's disease is increased in vivo by the presenilin 1 and 2 and APP mutations linked to familial Alzheimer's disease. *Nat Med* 2(8): 864-870.

Schliebs, R & Arendt, T (2011). The cholinergic system in aging and neuronal degeneration. *Behav Brain Res* 221(2): 555-563.

Schmitz, TW, Nathan Spreng, R & Alzheimer's Disease Neuroimaging, I (2016). Basal forebrain degeneration precedes and predicts the cortical spread of Alzheimer's pathology. *Nat Commun* 7: 13249.

Schnitzler, AC, Lopez-Coviella, I & Blusztajn, JK (2008). Purification and culture of nerve growth factor receptor (p75)-expressing basal forebrain cholinergic neurons. *Nat Protoc* 3(1): 34-40.

Scott, SA, Mufson, EJ, Weingartner, JA, Skau, KA & Crutcher, KA (1995). Nerve growth factor in Alzheimer's disease: increased levels throughout the brain coupled with declines in nucleus basalis. *J Neurosci* 15(9): 6213-6221.

Semba, K (2004). Phylogenetic and ontogenetic aspects of the basal forebrain cholinergic neurons and their innervation of the cerebral cortex. 145: 1-43.

Semba, K & Fibiger, HC (1988). Time of origin of cholinergic neurons in the rat basal forebrain. *J Comp Neurol* 269(1): 87-95.

Sharpe, LJ & Brown, AJ (2013). Controlling cholesterol synthesis beyond 3-hydroxy-3-methylglutaryl-CoA reductase (HMGCR). *J Biol Chem* 288(26): 18707-18715.

Shen, J, Bronson, RT, Chen, DF, Xia, W, Selkoe, DJ & Tonegawa, S (1997). Skeletal and CNS defects in Presenilin-1-deficient mice. *Cell* 89(4): 629-639.

Sherrington, R, Rogaev, EI, Liang, Y, Rogaeva, EA, Levesque, G, Ikeda, M, . . . St George-Hyslop, PH (1995). Cloning of a gene bearing missense mutations in early-onset familial Alzheimer's disease. *Nature* 375(6534): 754-760.

Shinotoh, H, Namba, H, Fukushi, K, Nagatsuka, S, Tanaka, N, Aotsuka, A, . . . Irie, T (2000). Progressive loss of cortical acetylcholinesterase activity in association with cognitive decline in Alzheimer's disease: a positron emission tomography study. *Ann Neurol* 48(2): 194-200.

Siebel, C & Lendahl, U (2017). Notch Signaling in Development, Tissue Homeostasis, and Disease. *Physiol Rev* 97(4): 1235-1294.

Sivandzade, F, Prasad, S, Bhalerao, A & Cucullo, L (2019). NRF2 and NF-B interplay in cerebrovascular and neurodegenerative disorders: Molecular mechanisms and possible therapeutic approaches. *Redox Biol* 21: 101059.

Sofroniew, MV, Howe, CL & Mobley, WC (2001). Nerve growth factor signaling, neuroprotection, and neural repair. *Annu Rev Neurosci* 24: 1217-1281.

Song, AJ & Palmiter, RD (2018). Detecting and Avoiding Problems When Using the Cre-lox System. *Trends Genet* 34(5): 333-340.

Sparks, DL, Hunsaker, JC, 3rd, Slevin, JT, DeKosky, ST, Kryscio, RJ & Markesbery, WR (1992). Monoaminergic and cholinergic synaptic markers in the nucleus basalis of Meynert (nbM): normal age-related changes and the effect of heart disease and Alzheimer's disease. *Ann Neurol* 31(6): 611-620.

Stadtman, ER (2006). Protein oxidation and aging. *Free Radic Res* 40(12): 1250-1258.

Steriade, M & Deschenes, M (1984). The thalamus as a neuronal oscillator. *Brain Res* 320(1): 1-63.

Strong, R, Reddy, V & Morley, JE (2003). Cholinergic deficits in the septal–hippocampal pathway of the SAM-P/8 senescence accelerated mouse. *Brain Research* 966(1): 150-156.

Sureda, FX, Gutierrez-Cuesta, J, Romeu, M, Mulero, M, Canudas, AM, Camins, A, . . . Pallas, M (2006). Changes in oxidative stress parameters and neurodegeneration markers in the brain of the senescence-accelerated mice SAMP-8. *Exp Gerontol* 41(4): 360-367.

Sweeney, JE, Hohmann, CF, Oster-Granite, ML & Coyle, JT (1989). Neurogenesis of the basal forebrain in euploid and trisomy 16 mice: an animal model for developmental disorders in Down syndrome. *Neuroscience* 31(2): 413-425.

Sykes, AM, Palstra, N, Abankwa, D, Hill, JM, Skeldal, S, Matusica, D, . . . Coulson, EJ (2012). The effects of transmembrane sequence and dimerization on cleavage of the p75 neurotrophin receptor by gamma-secretase. *J Biol Chem* 287(52): 43810-43824.

Takeda, T (1999). Senescence-accelerated mouse (SAM): a biogerontological resource in aging research. *Neurobiol Aging* 20(2): 105-110.

Takeda, T, Hosokawa, M & Higuchi, K (1991). Senescence-accelerated mouse (SAM): a novel murine model of accelerated senescence. *J Am Geriatr Soc* 39(9): 911-919.

Takeda, T, Hosokawa, M, Takeshita, S, Irino, M, Higuchi, K, Matsushita, T, . . . Yamamuro, T (1981). A new murine model of accelerated senescence. *Mech Ageing Dev* 17(2): 183-194.

Tanisawa, K, Mikami, E, Fuku, N, Honda, Y, Honda, S, Ohsawa, I, . . . Tanaka, M (2013). Exome sequencing of senescence-accelerated mice (SAM) reveals deleterious mutations in degenerative disease-causing genes. *BMC Genomics* 14: 248.

Taniuchi, M & Johnson, EM, Jr. (1985). Characterization of the binding properties and retrograde axonal transport of a monoclonal antibody directed against the rat nerve growth factor receptor. *J Cell Biol* 101(3): 1100-1106.

Teles-Grilo Ruivo, LM & Mellor, JR (2013). Cholinergic modulation of hippocampal network function. *Front Synaptic Neurosci* 5: 2.

Teng, HK, Teng, KK, Lee, R, Wright, S, Tevar, S, Almeida, RD, . . . Hempstead, BL (2005). ProBDNF induces neuronal apoptosis via activation of a receptor complex of p75NTR and sortilin. *J Neurosci* 25(22): 5455-5463.

Thinakaran, G, Harris, CL, Ratovitski, T, Davenport, F, Slunt, HH, Price, DL, . . . Sisodia, SS (1997). Evidence that levels of presenilins (PS1 and PS2) are coordinately regulated by competition for limiting cellular factors. *J Biol Chem* 272(45): 28415-28422.

Timucin, AC & Basaga, H (2017). Pro-apoptotic effects of lipid oxidation products: HNE at the crossroads of NF-kappaB pathway and anti-apoptotic Bcl-2. *Free Radic Biol Med* 111: 209-218.

Tomioka, T, Shimazaki, T, Yamauchi, T, Oki, T, Ohgoh, M & Okano, H (2014). LIM homeobox 8 (Lhx8) is a key regulator of the cholinergic neuronal function via a tropomyosin receptor kinase A (TrkA)-mediated positive feedback loop. *J Biol Chem* 289(2): 1000-1010.

Tonnies, E & Trushina, E (2017). Oxidative Stress, Synaptic Dysfunction, and Alzheimer's Disease. *J Alzheimers Dis* 57(4): 1105-1121.

Tooyama, I, Sasaki, K, Oomura, Y, Li, AJ & Kimura, H (1997). Effect of acidic fibroblast growth factor on basal forebrain cholinergic neurons in senescence-accelerated mice. *Exp Gerontol* 32(1-2): 171-179.

Torres, EM, Perry, TA, Blockland, A, Wilkinson, LS, Wiley, RG, Lappi, DA & Dunnet, SB (1994). Behavioural, histochemical and biochemical consequences of selective immunolesions in discrete regions of the basal forebrain cholinergic system. *Neuroscience* 63(1): 95-122.

Tuszynski, MH (2000). Intraparenchymal NGF infusions rescue degenerating cholinergic neurons. *Cell Transplant* 9(5): 629-636.

Tyurina, YY, Nylander, KD, Mirnics, ZK, Portugal, C, Yan, C, Zaccaro, C, . . . Schor, NF (2005). The intracellular domain of p75NTR as a determinant of cellular reducing potential and response to oxidant stress. *Aging Cell* 4(4): 187-196.

Ueno, M, Akiguchi, I, Hosokawa, M, Shinnou, M, Sakamoto, H, Takemura, M & Higuchi, K (1997). Age-related changes in the brain transfer of blood-borne horseradish peroxidase in the hippocampus of senescence-accelerated mouse. *Acta Neuropathol* 93(3): 233-240.

Ueno, M, Akiguchi, I, Yagi, H, Naiki, H, Fujibayashi, Y, Kimura, J & Takeda, T (1993). Age-related changes in barrier function in mouse brain I. Accelerated age-related increase of brain transfer of serum albumin in accelerated senescence prone SAM-P/8 mice with deficits in learning and memory. *Arch Gerontol Geriatr* 16(3): 233-248.

Unal, CT, Pare, D & Zaborszky, L (2015). Impact of basal forebrain cholinergic inputs on basolateral amygdala neurons. *J Neurosci* 35(2): 853-863.

Underwood, CK, Reid, K, May, LM, Bartlett, PF & Coulson, EJ (2008). Palmitoylation of the C-terminal fragment of p75(NTR) regulates death signaling and is required for subsequent cleavage by gamma-secretase. *Mol Cell Neurosci* 37(2): 346-358.

Unger, JW (1998). Glial reaction in aging and Alzheimer's disease. *Microsc Res Tech* 43(1): 24-28.

Urra, S, Escudero, CA, Ramos, P, Lisbona, F, Allende, E, Covarrubias, P, . . . Bronfman, FC (2007). TrkA receptor activation by nerve growth factor induces shedding of the p75 neurotrophin receptor followed by endosomal gamma-secretase-mediated release of the p75 intracellular domain. *J Biol Chem* 282(10): 7606-7615.

Van der Zee, CE, Ross, GM, Riopelle, RJ & Hagg, T (1996). Survival of cholinergic forebrain neurons in developing p75NGFR-deficient mice. *Science* 274(5293): 1729-1732.

Verkhratsky, A, Parpura, V, Pekna, M, Pekny, M & Sofroniew, M (2014). Glia in the pathogenesis of neurodegenerative diseases. *Biochem Soc Trans* 42(5): 1291-1301.

Vicario, A, Kisiswa, L, Tann, JY, Kelly, CE & Ibanez, CF (2015). Neuron-type-specific signaling by the p75NTR death receptor is regulated by differential proteolytic cleavage. *J Cell Sci* 128(8): 1507-1517.

Vilar, M (2017). Structural Characterization of the p75 Neurotrophin Receptor: A Stranger in the TNFR Superfamily. *Vitam Horm* 104: 57-87.

von Schack, D, Casademunt, E, Schweigreiter, R, Meyer, M, Bibel, M & Dechant, G (2001). Complete ablation of the neurotrophin receptor p75NTR causes defects both in the nervous and the vascular system. *Nat Neurosci* 4(10): 977-978.

Wang, F, Chen, H & Sun, X (2009). Age-related spatial cognitive impairment is correlated with a decrease in ChAT in the cerebral cortex, hippocampus and forebrain of SAMP8 mice. *Neurosci Lett* 454(3): 212-217.

Wang, W, Mutka, AL, Zmrzljak, UP, Rozman, D, Tanila, H, Gylling, H, . . . Ikonen, E (2014). Amyloid precursor protein alpha- and beta-cleaved ectodomains exert opposing control of cholesterol homeostasis via SREBP2. *FASEB J* 28(2): 849-860.

Wang, X, Zhou, X, Li, G, Zhang, Y, Wu, Y & Song, W (2017). Modifications and Trafficking of APP in the Pathogenesis of Alzheimer's Disease. *Front Mol Neurosci* 10: 294.

Ward, NL, Stanford, LE, Brown, RE & Hagg, T (2000). Cholinergic medial septum neurons do not degenerate in aged 129/Sv control or p75(NGFR)-/-mice. *Neurobiol Aging* 21(1): 125-134.

Wenk, GL (1997). The nucleus basalis magnocellularis cholinergic system: one hundred years of progress. *Neurobiol Learn Mem* 67(2): 85-95.

Wenk, GL, Stoehr, JD, Quintana, G, Mobley, S & Wiley, RG (1994). Behavioral, biochemical, histological, and electrophysiological effects of 192 IgG-saporin injections into the basal forebrain of rats. *J Neurosci* 14(10): 5986-5995.

Whitehouse, PJ, Price, DL, Struble, RG, Clark, AW, Coyle, JT & Delon, MR (1982). Alzheimer's disease and senile dementia: loss of neurons in the basal forebrain. *Science* 215(4537): 1237-1239.

Wiesmann, C, Ultsch, MH, Bass, SH & de Vos, AM (1999). Crystal structure of nerve growth factor in complex with the ligand-binding domain of the TrkA receptor. *Nature* 401(6749): 184-188.

Wiley, RG, Oeltmann, TN & Lappi, DA (1991). Immunolesioning: selective destruction of neurons using immunotoxin to rat NGF receptor. *Brain Res* 562(1): 149-153.

Wolfe, MS, Xia, W, Ostaszewski, BL, Diehl, TS, Kimberly, WT & Selkoe, DJ (1999). Two transmembrane aspartates in presenilin-1 required for presenilin endoproteolysis and gamma-secretase activity. *Nature* 398(6727): 513-517.

Wong, ST, Henley, JR, Kanning, KC, Huang, KH, Bothwell, M & Poo, MM (2002). A p75(NTR) and Nogo receptor complex mediates repulsive signaling by myelin-associated glycoprotein. *Nat Neurosci* 5(12): 1302-1308.

Woolf, NJ (1991). Cholinergic systems in mammalian brain and spinal cord. *Prog Neurobiol* 37(6): 475-524.

Wright, JW, Alt, JA, Turner, GD & Krueger, JM (2004). Differences in spatial learning comparing transgenic p75 knockout, New Zealand Black, C57BL/6, and Swiss Webster mice. *Behav Brain Res* 153(2): 453-458.

Wu, H, Williams, J & Nathans, J (2014). Complete morphologies of basal forebrain cholinergic neurons in the mouse. *Elife* 3: e02444.

Wu, Y, Zhang, AQ & Yew, DT (2005). Age related changes of various markers of astrocytes in senescence-accelerated mice hippocampus. *Neurochem Int* 46(7): 565-574.

Wyss-Coray, T (2016). Ageing, neurodegeneration and brain rejuvenation. *Nature* 539(7628): 180-186.

Xia, C, Higuchi, K, Shimizu, M, Matsushita, T, Kogishi, K, Wang, J, . . . Hosokawa, M (1999). Genetic typing of the senescence-accelerated mouse (SAM) strains with microsatellite markers. *Mamm Genome* 10(3): 235-238.

Yagi, H, Katoh, S, Akiguchi, I & Takeda, T (1988). Age-related deterioration of ability of acquisition in memory and learning in senescence accelerated mouse: SAM-P/8 as an animal model of disturbances in recent memory. *Brain Res* 474(1): 86-93.

Yamaguchi, Y, Katoh, H, Yasui, H, Mori, K & Negishi, M (2001). RhoA inhibits the nerve growth factor-induced Rac1 activation through Rho-associated kinase-dependent pathway. *J Biol Chem* 276(22): 18977-18983.

Yamashita, N & Kuruvilla, R (2016). Neurotrophin signaling endosomes: biogenesis, regulation, and functions. *Curr Opin Neurobiol* 39: 139-145.

Yamashita, T, Higuchi, H & Tohyama, M (2002). The p75 receptor transduces the signal from myelin-associated glycoprotein to Rho. *J Cell Biol* 157(4): 565-570.

Yamashita, T & Tohyama, M (2003). The p75 receptor acts as a displacement factor that releases Rho from Rho-GDI. *Nat Neurosci* 6(5): 461-467.

Yamashita, T, Tucker, KL & Barde, YA (1999). Neurotrophin binding to the p75 receptor modulates Rho activity and axonal outgrowth. *Neuron* 24(3): 585-593.

Yan, C, Mirnics, ZK, Portugal, CF, Liang, Y, Nylander, KD, Rudzinski, M, . . . Schor, NF (2005). Cholesterol biosynthesis and the pro-apoptotic effects of the p75 nerve growth factor receptor in PC12 pheochromocytoma cells. *Brain Res Mol Brain Res* 139(2): 225-234.

Yan, H & Chao, MV (1991). Disruption of cysteine-rich repeats of the p75 nerve growth factor receptor leads to loss of ligand binding. *J Biol Chem* 266(18): 12099-12104.

Yan, H, Pang, P, Chen, W, Zhu, H, Henok, KA, Li, H, . . . Lu, Y (2018). The Lesion Analysis of Cholinergic Neurons in 5XFAD Mouse Model in the Three-Dimensional Level of Whole Brain. *Mol Neurobiol* 55(5): 4115-4125.

Yanai, S & Endo, S (2016). Early onset of behavioral alterations in senescence-accelerated mouse prone 8 (SAMP8). *Behav Brain Res* 308: 187-195.

Yeaman, C, Le Gall, AH, Baldwin, AN, Monlauzeur, L, Le Bivic, A & Rodriguez-Boulan, E (1997). The O-glycosylated stalk domain is required for apical sorting of neurotrophin receptors in polarized MDCK cells. *J Cell Biol* 139(4): 929-940.

Yeiser, EC, Rutkoski, NJ, Naito, A, Inoue, J & Carter, BD (2004). Neurotrophin signaling through the p75 receptor is deficient in traf6-/- mice. *J Neurosci* 24(46): 10521-10529.

Yeo, TT, Chua-Couzens, J, Butcher, LL, Bredesen, DE, Cooper, JD, Valletta, JS, . . . Longo, FM (1997). Absence of p75NTR causes increased basal forebrain cholinergic neuron size, choline acetyltransferase activity, and target innervation. *J Neurosci* 17(20): 7594-7605.

Yin, F, Sancheti, H, Patil, I & Cadenas, E (2016). Energy metabolism and inflammation in brain aging and Alzheimer's disease. *Free Radic Biol Med* 100: 108-122.

Young, PW (2018). LNX1/LNX2 proteins: functions in neuronal signalling and beyond. *Neuronal Signal* 2(2): NS20170191.

Yu, H, Saura, CA, Choi, SY, Sun, LD, Yang, X, Handler, M, . . . Shen, J (2001). APP processing and synaptic plasticity in presenilin-1 conditional knockout mice. *Neuron* 31(5): 713-726.

Yuan, C, Aierken, A, Xie, Z, Li, N, Zhao, J & Qing, H (2020). The age-related microglial transformation in Alzheimer's disease pathogenesis. *Neurobiol Aging* 92: 82-91.

Zaborszky, L, Csordas, A, Mosca, K, Kim, J, Gielow, MR, Vadasz, C & Nadasdy, Z (2015). Neurons in the basal forebrain project to the cortex in a complex topographic organization that reflects corticocortical connectivity patterns: an experimental study based on retrograde tracing and 3D reconstruction. *Cereb Cortex* 25(1): 118-137.

Zaborszky, L, Gombkoto, P, Varsanyi, P, Gielow, MR, Poe, G, Role, LW, . . . Chiba, AA (2018). Specific Basal Forebrain-Cortical Cholinergic Circuits Coordinate Cognitive Operations. *J Neurosci* 38(44): 9446-9458.

Zaborszky, L, Pang, K, Somogyi, J, Nadasdy, Z & Kallo, I (1999). The basal forebrain corticopetal system revisited. *Ann N Y Acad Sci* 877: 339-367.

Zarubin, T & Han, J (2005). Activation and signaling of the p38 MAP kinase pathway. *Cell Res* 15(1): 11-18.

Zhang, J & Liu, Q (2015). Cholesterol metabolism and homeostasis in the brain. *Protein Cell* 6(4): 254-264.

Zhang, YH, Khanna, R & Nicol, GD (2013). Nerve growth factor/p75 neurotrophin receptor-mediated sensitization of rat sensory neurons depends on membrane cholesterol. *Neuroscience* 248: 562-570.

Zhao, Y, Flandin, P, Vogt, D, Blood, A, Hermesz, E, Westphal, H & Rubenstein, JL (2014). Ldb1 is essential for development of Nkx2.1 lineage derived GABAergic and cholinergic neurons in the telencephalon. *Dev Biol* 385(1): 94-106.

Zweifel, LS, Kuruvilla, R & Ginty, DD (2005). Functions and mechanisms of retrograde neurotrophin signalling. *Nat Rev Neurosci* 6(8): 615-625.

APPENDIX

Published Online: 3 February, 2021 | Supp Info: http://doi.org/10.26508/lsa.202000844
Downloaded from life-science-alliance.org on 5 February, 2021

Research Article

TRANSPARENT PROCESS SOURCE DATA OPEN ACCESS

Life Science Alliance

TrkA-mediated endocytosis of p75-CTF prevents cholinergic neuron death upon γ-secretase inhibition

María Luisa Franco[1,*], Irmina García-Carpio[1,*], Raquel Comaposada-Baró[1], Juan J Escribano-Saiz[1], Lucía Chávez-Gutiérrez[2], Marçal Vilar[1]

γ-secretase inhibitors (GSI) were developed to reduce the generation of Aβ peptide to find new Alzheimer's disease treatments. Clinical trials on Alzheimer's disease patients, however, showed several side effects that worsened the cognitive symptoms of the treated patients. The observed side effects were partially attributed to Notch signaling. However, the effect on other γ-secretase substrates, such as the p75 neurotrophin receptor (p75NTR) has not been studied in detail. p75NTR is highly expressed in the basal forebrain cholinergic neurons (BFCNs) during all life. Here, we show that GSI treatment induces the oligomerization of p75CTF leading to the cell death of BFCNs, and that this event is dependent on TrkA activity. The oligomerization of p75CTF requires an intact cholesterol recognition sequence (CRAC) and the constitutive binding of TRAF6, which activates the JNK and p38 pathways. Remarkably, TrkA rescues from cell death by a mechanism involving the endocytosis of p75CTF. These results suggest that the inhibition of γ-secretase activity in aged patients, where the expression of TrkA in the BFCNs is already reduced, could accelerate cholinergic dysfunction and promote neurodegeneration.

DOI 10.26508/lsa.202000844 | Received 8 July 2020 | Revised 11 January 2021 | Accepted 11 January 2021 | Published online 3 February 2021

Introduction

Alzheimer's disease (AD) is characterized by cognitive deficits and is one of the most commonly diagnosed types of dementia. Amyloid plaques are one of the neuropathological hallmarks of AD and are comprised of misfolded Aβ peptides. Aβ peptides are generated by sequential cleavage of the amyloid precursor protein (APP) by the β- and the γ-secretases. Mutations in the γ-secretase and APP cause autosomal dominant, early onset AD (De Strooper & Chávez Gutiérrez, 2015). Owing to its involvement in the production of Aβ production and close link to AD pathogenesis, γ-secretases have been considered to be one of the most promising targets as AD therapeutics. The development of γ-secretase inhibitors (GSIs) was in fact an area holding great expectations. GSIs were used in clinical trials to reduce the production of Aβ in AD patients. The GSI semagacestat (LY450139) Phase 3 clinical trial (Hopkins, 2010) was stopped because of adverse effects (such as increased risk of skin cancer) and a worsening of memory in the GSI treated group (Doody et al, 2013). The main reason of such failure likely relies on the fact that γ-secretases do not only process APP but also cleave many other type 1 transmembrane proteins (De Strooper & Chávez Gutiérrez, 2015), and thus, the concomitant GSI-mediated inhibition of the cleavage of other substrates of γ-secretase likely caused the observed undesirable consequences. The inhibition of the cleavage of Notch received great attention (Olsauskas-Kuprys et al, 2013; De Strooper, 2014); however, the impact that semagacestat could have had on other γ-secretase substrates is unclear. Although essential during development, Notch function in the adult central nervous system (CNS) is highly restricted to the population of neural stem cells and probably other substrates could better explain the worsening of the cognitive function seen in the clinical trial. One of the physiologically relevant substrates of γ-secretase in the brain is the p75 neurotrophin receptor. The p75 neurotrophin receptor ($p75^{NTR}$) is a member of the TNF receptor superfamily (Ibáñez & Simi, 2012; Bothwell, 2014), and it is best known by its role in programmed neuronal death during development or in response to injury in the adult brain (Ibáñez & Simi, 2012). It also regulates axonal growth and synaptic plasticity, as well as cell proliferation, migration, and survival (Kraemer et al, 2014; Vilar, 2017). These functions can be elicited by the association of $p75^{NTR}$ with different ligands and co-receptors leading to the activation of various signaling pathways (Roux & Barker, 2002). Importantly, $p75^{NTR}$ is highly expressed in the basal forebrain cholinergic neurons (BFCNs) during all stages of their development, a neuronal population well known for their involvement of complex cognitive tasks via their innervation to the cortex and hippocampus.

$p75^{NTR}$ undergoes regulated intramembrane proteolysis (RIP) (Kanning et al, 2003; Jung et al, 2003), a two-step process that

[1]Molecular Basis of Neurodegeneration Unit, Institute of Biomedicine of València (IBV-CSIC), València, Spain [2]Vlaams Instituut voor Biotechnologie Katholieke Universiteit (VIB-KU) Leuven Center for Brain and Disease, Leuven, Belgium

Correspondence: mvilar@ibv.csic.es
Irmina García-Carpio's present address is Division of Developmental Immunology, Biocenter, Medical University of Innsbruck, Innsbruck, Austria
*María Luisa Franco and Irmina García-Carpio contributed equally to this work

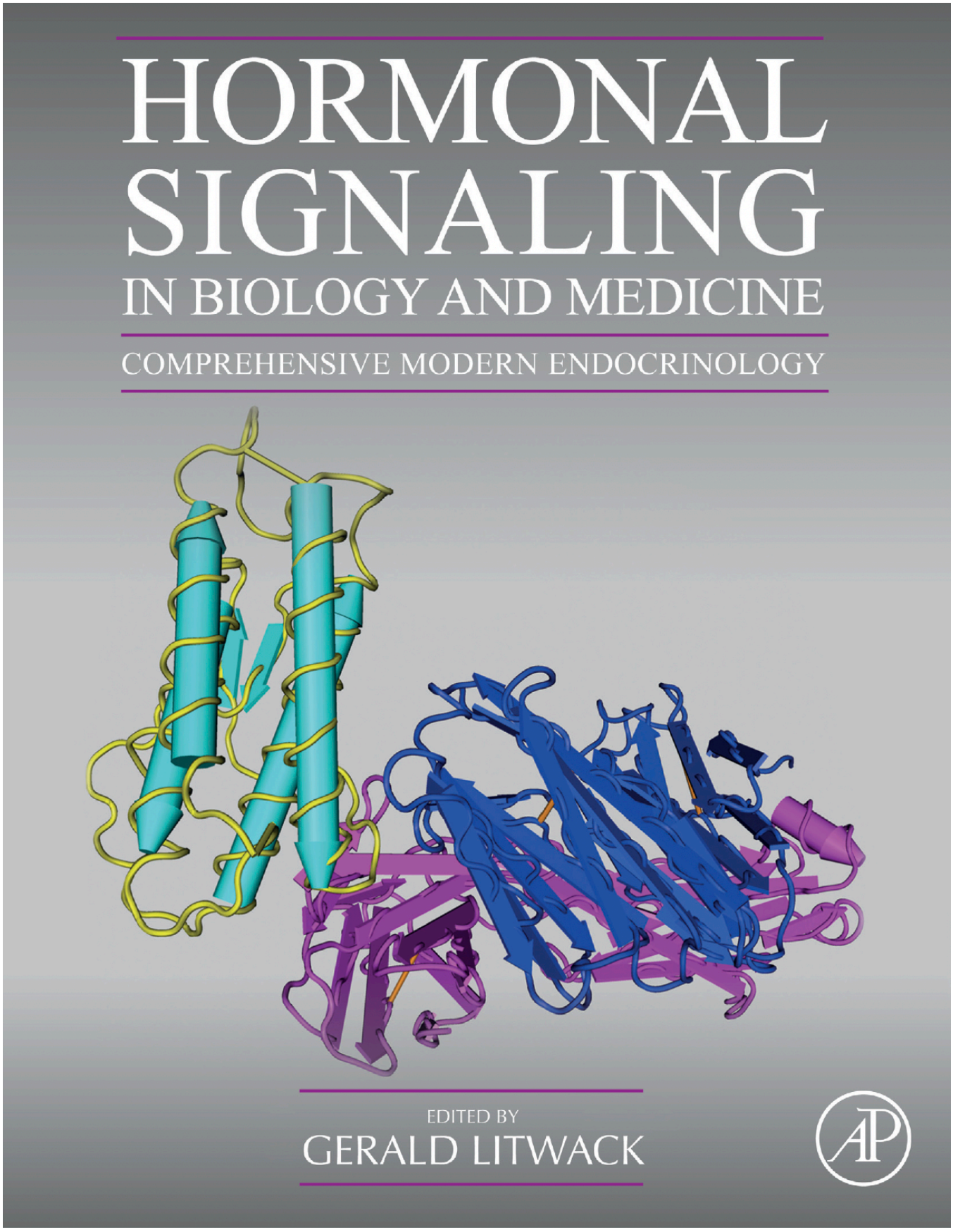
HORMONAL
SIGNALING
IN BIOLOGY AND MEDICINE
COMPREHENSIVE MODERN ENDOCRINOLOGY
EDITED BY
GERALD LITWACK

CHAPTER

5

Neurotrophins and Neurotrophin Receptors

M.L. Franco, R. Comaposada-Baró, M. Vilar

Molecular Basis of Neurodegeneration Unit, Instituto de Biomedicina de Valencia (IBV-CSIC), Valencia, Spain

1. INTRODUCTION

The discovery of nerve growth factor (NGF) by Rita Levi-Montalcini and Stanley Cohen in the 1950s represents an important milestone in the processes that led to modern cell biology and molecular neuroscience (Cohen et al., 1954; Levi-Montalcini et al., 1954; Levi-Montalcini and Hamburger, 1951). NGF was the first growth factor to be identified, paving the way to the identification of new soluble growth factors. NGF was discovered due to its trophic effects on sensory and sympathetic neurons. In 1982, brain-derived neurotrophic factor (BDNF), the second member of the "neurotrophic" family of neurotrophic factors, was shown to promote survival of a subpopulation of dorsal root ganglion neurons, and it subsequently was purified from pig brain (Barde et al., 1982). Since then, other members of the neurotrophin family such as neurotrophin-3 (NT-3) (Maisonpierre et al., 1990b) and neurotrophin-4/5 (NT-4/5) (Hallbook et al., 1991) have been described, each with a distinct profile of trophic effects on subpopulations of neurons in the peripheral and central nervous systems. The neurotrophin (NT) protein family is implicated in the maintenance and survival of the peripheral and central nervous systems (Ceni et al., 2014; Chao, 2003; Hempstead, 2014; Lu et al., 2014). NTs interact with two distinct receptors, a cognate member of the Trk receptor tyrosine kinase family and the common p75 neurotrophin receptor, which belongs to the tumor necrosis factor receptor superfamily of death receptors (Friedman and Greene, 1999; Huang and Reichardt, 2003). The interaction of mature neurotrophins with their receptors induces cell survival, cell death, differentiation, and synaptic plasticity activities. In this chapter we will describe the structural determinants of NTs binding to its receptors, the signalling pathways triggered, the functional consequences of deleting the NTs or their receptors in mice and the implication of the NTs in several human diseases.

2. STRUCTURES OF NEUROTROPHINS AND NEUROTROPHIN RECEPTORS

2.1 Neurotrophins

Neurotrophins are initially synthesized as precursors or proneurotrophins consisting of an N-terminal prodomain and a C-terminal mature domain. Following translation, proneurotrophins form noncovalent dimers via interactions of the mature domain. Mature neurotrophin proteins are noncovalent homodimers that contain a special three-dimensional structure, known as the *cysteine knot* (McDonald et al., 1991). The first reported structure of the cystine-knot family of growth factors was the one from NGF (McDonald et al., 1991). This structure is shared by other growth factors like transforming growth factor-β, platelet-derived growth factor, and others, forming a large superfamily of growth factors with a similar tertiary fold (McDonald and Hendrickson, 1993; Sun and Davies, 1995). The cysteine knot consists of three disulfide bonds that form a true knot of the polypeptide chain (Fig. 5.1A). The NGF protomer contains three pairs of antiparallel beta strands connected by three P-hairpin loop structures (Fig. 5.1A). Based on sequence alignments, neurotrophin residues are generally divided into two categories, conserved or variable. The dimer interface is composed of β-strands that maintain the conformation; these hydrophobic core residues are highly conserved. In addition, conserved residues are implicated in neurotrophin binding to their receptors (Fig. 5.1B). Variable residues represent elements of specificity to the different receptors and are usually located in the β-loops.

Hormonal Signaling in Biology and Medicine
https://doi.org/10.1016/B978-0-12-813814-4.00005-5